

DEVELOPMENT AND EXPERIMENTAL TESTING OF PRESS-BRAKE-FORMED STEEL TUB GIRDERS FOR SHORT SPAN BRIDGE APPLICATIONS

Karl E. Barth, Ph.D.

Gregory K. Michaelson, Ph.D.

Adam D. Roh

Robert M. Tennant, E.I.

VOLUME VII: FIELD EVALUATION OF A MODULAR PRESS-BRAKE-FORMED STEEL TUB GIRDER IN AN APPLICATION THAT INCLUDES SKEW AND SUPERELEVATION

Submitted to the AISI Steel Market

Development Institute Short Span

Steel Bridge Alliance

ABSTRACT

FIELD EVALUATION OF A MODULAR PRESS-BRAKE-FORMED STEEL TUB GIRDER IN AN APPLICATION THAT INCLUDES SKEW AND SUPERELEVATION

The Short Span Steel Bridge Alliance (SSSBA) is a group of bridge and culvert industry leaders (including steel manufacturers, fabricators, service centers, coaters, researchers, and representatives of related associations and government organizations) who have joined together to provide educational information on the design and construction of short span steel bridges in installations up to 140'-0" in length. A technical working group from within the SSSBA developed the notion for the modular shallow press-brake-formed steel tub girder as a solution for the short span steel bridge market.

After extensive testing at West Virginia University and multiple successful field demonstrations, members of the SSSBA collaborated with the West Virginia Division of Highways to arrange implementation of this system. The Fourteen Mile Bridge located in Lincoln County, West Virginia, was chosen as a prime candidate to demonstrate the system due to the significant superelevation and skew present. Upon completion of the Fourteen Mile Bridge, researchers from Marshall University and West Virginia University traveled to the bridge site to perform a live load field test.

This study presents the results and evaluation from experimental and analytical testing of the Fourteen Mile Bridge. Additionally, the research methods for both the experimental and analytical testing are outlined. Live load distribution factors were computed from the experimental and analytical data and compared to those computed following the AASHTO LRFD specifications. The results of this comparison reflect that the AASHTO LRFD specifications are conservative in the analysis of press-brake-formed tub girders. This report also includes an initial qualitative examination of bracing configurations for non-composite press-brake-formed tub girders. The results provide the basis for extending the work towards a closer investigation to determine the best practices of bracing.

TABLE OF CONTENTS

ABSTRACT	II
TABLE OF CONTENTS	III
LIST OF TABLES	VIII
LIST OF FIGURES	IX
CHAPTER 1: INTRODUCTION	1
1.1 BACKGROUND / OVERVIEW	1
1.2 PROJECT SCOPE & OBJECTIVES	2
1.3 REPORT ORGANIZATION	3
CHAPTER 2: LITERATURE REVIEW	4
2.1 INTRODUCTION	4
2.2 PREVIOUS APPLICATIONS OF COLD-BENT STEEL GIRDERS	4
<i>2.2.1 Prefabricated Press-Formed Steel T-Box Girder Bridge System (Taly & Gangarao, 1979)</i>	4
<i>2.2.2 Composite Girders with Cold Formed Steel U-sections (Nakamura, 2002)</i>	5
<i>2.2.3 Folded Plate Girders (Developed at the University of Nebraska)</i>	6
<i>2.2.4 Texas Department of Transportation Rapid Economical Bridge Replacement</i>	7
2.3 PREVIOUS RESEARCH AT WVU ON PRESS-BRAKE-FORMED STEEL TUB GIRDERS	8
<i>2.3.1 Development and Feasibility Assessment of Shallow Press-Brake-Formed Steel Tub Girders for Short-Span Bridge Applications (Michaelson 2014)</i>	8
<i>2.3.2 Experimental Evaluation of Non-Composite Shallow Press-Brake-Formed Steel Tub Girders (Kelly, 2014)</i>	13
<i>2.3.3 Evaluation of Modular Press-Brake-Formed Tub Girders with UHPC Joints (Kozhokin, 2016)</i>	14

2.3.4 <i>Field Performance Assessment of Press-Brake-Formed Steel Tub Girder Superstructures (Gibbs, 2017)</i>	16
2.3.5 <i>Fatigue Performance of Uncoated and Galvanized Composite Press-Brake-Formed Tub Girders (Tennant, 2018)</i>	18
2.3.6 <i>Field Performance and Rating Evaluation of a Modular Press-Brake-Formed Steel Tub Girder with a Steel Sandwich Plate Deck (Underwood, 2019)</i>	20
2.4 CURRENT AASHTO SPECIFICATIONS FOR TUB GIRDER DESIGN AND APPLICATION ..	22
2.4.1 <i>Multiple Presence Factors</i>	22
2.4.2 <i>Beam-Slab Bridges – Live Load Distribution Factors</i>	23
2.4.3 <i>Box-Section Flexural Members</i>	24
<u>2.4.3.1 Cross Section Proportion Limits</u>	<u>24</u>
<u>2.4.3.2 Constructability</u>	<u>25</u>
<u>2.4.3.3 Service Limit State</u>	<u>28</u>
<u>2.4.3.4 Fatigue and Fracture Limit State</u>	<u>30</u>
<u>2.4.3.5 Strength Limit State</u>	<u>31</u>
2.4.3.5.1 <i>General Flexure Requirements</i>	32
2.4.3.5.2 <i>Flexural Capacity of Composite Sections, Positive Flexure</i>	33
2.4.3.5.3 <i>Flexural Capacity of Non-composite Sections</i>	36
2.4.3.5.4 <i>Shear Capacity</i>	40
<u>2.4.3.6 AASHTO Equation References</u>	<u>42</u>
CHAPTER 3: DESIGN AND CONSTRUCTION OF THE FOURTEEN MILE BRIDGE	46
3.1 INTRODUCTION	46
3.2 SUMMARY OF DESIGN AND CONSTRUCTION	46
3.2.1 <i>Fabrication of Modular Components</i>	47
3.2.2 <i>Installation of Modular Components</i>	52

3.2.3 Accelerated Bridge Construction Strategies.....	55
CHAPTER 4: RESEARCH METHODS	56
4.1 INTRODUCTION	56
4.2 EXPERIMENTAL TESTING EQUIPMENT	56
4.2.1 BDI Strain Transducers	56
4.2.2 STS-WiFi Data Acquisition System.....	57
4.2.3 Load Truck and Wheel Scales.....	59
4.3 FINITE ELEMENT MODELING.....	60
4.3.1 Material Definitions.....	60
4.3.2 Element Selection.....	61
4.3.3 Mesh Discretization	61
4.3.4 Boundary Conditions and Multiple Point Constraints	63
4.3.5 Application of Live Loading.....	63
4.4 DATA REDUCTION METHODS.....	64
4.4.1 Computation of Quarter Span Bending Stresses	64
4.4.2 Computation of Live Load Distribution Factors	65
CHAPTER 5: FIELD TESTING OF THE FOURTEEN MILE BRIDGE	69
5.1 INTRODUCTION	69
5.2 LIVE LOAD FIELD TEST ASSESSMENT	69
5.2.1 Structure Instrumentation	69
5.2.2 Live Load Path Delineation.....	75
5.2.3 Live Load Testing.....	79
CHAPTER 6: RESULTS AND ANALYSIS	81
6.1 INTRODUCTION	81

6.2 COMPARISON OF RESULTS	81
6.2.1 <i>Live Load Field Test Results</i>	81
<u>6.2.1.1 Live Load Distribution Factors</u>	<u>82</u>
6.2.2 <i>Comparison of Analytical and Experimental Results</i>	83
6.3 COMPARISON OF LIVE LOAD DISTRIBUTION FACTORS WITH AASHTO LRFD SPECIFICATIONS	86
6.4 CONCLUSIONS.....	88
CHAPTER 7: QUALITATIVE ASSESSMENT OF BRACING EFFECTIVENESS AND TORSIONAL RESPONSE FOR NON-COMPOSITE TUB GIRDERS	89
7.1 INTRODUCTION	89
7.2 VERIFICATION WITH KELLY’S MODEL	89
7.2.1 <i>Geometric Imperfections</i>	89
7.2.2 <i>Material Modeling</i>	92
7.2.3 <i>Element Selection</i>	94
7.2.4 <i>Riks Loading Algorithm</i>	94
7.2.5 <i>Comparison with Kelly’s Model</i>	95
7.3 BRACING SCENARIOS	96
7.3.1 <i>Internal Bracing Scenarios</i>	96
7.3.2 <i>External Bracing Scenarios</i>	97
7.4 RESULTS OF FINITE ELEMENT ANALYSIS.....	98
7.4.1 <i>Comparison of Internal Bracing Scenarios</i>	99
7.4.2 <i>Comparison of External Bracing Scenarios</i>	100
7.5 CONCLUSIONS.....	102
CHAPTER 8: CONCLUSIONS AND RECOMMENDATIONS	103
8.1 PROJECT SUMMARY AND CONCLUSIONS	103

8.2 RECOMMENDATIONS FOR CONTINUED WORK	103
REFERENCES	104
APPENDIX A: RESULTS FOR ALL TRUCK RUNS.....	107
A.1 LIVE LOAD DISTRIBUTION FACTORS.....	107
<i>A.1.1 Live Load Field Test Results</i>	<i>107</i>
<i>A.1.2 Finite Element Analysis Results</i>	<i>111</i>
<i>A.1.3 Results Comparison: Live Load Field Test vs. Finite Element Analysis.....</i>	<i>111</i>
<i>A.1.4 Results Comparison: Live Load Field Test, Finite Element Analysis, AASHTO Calculations</i>	<i>116</i>
APPENDIX B: FINITE ELEMENT MODELING PROGRAM.....	121
APPENDIX C: FOURTEEN MILE BRIDGE DESIGN PLANS.....	174

LIST OF TABLES

<i>Table 2.1: Summary of Distribution Factors (Kozhokin, 2016)</i>	16
<i>Table 2.2: Multiple Presence Factors (AASHTO, 2017)</i>	22
<i>Table 2.3: Chapter 2 Equation Legend (AASHTO, 2017)</i>	43
<i>Table 4.1: Typical Aspect Ratio for Girder Elements</i>	62
<i>Table 4.2: Strain Values, Quarter Span Bending Stress</i>	65
<i>Table 4.3: Strain Values, Single Lane Loaded LLDF Sample Calculation</i>	66
<i>Table 4.4: Strain Values, Two Lanes Loaded LLDF Sample Calculation</i>	67
<i>Table 6.1: Measured Strain from Truck Run 1, Experimental</i>	82
<i>Table 6.2: Computed Live Load Distribution Factors from Truck Run 1, Experimental</i>	83
<i>Table 6.3: Comparison of Field and FEA Live Load Distribution Factors, One Lane Loaded</i> ... 84	
<i>Table 6.4: Comparison of Field and FEA Live Load Distribution Factors, Two Lanes Loaded</i> . 84	
<i>Table 6.5: Comparison of Field, FEA and AASHTO Live Load Distribution Factors, One Lane Loaded Truck Run 1</i>	86
<i>Table 6.6: Comparison of Field, FEA, and AASHTO Live Load Distribution Factors, Two Lanes Loaded Truck Run 1 and 4</i>	87
<i>Table 7.1: Expressions for Computing Steel Stress-Strain Behavior (Galindez, 2009)</i>	93

LIST OF FIGURES

<i>Figure 2:1: T-Box Girder System, Typical Girder Section with 5” Pre-cast, Prestressed Concrete Slab (Taly & Gangarao, 1979)</i>	5
<i>Figure 2:2: Nakamura’s Proposed Bridge System (Nakamura, 2002)</i>	6
<i>Figure 2:3: Folded Plate Girder and Composite Deck Cross Section (Burner, 2010)</i>	7
<i>Figure 2:4: Cross Section of Box Girder from Bridge FM 3267 (Chandar et al., 2010)</i>	8
<i>Figure 2:5: Design Comparison of 84” Wide Standard Mill Plate (Michaelson, 2014)</i>	9
<i>Figure 2:6: Typical Section, Composite Test Specimen (Michaelson, 2014)</i>	10
<i>Figure 2:7: Typical Ductile Failure of Composite Girder Section (Michaelson, 2014)</i>	11
<i>Figure 2:8: Typical Lateral Failure of Non-Composite Girder Section (Michaelson, 2014)</i>	11
<i>Figure 2:9: Comparison of Analytical and Experimental Results (Michaelson, 2014)</i>	12
<i>Figure 2:10: Initial Twist of Specimen #2 (Kelly, 2014)</i>	13
<i>Figure 2:11: Deflection at Quarter Points (Kelly, 2014)</i>	14
<i>Figure 2:12: Exposed Aggregate Finish of Shear Key Detail (Kozhokin, 2016)</i>	15
<i>Figure 2:13: New Amish Sawmill Bridge (Gibbs, 2017)</i>	17
<i>Figure 2:14: FEA v. Experimental v. AASHTO LLDFs (Gibbs, 2017)</i>	18
<i>Figure 2:15: Uncoated Steel Girder Under Fatigue Loading (Tennant, 2018)</i>	19
<i>Figure 2:16: Galvanized Steel Girder (Tennant, 2018)</i>	19
<i>Figure 2:17: Cannelville Road Bridge Modular Unit (Underwood, 2019)</i>	20
<i>Figure 2:18: Field v. FEA v. AASHTO LLDFs (Underwood, 2019)</i>	21
<i>Figure 2:19: Center-to-Center Flange Distance (AASHTO, 2017)</i>	23
<i>Figure 2:20 Live Load Deflection Limits (AASHTO, 2017)</i>	28
<i>Figure 3:1: Aerial View of Bridge Under Construction</i>	47
<i>Figure 3:2: Galvanized Tub Girder, Prior to Formwork Construction</i>	48
<i>Figure 3:3: Tub Girder with Completed Internal Formwork</i>	49
<i>Figure 3:4: Isometric View of Reusable External Formwork</i>	50
<i>Figure 3:5: Close View of Rebar Placement at Semi-Integral Abutment End</i>	50
<i>Figure 3:6: Casting of Fresh Concrete</i>	51
<i>Figure 3:7: Finished Concrete Deck</i>	51
<i>Figure 3:8: Test Fit of Two Precast Modules at Fabrication Yard</i>	52
<i>Figure 3:9: Composite Module Delivered to Site</i>	53

<i>Figure 3:10: Placement of First Composite Module On-Site</i>	53
<i>Figure 3:11: Verification of Fit of Adjacent Modules on Site</i>	54
<i>Figure 3:12: Pouring of UHPC Along Longitudinal Joint</i>	54
<i>Figure 3:13: Diamond Grinder Used to Finish Deck On-Site</i>	55
<i>Figure 4:1: BDI Strain Transducer, Typical Application to Girder</i>	57
<i>Figure 4:2: BDI STS-WiFi Wireless 4-Channel Node</i>	58
<i>Figure 4:3: BDI STS-WiFi Mobile Base Station</i>	58
<i>Figure 4:4: Tandem Axle Dump Truck used for Live Load Test</i>	59
<i>Figure 4:5: Haenni Wheel Load Weigher Scale</i>	60
<i>Figure 4:6: Typical Mesh Discretization for Each Tub Girder</i>	62
<i>Figure 4:7: Nodal Distribution of Point Loads (Michaelson, 2010)</i>	63
<i>Figure 5:1: Gage Locations on Girders, Looking Upstation</i>	70
<i>Figure 5:2: Aerial Lift Supplied by Contractor</i>	70
<i>Figure 5:3: Centerline of Gages at Quarter Span, Looking Upstream</i>	71
<i>Figure 5:4: Typical Bottom Flange Gage Mounting Points, Looking Upstream</i>	72
<i>Figure 5:5: Typical Web Gage Mounting Points, Looking Downstream</i>	72
<i>Figure 5:6: Typical Tab Mounting to Steel Surface</i>	73
<i>Figure 5:7: Typical View of Gages Installed on Bottom Flange, Looking Downstream</i>	74
<i>Figure 5:8: Overview of Instrumentation, Looking Backstation</i>	74
<i>Figure 5:9: Nail placement in Foam Joint with Construction String Line Wrapped Taut</i>	75
<i>Figure 5:10: Parallel Longitudinal Delineations on Deck with Construction String Line</i>	76
<i>Figure 5:11: Transverse Mark Completed with Blue Crayon</i>	76
<i>Figure 5:12: Plan View of Panel Point Grid</i>	77
<i>Figure 5:13: Live Load Truck Placement, Looking Upstation</i>	78
<i>Figure 5:14: Typical Truck Pass Location</i>	79
<i>Figure 5:15: Truck Dimensions and Field Weight Measurements</i>	80
<i>Figure 6:1: Deflected Shape of Finite Element Model, Truck Run 1, Panel Point 5</i>	84
<i>Figure 6:2: Comparison Between Analytical and Experimental Live Load Distribution Factors for Single and Two Lane Loaded Conditions</i>	85
<i>Figure 6:3: Comparison of Field, FEA and AASHTO Live Load Distribution Factors, One Lane Loaded Truck Run 1</i>	87

<i>Figure 6:4: Comparison of Field, FEA, and AASHTO Live Load Distribution Factors, Two Lanes Loaded Truck Run 1 and 4.....</i>	<i>88</i>
<i>Figure 7:1: Flange Inclinations (Kelly, 2014)</i>	<i>90</i>
<i>Figure 7:2: Web Inclinations (Kelly, 2014).....</i>	<i>90</i>
<i>Figure 7:3: Tub Girder Modeled with Flange Tilt.....</i>	<i>91</i>
<i>Figure 7:4: Tub Girder Modeled with Girder Twist</i>	<i>91</i>
<i>Figure 7:5: Tub Girder Modeled with Web Out of Flatness</i>	<i>92</i>
<i>Figure 7:6: Multi-linear Stress-Strain Curve.....</i>	<i>93</i>
<i>Figure 7:7: Vertical Deflection at Midspan for Unbraced Girder and Kelly (2014).....</i>	<i>96</i>
<i>Figure 7:8: Internal Bracing Scenarios</i>	<i>97</i>
<i>Figure 7:9: External Bracing Scenarios.....</i>	<i>98</i>
<i>Figure 7:10: Lateral Displacement Comparison for Internal Bracing Scenarios</i>	<i>99</i>
<i>Figure 7:11: Lateral Displacement Comparison for Internal Bracing Scenarios</i>	<i>100</i>
<i>Figure 7:12: Lateral Displacement Comparison for External Bracing Scenarios</i>	<i>101</i>
<i>Figure 7:13: Vertical Displacement Comparison for External Bracing Scenarios</i>	<i>101</i>

CHAPTER 1: INTRODUCTION

1.1 BACKGROUND / OVERVIEW

The Short Span Steel Bridge Alliance (SSSBA) is a group of bridge and culvert industry leaders (including steel manufacturers, fabricators, service centers, coaters, researchers, and representatives of related associations and government organizations) who have joined together to provide educational information on the design and construction of short span steel bridges in installations up to 140'-0" in length. The idea of the modular press-brake-formed steel tub girder was developed by a technical working group within the SSSBA. Initial research and testing began in the fall of 2011. After extensive laboratory demonstrations, the first implementation was installed in Buchanan County, Iowa in 2016. Following successful performance, a second bridge was installed in Muskingum County, Ohio the following year. The third bridge to employ this technology and the first to use a precast reinforced concrete deck in conjunction with the press-brake-formed tub girders is West Virginia State Project No. S322-37-3.29 00 along State Route 37 near Ranger, West Virginia (referred to hereafter as the Fourteen Mile Bridge). The Fourteen Mile Bridge is also unique due to both a skew and significant superelevation present. After completion of the Fourteen Mile Bridge, researchers from Marshall University (MU) and West Virginia University (WVU) traveled to the bridge site to perform a live load field test.

Strain data was recorded during the live load field test and the experimental results were compared to results from a finite element model developed to validate field data. 2017 American Association of State Highway and Transportation Officials (AASHTO) Load and Resistance Factor Design (LRFD) Bridge Design Specifications (hereafter referred to as AASHTO LRFD specifications) were applied and live load distribution factors (LLDFs) were computed for experimental data, analytical data, and AASHTO LRFD specifications.

This report also includes efforts to examine the effectiveness of bracing configurations of the non-composite press-brake-formed tub girder. When combined with a cast-in-place reinforced concrete deck, the non-composite section must resist the full construction load of the fresh concrete. It is imperative geometric imperfections be considered in order to account for second order amplification effects.

1.2 PROJECT SCOPE & OBJECTIVES

The scope of this report was to evaluate the field performance of a modular press-brake-formed steel tub girder bridge topped with a precast reinforced concrete deck in Lincoln County, West Virginia. This study also served to determine what effect skew and superelevation may have on the distribution of live load to each girder. A live load field test was performed, a finite element model was developed to verify the recorded data, and the results were used to compute LLDFs. This report also includes an initial qualitative investigation into the torsional response of the non-composite press-brake-formed tub girder under construction loading. The following objectives were assessed:

- A discussion of previous work relating to the implementation and design of press-brake-formed tub girders
- A brief review of the sections of the current AASHTO LRFD specifications relevant to the design of press-brake-formed steel tub girders and LLDFs
- An overview of the design and construction of the Fourteen Mile Bridge, in addition to the accelerated bridge construction methods employed
- An explanation of the research methodology and the field test performed on the Fourteen Mile Bridge with a description of the procedures used for the field testing and the finite element analysis completed
- A summary of the results and conclusions after comparing the experimental data, analytical data, and values determined following the AASHTO LRFD specifications
- A brief qualitative evaluation of the non-composite behavior of steel press-brake-formed tub girders with different interior and exterior bracing configurations under construction loading

1.3 REPORT ORGANIZATION

The organization of this report is as follows:

- Chapter 2:
 - This chapter discusses previous work on cold-bent steel tub girders. Also, current AASHTO LRFD specifications for steel box girders are reviewed.
- Chapter 3:
 - This chapter documents the design and construction of the composite press-brake-formed tub girder modules along with the installation of the Fourteen Mile Bridge in Lincoln County, West Virginia.
- Chapter 4:
 - This chapter details research methods utilized in the evaluation of the Fourteen Mile Bridge and discussion of equipment used during the physical load testing.
- Chapter 5:
 - This chapter describes the structure instrumentation and testing procedures for the live load field test performed on the Fourteen Mile Bridge.
- Chapter 6:
 - This chapter discusses a qualitative assessment of the non-composite behavior of press-brake-formed tub girders when varying bracing systems are employed.
- Chapter 7:
 - This chapter compares the results of the field test to the finite element analysis. This includes a comparison of the LLDFs determined by the field data, analytical model, and AASHTO LRFD specifications.
- Chapter 8:
 - This chapter summarizes the findings of this study and provides recommendations for future work in this field of research.

CHAPTER 2: LITERATURE REVIEW

2.1 INTRODUCTION

This chapter begins with an overview of previous work on cold-bent steel tub girders for utilization in bridge applications. Additionally, a summary of research performed by WVU in the area of design and evaluation of press-brake-formed steel tub girders will be discussed. This chapter concludes with a review of articles relevant to the design of tub girder bridges from the current 2017 AASHTO LRFD specifications.

2.2 PREVIOUS APPLICATIONS OF COLD-BENT STEEL GIRDERS

Cold-bent steel has been used in a variety of ways in bridge girders for several decades. Recent initiatives have encouraged further innovation and research to standardize a system of cold-bent girders for use in short span bridge applications. This section reviews previous research on the use of cold-bent steel girders in bridge applications.

2.2.1 Prefabricated Press-Formed Steel T-Box Girder Bridge System (Taly & Gangarao, 1979)

Taly and Gangarao (1979) performed early development of cold formed steel box girder systems. Two alternatives were proposed in the research: 1) An all steel deck and box girder assembly, and 2) A steel box girder topped with a pre-cast, prestressed, concrete deck. The girders were comprised of grade A36 steel plate bent into a trapezoidal shape. Shear studs were welded to the plates embedded in the pre-cast concrete planks, and plates were welded to the top flanges of the box girder. This enabled composite action between the steel box and the concrete deck. Load transfer between adjacent girders was achieved through shear keys and weld ties (Figure 2.1) and filled with a nonshrink grout.

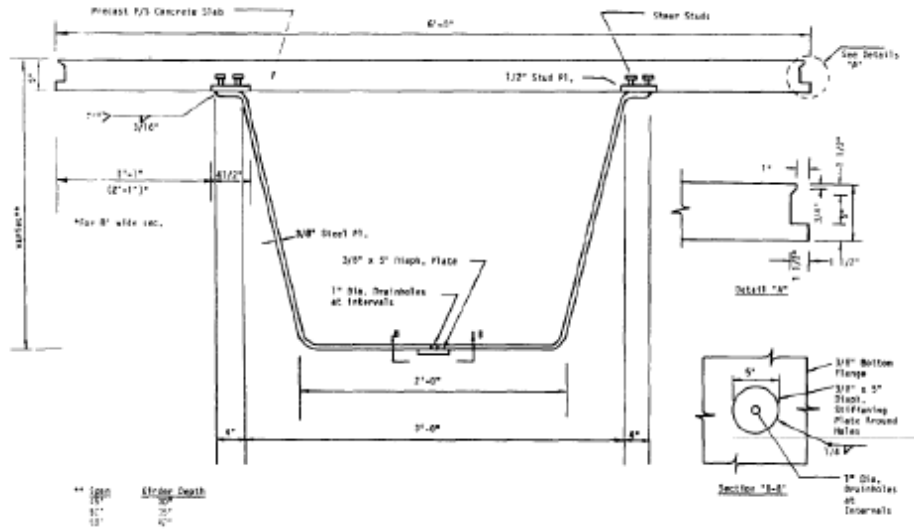


Figure 2:1: T-Box Girder System, Typical Girder Section with 5" Pre-cast, Prestressed Concrete Slab (Taly & Gangarao, 1979)

The box girders can be designed at a variety of depths to meet different span requirements, and the small size of each unit makes transportation to the site easier. Most fabrication for each unit can be completed offsite, greatly reducing the necessary time for construction on site. The low weight of the units requires less crane capacity and improves handling and erection characteristics.

2.2.2 Composite Girders with Cold Formed Steel U-sections (Nakamura, 2002)

Nakamura (2002) investigated the use of cold formed U-shape girders in continuous spans. The girders were cold formed from a single steel sheet, and a reinforced concrete slab was used for a deck (Figure 2.2). In the middle of the span where the positive bending moment was greatest, shear studs were welded to the top flange of the girder to allow composite action with the deck. Concern arose over the supports where the bridge was in negative bending, and the reinforced concrete deck was placed into tension. To prevent buckling, the U-section acted as a mold and was filled with reinforced concrete with prestressing bars. This increased dead load affected weight at the supports but did not affect the bending moment as the load was concentrated near the ends.

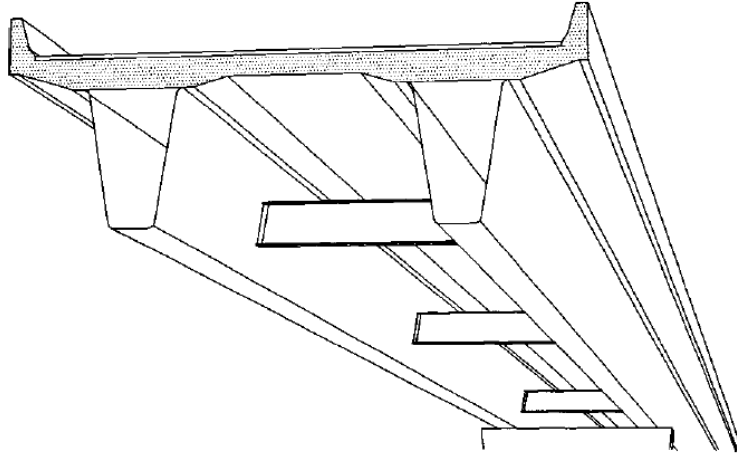


Figure 2:2: Nakamura's Proposed Bridge System (Nakamura, 2002)

Testing of the bending characteristics of this type of beam was performed on several specimens. The girder model performed similarly to typical composite beams on the positive bending sections, and the girder behaved as a prestressed beam near the supports in the regions of positive bending. It was also determined that the system was economical. Though a variety of materials were used to make each module, including structural steel, reinforced concrete, and prestressed concrete, savings from reduced fabrication improved the feasibility of the system.

2.2.3 Folded Plate Girders (Developed at the University of Nebraska)

Research performed at the University of Nebraska-Lincoln investigated rebar detailing between adjacent modules and non-composite behavior during construction of a trapezoidal, cold-bent plate box girder open at the bottom. Figure 2.3 presents an example cross section of the girder and a composite deck. The fabrication process to make each girder used readily available equipment and produced a consistent product in a limited amount of time. The inclusion of an open bottom improved the ease of inspection inside of the girder. Glaser (2010) determined the deformation under construction load was stable and the use of horizontal tie plates connected to each bottom flange serve to maintain the shape of the girder. Burner (2010) investigated the detailing of the reinforcement in the closure pour region and found that in addition to being resistant to fatigue, the hooked bar was more cost effective than the headed bar.

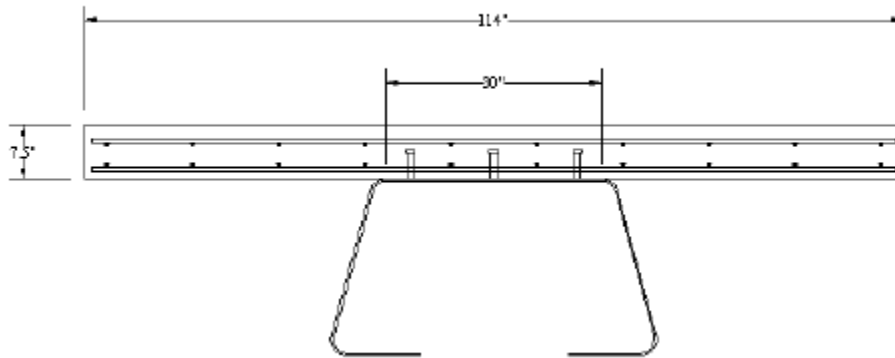


Figure 2:3: *Folded Plate Girder and Composite Deck Cross Section (Burner, 2010)*

2.2.4 Texas Department of Transportation Rapid Economical Bridge Replacement

The Texas Department of Transportation developed a standardized bridge system employing box girders as part of a large-scale corridor improvement of Interstate 35. FM 3267 was one of the bridges determined to be replaced (Chandar et al., 2010). To enable bridge replacements of large spans without creating height restrictions, shallow box girders were chosen due to the member's structural efficiency. Because of the lightweight nature of box girders, no bent caps were required for the pier columns, which helped maintain the original elevation of the bridge. The box girders were used in conjunction with a cast-in-place reinforced concrete deck. The design for each girder was standardized to reduced design and fabrications costs. As shown in Figure 2.4, the box girders were made up of several sizes of plate welded together to form a modular unit.

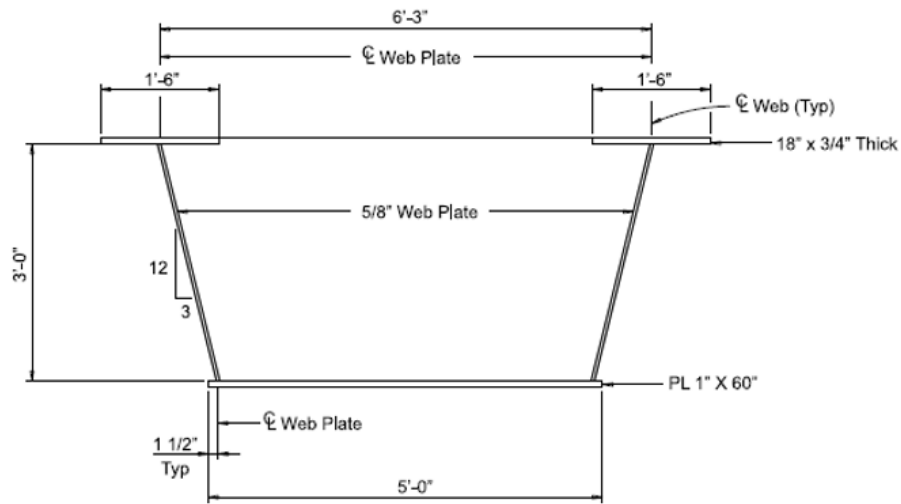


Figure 2:4: Cross Section of Box Girder from Bridge FM 3267 (Chandar et al., 2010)

2.3 PREVIOUS RESEARCH AT WVU ON PRESS-BRAKE-FORMED STEEL TUB GIRDERS

Research on press-brake-formed tub girders at WVU began in 2011 after researchers collaborated with the SSSBA to develop the modular cold formed box girder. This section describes the previous research performed at WVU concerning press-brake-formed tub girders.

2.3.1 Development and Feasibility Assessment of Shallow Press-Brake-Formed Steel Tub Girders for Short-Span Bridge Applications (Michaelson 2014)

Initial research at WVU on press-brake-formed tub girders was performed by Michaelson (2014) and the focus was to expand and refine the development of the modular notion from the SSSBA. The original concept included a cold-formed tub girder made composite with a precast deck. Each modular unit could be transported by truck to the bridge site to allow for accelerated bridge construction (ABC). In order to keep the system economical, an emphasis would be placed on utilizing plate sizes commonly available from mills.

To first grasp an understanding of the behavior of the shallow press-brake-formed tub girder, section properties were determined, and an iterative routine was developed in Microsoft

Excel and MATLAB. Several variables, such as web slope, bend radii, and top flange width, were kept constant across all the configurations to better compare the effect of varying plate width and thickness. Initial designs considered six standard plate widths (60", 72", 84", 96", 108", 120") and three standard thicknesses (7/16", 1/2", 5/8"). Yield moments were calculated for each plate width and plotted as a function of depth of the unit to determine the optimal cross section for each configuration (Figure 2.5).

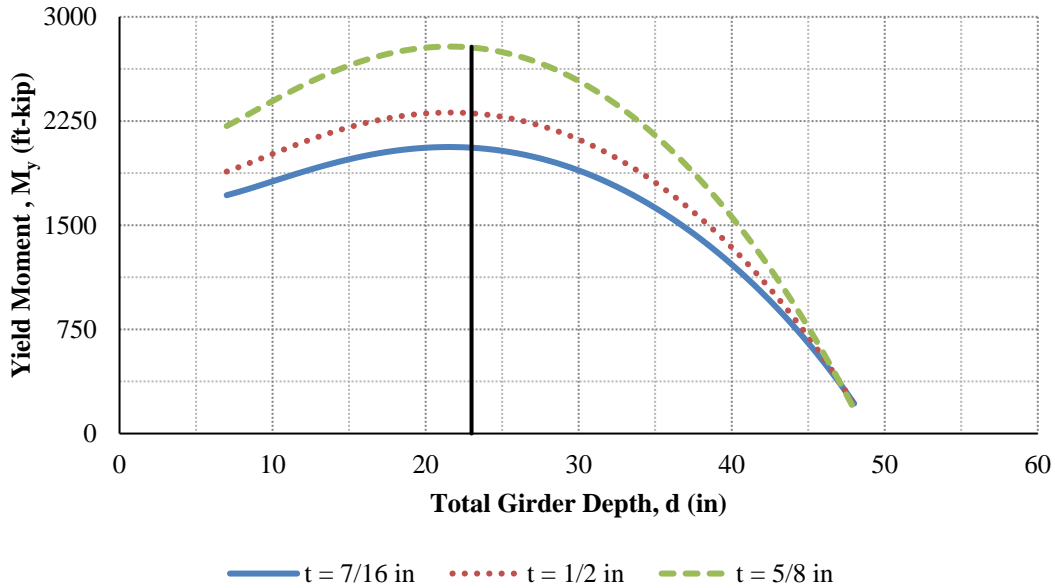


Figure 2.5: Design Comparison of 84" Wide Standard Mill Plate (Michaelson, 2014)

Once a methodology was selected for determining the geometry of the cross-section, experimental flexural testing was performed to assess composite and non-composite behavior. Four specimens were fabricated, each from 84" x 7/16" x 480" plate. To test the girders to failure, a deck thickness less than the AASHTO minimum 8" was employed. Experiments one and two used HPS-50 steel with a composite cast-in-place deck (Figure 2.6), while experiments three and four used HPS-50W weathering steel and HPS-50 steel hot-dip galvanized as a surface treatment, respectively.

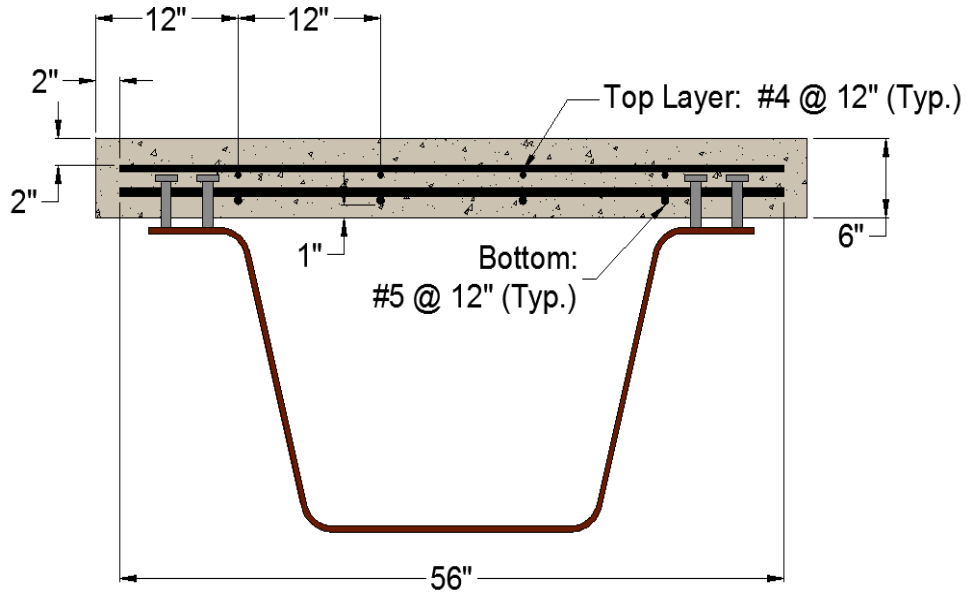


Figure 2:6: Typical Section, Composite Test Specimen (Michaelson, 2014)

Load was applied at the midspan of each specimen with a servo-hydraulic actuator and spreader beam and the displacement was increased in 0.05” increments until the specimen had reached failure. The composite specimens failed in ductility at approximately 304 kips (Figure 2.7). The non-composite specimens failed due to excessive lateral deflection and twist at relatively low-level loads as seen in Figure 2.8. This is not a significant issue as the intent of the system is to be topped with a precast deck.



Figure 2:7: Typical Ductile Failure of Composite Girder Section (Michaelson, 2014)



Figure 2:8: Typical Lateral Failure of Non-Composite Girder Section (Michaelson, 2014)

To verify the experimental testing, finite element models were developed and benchmarked against previous laboratory results. To fully capture the non-composite behavior, the model was adapted to consider second order effects due to geometric imperfections and residual stresses. A strain-compatibility approach was developed to assess each girder's capacity. The model was simulated for each experiment and little discrepancy existed between the experimental and analytical data (Figure 2.9).

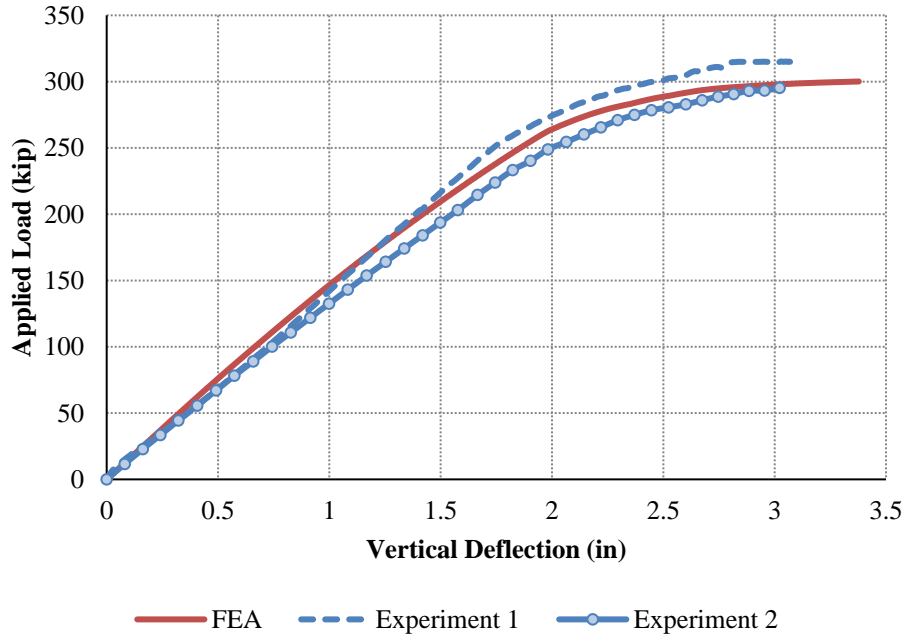


Figure 2:9: Comparison of Analytical and Experimental Results (Michaelson, 2014)

After the experimental results were verified against the analytical model, behavioral studies were performed to determine the applicability of the AASHTO LRFD specifications. Each girder configuration met the requirements to be considered as a box girder, and several of the configurations were determined to be compact. Comparisons were made to the analytical and experimental data, and it was determined the AASHTO LRFD specifications were conservative for calculating the nominal capacity of the section, and an equation that better fit data for nominal capacity was proposed.

A feasibility assessment was performed to determine if the proposed system could be economically competitive. In order to simplify the data set of possible configurations, plate widths outside the current industry standards were removed as options. The maximum span for each plate size was calculated and configurations not produced at that length were removed from the data set. Four standardized plate sizes were selected from this reduced plate matrix to be used in spans up to 80'-0" in length; however, the system was most competitive in spans up to 60'-0" in length. It should be noted that in the design of the system, a LLDF was assumed to be 1.0, so further work is necessary to accurately determine live load distribution.

2.3.2 Experimental Evaluation of Non-Composite Shallow Press-Brake-Formed Steel Tub Girders (Kelly, 2014)

In collaboration with Michaelson, Kelly (2014) furthered research efforts of stability and torsional behavior of non-composite press-brake-formed tub girders to determine the feasibility of a cast-in-place deck. The non-composite state is critical to understand as the girder must be able to withstand the full construction load, including wet concrete. To assess this condition, destructive flexural testing was performed, and a finite element model was developed.

Two specimens were tested in the laboratory using a servo-hydraulic actuator. The first specimen was fabricated from 84" x 7/16" HPS-50W weathering steel plate with a WT section bolted to the top flanges at midspan. Load was transferred to the WT section by a spreader beam and elastomeric pad. Elastic failure occurred at the critical load of 94 kips with a measured 2.25" of vertical deflection. The second specimen was fabricated from 84" x 7/16" HPS-50 plate but was hot-dip galvanized as a method of corrosion resistance. Unlike the first specimen, a noticeable initial twist due to fabrication was present and varied along the span of the girder as seen in Figure 2.10. Under flexural testing, the galvanized girder experienced lateral torsional buckling at a load of 33 kips and 0.73" of vertical deflection.

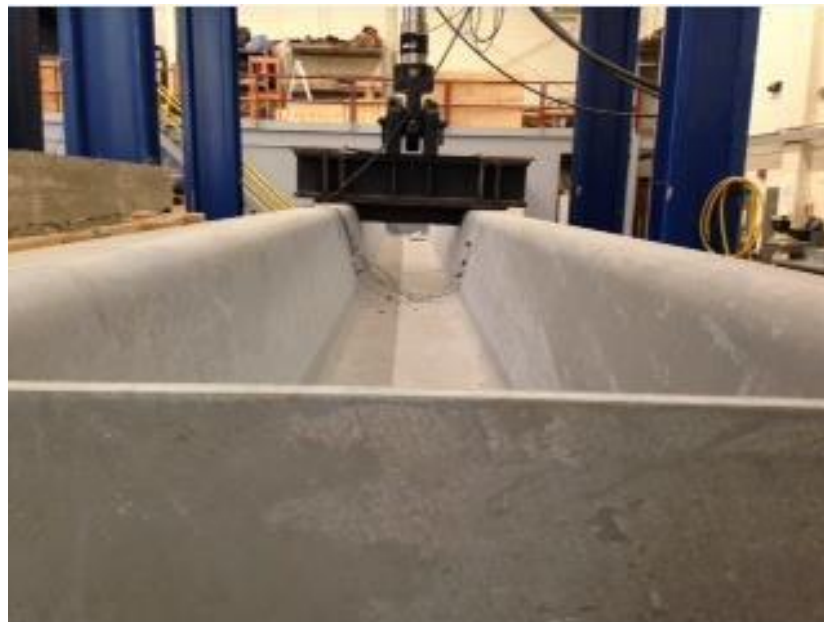


Figure 2:10: Initial Twist of Specimen #2 (Kelly, 2014)

A finite element model was developed to replicate the laboratory testing, and the results were compared to the measured experimental values as seen in Figure 2.11. The weathering steel specimen behaved nearly identical to the finite element model under the loading, while the galvanized specimen behaved similarly, until it reached the critical load of much less than the predicted value. This premature failure was largely attributed to second order effects due to the original deformity. To improve torsional stability under construction loads, it was recommended stay-in-place formwork be installed to each girder prior to erection.

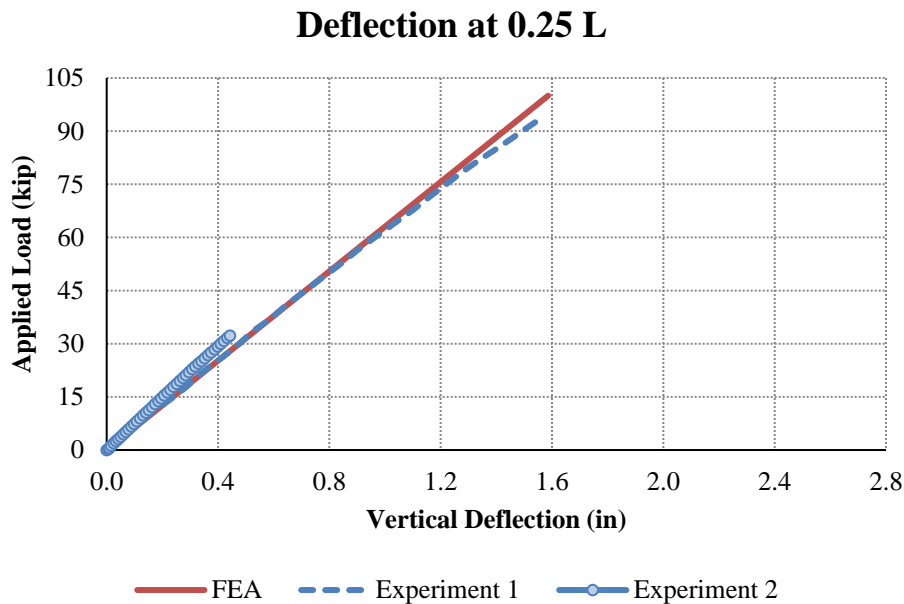


Figure 2:11: Deflection at Quarter Points (Kelly, 2014)

2.3.3 Evaluation of Modular Press-Brake-Formed Tub Girders with UHPC Joints (Kozhokin, 2016)

Research was extended by Kozhokin (2016) to evaluate the applicability of the press-brake-formed tub girder as a modular bridge component and the performance of joints between such modules. Following research from the Federal Highway Administration, ultra-high-performance concrete (UHPC) was chosen to be used for the closure pour between adjacent modules to develop durable connections. UHPC is a steel fiber reinforced Portland cement-based product with advantageous fresh and hardened properties. To ensure proper bonding between the

concrete deck and the UHPC joint, an exposed aggregate finish would be required. Techniques were assessed on sample slabs. The best results were produced by the application of a retarder to the shear key formwork and removal of the concrete paste using a wire brush (Figure 2.12).



Figure 2.12: Exposed Aggregate Finish of Shear Key Detail (Kozhokin, 2016)

After the appropriate approach was determined to produce the desired shear key detail, two full-scale modules were constructed to physically test the UHPC joint. Once the joint had cured, testing was performed by a servo-hydraulic actuator placed at midspan of one specimen along the girder's centerline. A steel plate replicating the contact area of a truck tire was attached to the actuator, and an elastomeric pad was placed between the deck and the steel plate. Loading was accomplished by the application of a Fatigue I moment due to a cyclic load of 67.43 kips over 2.8 million cycles and a Service II moment due to a static load of 90.78 kips applied at 10 predetermined cycle intervals. After approximately 1.6 million cycles, the concrete deck failed from punching shear. The actuator was moved to the adjacent, undamaged girder to continue testing. Subsequent testing found the UHPC joint satisfactorily transferred stress from the directly loaded girder to the indirectly loaded girder. Distribution factors were calculated, and a summary of the values are presented in Table 2.1.

Table 2.1: Summary of Distribution Factors (Kozhokin, 2016)

Average Distribution Factor		
Cycle Count	Directly Loaded Girder	Indirectly Loaded Girder
0	0.691	0.309
100,000	0.631	0.369
250,000	0.676	0.324
500,000	0.678	0.322
1,000,000	0.690	0.310
1,500,000	0.717	0.283
2,000,000	0.707	0.293
2,100,000	0.708	0.292
2,200,000	0.707	0.293
2,300,000	0.706	0.294
2,500,000	0.711	0.289
2,700,000	0.712	0.288
2,800,000	0.743	0.257

2.3.4 Field Performance Assessment of Press-Brake-Formed Steel Tub Girder Superstructures (Gibbs, 2017)

The first bridge to utilize the press-brake-formed tub girder concept developed by the SSSBA was installed in Buchanan County, Iowa in 2015. The bridge superstructure consisted of four tub girders constructed from 96” x 1/2” hot-dip galvanized plate. Unlike the original concept, this implementation employed the erection of non-composite girders topped with an 8 1/2” cast-

in-place deck and diaphragms between each girder to support the construction load. To further reduce the amount of time related to construction, Geosynthetic Reinforced Soil abutments were used. An overall view of the completed bridge is seen in Figure 2.13.



Figure 2:13: New Amish Sawmill Bridge (Gibbs, 2017)

Gibbs (2017), along with other researchers from WVU and MU, performed live load testing on site to further develop analytical models and verify AASHTO LRFD specifications could safely be used to design press-brake-formed tub girders. Upon arrival at the site, the girders were instrumented with Bridge Diagnostics, Inc. equipment to measure the strain in each of the girder's bottom flanges. A tandem-axle truck was positioned across the structure at various panel points, and the strain readings at each location were recorded. This strain data was used to calculate bottom flange bending stresses and LLDFs for single lane loaded and multiple lanes loaded conditions. A finite element model was developed, and LLDFs were calculated per AASHTO LRFD specifications; the LLDFs from all three methods were compared as seen in Figure 2.14. It should be noted, the stresses determined in the bottom flange by the finite element model were greater than those of the field testing. This was attributed to a difference in the boundary conditions as the

bridge was constructed with integral abutments, while the finite element model assumed simply supported boundary conditions. However, the LLDF's were similar to the experimental values. The experimental and finite element analysis (FEA) values were both significantly lower than those from AASHTO. Therefore, the AASHTO LRFD specifications were determined to be conservative in design applications for press-brake-formed tub girders.

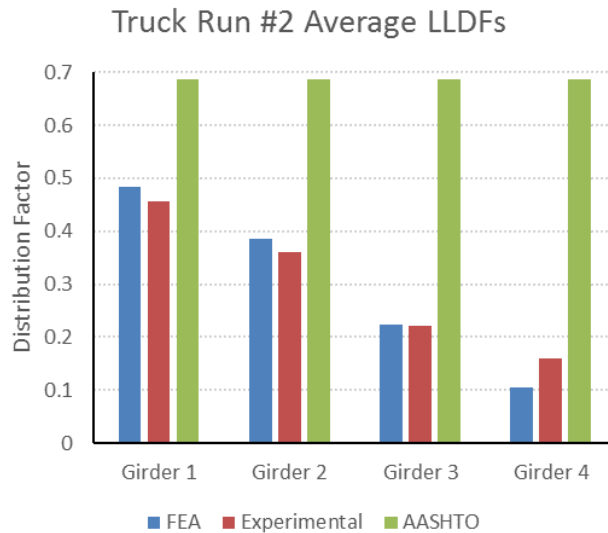


Figure 2:14: FEA v. Experimental v. AASHTO LLDFs (Gibbs, 2017)

2.3.5 Fatigue Performance of Uncoated and Galvanized Composite Press-Brake-Formed Tub Girders (Tennant, 2018)

Galvanic surface treatments are an effective means to provide corrosion resistance to steel members, but industry concern had arisen with the fatigue performance over the reheating of cold-formed members. Tennant (2018) examined the performance of two specimens with varying surface treatments; both girders were produced using ASTM A709 steel, but one was left uncoated (Figure 2.15), and the other was coated with a galvanic surface treatment (Figure 2.16). The composite system was fatigue loaded simulating a 75-year life in a rural environment. At a predetermined number of load cycles, a Service II load was applied to the system to observe the performance of the specimen. A combination of linear variable displacement transducers and strain gages were used to measure deflections that could be compared for each service loading interval.



Figure 2:15: Uncoated Steel Girder Under Fatigue Loading (Tennant, 2018)



Figure 2:16: Galvanized Steel Girder (Tennant, 2018)

A 6” thick concrete deck was cast-in-place for each girder to become composite. Compressive testing of cylinder samples taken from casting reflected the deck on the galvanized girder had significantly lower compressive strength than the deck on the uncoated girder. To confirm precision, loads applied by the servo-hydraulic actuator were compared to loads calculated from the measured strain data, and the differences were small. The project concluded the heat of galvanization had no adverse effect on the fatigue performance of a press-brake-formed tub girder.

2.3.6 Field Performance and Rating Evaluation of a Modular Press-Brake-Formed Steel Tub Girder with a Steel Sandwich Plate Deck (Underwood, 2019)

The Cannelville Road Bridge in Muskingum County, Ohio was the second bridge built utilizing press-brake-formed tub girders. The bridge was composed of two modular units each made up of two press-brake-formed tub girders attached to a sandwich plate steel (SPS®) deck with bolts. SPS® decks are a thin, lightweight option particularly useful in areas with limited hydraulic openings. The tub girders were fabricated from 5/8” thick plate and were braced at various locations internally and externally. The entire unit was hot-dip galvanized to provide corrosion resistance. Figure 2.17 shows one of the modular units on site. Erection of most of the superstructure was placed in approximately 20 minutes, and the entire project used only 26 of the allotted 30 days from demolition of the old bridge to carrying traffic on the new bridge.



Figure 2:17: Cannelville Road Bridge Modular Unit (Underwood, 2019)

Underwood (2019) worked with researchers at WVU and MU to perform live load testing of the bridge to assess the applicability of AASHTO LRFD specifications for press-brake-formed tub girders topped with a SPS® deck. The structure was instrumented with Bridge Diagnostics, Inc. equipment and a tandem axle load truck was placed at predetermined grid points. The bottom flange strains of each girder and the weight of each wheel on the load truck were recorded.

A finite element model was produced to make comparisons to the data collected in the field. LLDFs were calculated for the finite element model and the experimental data and the results were compared to LLDFs calculated per the AASHTO LRFD specifications as seen in Figure 2.18. Inventory and operating load ratings for interior and exterior girders were computed from field data and the analytical model. Live load ratings were compared to AASHTO serviceability and strength requirements. As in other tests, the data reflected that the AASHTO LRFD specifications tend to be conservative and underpredict the performance of the press-brake-formed tub girder system; therefore, the provisions used safely model press-brake-formed tub girders.

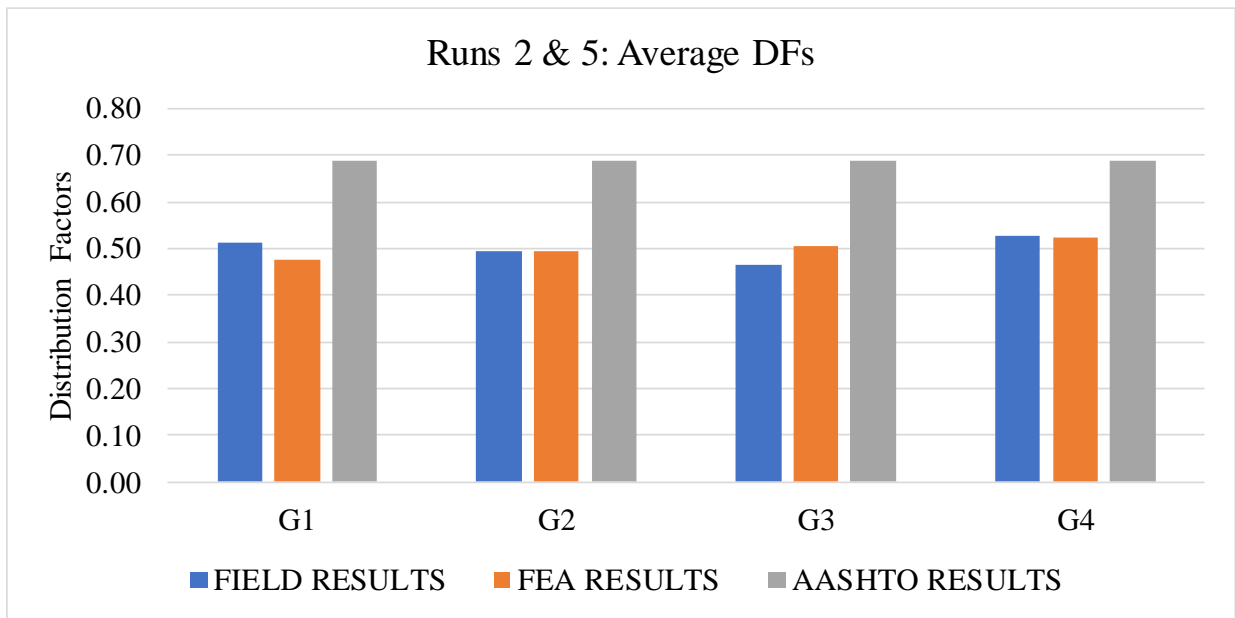


Figure 2:18: Field v. FEA v. AASHTO LLDFs (Underwood, 2019)

2.4 CURRENT AASHTO SPECIFICATIONS FOR TUB GIRDER DESIGN AND APPLICATION

AASHTO is the governing body regulated the practice of roadway design. AASHTO's presence extends into the design and analysis of bridge structures with the LRFD Bridge Design Specifications, a code manual that is updated approximately every three years based on improvements in behavioral understandings and to improve safety of the traveling public. Design under the LRFD philosophy accounts for varying levels of loadings that may be applied to structures and the varying capacity that members may have based on sound statistical evidence. The current AASHTO LRFD Bridge Design Specifications (hereafter referred to as AASHTO LRFD specifications), is the 8th edition which was published in September 2017. This section summarizes the relevant portions of the code related to the design of the Fourteen Mile Bridge.

2.4.1 Multiple Presence Factors

Multiple presence factors are empirical values used to investigate the extreme live load force effect by considering the probability of simultaneous lane occupation by the HL-93 design live load. Each design lane is defined to be 12'-0" in width or lesser if the traffic lanes are less than 12'-0". When calculating distribution factors per Articles 4.6.2.2 and 4.6.2.3, the appropriate multiple presence factor has already been included in the expressions and need not be taken into consideration. The values are based on an average daily truck traffic of 5,000 trucks in a single direction. Table 2.2 presents the multiple presence factors from the AASHTO LRFD specifications for each scenario of the number of lanes loaded. Multiple presence factors shall not be considered for the fatigue limit state where only a single design truck is applied.

Table 2.2: Multiple Presence Factors (AASHTO, 2017)

Number of Loaded Lanes	Multiple Presence Factors, m
1	1.20
2	1.00
3	0.85
>3	0.65

2.4.2 Beam-Slab Bridges – Live Load Distribution Factors

Provisions for calculated LLDFs in Article 4.6.2.2 require the cross-sections of bridges containing multiple boxes meet geometric criteria in Article 6.11.2.3. These specifications require the top flanges of adjacent girders must be at least 80% and not more than 120% of the top flange spacing of one of the girders. These distances are represented by a and w , respectively, in Figure 2.19. In addition, the inclination of web plate to the plane normal to the bottom flange shall be limited to 1 to 4. The provisions of Article 4.6.2.2 are only applicable in situations where the bearing lines are not skewed; in cases of skew at the supports, a more refined structural analysis must occur. Cantilevered overhang of the concrete deck including the curb and parapet is limited to either 60 percent of the interior spacing of the center of top flanges, w , or 6'-0".

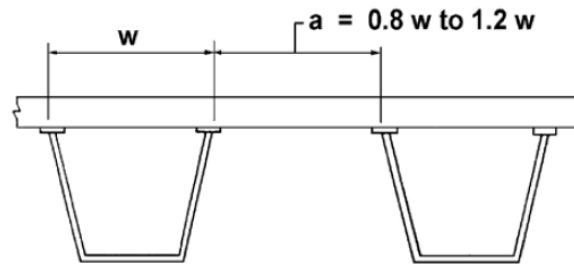


Figure 2:19: Center-to-Center Flange Distance (AASHTO, 2017)

If the cross-section of a bridge constructed from multiple boxes meets these criteria, Article 4.6.2.2 may be used to calculate the LLDFs. Article 4.6.2.2 refers to use of Table 4.6.2.2b-1 for multiple steel box girders with a concrete deck; the appropriate cross section is matched to the list provided in Table 4.6.2.2.1-1. For bridges constructed of multiple steel box girders topped with a concrete deck, only one equation for determining the LLDFs, regardless of the number of lanes loaded. The applicable expression is listed as Equation 2-1 and is valid for moment and shear in interior beams. Table 4.6.2.2d-1 specifies that Equation 2-1 may also be used for calculation of LLDFs in exterior beams. Multiple presence factors are already incorporated into the expression for the calculation of distribution factors by approximate means.

$$LLDF_{INT} = 0.05 + 0.85 \left(\frac{N_L}{N_b} \right) + \frac{0.425}{N_L} \quad \text{Equation 2-1}$$

$$\text{Where: } 0.5 \leq \frac{N_L}{N_b} \leq 1.5$$

N_L = number of design lanes

N_b = number of girders

2.4.3 Box-Section Flexural Members

This section details the relevant limit states and capacity requirements that must be checked in the design of box-section flexural members.

2.4.3.1 Cross Section Proportion Limits

Webs may be either vertical or inclined; the inclination of the web plates to the plane perpendicular to the bottom flange shall be limited to 1 to 4. In addition, the criteria of Equation 2-2 and Equation 2-3 must be met regarding web proportions.

For webs without longitudinal stiffeners:

$$\frac{D}{t_w} \leq 150 \quad \text{Equation 2-2}$$

For webs with longitudinal stiffeners:

$$\frac{D}{t_w} \leq 300 \quad \text{Equation 2-2}$$

Where: D = web depth (in)

t_w = web thickness (in)

Top flanges of tub sections shall meet the criteria specified in Equation 2-4, Equation 2-5, and Equation 2-6, regardless if the flange section is subjected to compression or tension.

$$\frac{b_f}{2t_f} \leq 12.0 \quad \text{Equation 2-4}$$

$$b_f \leq D/6 \quad \text{Equation 2-5}$$

$$t_f \geq 1.1t_w \quad \text{Equation 2-6}$$

Where: b_f = flange width (in)

t_f = flange thickness (in)

D = web depth measure along inclination (in)

t_w = web thickness (in)

2.4.3.2 Constructability

To ensure the geometry of the box section is maintained during construction, the section must be checked in various states to verify adequate capacity. Through investigation, it may be determined additional internal and/or external cross-frames may be temporarily required during construction or as a permanent fixture to support possible eccentric loads. Load factors for construction are taken from Article 3.4.2. Article 6.11.3 specifies the provisions of Article 6.10.3 are to be applied unless otherwise stated.

For sections in flexure, Articles 6.10.3.2.1 through 6.10.3.2.3 shall be applied to only the top flanges of tub sections. Equations 2-8, 2-10, and 2-11 shall be checked as applicable. The unbraced length is defined as the distance between interior cross-frames or diaphragms. Equation 2-9 shall not be checked in cases of either compact or noncompact webs and when $f_l = 0$. If the section contains a slender web, Equation 2-7 shall not be checked. The provisions specify non-composite sections with slender webs and flanges in compression shall also satisfy Equation 2-9.

For discretely braced flanges in compression:

$$f_{bu} + f_l \leq \phi_f R_h F_{yc} \quad \text{Equation 2-7}$$

$$f_{bu} + \frac{1}{3}f_l \leq \phi_f F_{nc} \quad \text{Equation 2-8}$$

$$f_{bu} \leq \phi_f F_{crw} \quad \text{Equation 2-9}$$

Where: ϕ_f = resistance factor for flexure specified in Article 6.5.4.2

f_{bu} = flange stress calculated without consideration of flange lateral bending determined as specified in Article 6.10.1.6 (ksi)

f_l = flange lateral bending stress determined as specified in Article 6.10.1.6 (ksi)

F_{crw} = nominal bend-buckling resistance for webs specified in Article 6.10.1.6 (ksi)

F_{nc} = nominal flexural resistance of the flange as specified in Article 6.10.8.2 (ksi), with the web load-shedding factor, R_b , taken as 1.0 for constructability

R_h = hybrid factor as specified in Article 6.10.1.10.1, $R_h = 1.0$ when f_{bu} does not exceed the specified yield strength of the web

F_{yc} = specified minimum yield strength of compression flange (ksi)

For discretely braced flanges in tension:

$$f_{bu} + f_l \leq \phi_f R_h F_{yt} \quad \text{Equation 2-10}$$

Where: F_{yt} = specified minimum yield strength of tension flange (ksi)

For continuously braced flanges in compression or tension:

$$f_{bu} \leq \phi_f R_h F_{yf} \quad \text{Equation 2-11}$$

Where: F_{yf} = specified minimum yield strength of flange (ksi)

For critical stages of construction, non-composite box flanges in compression must meet the criteria specified in Equation 2-12 and Equation 2-13.

$$f_{bu} \leq \phi_f F_{nc} \quad \text{Equation 2-12}$$

$$f_{bu} \leq \phi_f F_{crw} \quad \text{Equation 2-13}$$

For critical stages of construction, non-composite box flanges in tension and continuously braced box flanges in compression or tension must meet the criteria specified in Equation 2-14.

$$f_{bu} \leq \phi_f R_h F_{yf} \Delta \quad \text{Equation 2-14}$$

$$\text{Where: } \Delta = \sqrt{1 - 3 \left(\frac{f_v}{F_{yf}} \right)^2} \quad \text{Equation 2-15}$$

$$f_v = \frac{T}{2A_o t_f} \quad \text{Equation 2-16}$$

f_v = St. Venant torsional shear stress in the flange due to the factored loads at the section under consideration (ksi)

T = internal torque due to the factored loads (kip-in)

A_o = enclosed area within box section (in²)

Requirements for shear strength during critical stages of construction are extended from the beam-slab provisions. Sections must meet the requirements of Article 6.10.3.3 in addition to Article 6.11.9 if applicable. Equation 2-17 specifies the requirements for webs of box sections.

$$V_u \leq \phi_v V_{cr} \quad \text{Equation 2-17}$$

Where: ϕ_v = resistance factor for shear as specified in Article 6.5.4.2

V_u = shear in the web at the section under consideration due to the factored permanent loads and factored construction loads applied to the non-composite section (kips)

V_{cr} = shear-yielding or shear buckling resistance per Article 6.10.9.3.3 (kip)

For inclined webs:

$$V_{ui} = \frac{V_u}{\cos(\theta)} \quad \text{Equation 2-18}$$

Where: V_{ui} = vertical shear due to factored loads along an inclined web (kip)

θ = angle of inclination of the web plate to vertical (degrees)

2.4.3.3 Service Limit State

Service limit states are employed to control deflection under typical live loads. Limited deflection not only provides user comfort, but it ensures adequate performance of bearings, joints, and other critical features of the bridge structure. Box sections must meet the provisions of Article 6.10.4, except in Equation 2-20, f_i shall be taken as zero, and Equation 2-21 shall not apply.

Elastic deformation limits are specified in Article 2.5.2.6, and when applying the relevant criteria, the vehicular live load taken from Article 3.6.1.3.2 shall include the dynamic load allowance, IM per Table 3.4.1-1. The provisions specify all design lanes should be loaded, and all components can be assumed to deflect uniformly. In cases where a bridge is skewed, a right cross section may be employed. The following deflection limit is to be considered for steel bridges:

- Vehicular load, general Span/800,
- Vehicular and pedestrian loads Span/1,000,
- Vehicular load on cantilever arms..... Span/300, and
- Vehicular and pedestrian loads on cantilever arms
Span/375.

Figure 2:20 Live Load Deflection Limits (AASHTO, 2017)

Permanent deformations are governed by Article 6.10.4.2, and Service II load combinations per Table 3.4.1-1 shall apply. The criteria specified by Equations 2-19, 2-20, and 2-21 shall be met for flanges in flexure.

Top steel flange, composite sections

$$f_f \leq 0.95R_h F_{yf} \qquad \text{Equation 2-19}$$

Bottom steel flange, composite sections

$$f_f + \frac{f_l}{2} \leq 0.95R_h F_{yf} \quad \text{Equation 2-20}$$

Both steel flanges, non-composite sections

$$f_f + \frac{f_l}{2} \leq 0.80R_h F_{yf} \quad \text{Equation 2-21}$$

Where: f_f = flange stress at the section under consideration due to the Service II loads calculated without consideration of flange lateral bending (ksi)

f_l = flange lateral bending stress at the section under consideration due to the Service II loads determined as specific in Article 6.10.1.6 (ksi)

R_h = hybrid factor as specified in Article 6.10.1.10.1

In addition to flange stress criteria, limits also apply to the web of the composite section. Except for sections in positive flexure in which the web satisfies Article 6.11.2.1.2, all sections shall satisfy Equation 2-22.

$$f_c \leq F_{crw} \quad \text{Equation 2-22}$$

Where: f_c = compression flanges stress at section under consideration due to Service II loads calculated without consideration of flange lateral bending (ksi)

F_{crw} = nominal bend-buckling resistance for webs with or without longitudinal stiffeners, as applicable, determined as specified in Article 6.10.1.9 (ksi)

2.4.3.4 Fatigue and Fracture Limit State

Fatigue limits shall be considered to ensure cracks in steel members due to cyclic loading are limited and do not propagate. Article 6.10.5 specifies the general provisions that must be met, while Article 6.11.10 specifies criteria for shear connectors. In cases where the cross section of a bridge with multiple straight box girders does not meet the requirements of Article 6.11.2.3, longitudinal warping stress and transverse bending stress due to distortion shall be considered. Connection details shall be investigated per the specifications in Article 6.6.1 with the appropriate load combination for fatigue from Table 3.4.1-1.

Fatigue is separated into two categories, load-induced and distortion-induced. Load-induced fatigue is a result of the live load stresses present in members. In concrete deck casting scenarios, the long-term composite section shall be used when resisting dead loads, and the short-term composite section shall be used when resisting live loads. The provisions are only applicable to details with a net tensile stress; residual stresses are to be neglected in fatigue considerations.

For load-induced fatigue considerations, each detail shall satisfy:

$$\gamma(\Delta f) \leq (\Delta F)_n \quad \text{Equation 2-23}$$

Where: γ = load factor as specified in Table 3.4.1-1 for the fatigue load combination

(Δf) = force effect, live load stress range due to the passage of the fatigue load as specified in Article 3.6.1.4 (ksi)

$(\Delta F)_n$ = nominal fatigue resistance specified in Article 6.6.1.2.5 (ksi)

For the Fatigue I load combination (infinite life), nominal fatigue resistance is computed as shown in Equation 2-24:

$$(\Delta F)_n = (\Delta F)_{TH} \quad \text{Equation 2-24}$$

For the Fatigue II load combination (finite life), nominal fatigue resistance is computed as shown in Equation 2-25:

$$(\Delta F)_n = \left(\frac{A}{N}\right)^{\frac{1}{3}} \quad \text{Equation 2-25}$$

Where: $N = (365)(75)n(ADTT)_{SL}$ Equation 2-26

A = constant taken from table 6.6.1.2.5-1 (ksi³)

n = number of stress range cycles per truck passage taken from Table 6.6.1.2.5-2

(ADTT)_{SL} = single-lane ADTT as specified in Article 3.6.1.4

(ΔF)_{TH} = constant-amplitude fatigue threshold taken from Table 6.6.1.2.5-3 (ksi)

Distortion-induced fatigue limits are provided in Article 6.6.1.3. Load paths shall be sufficient to carry all intended and unintended forces provided by connecting transverse members to longitudinal members by either welding or bolting. Specifications are provided for transverse connection plates and lateral connection plates. In cases where the required load is unknown, the connection shall be designed to resist a 20.0 kip lateral load for straight bridges with no skew.

Fracture requirements are specified in Article 6.6.2. Members and components shall follow Table 6.6.2.1-1 to be classified as either primary or secondary. Primary members or components subject to a net tensile stress under the Strength I load combination shall be designated on the contract plans. All primary members and any members or components subject to net tensile stress under Strength I load combination shall require the performance of Charpy V-notch testing.

2.4.3.5 Strength Limit State

The strength limit state is employed to ensure the structure has adequate capacity to resist moments and shears generated during loading. Article 6.11.6 specifies the provisions that must be met. Applicable load combinations are taken from Table 3.4.1-1.

2.4.3.5.1 General Flexure Requirements

In box sections with holes in the tension flange at the section under consideration, the tension flange shall satisfy provisions of Article 6.10.1.8 and Equation 2-27.

$$f_t \leq 0.84 \left(\frac{A_n}{A_g} \right) F_u \leq F_{yt} \quad \text{Equation 2-27}$$

Where: A_n = net area of the tension flange determined as specified in Article 6.8.3 (in²)

A_g = gross area of the tension flange (in²)

f_t = stress on the gross area of the tension flange due to the factored loads calculated without consideration of flange lateral bending (ksi)

F_u = specified minimum tensile strength of the tension flange determines as specified in Table 6.4.1-1 (ksi)

Sections in straight bridges in positive flexure must meet the following criteria to be considered compact:

- The specified minimum yield strengths of flanges and web do not exceed 70.0 ksi
- The web satisfies the requirement of Article 6.11.2.1.2
- The section under consideration is part of a bridge that satisfies Article 6.11.2.3
- The box flange is fully effective as specified in Article 6.11.1.1
- The section satisfies the requirements of Article 6.11.7.1
- The section satisfies the web slenderness limit of Equation 2-28:

$$\frac{2D_{cp}}{t_w} \leq 3.76 \sqrt{\frac{E}{F_{yc}}} \quad \text{Equation 2-28}$$

Where: D_{cp} = depth of the web in compression at the plastic moment determined as specified in Article D6.3.2 (in)

E = modulus of elasticity of steel (ksi)

If the section does not meet these criteria, it will be considered noncompact and must satisfy the requirements of Article 6.11.7.2. Both compact and noncompact sections must satisfy ductile requirements of Article 6.10.7-3 and Equation 2-29:

$$D_p \leq 0.42D_t \quad \text{Equation 2-29}$$

Where: D_p = distance from the top of the concrete deck to the neutral axis of the composite section (in)

D_t = total depth of the composite section (in)

2.4.3.5.2 Flexural Capacity of Composite Sections, Positive Flexure

For compact composite sections, Equation 2-30 shall be satisfied at the strength limit state. Lateral bending need not be considered in the compression flanges of the tub sections because the flanges are continuously supported by the concrete deck.

$$M_u \leq \phi_f M_n \quad \text{Equation 2-30}$$

Where: ϕ_f = resistance factor for flexure as specified in Article 6.5.4.2

M_n = nominal flexural resistance of the section determined as specified in Article 6.11.7.1.2 (kip-in)

M_u = bending moment about the major axis of the cross-section due to factored loads at the section under consideration (kip-in)

Nominal flexural resistance of a section shall be calculated using the applicable equations: Equation 2-31 or Equation 2-32.

If $D_p \leq 0.1D_t$:

$$M_n = M_p \quad \text{Equation 2-31}$$

Otherwise:

$$M_n = M_p \left(1.07 - 0.7 \frac{D_p}{D_t} \right) \quad \text{Equation 2-32}$$

Where: D_p = distance from the top of the concrete deck to the neutral axis of the composite section at the plastic moment (in)

D_t = total depth of the composite section (in)

M_p = plastic moment of the composite section as specified in Article D6.1 (kip-in)

It should be noted that Michaelson (2014) modelled several scenarios for the press-brake-formed tub girder and found Equation 2-32 from AASHTO did not accurately depict the nominal flexural resistance of the girders and was significantly conservative. The study recommended a similar expression with constants that better predicted capacity presented as Equation 2-33:

$$M_n = \begin{cases} M_p & D_p \leq 0.1D_t \\ M_p \left(1.0229 - 0.229 \frac{D_p}{D_t} \right) & 0.1D_t < D_p \leq 0.42D_t \end{cases} \quad \text{Equation 2-33}$$

In cases where a continuous span is employed, the nominal flexural resistance of the section shall satisfy Equation 2-34.

$$M_n \leq 1.3R_h M_y \quad \text{Equation 2-34}$$

Where: M_n = nominal flexural resistance calculated per Equation 2-31 and Equation 2-32 as applicable(kip-in)

M_y = yield moment as determined by Article D6.2 (kip-in)

R_h = hybrid factor as determined by Article 6.10.1.10.1

For noncompact composite sections, Equation 2-35 shall be satisfied for compression flanges at the strength limit state.

$$f_{bu} \leq \phi_f F_{nc} \quad \text{Equation 2-35}$$

Where: ϕ_f = resistance factor for flexure as specified in Article 6.5.4.2

f_{bu} = longitudinal flange stress at the section under consideration calculated without consideration of flange lateral bending or longitudinal warping as applicable (ksi)

F_{nc} = nominal flexural resistance of the compression flange determined as specified in Article 6.11.7.2.2 and Equation 2-36 (kip-in)

$$F_{nc} = R_b R_h F_{yc} \quad \text{Equation 2-36}$$

Where: R_b = web load-shedding factor determined as specified in Article 6.10.1.10.2

R_h = hybrid factor determined as specified in Article 6.10.1.10.1

Equation 2-37 shall be satisfied for compression flanges at the strength limit state.

$$f_{bu} \leq \phi_f F_{nt} \quad \text{Equation 2-37}$$

Where: F_{nt} = nominal flexural resistance of the tension flange determined as specified in Article 6.11.7.2.2 (kip-in)

$$F_{nt} = R_h F_{yt} \Delta \quad \text{Equation 2-38}$$

$$\text{Where: } \Delta = \sqrt{1 - 3 \left(\frac{f_v}{F_{yf}} \right)^2} \quad \text{Equation 2-39}$$

$$f_v = \frac{T}{2A_o t_f} \quad \text{Equation 2-40}$$

The maximum longitudinal compressive stress in the concrete deck at the strength limit state, determined as specified in Article 6.10.1.1.1d, shall not exceed $0.6f'_c$.

2.4.3.5.3 Flexural Capacity of Non-composite Sections

Compression flanges of box sections not made composite must satisfy Equation 2-41 at the strength limit state.

$$f_{bu} \leq \phi_f F_{nc} \quad \text{Equation 2-41}$$

Where: ϕ_f = resistance factor for flexure as specified in Article 6.5.4.2

f_{bu} = longitudinal flange stress due to the factored loads at the section under consideration calculated without consideration of longitudinal warping (ksi)

F_{nc} = nominal flexural resistance of the flange as specified in Article 6.11.8.2 (ksi)

Nominal flexural resistance is computed by the following equations when flange longitudinal stiffeners are not used:

$$F_{nc} = F_{cb} \sqrt{1 - \left(\frac{f_v}{\phi_v F_{cv}} \right)^2} \quad \text{Equation 2-42}$$

Where: F_{cb} = nominal axial compression buckling resistance of the flange under compression alone, calculated per Equation 2-43 through Equation 2-45 as applicable (ksi)

If $\lambda_f \leq \lambda_p$ then:

$$F_{cb} = R_b R_h F_{yc} \Delta \quad \text{Equation 2-43}$$

If $\lambda_p < \lambda_f \leq \lambda_r$ then:

$$F_{cb} = R_b R_h F_{yc} \left[\Delta - \left(\Delta - \frac{\Delta - 0.3}{R_h} \right) \left(\frac{\lambda_f - \lambda_p}{\lambda_r - \lambda_p} \right) \right] \quad \text{Equation 2-44}$$

If $\lambda_f > \lambda_r$ then:

$$F_{cb} = \frac{0.9 E R_b k}{\lambda_f^2} \quad \text{Equation 2-45}$$

Where: F_{cv} = nominal shear buckling resistance of the flange under shear alone and is determined by Equation 2-46 through Equation 2-48 as applicable

If $\lambda_f \leq 1.12 \sqrt{\frac{E k_s}{F_{yc}}}$, then:

$$F_{cv} = 0.58 F_{yc} \quad \text{Equation 2-46}$$

If $1.12 \sqrt{\frac{E k_s}{F_{yc}}} < \lambda_f \leq 1.40 \sqrt{\frac{E k_s}{F_{yc}}}$, then:

$$F_{cv} = \frac{0.65 \sqrt{F_{yc} E k_s}}{\lambda_f} \quad \text{Equation 2-47}$$

If $\lambda_f > 1.40 \sqrt{\frac{E k_s}{F_{yc}}}$, then:

$$F_{cv} = \frac{0.9 E k_s}{\lambda_f^2} \quad \text{Equation 2-48}$$

Where: λ_f = slenderness ratio of compression flange per Equation 2-49

$$\lambda_f = \frac{b_{fc}}{t_{fc}} \quad \text{Equation 2-49}$$

$$\lambda_p = 0.57 \sqrt{\frac{E k}{F_{yc} \Delta}} \quad \text{Equation 2-50}$$

$$\lambda_r = 0.95 \sqrt{\frac{Ek}{F_{yr}}} \quad \text{Equation 2-51}$$

$$\Delta = \sqrt{1 - 3 \left(\frac{f_v}{F_{yt}} \right)^2} \quad \text{Equation 2-52}$$

Where: f_v = St. Venant torsional shear stress in the flange due to the factored loads at the section under consideration per Equation 2-53 (ksi)

$$f_v = \frac{T}{2A_o t_f} \quad \text{Equation 2-53}$$

Where: F_{yr} = smaller of the compression-flange stress at the onset of nominal yielding, with consideration of residual stress effects, or the specified yield strength of the web determined per Equation 2-54 (ksi)

$$f_v = (\Delta - 0.3)F_{yc} \quad \text{Equation 2-54}$$

Where: k = plate-buckling coefficient for uniform normal stress = 4.0

k_s = plate-buckling coefficient for shear stress = 5.34

ϕ_f = resistance factor for flexure specified in Article 6.5.4.2

ϕ_v = resistance factor for shear specified in Article 6.5.4.2

b_{fc} = compression-flange width between webs (in)

A_o = enclosed area within the box section (in²)

R_b = web load-shedding factor determined as specified in Article 6.10.1.10.2

R_h = hybrid factor determined as specified in Article 6.10.1.10.1

T = internal torque due to the factored loads (kip-in)

The nominal flexural resistance of a longitudinally stiffened compression flange shall be calculated in the same manner as the compression flange when flange longitudinal stiffeners are not used with the following substitutions:

- w shall be substituted for b_{fc}
- the plate-buckling coefficient for uniform normal stress, k , shall be taken as:
 - If $n = 1$, then:

$$k = \left(\frac{8I_s}{wt^3_{fc}} \right)^{\frac{1}{3}} \quad \text{Equation 2-55}$$

- If $n = 2$, then:

$$k = \left(\frac{0.894I_s}{wt^3_{fc}} \right)^{\frac{1}{3}} \quad \text{Equation 2-56}$$

$$1.0 \leq k \leq 4.0$$

- the plate-buckling coefficient for shear stress, k_s , shall be taken per Equation 2-57:

$$k_s = \frac{5.34 + 2.84 \left(\frac{I_s}{wt^3_{fc}} \right)^{\frac{1}{3}}}{(n + 1)^2} \leq 5.34 \quad \text{Equation 2-57}$$

Where: I_s = moment of inertia of a single longitudinal flange stiffener about an axis parallel to the flange and taken at the base of the stiffener (in^4)

n = number of equally spaced longitudinal flange stiffeners

w = larger of the width of the flange between longitudinal flange stiffeners or the distance from a web to the nearest longitudinal flange stiffener (in)

Compression-flange longitudinal stiffeners shall satisfy the requirements specified in Article 6.11.11.2. Nominal flexural resistance of tension flanges of tub sections shall be determined in Equation 2-58.

$$F_{nt} = R_h F_{yt} \quad \text{Equation 2-58}$$

Where: R_h = hybrid factor determined as specified in Article 6.10.1.10.1

2.4.3.5.4 Shear Capacity

Shear resistance shall be defined by the provisions of Article 6.10.9 for single webs. In cases where the web is inclined, D in Article 6.10.9 shall be taken as the depth of the web plate measured along the inclination. Straight and curved web panels shall satisfy Equation 2-59 at the strength limit state.

$$V_u \leq \phi_v V_n \quad \text{Equation 2-59}$$

Where: ϕ_v = resistance factor for shear as specified in Article 6.5.4.2

V_u = factored shear in the web at the section under consideration
(kip)

V_n = nominal shear resistance determined as specified in Article 6.10.9.2 and 6.10.9.3 for unstiffened and stiffened webs, respectively (kip)

Nominal shear resistance is computed by the following equations for unstiffened webs:

$$V_n = V_{cr} = C V_p \quad \text{Equation 2-60}$$

$$V_p = 0.58 F_{yw} D t_w \quad \text{Equation 2-61}$$

Where: C = ratio of the shear-buckling resistance to the shear yield strength determined by Equations 2-65, 2-66, and 2-67 with, $k = 5.0$

V_{cr} = shear-yielding or shear-buckling resistance (kip)

V_n = nominal shear resistance (kip)

V_p = plastic shear force (kip)

The nominal shear resistance of stiffened interior web panels is determined by Equations 2-63 and 2-64. The section proportions must satisfy Equation 2-61 and must meet the provisions of Article 6.10.9.1.

$$\frac{2Dt_w}{(b_{fc}t_{fc} + b_{ft}t_{ft})} \leq 2.5 \quad \text{Equation 2-62}$$

$$V_n = V_p \left[C + \frac{0.87(1 - C)}{\sqrt{1 + \left(\frac{d_o}{D}\right)^2}} \right] \quad \text{Equation 2-63}$$

$$V_p = 0.58F_{yw}Dt_w \quad \text{Equation 2-64}$$

Where: d_o = transverse stiffener spacing (in)

V_n = nominal shear resistance of the web panel (kip)

V_p = plastic shear force (kip)

C = ratio of shear-buckling resistance to shear yield strength

The ratio, C , shall be determined as specified by Equations 2-65 through 2-67:

If $\frac{D}{t_w} \leq 1.12 \sqrt{\frac{Ek}{F_{yw}}}$, then:

$$C = 1.0 \quad \text{Equation 2-65}$$

If $1.12 \sqrt{\frac{Ek}{F_{yw}}} < \frac{D}{t_w} \leq 1.40 \sqrt{\frac{Ek}{F_{yw}}}$, then:

$$C = \frac{1.12}{\frac{D}{t_w}} \sqrt{\frac{Ek}{F_{yw}}} \quad \text{Equation 2-66}$$

If $\frac{D}{t_w} > 1.40 \sqrt{\frac{Ek}{F_{yw}}}$, then:

$$C = \frac{1.57}{\left(\frac{D}{t_w}\right)^2} \left(\frac{Ek}{F_{yw}}\right) \quad \text{Equation 2-67}$$

Where: k = shear-buckling coefficient

$$k = 5 + \frac{5}{\left(\frac{d_o}{D}\right)^2} \quad \text{Equation 2-68}$$

If the section proportions do not satisfy Equation 2-62, Equation 2-69 shall be used to determine the nominal shear resistance.

$$V_n = V_p \left[C + \frac{0.87(1 - C)}{\left(\sqrt{1 + \left(\frac{d_o}{D}\right)^2} + \frac{d_o}{D}\right)} \right] \quad \text{Equation 2-69}$$

The nominal shear resistance of stiffened end panels shall be determined as specified in Equations 2-70 and 2-71.

$$V_n = V_{cr} = CV_p \quad \text{Equation 2-70}$$

$$V_p = 0.58F_{yw}Dt_w \quad \text{Equation 2-71}$$

Where: C = ratio of the shear buckling resistance to the shear yield strength determined by Equations 2-62 through 2-64.

V_{cr} = shear-yielding or shear-buckling resistance (kip)

V_p = plastic shear force (kip)

Transverse stiffener spacing for stiffened end panels, with or without longitudinal stiffeners, shall not exceed 1.5 times the section depth.

2.4.3.6 AASHTO Equation References

Table 2.3 includes a summary of the equations referenced and included in this chapter from the ASHTO LRFD Specifications with the appropriate AASHTO equation references.

Table 2.3: Chapter 2 Equation Legend (AASHTO, 2017)

Chapter 2 Equations	AASHTO 8th Edition
Equation 2-1	Table 4.6.2.2.2b-1
Equation 2-2	Equation 6.11.2.1.2-1
Equation 2-3	Equation 6.11.2.1.3-1
Equation 2-4	Equation 6.11.2.2-1
Equation 2-5	Equation 6.11.2.2-2
Equation 2-6	Equation 6.11.2.2-3
Equation 2-7	Equation 6.10.3.2.1-1
Equation 2-8	Equation 6.10.3.2.1-2
Equation 2-9	Equation 6.10.3.2.1-3
Equation 2-10	Equation 6.10.3.2.2-1
Equation 2-11	Equation 6.10.3.2.3-1
Equation 2-12	Equation 6.11.3.2-1
Equation 2-13	Equation 6.11.3.2-2
Equation 2-14	Equation 6.11.3.2-3
Equation 2-15	Equation 6.11.3.2-4
Equation 2-16	Equation 6.11.3.2-5
Equation 2-17	Equation 6.10.3.3-1
Equation 2-18	Equation 6.11.9-1
Equation 2-19	Equation 6.10.4.2.2-1
Equation 2-20	Equation 6.10.4.2.2-2
Equation 2-21	Equation 6.10.4.2.2-3
Equation 2-22	Equation 6.10.4.2.2-4
Equation 2-23	Equation 6.6.1.2.2-1
Equation 2-24	Equation 6.6.1.2.5-1
Equation 2-25	Equation 6.6.1.2.5-2
Equation 2-26	Equation 6.6.1.2.5-3

Table 2.3 (cont.): Chapter 2 Equation Legend (AASHTO, 2017)

Equation 2-27	Equation 6.10.1.8-1
Equation 2-28	Equation 6.11.6.2.2-1
Equation 2-29	Equation 6.10.7.3-1
Equation 2-30	Equation 6.11.7.1.1-1
Equation 2-31	Equation 6.10.7.1.2-1
Equation 2-32	Equation 6.10.7.1.2-2
Equation 2-34	Equation 6.10.7.1.2-3
Equation 2-35	Equation 6.11.7.2.1-1
Equation 2-36	Equation 6.11.7.2.2-1
Equation 2-37	Equation 6.11.7.2.1-2
Equation 2-38	Equation 6.11.7.2.2-5
Equation 2-39	Equation 6.11.7.2.2-6
Equation 2-40	Equation 6.11.7.2.2-7
Equation 2-41	Equation 6.11.8.1.1-1
Equation 2-42	Equation 6.11.8.2.2-1
Equation 2-43	Equation 6.11.8.2.2-2
Equation 2-44	Equation 6.11.8.2.2-3
Equation 2-45	Equation 6.11.8.2.2-4
Equation 2-46	Equation 6.11.8.2.2-5
Equation 2-47	Equation 6.11.8.2.2-6
Equation 2-48	Equation 6.11.8.2.2-7
Equation 2-49	Equation 6.11.8.2.2-8
Equation 2-50	Equation 6.11.8.2.2-9
Equation 2-51	Equation 6.11.8.2.2-10
Equation 2-52	Equation 6.11.8.2.2-11
Equation 2-53	Equation 6.11.8.2.2-12
Equation 2-54	Equation 6.11.8.2.2-13
Equation 2-55	Equation 6.11.8.2.3-1

Table 2.3 (cont.): Chapter 2 Equation Legend (AASHTO, 2017)

Equation 2-56	Equation 6.11.8.2.3-2
Equation 2-57	Equation 6.11.8.2.3-3
Equation 2-58	Equation 6.10.8.3-1
Equation 2-59	Equation 6.10.9.1-1
Equation 2-60	Equation 6.10.9.2-1
Equation 2-61	Equation 6.10.9.2-2
Equation 2-62	Equation 6.10.9.3.2-1
Equation 2-63	Equation 6.10.9.3.2-2
Equation 2-64	Equation 6.10.9.3.2-3
Equation 2-65	Equation 6.10.9.3.2-4
Equation 2-66	Equation 6.10.9.3.2-5
Equation 2-68	Equation 6.10.9.3.2-7
Equation 2-69	Equation 6.10.9.3.2-8
Equation 2-70	Equation 6.10.9.3.3-1
Equation 2-71	Equation 6.10.9.3.3-2

CHAPTER 3: DESIGN AND CONSTRUCTION OF THE FOURTEEN MILE BRIDGE

3.1 INTRODUCTION

This chapter details the design and construction of the Fourteen Mile Bridge in Lincoln County, West Virginia. This was the first installation of a bridge in West Virginia utilizing press-brake-formed tub girders. This bridge site has unique characteristics, such as significant skew and superelevation. The full bridge plans are in Appendix C of this report.

3.2 SUMMARY OF DESIGN AND CONSTRUCTION

The Fourteen Mile Bridge is a 58'-0" long, single span press-brake-formed tub girder bridge near the community of Ranger, West Virginia. The bridge carries traffic across Fourteenmile Creek on State Route Number 37. The bridge has a skew angle of 10° and a superelevation of 8%. Construction started in the spring of 2019 and completed on November 6, 2019 by Orders Construction Company. An aerial image of the bridge under construction is shown in Figure 3.1.



Figure 3.1: Aerial View of Bridge Under Construction

3.2.1 Fabrication of Modular Components

The press-brake-formed tub girders used in construction of the bridge were assembled in five fully composite modular components each brought to the site by truck and lifted into place by crane. This offsite manufacture enabled each step of the fabrication to be closely monitored and for progress to continue before the field would typically allow certain steps to be undertaken.

The five press-brake-formed tub girders began as 96” wide by 1/2” thick plate of AASHTO M270 steel shaped using a large capacity press-brake. Once formed, additional details such as shear studs, end bearing diaphragms, and mounting angles for the internal formwork were welded onto the steel tub. The entire assembly was hot-dipped galvanized for corrosion resistance. A photo of the galvanized press-brake-formed tub girder is seen in Figure 3.2.

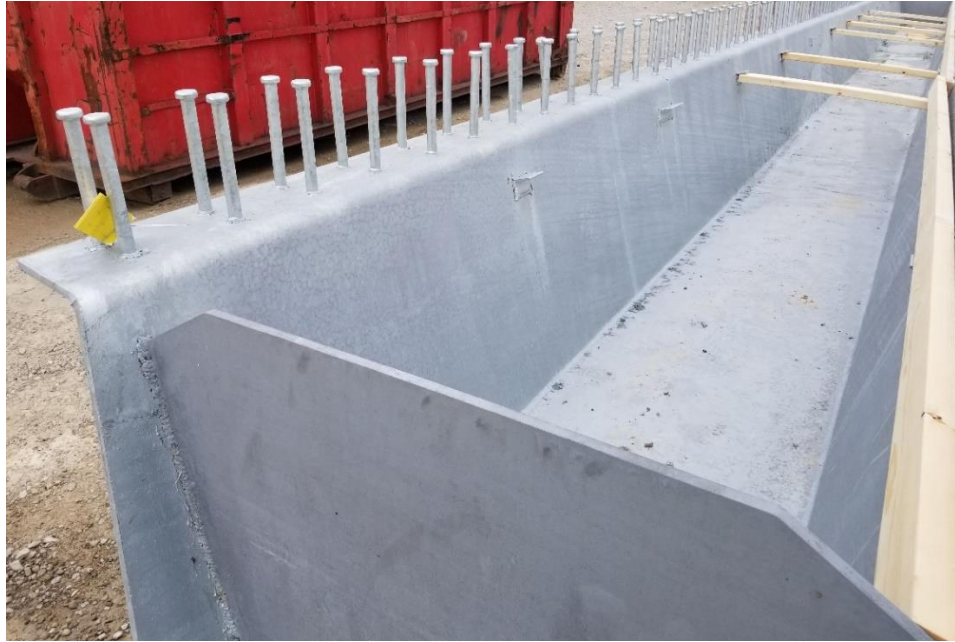


Figure 3.2: Galvanized Tub Girder, Prior to Formwork Construction

Once the press-brake-formed tub girders were galvanized, the girder were shipped to Carr Concrete in Waverly, West Virginia where the formwork was assembled and a concrete deck was cast. The precaster used wooden studs and plywood to create the internal sacrificial formwork. Figure 3.3 shows a press-brake-formed tub girder module with the internal formwork.



Figure 3:3: Tub Girder with Completed Internal Formwork

While internal formwork was fabricated, reusable external formwork was constructed. The external formwork used a combination of steel formwork panels, wooden studs, and plywood. Upon completion of the external formwork, each press-brake-formed tub girder was placed into the forms (Figure 3.4) and the mats of rebar were added (Figure 3.5). A retardant was placed on the edges of the shear key detail on the external formwork where the UHPC joints would connect. This retardant allowed the concrete paste at the edge to be removed by a pressure washer, leaving exposed aggregate to which the UHPC could properly bond.



Figure 3:4: Isometric View of Reusable External Formwork



Figure 3:5: Close View of Rebar Placement at Semi-Integral Abutment End

Following the placement of the rebar, concrete casting began. The crew used two concrete buckets, so any downtime from waiting for more material was minimized, and the deck could be cast continuously. Once pouring was completed, the deck was finished, and a plastic sheet covering was applied, so the deck could cure. Figure 3.6 and Figure 3.7 show the casting of the concrete and finishing of the deck, respectively.



Figure 3:6: Casting of Fresh Concrete



Figure 3:7: Finished Concrete Deck

After the concrete had set, the external formwork was removed, and the next press-brake-formed tub girder was placed into the formwork. After the first two modules had been cast, a test fit was performed to ensure compatibility of the composite modules in the field. Figure 3.8 shows the test fit in the fabrication yard.



Figure 3:8: Test Fit of Two Precast Modules at Fabrication Yard

3.2.2 Installation of Modular Components

Once all five composite modules were completed, they were transported by truck to the bridge site and lifted into place by crane. The UHPC closure pours were cast, and the deck was diamond ground for the appropriate finish. In order to reduce traffic congestion during placement and the amount of time necessary to rent the cranes, each successive truck was staged. This allowed the next modular unit to be delivered and set in minimal time. A typical composite module loaded on a staged truck is shown in Figure 3.9.



Figure 3:9: Composite Module Delivered to Site

Two cranes operated in tandem to lift each composite module from the trailer to the abutment seats. Workers on the ground verified measurements for the first composite module as this placement defined further composite module positions. Figure 3.10 shows the placement of the first composite module, and Figure 3.11 shows the placement of the second composite module and the appropriate fit of the two.



Figure 3:10: Placement of First Composite Module On-Site



Figure 3:11: Verification of Fit of Adjacent Modules on Site

After all composite modules were placed, formwork was erected around the joints for the UHPC closure pours. The UHPC was mixed onsite with a pan mixer, then concrete buggies moved the concrete from the mixer to the bridge to place along the joints. The pouring of the UHPC is shown in Figure 3.12.

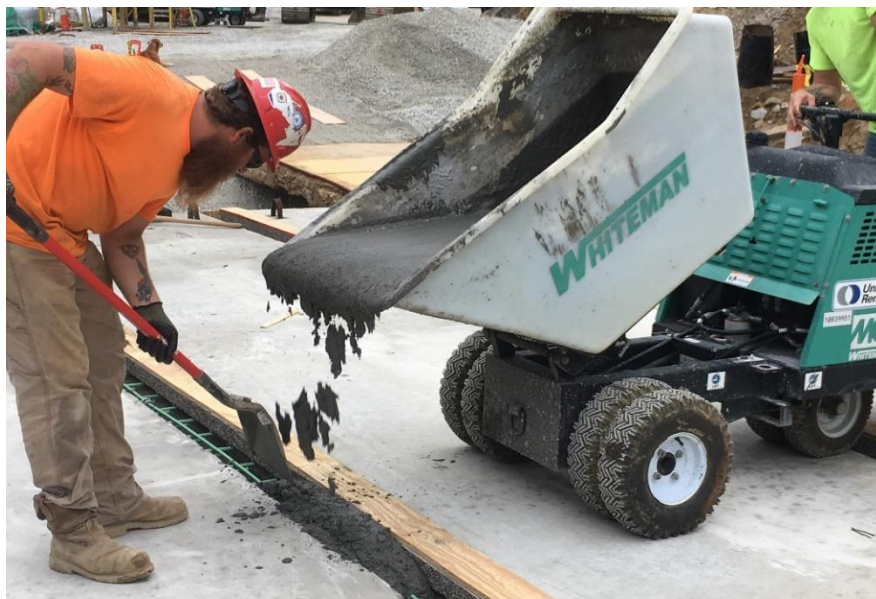


Figure 3:12: Pouring of UHPC Along Longitudinal Joint

After the UHPC set, the forms were removed, and a diamond grinder was used to adjust the deck profile as desired (Figure 3.13). This enabled a smooth transition from the cast-in-place concrete approach slab to the precast concrete deck modules.



Figure 3.13: Diamond Grinder Used to Finish Deck On-Site

3.2.3 Accelerated Bridge Construction Strategies

Several accelerated bridge construction (ABC) strategies were employed in this bridge replacement project to minimize project duration and improve the finished structure. Instead of a traditional cast-in-place deck for the bridge superstructure, the Fourteen Mile Bridge used five composite modules manufactured individually off site. By having the deck precast in a controlled shop environment, the contractor was able to closely monitor the application of the fresh concrete. The minimal difference between the pouring of each bucket of concrete ensured that no cold joints formed in the deck structure. The controlled shop environment was also beneficial for the curing process to allow the concrete to gain maximum strength. Once the composite modules were complete, they were transported by truck to the bridge site and the modules were placed directly from the trucks to the abutments. The removal of a staging yard for construction reduced the time spent handling material and the necessary footprint of the construction site. The choice of UHPC was advantageous for the closure pours due to the high compressive strength and the short amount of time required to develop full strength of UHPC.

CHAPTER 4: RESEARCH METHODS

4.1 INTRODUCTION

This chapter serves to provide an overview of the research methodology employed during the field evaluation of the Fourteen Mile Bridge. This includes descriptions of the field-testing equipment and finite element modeling, along with the data reduction approaches.

4.2 EXPERIMENTAL TESTING EQUIPMENT

This section details the pieces of field equipment used to assess the performance of the Fourteen Mile Bridge during the live load field test. Instrumentation and software were developed by Bridge Diagnostics, Inc. (BDI).

4.2.1 BDI Strain Transducers

BDI strain transducers (Figure 4.1) were chosen as the data sensors to measure strain during the live load field test. These gages are an appropriate choice for outdoor field tests because the gages are reusable and resistant to adverse weather conditions. Each gage is fully sealed to the elements, has been rated IP67 for dust and moisture resistance, and has an operating temperature range of -58°F to $+185^{\circ}\text{F}$. Inside of each gage is a full Wheatstone bridge with four active 350Ω foil gages. The applicable range for strain measurements of the gage is $\pm 2000\mu\epsilon$. Each gage is individually calibrated to meet National Institute of Standards and Technology specifications and has a variation in readings of less than $\pm 1\%$. The BDI strain transducers attach to the surface of the steel member with reusable tabs that included a $1/4''$ -20 threaded mounting shaft. For this live load field test, Loctite HY 4070 Structural Repair Hybrid Adhesive was used to affix the transducers to the girder. More details on structure instrumentation are available in section 5.2.1.



Figure 4.1: BDI Strain Transducer, Typical Application to Girder

4.2.2 STS-WiFi Data Acquisition System

In order to record the data measured with the strain transducers, BDI created the STS-WiFi Data Acquisition System. This system consists of nodes collecting data from various sensors and a base station serving as the interface between the nodes and the computer software. The STS-WiFi Data Acquisition System is especially useful for field testing where access to a power source is difficult or running cables between devices is limited. Sensors, such as a strain transducer, plug into one of the four connectors of the wireless four-channel node (Figure 4.2). These nodes transmit the data readings over a local wireless broadcast to the mobile base station as seen in Figure 4.3. Power is supplied to the wireless nodes and base station by rechargeable NiMH batteries. In cases where a source of continuous AC power is available, the wireless nodes may also be powered by a DC power adapter.



Figure 4:2: BDI STS-WiFi Wireless 4-Channel Node



Figure 4:3: BDI STS-WiFi Mobile Base Station

Even though the units are designed with the capability to wirelessly transmit data for use in applications with limited access, there is the option to use wired ethernet connections between each node and the base station. Like the strain transducers, BDI designed the base stations and wireless nodes to be able to resist dust and water. A weather seal and locking mechanism is provided on the access door to both the base station and wireless node. BDI also provided mounting locations on the wireless nodes and base station; these mounts were combined with high

strength magnets to affix the testing equipment to the outside of the girders in a sturdy and temporary fashion. To improve data reduction efforts, each piece of equipment in the BDI Data Acquisition System is equipped with a BDI “Intelliducer” chip. This chip allows the equipment to identify itself inside of the software package. The ease of installation and durable nature of the BDI system makes its use in field testing an appropriate choice.

4.2.3 Load Truck and Wheel Scales

The live load was produced by a loaded tandem axle dump truck provided by Lusher Trucking of Prichard, West Virginia (Figure 4.4). The total weight of the truck was measured prior to arrival on site. The weight of each wheel was measured on site using Haenni Wheel Load Weigher scales as seen in Figure 4.5. The wheel scales were provided by the Public Service Commission of West Virginia Transportation Enforcement Division.



Figure 4:4: Tandem Axle Dump Truck used for Live Load Test

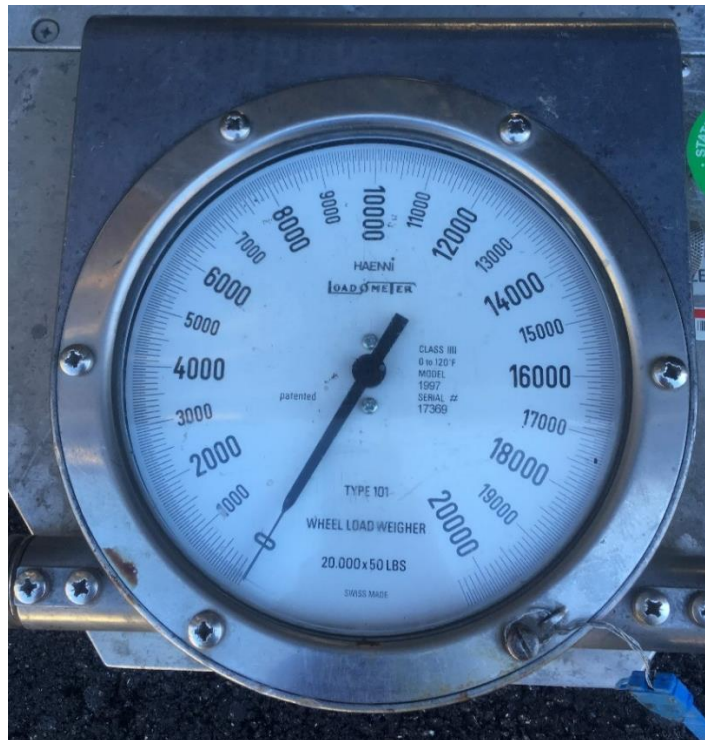


Figure 4.5: Haenni Wheel Load Weigher Scale

4.3 FINITE ELEMENT MODELING

This section details the process followed to conduct a finite element analysis to compare analytical values to the results from the field. Abaqus/CAE 6.14-1 (Dassault Systèmes, 2014) was used to develop a finite element model of the Fourteen Mile Bridge. Load simulating a tandem axle truck was applied and an analysis was conducted. Article 4.6.3.3 of the AASHTO LRFD specifications was used as a guide for the considerations in a refined analysis approach. Data from the model was used to compare the girder strains and LLDFs calculated from the field results.

4.3.1 Material Definitions

The Fourteen Mile Bridge superstructure consists of AASHTO M270 Grade 50 plate for the girders and Class H concrete for the deck. Due to the narrow widths of the UHPC closure pours, Class H concrete was assumed for the entire deck. Following AASHTO 6.4.1, the structural

steel had a modulus of elasticity of 29,000 ksi, a minimum yield strength of 50 ksi, and a Poisson's ratio of 0.3. The compressive strength of the concrete was 4,000 psi as stated in the design plans. Following AASHTO Article 5.4.2, the concrete had a modulus of elasticity of 3,640 ksi and a Poisson's ratio of 0.2. Linear elastic behavior was assumed in this analysis and all materials were assumed to be isotropic.

4.3.2 Element Selection

Due to the uniform geometry of the Fourteen Mile Bridge, quadrilateral shell elements were employed in the finite element model. Following the Abaqus/Standard User's Manual and work from previous analytical models of press-brake-formed tub girders (Gibbs, 2017; Underwood, 2019), S4R shell elements were chosen to be used. S4R elements are four-noded stress/displacement shell elements with reduced integration. These properties make S4R elements a suitable choice for a wide variety of uses. Comparison of analytical results to the field data indicated the element produced accurate results for finite element analysis.

4.3.3 Mesh Discretization

Following Article 4.6.3.3 of the AASHTO LRFD specifications, abrupt changes in the sizes or shapes of finite elements should be avoided, and the aspect ratio of finite elements and grid panels should not exceed 5.0. This controls the shapes used in the mesh and the relative element sizes.

The mesh discretization of the finite element model for the Fourteen Mile Bridge adhered to the guidelines set by AASHTO to produce accurate results. Each portion of the cross section was seeded to generate a desired number of elements. The typical mesh discretization for the cross section is presented in Figure 4.6. Nodes were spaced in the longitudinal dimension of the girders at 6" increments for 116 elements along the length of each girder. Both top flanges consist of two elements each, top and bottom bends consist of three elements each, webs consist of 12 elements each, and the bottom flange consists of 10 elements.

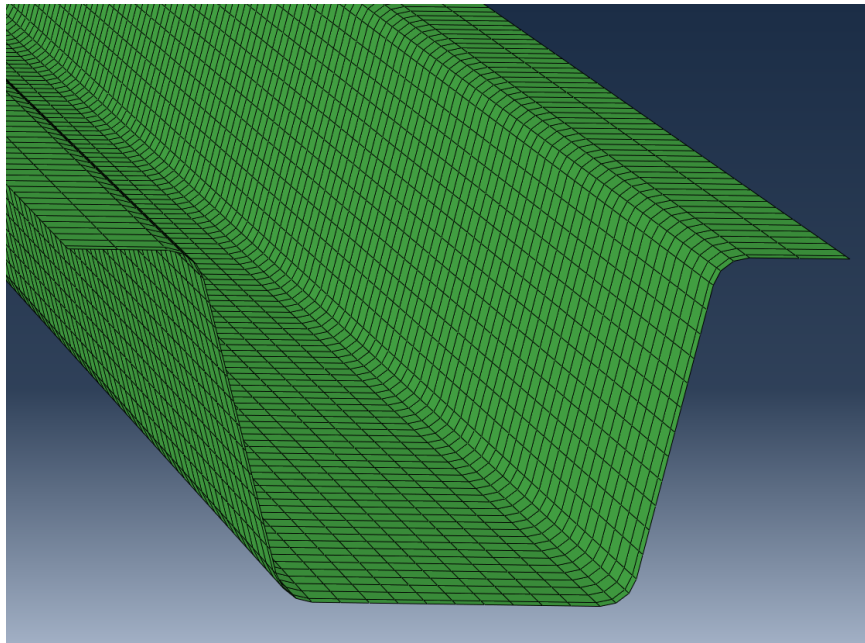


Figure 4.6: Typical Mesh Discretization for Each Tub Girder

Elements were grouped by similar geometries, and each was checked to verify the aspect ratios met the guidelines set by AASHTO. The results of this validation are presented in Table 4.1.

Table 4.1: Typical Aspect Ratio for Girder Elements

Geometry	Number of Elements	Depth, D (in)	Length, L (in)	Aspect Ratio (D/L)
Top Flange	2	3.00	3.74	0.80
Bend	3	3.00	1.21	2.48
Web	12	3.00	1.89	1.59
Bottom Flange	10	3.00	2.16	1.39

Seeding of the deck nodes in the longitudinal direction matched the 6” spacing used to seed the girder. However, for the multiple-point constraints to be collinear between deck and girder nodes, transverse spacings of nodes varied between 6.77” for exterior overhangs, 6.41” over each girder, and 5.77” for interior overhangs. Aspect ratios for each deck element met the AASHTO guidelines for advanced modeling techniques.

4.3.4 Boundary Conditions and Multiple Point Constraints

The boundary conditions of the Fourteen Mile Bridge were modeled as a “hinge-roller” simple span which limited horizontal and vertical displacement. The girders were restrained from lateral movement at the ends. All boundary conditions were applied to the nodes on the bottom flange of each girder. Multiple-Point Constraints are used to associate disconnected nodes of a finite element model to limit displacement between the two points. This feature is useful in the analysis of beam-slab bridges when the deck is composite where the deck and girders can be modeled to act together.

4.3.5 Application of Live Loading

Load placement on the finite element model simulated the loading performed in the field to maximize the strain in the bottom flange of each girder. Because the point loads were applied in the middle of elements and not at distinct nodes, the load from each wheel would need to be statically distributed to each node defining the element (Figure 4.7). The proportion of the applied load taken to each node was computed by Equations 4-1 through 4-4, which follows AASHTO Article 4.6.3.3.1 as the sum for each nodal load is statically equivalent to the applied load.

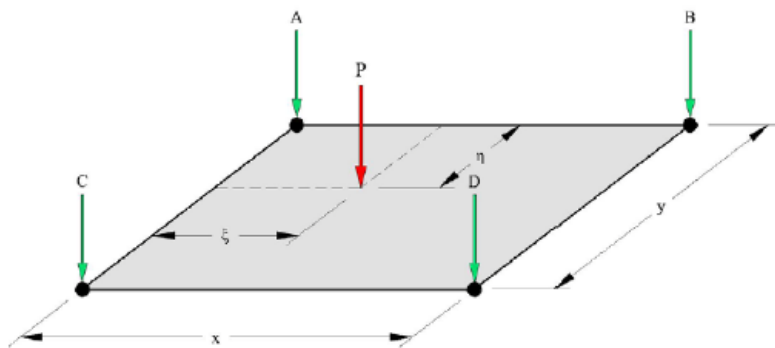


Figure 4.7: Nodal Distribution of Point Loads (Michaelson, 2010)

$$A = P \left(1 - \frac{\xi}{x}\right) \left(1 - \frac{\eta}{y}\right)$$

Equation 4-1

$$B = P \left(\frac{\xi}{x} \right) \left(1 - \frac{\eta}{y} \right) \quad \text{Equation 4-2}$$

$$C = P \left(1 - \frac{\xi}{x} \right) \left(\frac{\eta}{y} \right) \quad \text{Equation 4-3}$$

$$D = P \left(\frac{\xi}{x} \right) \left(\frac{\eta}{y} \right) \quad \text{Equation 4-4}$$

4.4 DATA REDUCTION METHODS

This section details the methods used to analyze the data collected in the field and from the finite element model used to calculate the LLDFs. Example calculations for the quarter span bending stress and LLDFs are also included. Structure instrumentation is further described in Section 5.2. Raw data from the field testing included the strain readings (measured in microstrain, $\mu\epsilon$) and corresponding gage numbers. The five strain readings from each panel point were averaged to a single strain reading for each gage; the initial strain recorded from when the truck was located off the bridge was subtracted from the strain at each panel point. The location of each gage on the structure was determined from field notes, and the gages were grouped by girders. For simplicity, the truck passes were defined as the physical positions of the truck during live load testing and the truck runs were the positions that maximized the strains on targeted girders. More information on the distinction between truck passes and runs is provided in Section 5.2.2. The three gage measurements for each girder were averaged to obtain the strain at each panel point on each girder for each truck pass. The strains were subsequently linearly interpolated to determine the strain at each panel point for each truck run.

4.4.1 Computation of Quarter Span Bending Stresses

Recorded strain data was separated by girder and the readings were averaged to obtain a single strain value for each panel point measured in microstrain, $\mu\epsilon$. These strain values were used in combination with Hooke's Law to compute the bending stress at the gage locations at quarter span. The strain values were averaged for each girder, then divided by $1e6$ to convert to strains.

The values were multiplied by Young's Modulus of steel, $E_s = 29,000$ ksi. The resultant value is the stress in ksi at the quarter span for each girder. An example of these calculations for the selected data shown in Table 4.2 is presented below as Equations 4-5 and 4-6.

Table 4.2: Strain Values, Quarter Span Bending Stress

Truck Pass 4, Girder 3, Panel Point 5				
Panel Point		Strain in Gages, Girder 3 ($\mu\epsilon$)		
x (ft)	x/L	G01	G02	G03
29	0.5	37.83	39.39	39.58

Average Strain in Girder 3:

$$\epsilon_{avg} = \frac{\sum \epsilon}{n} = \frac{37.83 + 39.39 + 39.58}{3} = 38.93 \mu\epsilon \quad \text{Equation 4-5}$$

Application of Hooke's Law to Compute Bending Stress

$$\sigma = \frac{\epsilon_{avg}}{1,000,000} * E_s = \frac{38.93}{1,000,000} * 29000 = \mathbf{1.13 \text{ ksi}} \quad \text{Equation 4-6}$$

Where: n = number of gages

ϵ_{avg} = average bottom flange strain ($\mu\epsilon$)

σ = bottom flange bending stress (ksi)

E_s = Young's Modulus of Steel (ksi)

4.4.2 Computation of Live Load Distribution Factors

The average girder strain for each panel point was used to calculate the LLDFs for each girder following Equation 4-7. The strain in each girder is divided by the total amount of strain in all girders. This value is multiplied by the number of applied design trucks and the multiple presence factor, which is described in Section 2.4.1. For the single lane loaded condition, the

multiple presence factor is taken as 1.2, and for the two lanes loaded condition, the multiple presence factor is taken as 1.0.

$$LLDF_{gi} = \frac{n\varepsilon_i}{\sum_{i=1}^k \varepsilon_i} * m \quad \text{Equation 4-7}$$

Where: $LLDF_{gi}$ = distribution factor for a target “i”th” girder

ε_i = bottom flange static strain for a target “i”th” girder

n = number of applied design trucks

m = AASHTO multiple presence factor

k = number of girders

Sample calculations will first be shown for calculating the LLDFs for the single lane loaded condition at Panel Point 5 for Truck Pass 4 and Girder 2. This computation for the data shown in Table 4.3 is represented by Equation 4-8. In the case of multiple lanes loaded, strain data from separate passes must be superimposed to simulate the loading of two trucks. This means the strain would be the sum of the strain on a given girder due to each relevant pass. Data presented in Table 4.4 represents the average girder strain for each pass and the summation of girder strains for each respective girder. The two lanes loaded calculations are shown in Equation 4-9 for the summation of Panel Point 5 for Truck Pass 1 and 7 on Girder 1.

Table 4.3: Strain Values, Single Lane Loaded LLDF Sample Calculation

Truck Pass 4, Panel Point 5						
Panel Point		Girder Average Strain ($\mu\varepsilon$)				
x (ft)	x/L	G1	G2	G3	G4	G5
29	0.5	38.75	45.52	38.93	25.21	9.67

$$LLDF_{G2,PP5} = \frac{1.2 * (45.52)}{38.75 + 45.52 + 38.93 + 25.21 + 9.67} * 1 = \mathbf{0.346}$$

Equation 4-8

Table 4.4: Strain Values, Two Lanes Loaded LLDF Sample Calculation

Truck Pass 1, Panel Point 5						
Panel Point		Girder Average Strain (μϵ)				
x (ft)	x/L	G1	G2	G3	G4	G5
29	0.5	64.28	59.56	35.36	17.46	6.42
Truck Pass 7, Panel Point 5						
Panel Point		Girder Average Strain (μϵ)				
x (ft)	x/L	G1	G2	G3	G4	G5
29	0.5	26.81	39.31	47.95	46.40	28.26
Truck Pass 2+7, Panel Point 5						
Panel Point		Girder Average Strain (μϵ)				
x (ft)	x/L	G1	G2	G3	G4	G5
29	0.5	91.09	98.88	83.31	63.86	34.68

$$LLDF_{G1,PP5} = \frac{1.0 * (91.09)}{91.09 + 98.88 + 83.31 + 63.86 + 34.68} * 2.0 = \mathbf{0.490}$$

Equation 4-9

LLDFs were calculated following AASHTO Article 4.6.2.2. The specifications within Article 4.6.2.2 are discussed earlier in Section 2.4.2 and Equation 4-10 represents the LLDF equation for steel box girders. In the AASHTO LRFD specifications, no differentiation is made

for the calculation of interior girder or exterior girder LLDFs, or for the number of design lanes loaded. Note the multiple presence factor is already taken into consideration by Equation 4-10.

$$LLDF = 0.05 + 0.85 * \frac{N_L}{N_b} + \frac{0.425}{N_L} \quad \text{Equation 4-10}$$

Where: N_L = number of design lanes as specified in Article 3.6.1.1.1

N_b = number of girders

$$0.5 \leq \frac{N_L}{N_b} \leq 1.5$$

In the case of the Fourteen Mile Bridge, there are five girders and two design lanes. As shown in Equation 4-11, the LLDF determined by the methods specified in the AASHTO LRFD specifications Article 4.6.2.2 is 0.603. It should be noted this bridge does not fall within the range of applicability. The calculation of N_L/N_b is 2/5, or 0.4, which is below the minimum requirement the equation may be utilized for. No provisions are described by AASHTO for steel box bridges that lie outside this range.

$$LLDF = 0.05 + 0.85 * \frac{2}{5} + \frac{0.425}{2} = \mathbf{0.603} \quad \text{Equation 4-11}$$

CHAPTER 5: FIELD TESTING OF THE FOURTEEN MILE BRIDGE

5.1 INTRODUCTION

This section details the loading and data recording process performed for the physical field testing of the Fourteen Mile Bridge in October 2019. Researchers from MU and WVU traveled to Ranger, West Virginia to perform a live load field test on the bridge. The goal of the field test was to compare measured strains due to physical loading to strains determined from analytical modeling to assess performance of the structure.

5.2 LIVE LOAD FIELD TEST ASSESSMENT

The field test of the Fourteen Mile Bridge was completed over two days. The first day was used to measure and apply instruments to the structure. The field testing and data collection was completed on the second day.

5.2.1 Structure Instrumentation

The BDI STS Wi-Fi Data Acquisition System was used to instrument the structure and record results. Nineteen gage locations were identified for this field test; three gages were located on the bottom of each girder (15 total) and one gage was located on each web of Girders 1 and 2. Gages were placed at quarter span to allow for easier access for preparation and removal. An overview of the gage layout is shown in Figure 5.1.

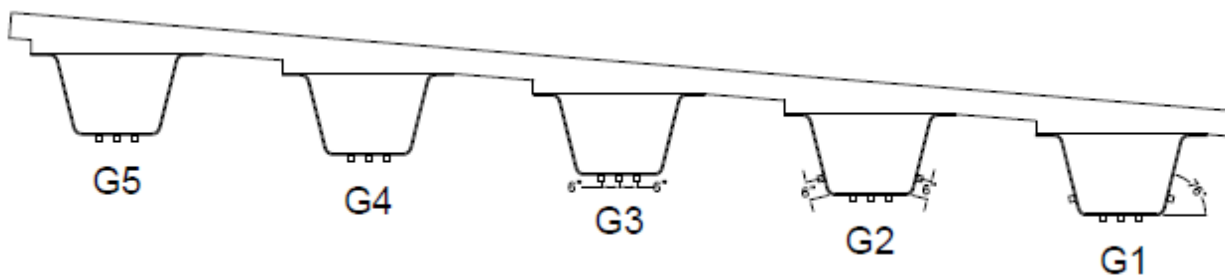


Figure 5:1: Gage Locations on Girders, Looking Upstation

To improve access to mark and prepare the girders and apply the instrumentation, an all-terrain aerial lift was supplied by the contractor for use during the field testing. The aerial lift is presented in Figure 5.2.

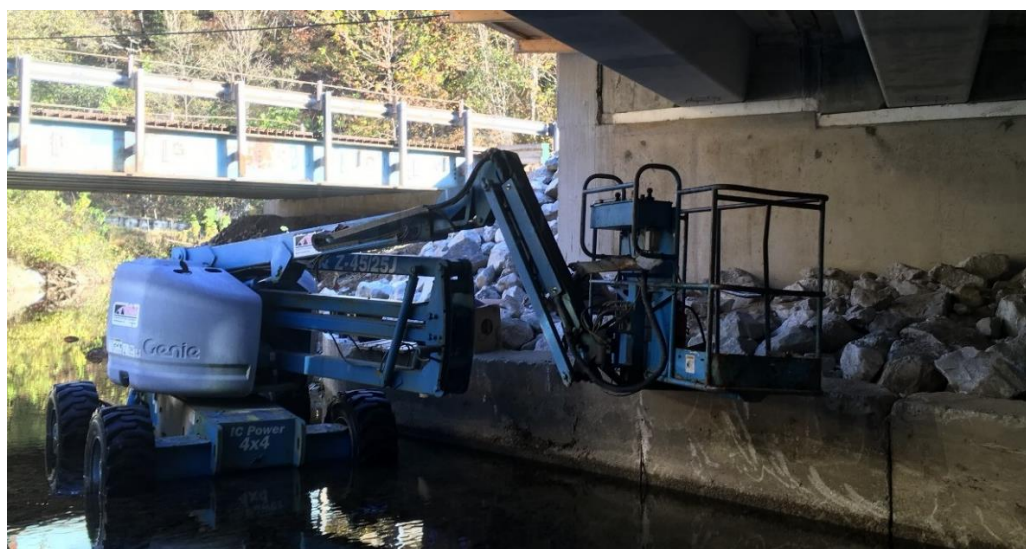


Figure 5:2: Aerial Lift Supplied by Contractor

Quarter span locations were determined by measuring the distance from the inside face of one precast abutment to the inside face of the other. This distance was 60'-6", which was divided by four to find quarter span. The resulting distance measured from the back-station abutment to quarter span was 13'-7⁵/₁₆." A mark was made at quarter span for the transverse middle of each girder. Quarter points were also measured the along the bends of each girder; a square was used to

mark the resulting diagonal. The middle of the gages, as seen in Figure 5.3, is at an angle parallel to the skew. After this mark was made, measurements were made at 6" normal to the longitudinal direction at each side from the center and then 1.5" from each intersection point to determine the tab locations for the gages. The resulting grid of markings is seen in Figure 5.4. Web locations were measured using an angled rule; the web gages were placed 6" from the bottom flange measured along the inclination of the web. The web gage mounting points were determined in a similar fashion as the bottom flange mounting points. Typical web gage mounting locations are seen in Figure 5.5.

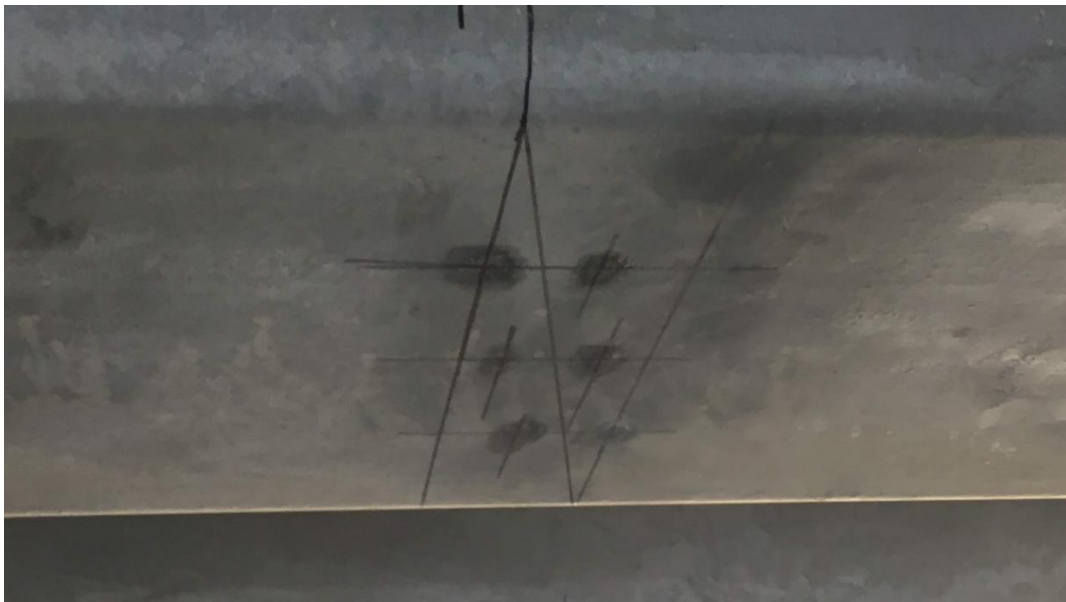


Figure 5:3: Centerline of Gages at Quarter Span, Looking Upstream



Figure 5:4: Typical Bottom Flange Gage Mounting Points, Looking Upstream

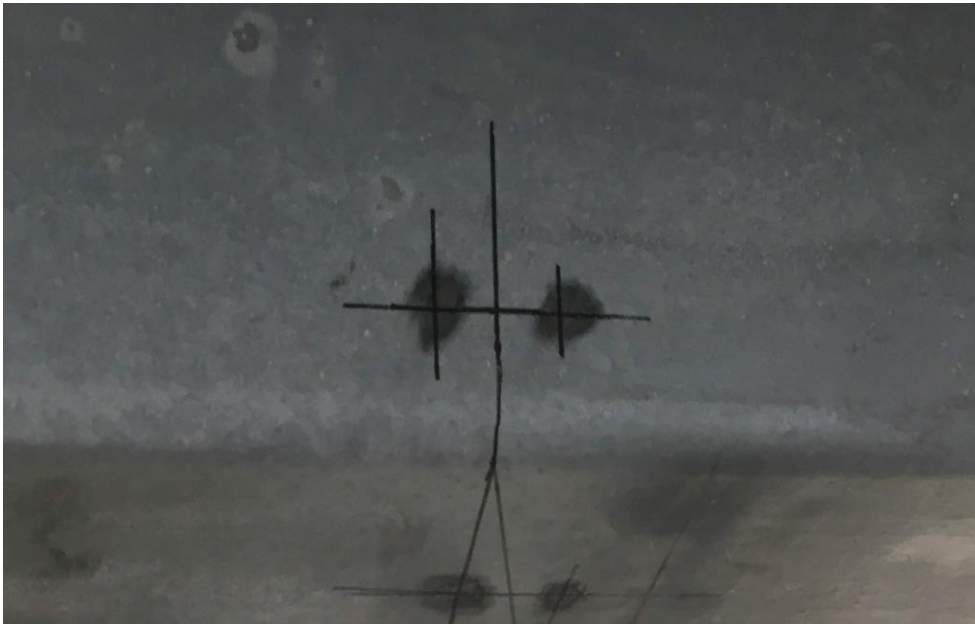


Figure 5:5: Typical Web Gage Mounting Points, Looking Downstream

After the gage locations had been marked, a battery-powered angle grinder with a wire brush attachment was used to buff the surface of the girder to allow the adhesive to bond to the bare steel. After the surface was prepared, the marks were replaced so the gages could be installed at the correct locations. A gage blank was used in combination with the tab jig provided by BDI to ensure correct spacing of the mounting locations. A small bead of Loctite® HY 4070 Superfast Fixture Structural Repair Hybrid Adhesive was applied to the bottom of each tab and uniform pressure was used to fix the tabs against the steel surface. Approximately 90 seconds after the initial contact, the adhesive set, and pressure could be released. Figure 5.6 shows the tab mounts in place on the girder.

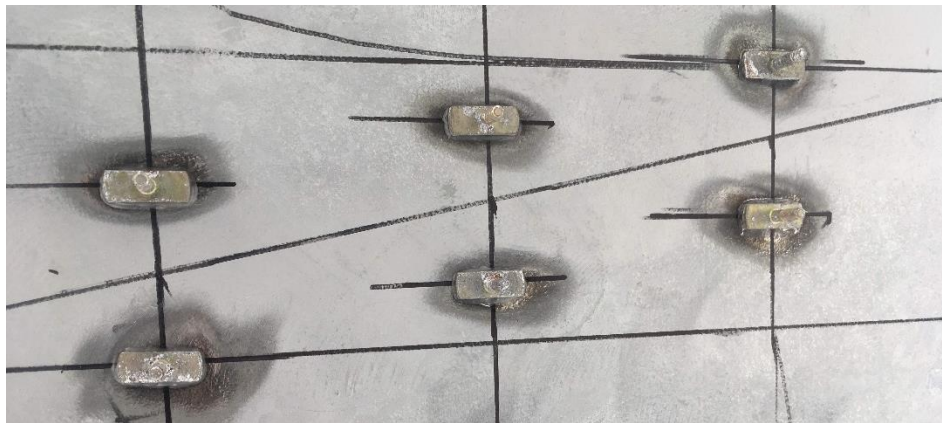


Figure 5.6: Typical Tab Mounting to Steel Surface

Approximately 20 minutes following the original application, the gage blank was removed, and the appropriate BDI strain transducer was installed based on the necessary cable length. The gages attached to the two tabs with 7/16" nuts tightened with a wrench until snug. The cables were connected to the appropriate wireless node. Nodes were attached to the surface of the steel using a magnetic mounting assembly. Figure 5.7 shows the gages installed on the girder.

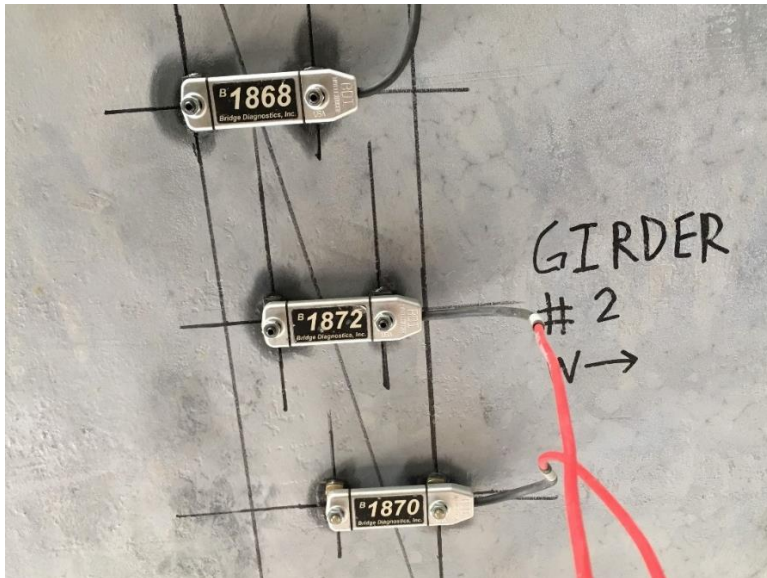


Figure 5:7: Typical View of Gages Installed on Bottom Flange, Looking Downstream

Because a portable generator was available, it was determined that using DC power adapters with the wireless nodes and base station would be an appropriate option. A wired ethernet cable connected one of the five nodes to the base station. Figure 5.8 shows an overview of the instrumentation once all connections were completed.



Figure 5:8: Overview of Instrumentation, Looking Backstation

5.2.2 Live Load Path Delineation

The second day of the study began with troubleshooting all connections and verifying the system recorded data correctly. The live load paths were developed from the AASHTO LRFD specifications for maximizing load on individual girders. Measurements to determine the panel points started with identification of the centerline of the road survey. A straight line was marked between both survey points. Subsequent parallel lines were measured in 2'-0" measurements, resulting in the last longitudinal marking located 2'-0" from the edge of the downstream parapet. In total, 13 longitudinal markings were made. To determine transverse locations, the distance between the survey points was measured and was broken into 10 equal panel points, each 6'-⁵/₈" in length.

Delineation of load paths was accomplished by marking the deck by string and crayon. At 2'-0" increments from the centerline of road survey, nails were placed in the deck at the foam joints at the end of the precast modules. Yellow construction string lines were wrapped around the nails and care was taken to ensure the string was taut (Figure 5.9). Figure 5.10 shows several longitudinal markings with the construction string lines. In the transverse direction, blue crayon was used to mark the 10 panel points as seen in Figure 5.11.



Figure 5:9: Nail placement in Foam Joint with Construction String Line Wrapped Taut



Figure 5:10: Parallel Longitudinal Delineations on Deck with Construction String Line



Figure 5:11: Transverse Mark Completed with Blue Crayon

Once the markings had been placed on the deck, a grid was created with the intersections representing the panel points for each placement where the truck would be located. For the purpose of this study, passes will refer to the particular transverse spacing that the truck path is following, and panel point will refer to the truck's position in the longitudinal direction. This grid is indicated by Figure 5.12. It should be noted, due to the radius of curvature of the roadway, the truck would not be able to be placed at either the upstation or backstation end of the longitudinal pass for passes 12 and 13. Subsequently, there is no data from either pass.

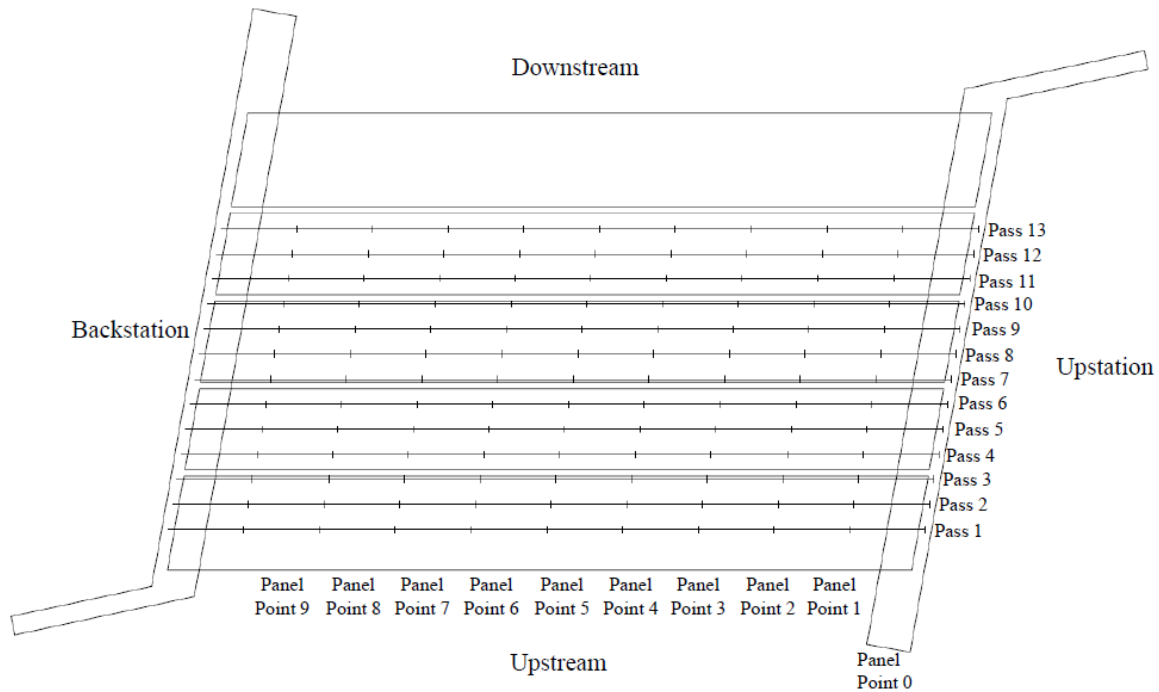


Figure 5.12: Plan View of Panel Point Grid

Referencing work from Gibbs on the Amish Sawmill Bridge (2017) and Underwood on the Cannelville Road Bridge (2019), these delineated truck passes were linearly interpolated to maximize loading on specific girders. Strain values from multiple passes could be added together for each respective girder to simulate the effects of multiple lane loaded scenarios. The following methodology was performed to determine the appropriate location of runs. All transverse distances were measured along the grade of the deck. Girder 1, an exterior girder, would have the strains maximized by having the truck run located 2'-0" from the inside edge of the downstream parapet.

To simulate the two lanes loaded scenario, a second truck located 12'-0", the spacing of a design lane, away from the first truck run, or 14'-0", from the inside edge of the downstream parapet. These two runs are shown in Figure 5.13, along with their distance to the inside edge of the downstream parapet as Runs 1 and 4, respectively. A similar procedure is followed for Girders 2 and 3. To maximize the strain for the single lane load in Girder 2, an interior girder, the truck run must be placed so the middle of the tire is along the centerline of Girder 1, 3'- $\frac{13}{16}$ " from the inside edge of the downstream parapet, labeled as Run 2. To induce the multiple lane loaded scenario, the strains from Run 2 must be superimposed with Run 5, located 12'-0" in the upstream direction. Runs 3 and 6 are used to maximize strain from the single and multiple lanes loaded scenarios, respectively, for girder 3.

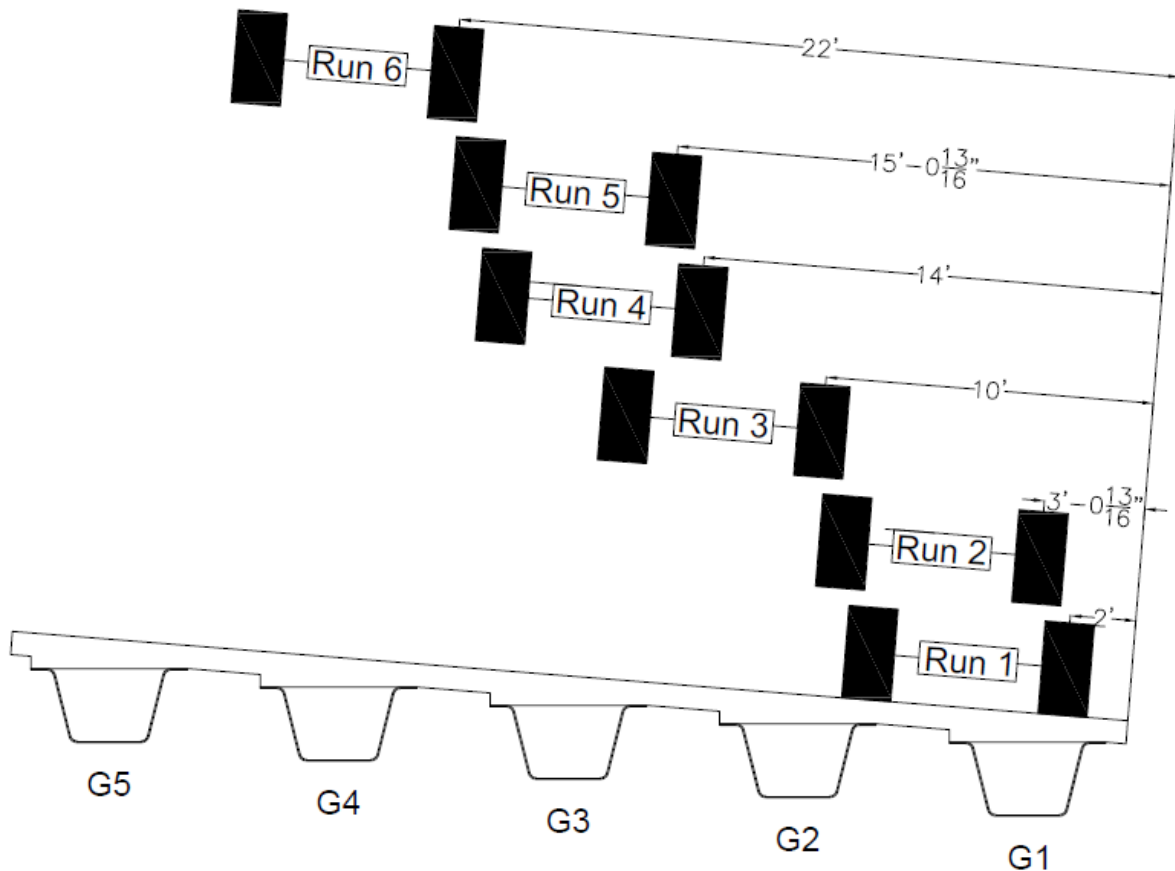


Figure 5:13: Live Load Truck Placement, Looking Upstation

5.2.3 Live Load Testing

Upon arrival of the tandem axle truck to the bridge site, testing began. The truck was deemed fit for use in the live load test due to the similarity with the HS-20 design load truck from AASHTO. The initial truck pass began at the downstream edge of the deck oriented in the direction of back station. Successive passes were worked in the upstream direction. Before the truck moved onto the bridge, the right edge of the front left tire, wheel 1, was lined up with the construction string line. Once the physical testing began, 10 Hz was chosen as the sample rate within the BDI Software to record strain values. Five measurements were taken before the bridge was loaded to serve as a baseline. The truck would be positioned at each panel point at the intersection of the string line and crayon mark. A typical pass location can be seen in Figure 5.14. Once the truck stopped and the bridge returned to a static condition, five readings were taken. At the conclusion of the testing, each wheel was weighed and the geometry of the axle spacings were measured. Figure 5.15 shows the weight of each wheel along with the geometric configuration of the axles.

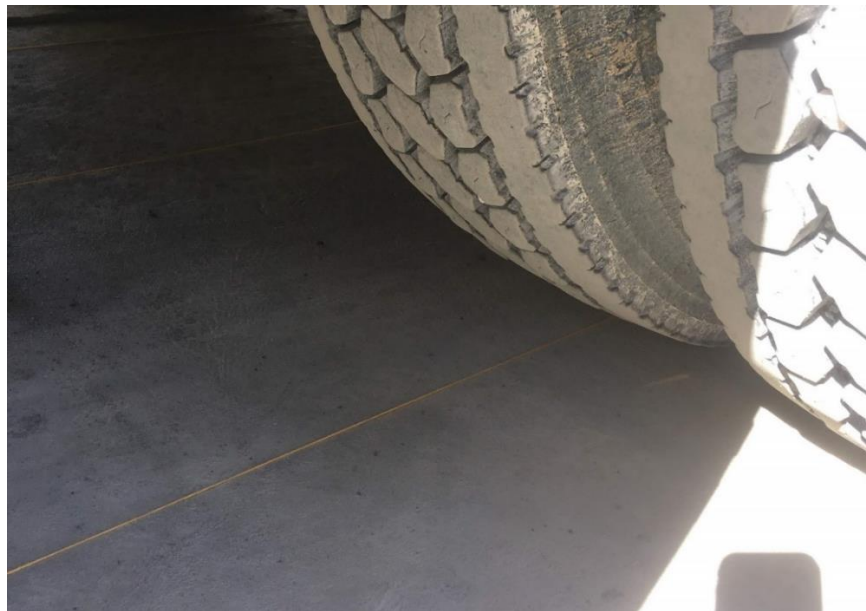


Figure 5:14: Typical Truck Pass Location

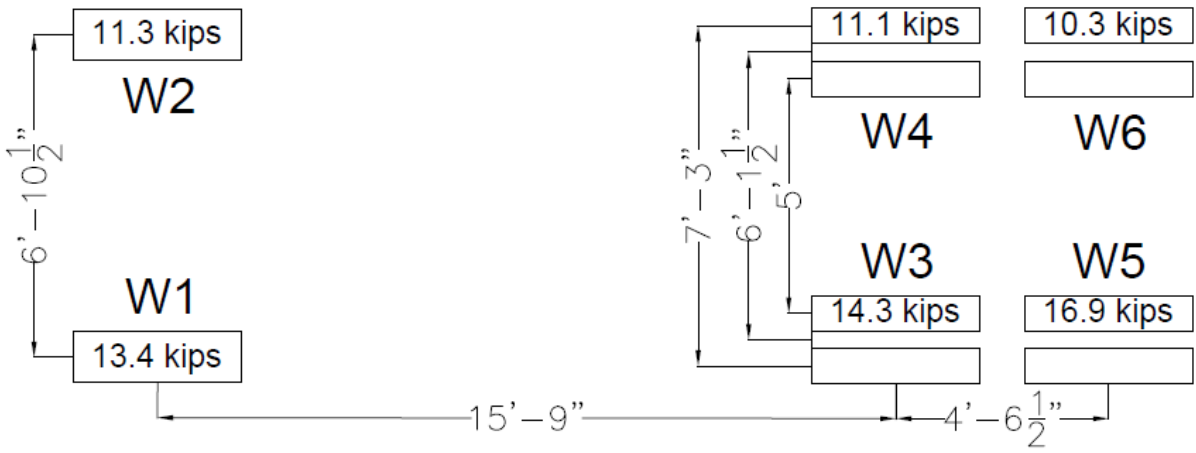


Figure 5:15: Truck Dimensions and Field Weight Measurements

CHAPTER 6: RESULTS AND ANALYSIS

6.1 INTRODUCTION

This chapter summarizes the results of the Fourteen Mile Bridge live load field test and compares the values to those computed by analytical models. LLDFs will be compared from the live load field test, the finite element analysis, and the AASHTO LRFD specification (2017).

6.2 COMPARISON OF RESULTS

This section presents the results determined from the live load field test and the finite element model. The raw data from the live load field test is included, and the subsequent LLDFs are discussed. Truck Run 1 will be the focus of this section. The full results for all truck runs with all relevant tables and charts are shown in Appendix A.

6.2.1 Live Load Field Test Results

The following section discusses the results collected from the live load field test of the Fourteen Mile Bridge. Data was collected with the BDI STS Wi-Fi Data Acquisition System, and data reduction was performed following the methods outlined in Section 4.4. The three strain readings across the bottom flange of each girder were averaged respectively to account for torsion; the strain readings from the webs were not used. Girder stresses at quarter span, where the gages were located, were computed and LLDFs were determined for comparison with the finite element model and AASHTO LRFD specifications. A sample of the raw strain data from Truck Run 1 is shown in Table 6.1.

Table 6.1: Measured Strain from Truck Run 1, Experimental

Truck Run 1, Measured Strain (Field)						
Panel Points		Average Bottom Flange Strain ($\mu\epsilon$)				
x (ft)	x/L	G1	G2	G3	G4	G5
0	0	0	0	0	0	0
5.8	0.1	5.513	2.877	0.157	-1.270	-3.635
11.6	0.2	17.992	14.074	9.539	5.401	0.336
17.4	0.3	34.632	30.154	21.157	12.541	4.579
23.2	0.4	52.685	49.797	30.625	16.274	6.498
29	0.5	64.277	59.563	35.360	17.456	6.418
34.8	0.6	66.936	64.148	37.530	16.816	5.658
40.6	0.7	72.247	71.656	32.655	11.770	2.987
46.4	0.8	70.454	65.424	25.459	7.196	0.984
52.2	0.9	42.457	36.502	12.600	0.863	-2.546
58	1	0	0	0	0	0

6.2.1.1 Live Load Distribution Factors

The girder strains were used to calculate the LLDFs following the procedures discussed in Section 4.4.2. The multiple presence factor was applied following the AASHTO LRFD specifications. LLDFs were calculated for each panel point in the field test, but only the LLDFs at Panel Point 5 ($0.5*L$) were compared to the analytical model because that position would have the maximum effect of the truck on the girders. A sample of the calculated LLDFs for Truck Run 1 is presented in Table 6.2.

Table 6.2: Computed Live Load Distribution Factors from Truck Run 1, Experimental

Truck Run 1, Simplified Distribution Factors (Field)						
Panel Points		Distribution Factors				
x (ft)	x/L	G1	G2	G3	G4	G5
0	0	---	---	---	---	---
5.8	0.1	1.514	0.790	0.043	-0.349	-0.998
11.6	0.2	0.380	0.297	0.201	0.114	0.007
17.4	0.3	0.336	0.293	0.205	0.122	0.044
23.2	0.4	0.338	0.319	0.196	0.104	0.042
29	0.5	0.351	0.325	0.193	0.095	0.035
34.8	0.6	0.350	0.336	0.196	0.088	0.030
40.6	0.7	0.378	0.375	0.171	0.062	0.016
46.4	0.8	0.416	0.386	0.150	0.042	0.006
52.2	0.9	0.472	0.406	0.140	0.010	-0.028
58	1	---	---	---	---	---
Average		0.504	0.392	0.166	0.032	-0.094
MPF applied (1.2*PP5)		0.421	0.390	0.232	0.114	0.042
St. Dev.		0.381	0.154	0.052	0.147	0.340

6.2.2 Comparison of Analytical and Experimental Results

This section details the comparison between the results developed from the experimental data collected in the field and the analytical values determined from the finite element analysis. The deflected shape of the finite element model is shown in Figure 6.1 and additional information is provided in Section 4.3. Table 6.3 presents a comparison between the analytical and experimental LLDFs for each girder at Panel Point 5 for the single lane loaded condition of Truck

Run 1. Table 6.4 presents a similar comparison for the two lanes loaded condition of Truck Runs 1 and 4. Note the appropriate AASHTO multiple presence factor is applied in each scenario.

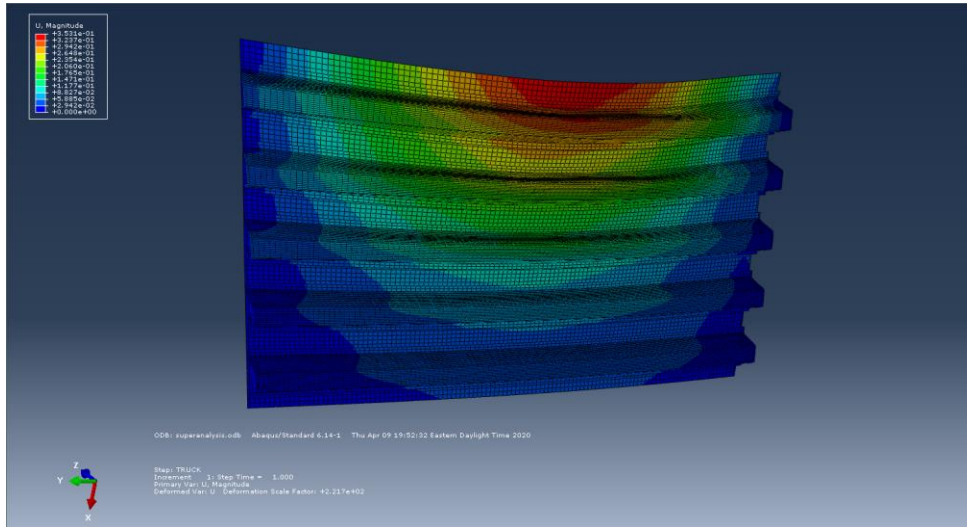


Figure 6.1: Deflected Shape of Finite Element Model, Truck Run 1, Panel Point 5

Table 6.3: Comparison of Field and FEA Live Load Distribution Factors, One Lane Loaded

Truck Run 1, Distribution Factors at Panel Point 5					
Girder	G1	G2	G3	G4	G5
Field Results	0.421	0.390	0.232	0.114	0.042
FEA Results	0.440	0.355	0.217	0.116	0.072

Table 6.4: Comparison of Field and FEA Live Load Distribution Factors, Two Lanes Loaded

Truck Run 1 & 4, Distribution Factors at Panel Point 5					
Girder	G1	G2	G3	G4	G5
Field Results	0.490	0.532	0.448	0.343	0.187
FEA Results	0.502	0.503	0.440	0.334	0.221

While the two methods produce similar results, some variance is still present. This may be partially due to varying boundary conditions. The Fourteen Mile Bridge utilized integral abutments as described in Section 3.2, which would yield similar results to a “fixed-fixed” end condition and a stiffer structure due to the decrease in rotation at the supports. There is not an adequate manner to model integral abutments in the finite element analysis, so simply supported (“hinge-roller”) conditions were used in the analytical model. The results show the LLDFs are similar in both cases. Figure 6.2 presents a Q-Q plot reflecting the comparison of each girder’s distribution factors at Panel Point 5. Note the R^2 value represents the correlation of the entire data set, both single and two-lane loaded scenarios.

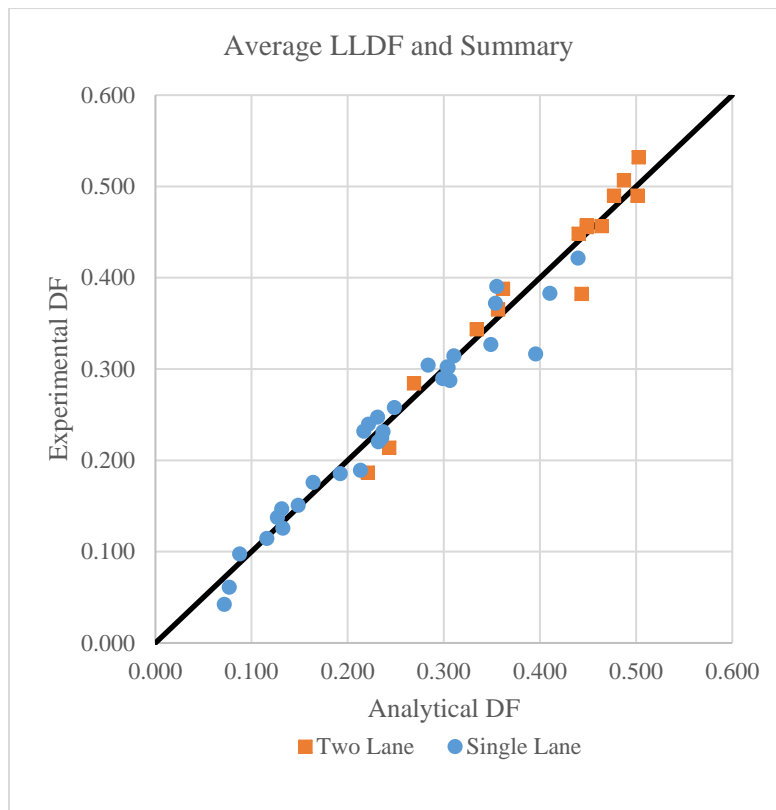


Figure 6:2: Comparison Between Analytical and Experimental Live Load Distribution Factors for Single and Two Lane Loaded Conditions

6.3 COMPARISON OF LIVE LOAD DISTRIBUTION FACTORS WITH AASHTO LRFD SPECIFICATIONS

This section will provide a comparison between LLDFs determined from the experimental data of the live load field test, the analytical data from the finite element model, and the relevant AASHTO LRFD specifications. LLDFs calculated with the expressions from the 2017 AASHTO LRFD specifications already take the multiple presence factors into consideration, so the comparison for each scenario will have the appropriate multiple presence factors applied. Calculations for the AASHTO LLDFs are presented in Section 4.4.2. Truck Run 1 will be used for comparison between the three methods for the single lane condition. Table 6.5 and Figure 6.3 provide a comparison of the three methods.

Table 6.5: Comparison of Field, FEA and AASHTO Live Load Distribution Factors, One Lane Loaded Truck Run 1

Truck Run 1, Distribution Factors at Panel Point 5					
Girder	G1	G2	G3	G4	G5
Field Results	0.421	0.390	0.232	0.114	0.042
FEA Results	0.440	0.355	0.217	0.116	0.072
AASHTO	0.603	0.603	0.603	0.603	0.603

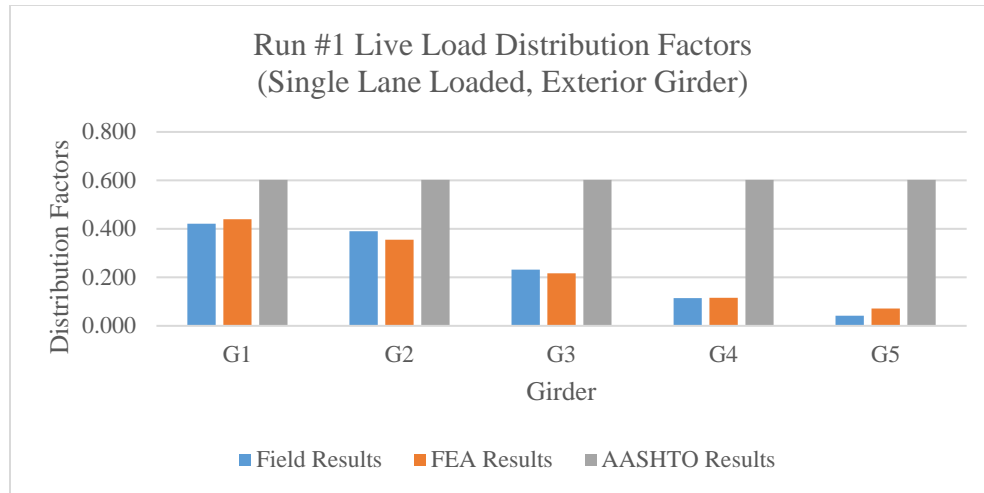


Figure 6.3: Comparison of Field, FEA and AASHTO Live Load Distribution Factors, One Lane Loaded Truck Run 1

LLDFs determined from the field test and the analytical model are similar; the AASHTO equations predict a much higher distribution factor for the single lane loaded condition. A comparison between the three methods for the two-lane loaded scenario is presented in Table 6.6 and Figure 6.4. Again, the LLDFs for both the analytical and experimental methods are close, but the AASHTO values are significantly higher. The discrepancy between AASHTO and the analytical and experimental methods is increased for girders further away from the placement of the load truck.

Table 6.6: Comparison of Field, FEA, and AASHTO Live Load Distribution Factors, Two Lanes Loaded Truck Run 1 and 4

Truck Run 1 & 4, Distribution Factors at Panel Point 5					
Girder	G1	G2	G3	G4	G5
Field Results	0.490	0.532	0.448	0.343	0.187
FEA Results	0.502	0.503	0.440	0.334	0.221
AASHTO	0.603	0.603	0.603	0.603	0.603

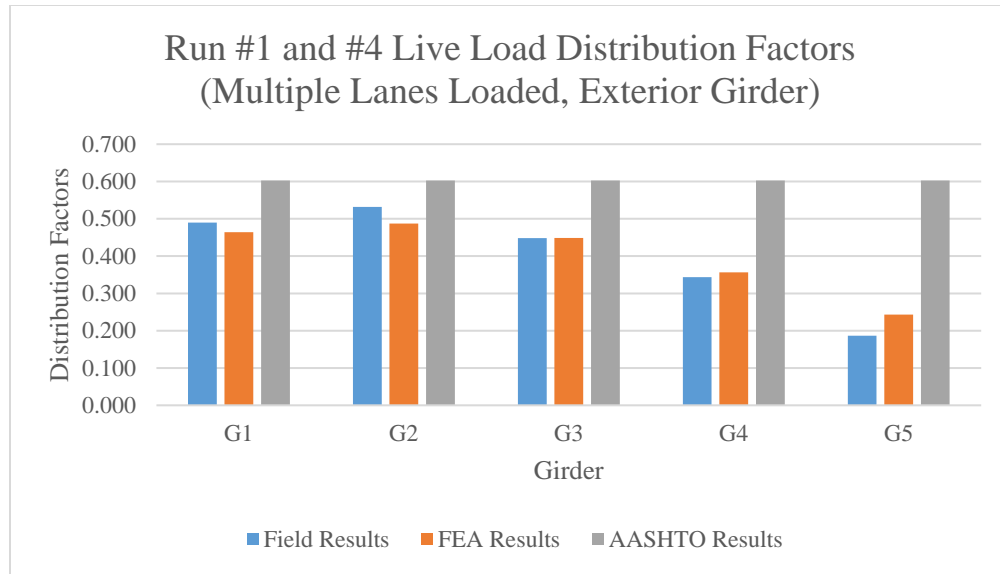


Figure 6:4: Comparison of Field, FEA, and AASHTO Live Load Distribution Factors, Two Lanes Loaded Truck Run 1 and 4

6.4 CONCLUSIONS

This chapter provided a summary of the results computed from the experimental data from the field test of the Fourteen Mile Bridge along with the finite element analysis performed. The data was used to calculate the LLDFs from the field test and the analytical model. The computed LLDFs were compared to the LLDFs calculated following the AASHTO LRFD specifications to assess the applicability of AASHTO in regards to press-brake-formed tub girders. The comparison showed minor differences in LLDFs between the finite element model and the experimental results, likely due to the differing boundary conditions. In all cases, the AASHTO LLDFs underpredicted the performance of the press-brake-formed tub girder and were more conservative than the experimental and analytical values. Therefore, AASHTO LLDFs may be safely used in the application of press-brake-formed steel tub girder bridges.

CHAPTER 7: QUALITATIVE ASSESSMENT OF BRACING EFFECTIVENESS AND TORSIONAL RESPONSE FOR NON-COMPOSITE TUB GIRDERS

7.1 INTRODUCTION

When press-brake-formed tub girders are used in conjunction with a precast reinforced concrete deck, the top flanges are fully supported during casting. In cases where a cast-in-place reinforced concrete deck is used, significant loading is placed on the top flanges. This can lead to instability issues as the open shape of the non-composite tub girder is susceptible to torsional effects. Bracing may be added either to the interior or exterior of the tub shape to control undesirable deflection. This chapter examines work performed by Kelly (2014) on non-composite behavior of press-brake-formed steel tub girders and evaluates different bracing scenarios from a qualitative view. Abaqus/CAE 6.14-1 (Dassault Systèmes, 2014) was utilized to create a finite element model for each scenario and a nonlinear analysis was performed. Program files from MATLAB (The Mathworks, Inc., 2020) were used to write the Abaqus input files, which are included in Appendix B of this report.

7.2 VERIFICATION WITH KELLY'S MODEL

7.2.1 Geometric Imperfections

A significant discrepancy in the critical load that led to buckling in the experiments performed by Kelly (2014) was attributed to geometric imperfections induced during the fabrication process of the press-brake-formed tub girder. Flange inclinations and web inclinations were recorded for each specimen (Figure 7.1 and 7.2).

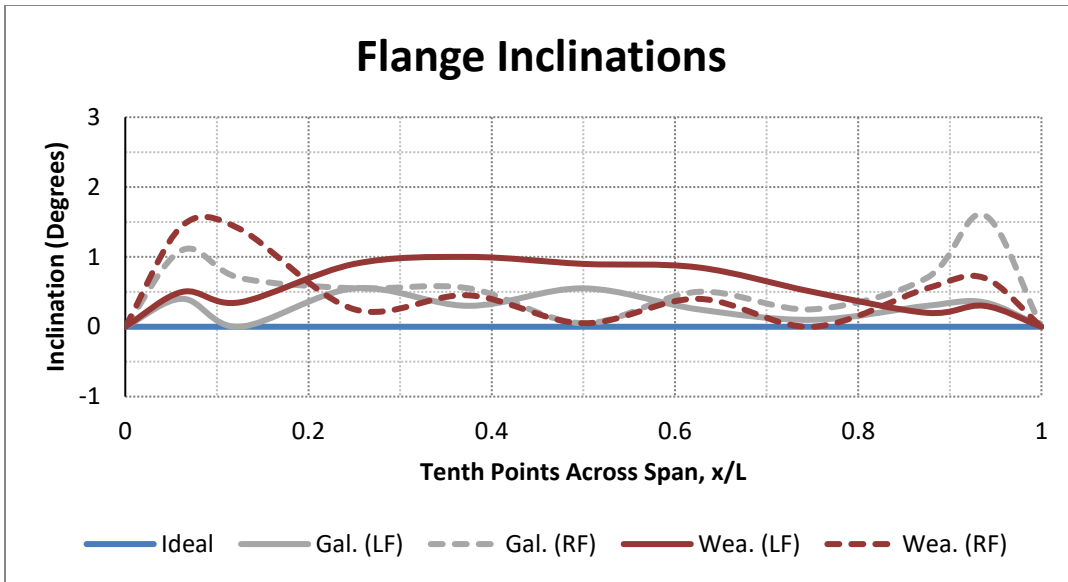


Figure 7:1: Flange Inclinations (Kelly, 2014)

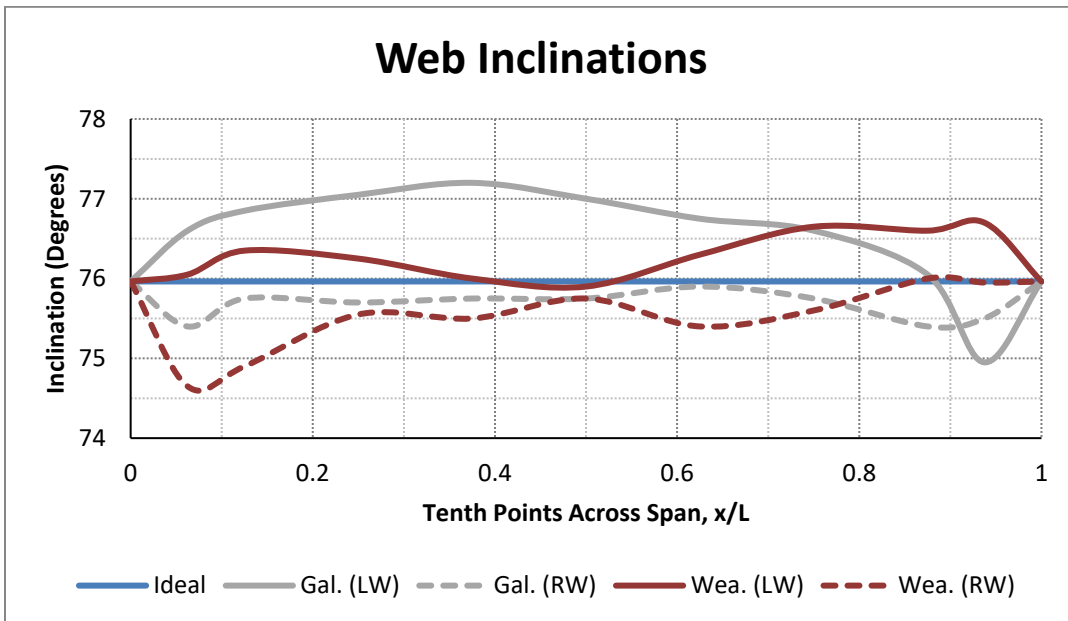


Figure 7:2: Web Inclinations (Kelly, 2014)

The finite element model was developed to induce imperfections onto the generated mesh based on user inputs. The geometric imperfections were separated into flange tilt, girder twist, and web out of flatness. Each of the geometric imperfections was modeled to follow a sine curve with the maximum amplitude and anchor points specified by the user to control the imperfection across the mesh. Figures 7.3 through 7.5 present an exaggerated view of the effect of flange tilt, girder twist, and web out of flatness, respectively.

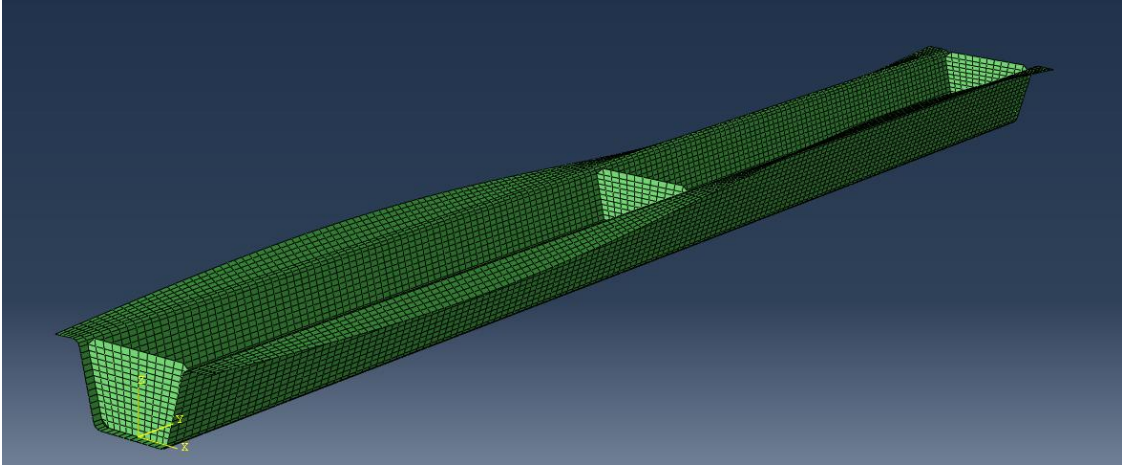


Figure 7:3: Tub Girder Modeled with Flange Tilt

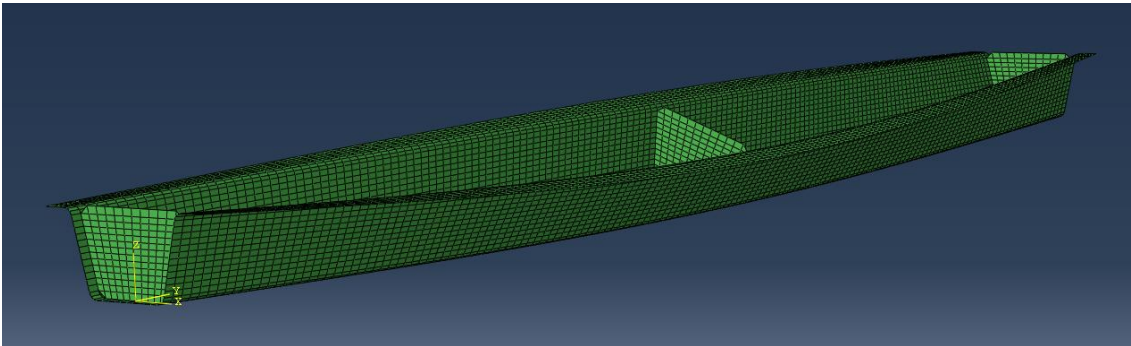


Figure 7:4: Tub Girder Modeled with Girder Twist

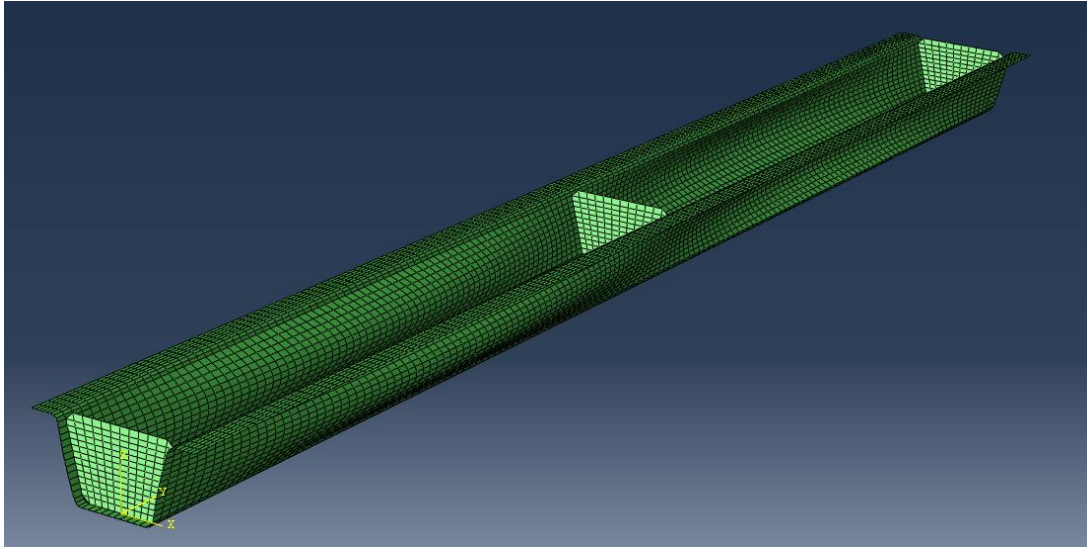


Figure 7:5: Tub Girder Modeled with Web Out of Flatness

To best fit the geometric imperfections recorded by Kelly (2014), only the flange tilt and girder twist were considered. Using the recorded data previously mentioned in Figures 7.1 and 7.2, the amplitude for each imperfection was determined. The peak values were input as 1° of flange tilt clockwise and 1° of girder twist clockwise. For both imperfections, the end supports were selected as the anchor points to best fit the model.

7.2.2 Material Modeling

To capture the behavior of a nonlinear analysis, steel material in the finite element model was modeled using an elastic-plastic constitutive law following work by Michaelson (2014) and Kelly (2014). A multilinear relationship (Galindez, 2009) was used to represent the stress-strain behavior of material modeling (Figure 7.6 and Table 7.1). The plastic material properties were a function of the true stress and strain, and these were input into the Abaqus input file.

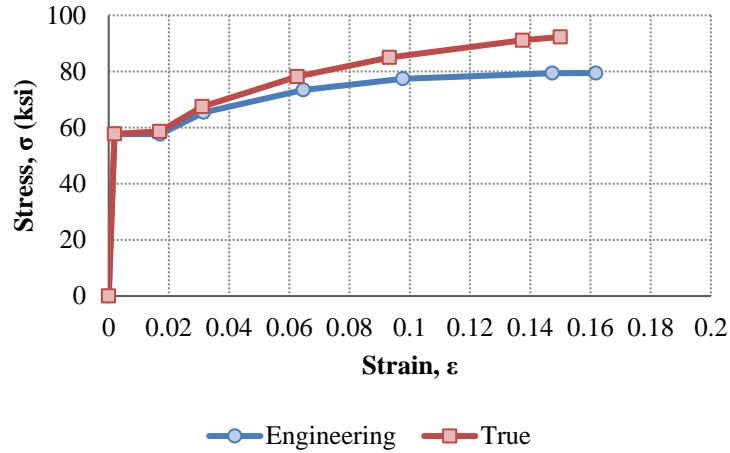


Figure 7.6: Multi-linear Stress-Strain Curve

Table 7.1: Expressions for Computing Steel Stress-Strain Behavior (Galindez, 2009)

Point	Strain	Stress
1	$\varepsilon_1 = \frac{\sigma_y}{E}$	$\sigma_1 = \sigma_y$
2	$\varepsilon_2 = \varepsilon_{st}$	$\sigma_2 = \sigma_y$
3	$\varepsilon_3 = \frac{1}{10}(\varepsilon_u - \varepsilon_{st}) + \varepsilon_{st}$	$\sigma_3 = \frac{E_{st}}{10}(\varepsilon_u - \varepsilon_{st}) + \sigma_y$
4	$\varepsilon_4 = \frac{2}{7}(\varepsilon_6 - \varepsilon_3) + \varepsilon_3$	$\sigma_4 = \frac{4}{7}(\sigma_6 - \sigma_3) + \sigma_3$
5	$\varepsilon_5 = \frac{2}{7}(\varepsilon_6 - \varepsilon_3) + \varepsilon_4$	$\sigma_5 = \frac{2}{7}(\sigma_6 - \sigma_3) + \sigma_4$
6	$\varepsilon_6 = \varepsilon_u - \frac{1}{10}(\varepsilon_u - \varepsilon_{st})$	$\sigma_6 = \left(\frac{\sigma_y}{\sigma_{0.2\%}} \right) \sigma_u - \frac{100}{E_{st}}(\varepsilon_u - \varepsilon_{st})$
7	$\varepsilon_7 = \varepsilon_u$	$\sigma_7 = \left(\frac{\sigma_y}{\sigma_{0.2\%}} \right) \sigma_u$

7.2.3 Element Selection

Abaqus (2014) provides complete geometric modeling capabilities with a variety of available element types. General shell elements with reduced integration (S4R) are used for modeling the steel girders in this study. As shown by several researchers (Barth, 1996; Yang, 2004; Roberts, 2004; Righman, 2005), S4R shell elements are very accurate in modeling the physical behavior of non-composite steel plate girders. These 4-node general-purpose elements are intended to provide accurate solutions for both thin and thick shells, using classical (Kirchoff) shell theory when appropriate for thin shells and (Mindlin) shell theory as the thickness increases.

These elements allow for finite membrane strains and rotations of the shell, change in shell thickness as a function of the membrane strain, and transverse shear deformation. Therefore, they are suitable for large-strain analysis involving inelastic deformation of materials. The S4R element is a first-order element having only one integration point used to form the element stiffness matrix. S4R elements offer many advantages over traditional shell elements, including strains and stresses computed at the integration points, providing optimal accuracy, and fewer integration points, resulting in reduced computing time and storage requirements.

The primary disadvantage of using reduced integration is that deformation modes which cause no strain at the integration points may develop. This may lead to inaccurate results if these zero-energy modes propagate through the structure in a phenomenon commonly known as hourglassing. However, this can be prevented by the user by introducing a small artificial stiffness associated with zero-energy deformation modes using the *SECTION CONTROLS command in an Abaqus input file (Kelly 2014; Michaelson, 2014).

7.2.4 Riks Loading Algorithm

The girders studied in this work are analyzed using the modified Riks algorithm available in Abaqus (2014). This solution method captures the nonlinear load deflection response of the finite element model at and beyond maximum loading. The modified Riks method is capable of obtaining a complete nonlinear solution and giving information on girder behavior in both loading and unloading regions (Yang, 2004).

It is assumed the loading is proportional and the response is smooth (no sudden bifurcations). Furthermore, this method uses the load magnitude as an additional unknown and solves simultaneously for loads and displacements. Because the progress of the solution is independent of the load increment, Abaqus uses the “arc length” to control the increment size. The arc length is the distance along the static equilibrium path in the load-displacement space. This value is initially provided by the user and later adjusted by the Abaqus automatic load increment algorithm, which is based on convergence rate.

The essence of this method is that the solution is viewed as the discovery of a single equilibrium path in a space defined by the nodal variables and loading parameter. The solution is found during each increment by moving a given distance along a tangent to the current solution point and searching for equilibrium in the plane, that not only passes through the point, but also is orthogonal to the same tangent line (Yang, 2004). The total path length is determined by the load magnitudes the user specifies. The user also determines the number of increments (Kelly, 2014).

7.2.5 Comparison with Kelly's Model

Once the finite element model was developed, an evaluation of an unbraced girder was performed as a benchmark with the experimental and analytical data that Kelly (2014) had recorded. A plot of the comparisons between the two analyses is presented in Figure 7.7. Note that little discrepancy exists between the two models; when full load is applied, approximately a 0.05” difference between the vertical displacement of each model exists. Therefore, this developed finite element model is suitable for use in comparison between bracing options and an unbraced girder.

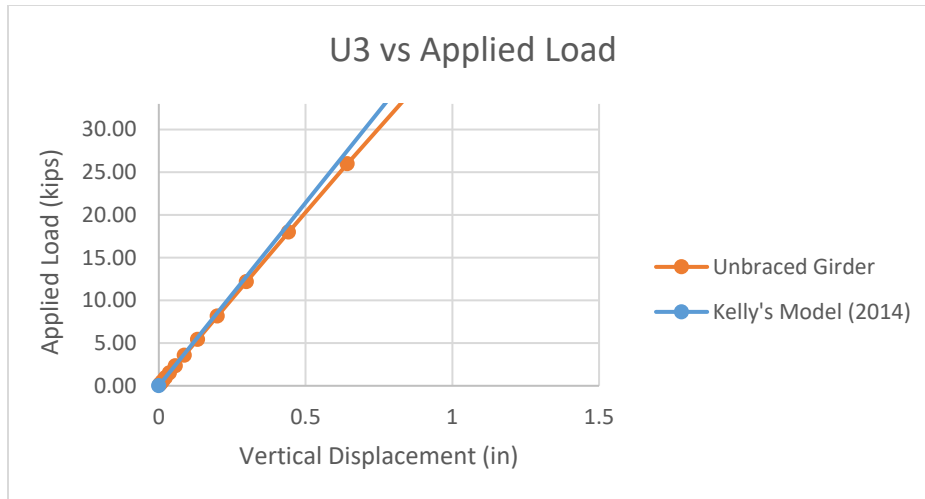


Figure 7:7: Vertical Deflection at Midspan for Unbraced Girder and Kelly (2014)

7.3 BRACING SCENARIOS

7.3.1 Internal Bracing Scenarios

Bracing schemes were examined for both the interior and exterior of the girder. Braces were modeled on a press-brake-formed tub girder constructed from an 84"x⁷/₁₆" plate. Four different bracing scenarios were implemented, each using L4x4x⁵/₈" angle for the brace members. Each transverse brace was spaced at three times the depth of the girder from one another, or 69", in the case of the modeled girder. A visual representation of the four internal bracing scenarios is provided in Figure 7.8.

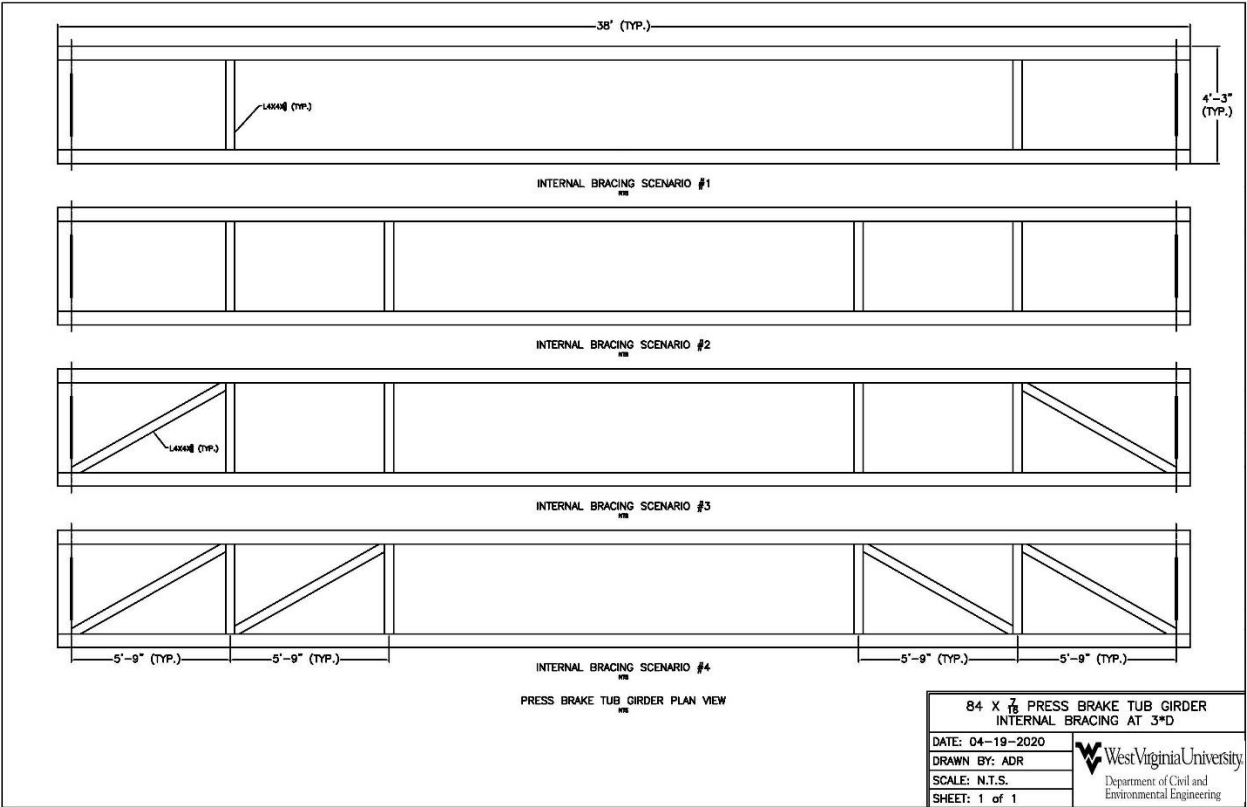


Figure 7:8: Internal Bracing Scenarios

7.3.2 External Bracing Scenarios

In addition to the internal bracing scenarios, three external bracing options were modeled. A press-brake-formed tub girder constructed from 84"x^{7/16}" plate was used for each external bracing scenario, so adequate comparisons could be made. External braces were placed at midspan for scenario 1, third points for scenario 2, and quarter points for scenario 3. External bracing was modeled in Abaqus/CAE through the use of boundary conditions to provide lateral support at the locations of interest. A visual representation of the three external bracing scenarios is provided in Figure 7.9.

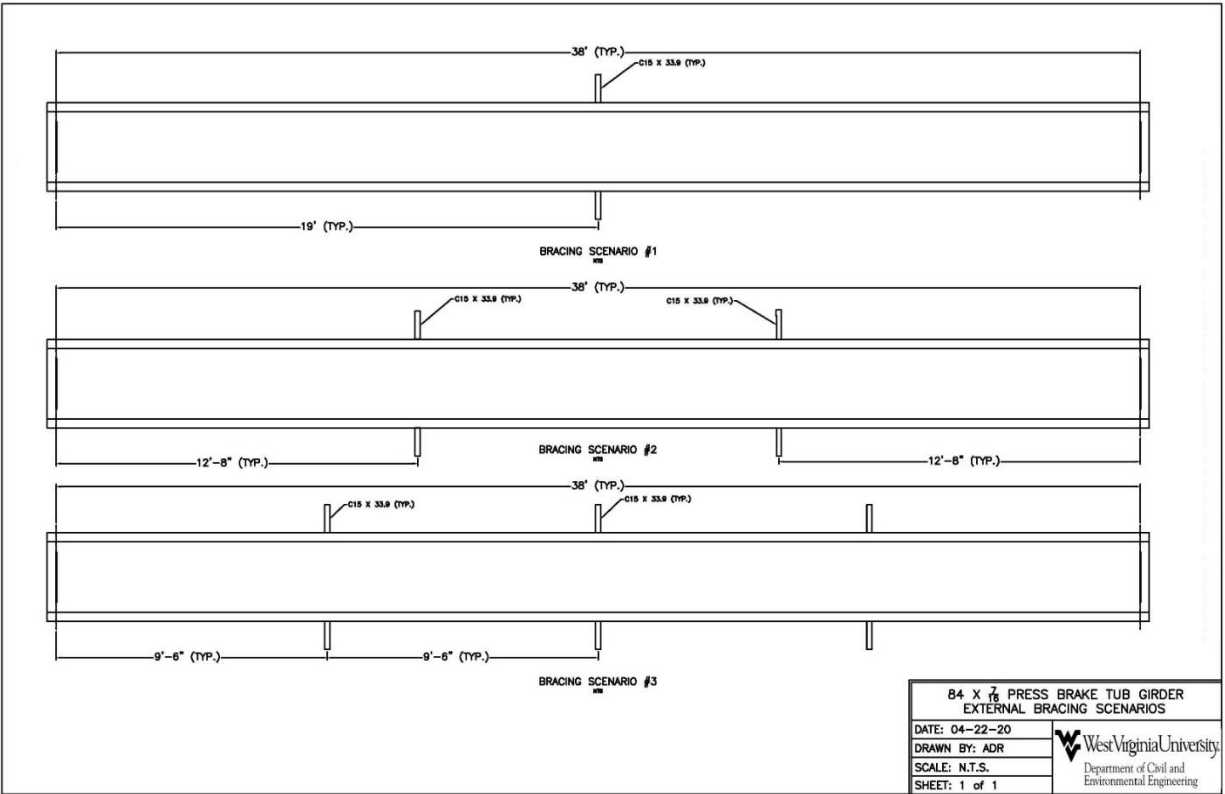


Figure 7.9: External Bracing Scenarios

7.4 RESULTS OF FINITE ELEMENT ANALYSIS

This section discusses the results achieved as a function of the finite element analysis. Both the set of internal braces and external braces were compared to the unbraced girder as a benchmark to assess resistance to torsion. Static Riks loading was applied to the structure and plots were developed from the load proportionality factors available in the Abaqus/CAE .dat file. For the purposes of these plots, U1 refers to the lateral displacement and U3 refers to the vertical displacement. The plots stop at 33 kips of applied load because this was the critical load to induce buckling in the unbraced girder in Kelly’s experiment (2014).

7.4.1 Comparison of Internal Bracing Scenarios

The first analyses were performed on the internal bracing options. L4x4x⁵/₈” angle was used for each interior bracing member and each member was modeled as a beam element in the finite element model. From the load proportionality factors, plots of U1 and U3 for each load increment were produced. Figure 7.10 shows the lateral displacement for each of the internal bracing options and Figure 7.11 shows the vertical displacement for each of the internal bracing options. It should be noted that while internal bracing has little effect on the vertical displacement at midspan, lateral displacement is reduced. Specifically, in the cases of internal bracing options where a diagonal brace is used, the decrease in lateral displacement is significant.

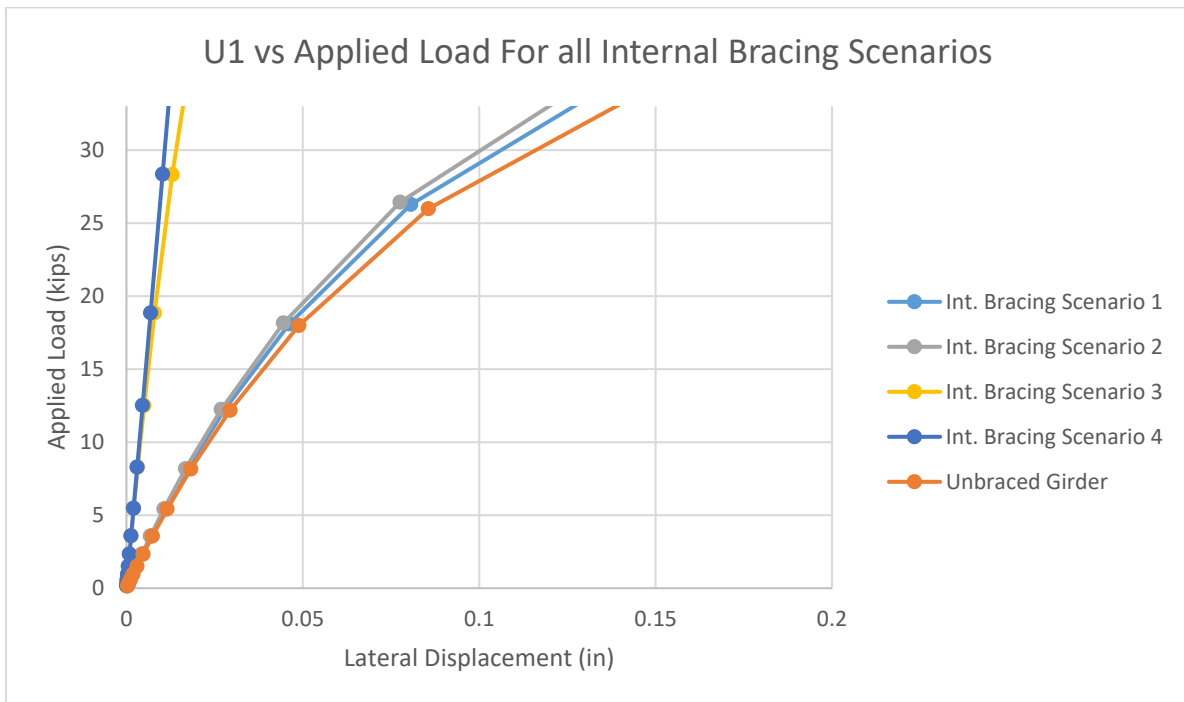


Figure 7:10: Lateral Displacement Comparison for Internal Bracing Scenarios

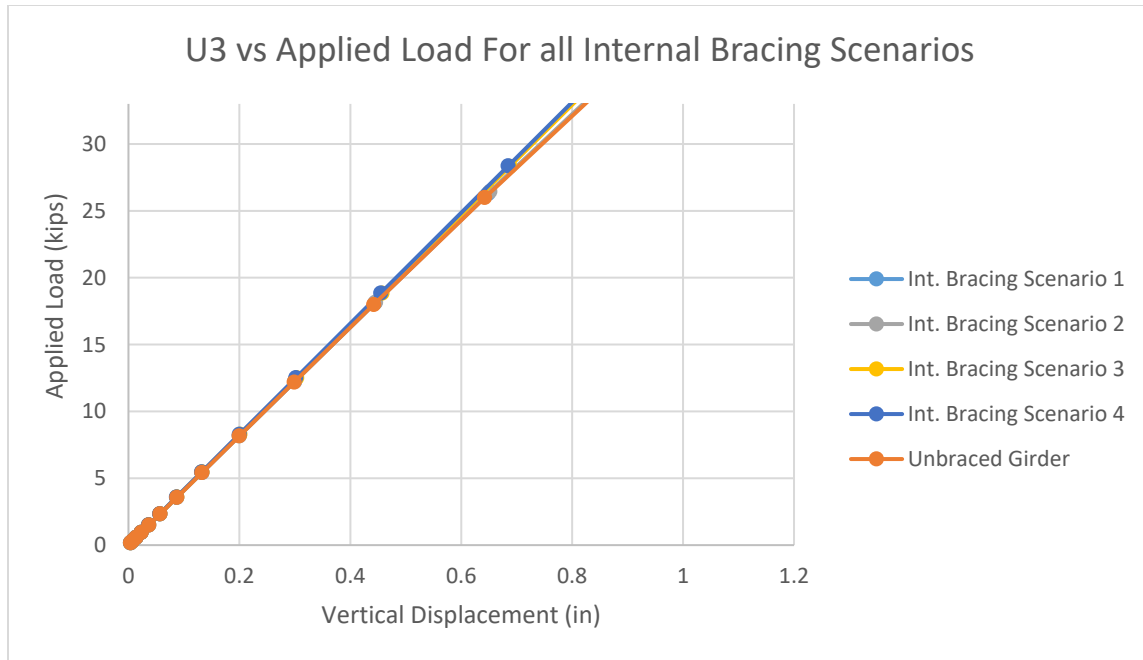


Figure 7:11: Lateral Displacement Comparison for Internal Bracing Scenarios

7.4.2 Comparison of External Bracing Scenarios

After the internal bracing analyses were completed, analyses were performed on the external bracing options. Lateral support was added at points of interest through boundary conditions at the web to resist lateral movement. From the load proportionality factors, plots of U1 and U3 for each load increment were produced. Figure 7.12 shows the lateral displacement for each of the external bracing options and Figure 7.13 shows the vertical displacement for each of the external bracing options. Similar to the internal bracing, external bracing has little effect on the vertical displacement at midspan. However, all three exterior bracing options have comparable resistance to lateral displacement, which differs significantly from the unbraced girder.

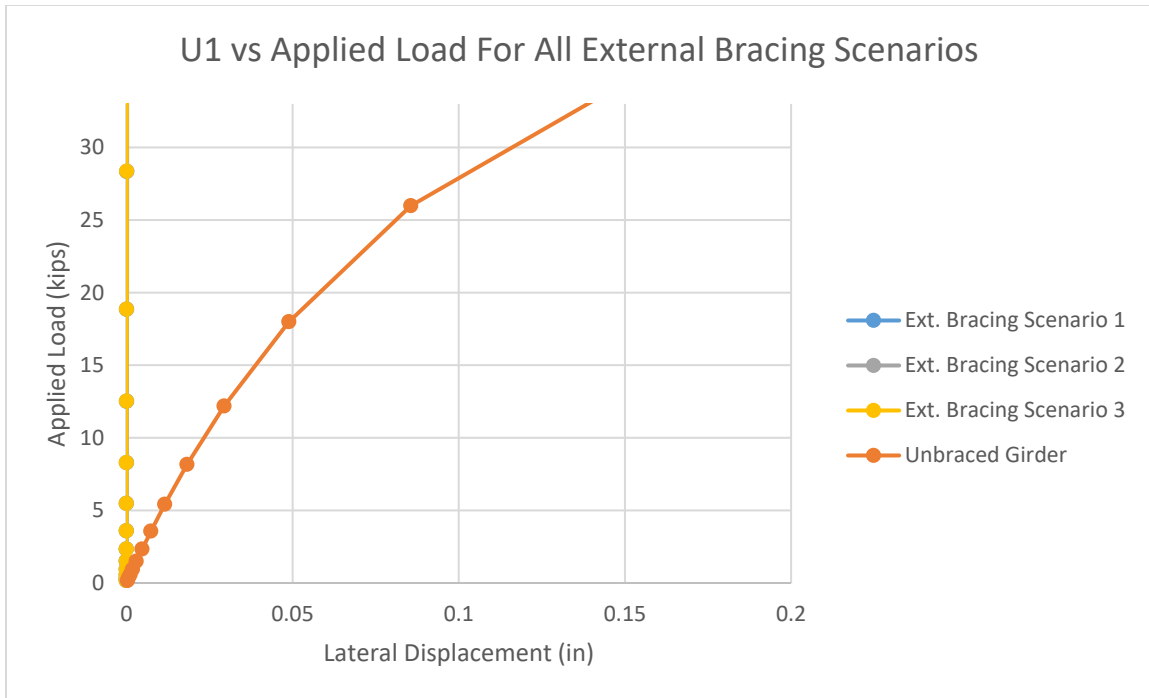


Figure 7:12: Lateral Displacement Comparison for External Bracing Scenarios

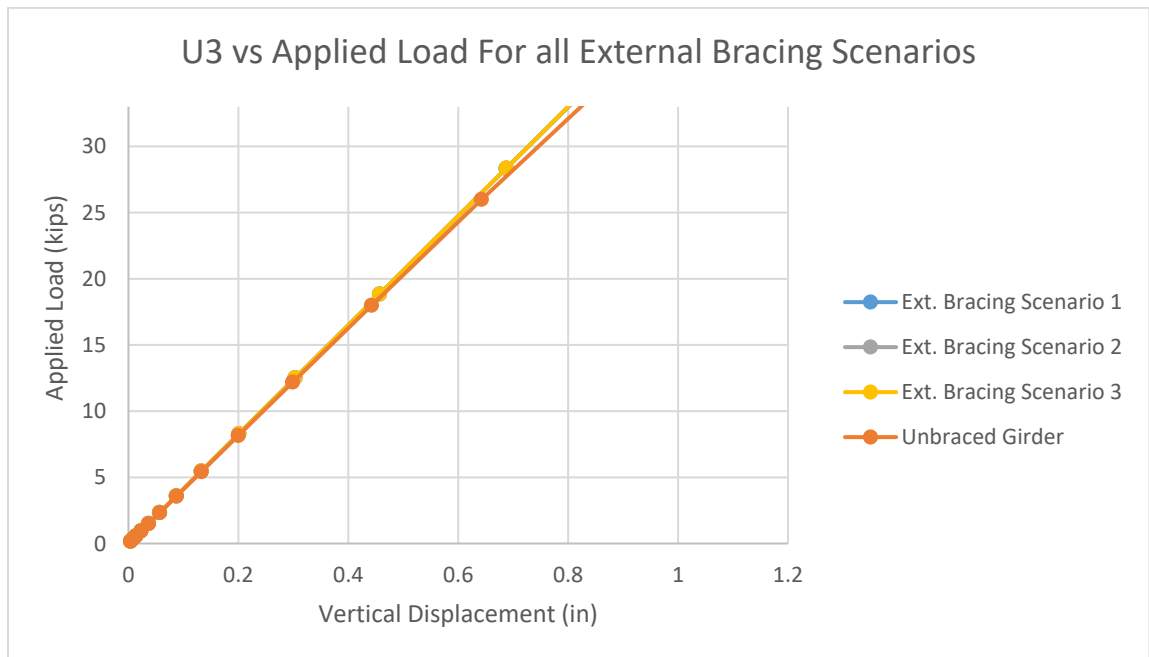


Figure 7:13: Vertical Displacement Comparison for External Bracing Scenarios

7.5 CONCLUSIONS

When employing a cast-in-place reinforced concrete deck in conjunction with press-brake-formed steel tub girders, it is important to consider the stability of the non-composite section under the effect of construction loading from placement of the wet concrete. Significant torsional amplification is possible, and the non-composite girder must have adequate lateral support to resist rotation and buckling. From the analyses ran, it was observed that the effect of diagonal struts for internal braces lead to a greater reduction in lateral displacement than the use of transverse braces alone. All external bracing options performed similar and each provided a significant reduction in lateral displacement. Further work is necessary to extend this initial qualitative modeling into sound reasoning for best practices for maintaining stability of the non-composite girder.

CHAPTER 8: CONCLUSIONS AND RECOMMENDATIONS

8.1 PROJECT SUMMARY AND CONCLUSIONS

The scope of this report was to evaluate the field performance of a modular press-brake-formed steel tub girder topped with a precast reinforced concrete deck in an application including skew and significant superelevation and compare that to analytical testing through finite element analysis and expected performance determined by AASHTO LRFD specifications. Bottom flange strain was recorded, and the LLDFs were determined for each method. The LLDFs determined with the experimental data and the analytical results showed little discrepancy, but both were lower than the LLDFs computed per AASHTO LRFD specifications. However, AASHTO does not specify a different expression for the calculation of LLDFs in regards to interior and exterior girders or the loading of single or multiple lanes. In either case, the AASHTO LLDFs were conservative, and are therefore safe to use in the design of press-brake-formed-tub girder systems.

8.2 RECOMMENDATIONS FOR CONTINUED WORK

The following are recommended for future work in this area:

- Current manufacturing methods limit the span length of press-brake-formed steel tub girders to 80'-0". Research could be performed to determine methods to increase span length and to determine the economic feasibility of longer spans.
- In cases where several spans are used, preferred detailing of the pier region should be examined to understand how the girders behave in the negative bending regions.
- Further work can investigate the ideal detailing and best practices for non-composite bracing of girders.
- Additional work could be performed to further define the lateral torsional buckling behavior of the press-brake-formed tub girders as a function of unbraced length.

REFERENCES

- (2017). *AASHTO LRFD Bridge Design Specifications*. Washington, DC: American Association of State Highway and Transportation Officials.
- Barth, K. E. (1996). *Moment-Rotation Characteristics for Inelastic Design of Steel Bridge Beams and Girders*. School of Civil Engineering. West Lafayette, IN, Purdue University. Doctor of Philosophy.
- Barth, K. E., Barth, A. S., Michaelson, G. K., Gibbs, C. L., & Tennant, R. M. (2017). *Evaluation of SMDI short span steel bridge design standards*.
- Bertoldi, A. G. (2009). *A strength and serviceability assesement of high performance steel bridge 10462* (Master's thesis). Available from ProQuest.
- Bridge Diagnostics, Inc. (n.d.). *STS-WiFi Operations Manual*. Boulder, CO.
- Bridge Engineering Software & Technology (BEST) Center. (2000). *Report on the Determination of Redundancy of the U.S. Bridge Corporation Bridge 3000*. University of Maryland, Civil Engineering.
- Burgueño, R., & Pavlich, B. S. (2008). *Evaluation of prefabricated composite steel box girder systems for rapid bridge construction*. (Report No. RC-1507).
- Burner, K. A. (2010). *Experimental investigation of folded plate girders and slap joints used in modular construction* (Master's Thesis). Available from University of Nebraska-Lincoln Database.
- Chandar, G., Hyzak, M. D., & Wolf, L. M. (2010). *Rapid, economical bridge replacement*. Available from Modern Steel Construction.
- Connor, R. J., Dexter, R., & Mahmoud, H. (2005). *NCHRP Synthesis 354: Inspection and Management of Bridges with Fracture-Critical Details*. National Cooperative Highway Research Program.

- Culmo, M. P. (2011). *Accelerated bridge construction: Experience in design, fabrication and erection of prefabricated bridge elements and systems* (Report No. FHWA-HIF-12-013). U. S. Department of Transportation, Federal Highway Administration.
- Dassault Systèmes (n.d.) *Abaqus/CAE User's Guide*. Providence, RI.
- Galindez, N. Y. (2009). *Levels of Lateral Flange Bending in Straight, Skewed and Curved Steel I-Girder Bridges During Deck Placement* (Doctoral dissertation). Available from ProQuest.
- Gibbs, C. L. (2017). *Field performance assessment of press-brake-formed steel tub girder superstructures* (Master's thesis). Available from ProQuest.
- Glaser, L. A. (2010). *Constructability testing of folded plate girders* (Master's Thesis). Available from University of Nebraska-Lincoln Database.
- Graybeal, B.A. and Swenty, M., "UHPFRC for Prefabricated Bridge Component Connections," *Proceedings of Hipermat 2012 3rd International Symposium on UHPC and Nanotechnology for High Performance Construction Materials*, Ed., Schmidt, M., Fehling, E., Glotzbach, C., Fröhlich, S., and Piotrowski, S., Kassel University Press, Kassel, Germany, 2012, pp. 663–668.
- Helwig, T. A., & Fan, Z. (2000). *Field and computational studies of steel trapezoidal box girder bridges* (Report No. 1395-3). Austin, Texas: Texas Department of Transportation.
- Kassimali, A. (2015). *Structural analysis* (5th ed.). Stamford, CT: Cengage Learning.
- Kelly, L. T. (2014). *Experimental evaluation of non-composite shallow press-brake-formed steel tub girders* (Master's thesis). Available from ProQuest.
- Kozhokin, P. (2016). *Evaluation of modular press-brake-formed tub girders with UHPC joints* (Master's thesis). Available from ProQuest.
- Michaelson, G. K. (2010). *Live Load Distribution Factors for Exterior Girders in Steel I-Girder Bridges* (Master's thesis). Available from ProQuest.
- Michaelson, G. K. (2014). *Development and feasibility assessment of shallow press-brake-formed steel tub girders for short-span bridge applications* (Doctoral dissertation). Available from ProQuest.

- Nakamura, S. (2002). Bending behavior of composite girders with cold formed steel U section. *ASCE Journal of Structural Engineering*, 128(9), 1169-1176. Doi: 10.1061-(ASCE)0733-9455(2002)128:9(1169).
- National Steel Bridge Alliance. (2010). Redundancy. In NSBA, *Steel Bridge Design Handbook*.
- Righman, J. E. (2005). Rotation Compatibility Approach to Moment Redistribution for Design and Rating of Steel I-Girders. Department of Civil & Environmental Engineering. Morgantown, WV, West Virginia University. Doctor of Philosophy.
- Roberts, N. R. (2004). Evaluation of the Ductility of Composite Steel I-Girders in Positive Bending. Department of Civil & Environmental Engineering. Morgantown, WV, West Virginia University. Master of Science.
- Phares, B., Deng, Y., & Steffens, O. (2017). *Evaluation of a folded plate girder bridge system*. (Report No. InTrans Project 13-458).
- Taly, N. B., & GangaRao, H. V. S. (1976). *Development and design of standardized short span bridge superstructural*. (Report No. FHWA-WV-76-5).
- The Mathworks, Inc. (2020). MATLAB. Natick, MA, The Mathworks, Inc.
- Tennant, R. M. (2018). *Fatigue Performance of Uncoated and Galvanized Composite Press-Brake-Formed Tub Girders* (Master's thesis). Available from ProQuest.
- Tricon Engineering Group, Ltd. (2008). *Standard design and details of press-brake-formed steel tub girder*. Tricon Engineering Group: Michigan.
- Underwood, N. M. H. (2019). *Field Performance and Rating Evaluation of a Modular Press-Brake-Formed Steel Tub Girder with a Steel Sandwich Plate Deck* (Master's thesis). Available from ProQuest.
- Yang, L. (2004). Evaluation of Moment Redistribution for Hybrid HPS 70W Bridge Girders. Department of Civil & Environmental Engineering. Morgantown, WV, West Virginia University. Master of Science.

APPENDIX A: RESULTS FOR ALL TRUCK RUNS

This appendix includes the following: results, tables, and graphs, generated from both the live load field test and finite element analysis of the Fourteen Mile Bridge. The data presented is for all girders, for all load runs.

The following is the order that the data is presented:

- Live Load Distribution Factors (LLDFs)
 - Live Load Test Data
 - Finite Element Analysis
 - Results Comparison: Live Load Test Data vs. Finite Element Analysis
 - Results Comparison: Live Load, FEA, & AASHTO LRFD

A.1 LIVE LOAD DISTRIBUTION FACTORS

A.1.1 Live Load Field Test Results

Truck Run 1, Simplified Distribution Factors (Field)												
Panel Points		Averages ($\mu\epsilon$)					Distribution Factors					
x (ft)	x/L	G1	G2	G3	G4	G5	G1	G2	G3	G4	G5	
0	0	0	0	0	0	0	---	---	---	---	---	
5.8	0.1	5.513	2.877	0.157	-1.270	-3.635	1.514	0.790	0.043	-0.349	-0.998	
11.6	0.2	17.992	14.074	9.539	5.401	0.336	0.380	0.297	0.201	0.114	0.007	
17.4	0.3	34.632	30.154	21.157	12.541	4.579	0.336	0.293	0.205	0.122	0.044	
23.2	0.4	52.685	49.797	30.625	16.274	6.498	0.338	0.319	0.196	0.104	0.042	
29	0.5	64.277	59.563	35.360	17.456	6.418	0.351	0.325	0.193	0.095	0.035	
34.8	0.6	66.936	64.148	37.530	16.816	5.658	0.350	0.336	0.196	0.088	0.030	
40.6	0.7	72.247	71.656	32.655	11.770	2.987	0.378	0.375	0.171	0.062	0.016	
46.4	0.8	70.454	65.424	25.459	7.196	0.984	0.416	0.386	0.150	0.042	0.006	
52.2	0.9	42.457	36.502	12.600	0.863	-2.546	0.472	0.406	0.140	0.010	-0.028	
58	1	0	0	0	0	0	---	---	---	---	---	
							DF @ 0.5L (PP 5)	0.351	0.325	0.193	0.095	0.035
							MPF Applied	0.421	0.390	0.232	0.114	0.042
							St. Dev.	0.381	0.154	0.052	0.147	0.340

Truck Run 2, Simplified Distribution Factors (Field)											
Panel Points		Averages ($\mu\epsilon$)					Distribution Factors				
x (ft)	x/L	G1	G2	G3	G4	G5	G1	G2	G3	G4	G5
0	0	0	0	0	0	0	---	---	---	---	---
5.8	0.1	8.505	6.033	4.168	3.289	0.563	0.377	0.267	0.185	0.146	0.025
11.6	0.2	22.117	17.984	14.678	11.505	5.427	0.308	0.251	0.205	0.160	0.076
17.4	0.3	36.747	32.747	26.117	18.402	9.268	0.298	0.266	0.212	0.149	0.075
23.2	0.4	51.932	50.893	35.910	21.822	10.490	0.304	0.298	0.210	0.128	0.061
29	0.5	63.244	61.446	40.824	22.688	10.049	0.319	0.310	0.206	0.114	0.051
34.8	0.6	64.947	64.901	42.363	21.576	9.032	0.320	0.320	0.209	0.106	0.045
40.6	0.7	68.440	73.760	39.378	16.644	6.491	0.334	0.360	0.192	0.081	0.032
46.4	0.8	65.714	68.033	31.426	11.322	3.890	0.364	0.377	0.174	0.063	0.022
52.2	0.9	40.242	37.619	16.690	4.385	0.289	0.406	0.379	0.168	0.044	0.003
58	1	0	0	0	0	0	---	---	---	---	---
DF @ 0.5L (PP 5)							0.319	0.310	0.206	0.114	0.051
MPF Applied							0.383	0.372	0.247	0.137	0.061
St. Dev.							0.037	0.049	0.016	0.040	0.025

Truck Run 3, Simplified Distribution Factors (Field)											
Panel Points		Averages ($\mu\epsilon$)					Distribution Factors				
x (ft)	x/L	G1	G2	G3	G4	G5	G1	G2	G3	G4	G5
0	0	0	0	0	0	0	---	---	---	---	---
5.8	0.1	10.424	8.054	6.671	8.875	7.108	0.253	0.196	0.162	0.216	0.173
11.6	0.2	19.645	16.209	14.286	17.690	13.036	0.243	0.200	0.177	0.219	0.161
17.4	0.3	26.596	25.038	24.290	26.307	16.946	0.223	0.210	0.204	0.221	0.142
23.2	0.4	32.323	37.612	39.361	34.264	19.479	0.198	0.231	0.241	0.210	0.119
29	0.5	38.505	50.209	50.322	39.875	20.914	0.193	0.251	0.252	0.200	0.105
34.8	0.6	40.285	53.099	54.568	41.034	19.320	0.193	0.255	0.262	0.197	0.093
40.6	0.7	34.296	58.382	63.334	36.887	14.382	0.165	0.282	0.306	0.178	0.069
46.4	0.8	26.985	56.118	57.170	29.157	9.991	0.150	0.313	0.319	0.163	0.056
52.2	0.9	17.820	33.427	31.944	18.003	5.581	0.167	0.313	0.299	0.169	0.052
58	1	0	0	0	0	0	---	---	---	---	---
DF @ 0.5L (PP 5)							0.193	0.251	0.252	0.200	0.105
MPF Applied							0.231	0.302	0.302	0.239	0.126
St. Dev.							0.035	0.045	0.057	0.022	0.045

Truck Run 4, Simplified Distribution Factors (Field)											
Panel Points		Averages ($\mu\epsilon$)					Distribution Factors				
x (ft)	x/L	G1	G2	G3	G4	G5	G1	G2	G3	G4	G5
0	0	0	0	0	0	0	---	---	---	---	---
5.8	0.1	7.419	6.902	4.758	6.622	7.862	2.038	1.896	1.307	1.819	2.159
11.6	0.2	14.049	14.062	11.014	14.329	15.004	0.297	0.297	0.233	0.303	0.317
17.4	0.3	19.815	22.314	20.415	24.759	21.447	0.192	0.217	0.198	0.240	0.208
23.2	0.4	24.036	31.182	35.360	38.414	25.988	0.154	0.200	0.227	0.246	0.167
29	0.5	26.808	39.315	47.951	46.401	28.264	0.146	0.215	0.262	0.253	0.154
34.8	0.6	26.434	41.748	49.072	47.439	26.622	0.138	0.218	0.257	0.248	0.139
40.6	0.7	21.341	39.722	58.573	49.935	20.828	0.112	0.208	0.306	0.261	0.109
46.4	0.8	14.110	33.535	57.812	42.109	14.042	0.083	0.198	0.341	0.248	0.083
52.2	0.9	6.266	19.831	28.734	21.032	5.861	0.070	0.221	0.320	0.234	0.065
58	1	0	0	0	0	0	---	---	---	---	---
DF @ 0.5L (PP 5)							0.146	0.215	0.262	0.253	0.154
MPF Applied							0.176	0.258	0.314	0.304	0.185
St. Dev.							0.633	0.559	0.349	0.522	0.672

Truck Run 5, Simplified Distribution Factors (Field)											
Panel Points		Averages ($\mu\epsilon$)					Distribution Factors				
x (ft)	x/L	G1	G2	G3	G4	G5	G1	G2	G3	G4	G5
0	0	0	0	0	0	0	---	---	---	---	---
5.8	0.1	6.770	6.963	5.457	6.900	8.822	0.300	0.309	0.242	0.306	0.391
11.6	0.2	13.043	13.785	11.549	14.346	16.233	0.182	0.192	0.161	0.200	0.226
17.4	0.3	18.791	22.109	21.456	25.369	23.667	0.152	0.179	0.174	0.206	0.192
23.2	0.4	22.567	29.653	35.506	39.254	28.584	0.132	0.173	0.208	0.229	0.167
29	0.5	24.876	36.364	47.468	47.821	31.227	0.125	0.183	0.239	0.241	0.158
34.8	0.6	23.978	38.349	48.333	49.065	29.739	0.118	0.189	0.238	0.242	0.147
40.6	0.7	19.898	36.238	57.930	54.053	24.878	0.097	0.177	0.283	0.264	0.122
46.4	0.8	14.699	31.272	58.569	48.251	19.207	0.081	0.173	0.325	0.267	0.106
52.2	0.9	8.868	20.593	32.454	26.639	11.212	0.089	0.208	0.327	0.268	0.113
58	1	0	0	0	0	0	---	---	---	---	---
DF @ 0.5L (PP 5)							0.125	0.183	0.239	0.241	0.158
MPF Applied							0.151	0.220	0.287	0.289	0.189
St. Dev.							0.067	0.043	0.059	0.033	0.088

Truck Run 6, Simplified Distribution Factors (Field)											
Panel Points		Averages ($\mu\epsilon$)					Distribution Factors				
x (ft)	x/L	G1	G2	G3	G4	G5	G1	G2	G3	G4	G5
0	0	0	0	0	0	0	---	---	---	---	---
5.8	0.1	4.692	6.266	7.309	7.581	10.082	0.114	0.152	0.178	0.184	0.245
11.6	0.2	9.066	12.474	14.712	15.602	20.162	0.112	0.154	0.182	0.193	0.249
17.4	0.3	12.042	17.365	22.484	26.079	31.446	0.101	0.146	0.189	0.219	0.264
23.2	0.4	14.500	21.298	30.378	41.059	44.683	0.089	0.131	0.186	0.252	0.274
29	0.5	16.202	24.443	37.352	54.404	52.674	0.081	0.122	0.187	0.272	0.264
34.8	0.6	16.196	24.853	40.422	57.132	54.459	0.078	0.119	0.194	0.274	0.261
40.6	0.7	11.886	19.162	36.254	63.694	54.936	0.057	0.092	0.175	0.307	0.265
46.4	0.8	7.708	12.997	29.689	62.683	47.209	0.043	0.072	0.165	0.349	0.263
52.2	0.9	5.491	8.489	20.109	37.463	28.538	0.051	0.079	0.188	0.351	0.267
58	1	0	0	0	0	0	---	---	---	---	---
DF @ 0.5L (PP 5)							0.081	0.122	0.187	0.272	0.264
MPF Applied							0.097	0.147	0.224	0.327	0.316
St. Dev.							0.026	0.031	0.009	0.062	0.009

Truck Runs 1 and 4, Simplified Distribution Factors (Field)											
Panel Points		Averages ($\mu\epsilon$)					Distribution Factors				
x (ft)	x/L	G1	G2	G3	G4	G5	G1	G2	G3	G4	G5
0	0	0	0	0	0	0	---	---	---	---	---
5.8	0.1	12.932	9.779	4.914	5.352	4.227	0.348	0.263	0.132	0.144	0.114
11.6	0.2	32.041	28.135	20.554	19.731	15.341	0.277	0.243	0.177	0.170	0.132
17.4	0.3	54.448	52.468	41.572	37.300	26.026	0.257	0.248	0.196	0.176	0.123
23.2	0.4	76.721	80.979	65.985	54.688	32.486	0.247	0.261	0.212	0.176	0.105
29	0.5	91.085	98.877	83.310	63.857	34.681	0.245	0.266	0.224	0.172	0.093
34.8	0.6	93.370	105.896	86.602	64.255	32.280	0.244	0.277	0.226	0.168	0.084
40.6	0.7	93.589	111.379	91.229	61.705	23.815	0.245	0.292	0.239	0.162	0.062
46.4	0.8	84.565	98.959	83.272	49.304	15.026	0.255	0.299	0.251	0.149	0.045
52.2	0.9	48.723	56.333	41.333	21.895	3.316	0.284	0.328	0.241	0.128	0.019
58	1	0	0	0	0	0	---	---	---	---	---
DF @ 0.5L (PP 5)							0.245	0.266	0.224	0.172	0.093
MPF Applied							0.490	0.532	0.448	0.343	0.187
St. Dev.							0.034	0.027	0.038	0.017	0.038

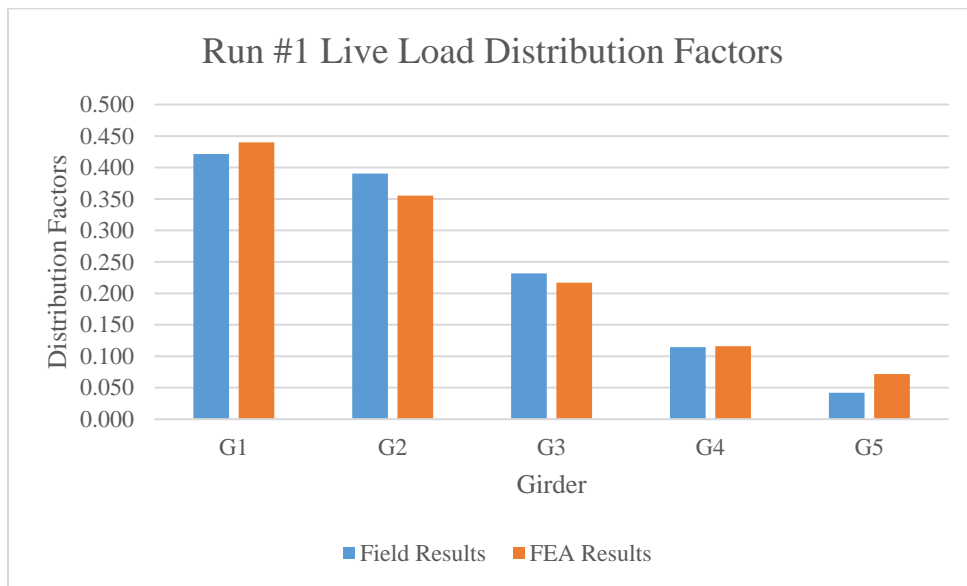
Truck Runs 2 and 5, Simplified Distribution Factors (Field)											
Panel Points		Averages ($\mu\epsilon$)					Distribution Factors				
x (ft)	x/L	G1	G2	G3	G4	G5	G1	G2	G3	G4	G5
0	0	0	0	0	0	0	---	---	---	---	---
5.8	0.1	15.275	12.995	9.626	10.189	9.385	0.266	0.226	0.167	0.177	0.163
11.6	0.2	35.160	31.769	26.227	25.851	21.660	0.250	0.226	0.186	0.184	0.154
17.4	0.3	55.539	54.856	47.573	43.771	32.935	0.237	0.234	0.203	0.187	0.140
23.2	0.4	74.498	80.546	71.417	61.077	39.075	0.228	0.247	0.219	0.187	0.120
29	0.5	88.119	97.811	88.293	70.508	41.275	0.228	0.253	0.229	0.183	0.107
34.8	0.6	88.925	103.251	90.696	70.641	38.770	0.227	0.263	0.231	0.180	0.099
40.6	0.7	88.338	109.998	97.308	70.697	31.370	0.222	0.277	0.245	0.178	0.079
46.4	0.8	80.413	99.305	89.996	59.574	23.098	0.228	0.282	0.255	0.169	0.066
52.2	0.9	49.111	58.211	49.144	31.024	11.501	0.247	0.293	0.247	0.156	0.058
58	1	0	0	0	0	0	---	---	---	---	---
DF @ 0.5L (PP 5)							0.228	0.253	0.229	0.183	0.107
MPF Applied							0.457	0.507	0.457	0.365	0.214
St. Dev.							0.014	0.025	0.030	0.010	0.038

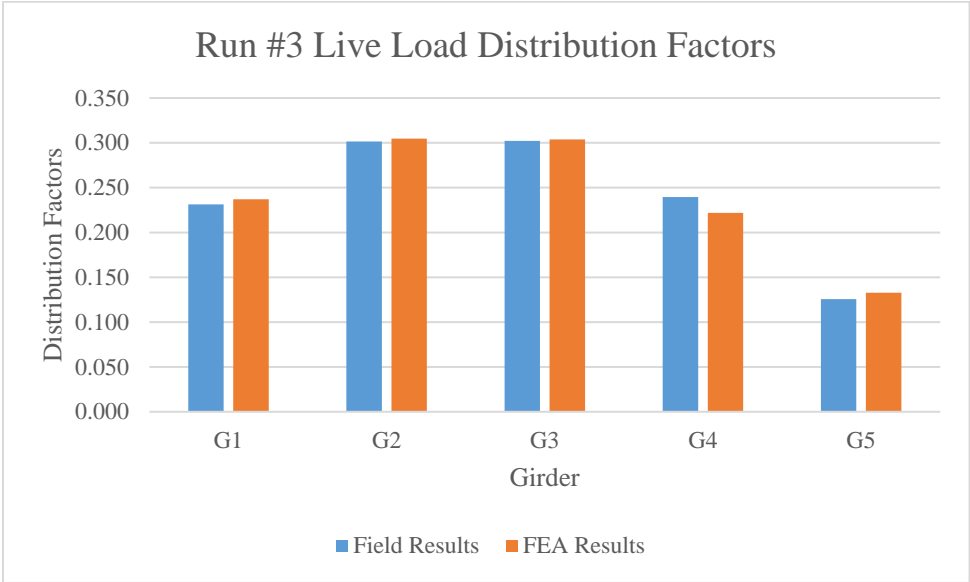
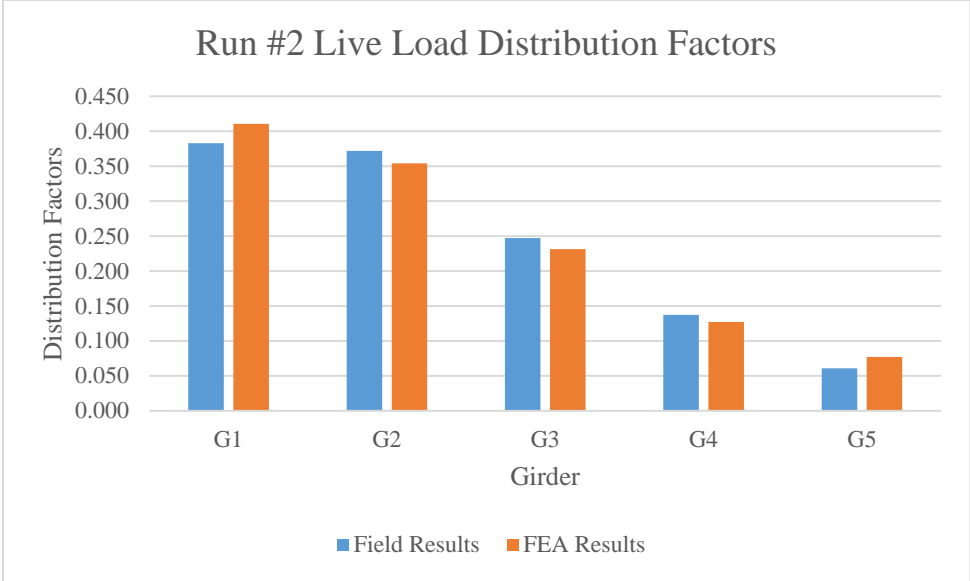
Truck Runs 3 and 6, Simplified Distribution Factors (Field)											
Panel Points		Averages ($\mu\epsilon$)					Distribution Factors				
x (ft)	x/L	G1	G2	G3	G4	G5	G1	G2	G3	G4	G5
0	0	0	0	0	0	0	---	---	---	---	---
5.8	0.1	15.116	14.319	13.980	16.456	17.190	0.196	0.186	0.181	0.214	0.223
11.6	0.2	28.711	28.682	28.997	33.292	33.198	0.188	0.188	0.190	0.218	0.217
17.4	0.3	38.638	42.403	46.774	52.386	48.392	0.169	0.185	0.205	0.229	0.212
23.2	0.4	46.823	58.911	69.739	75.322	64.162	0.149	0.187	0.221	0.239	0.204
29	0.5	54.707	74.652	87.673	94.279	73.587	0.142	0.194	0.228	0.245	0.191
34.8	0.6	56.481	77.952	94.990	98.166	73.779	0.141	0.194	0.237	0.245	0.184
40.6	0.7	46.182	77.544	99.588	100.581	69.318	0.117	0.197	0.253	0.256	0.176
46.4	0.8	34.693	69.115	86.859	91.840	57.200	0.102	0.203	0.256	0.270	0.168
52.2	0.9	23.311	41.916	52.053	55.466	34.119	0.113	0.203	0.252	0.268	0.165
58	1	0	0	0	0	0	---	---	---	---	---
DF @ 0.5L (PP 5)							0.142	0.194	0.228	0.245	0.191
MPF Applied							0.284	0.388	0.456	0.490	0.382
St. Dev.							0.033	0.007	0.028	0.020	0.022

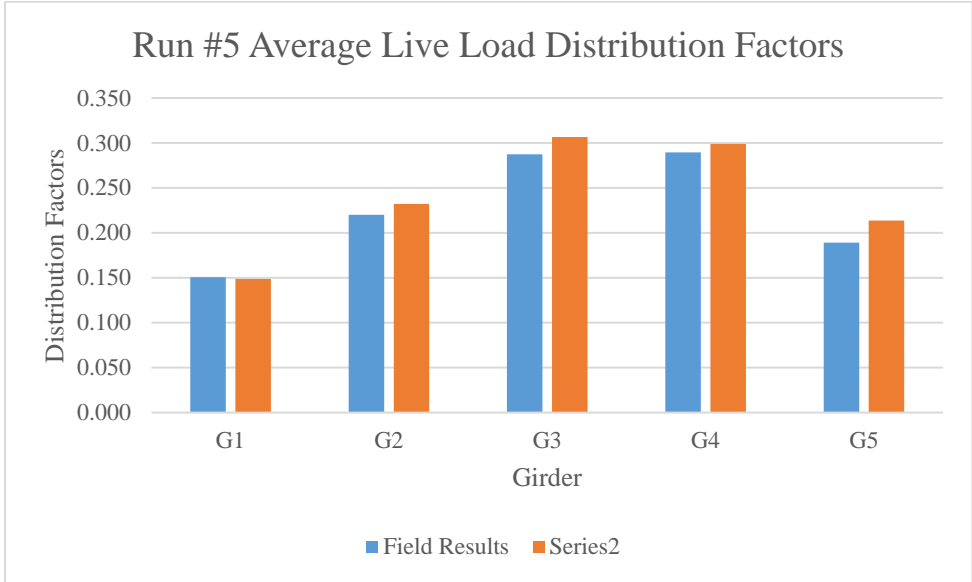
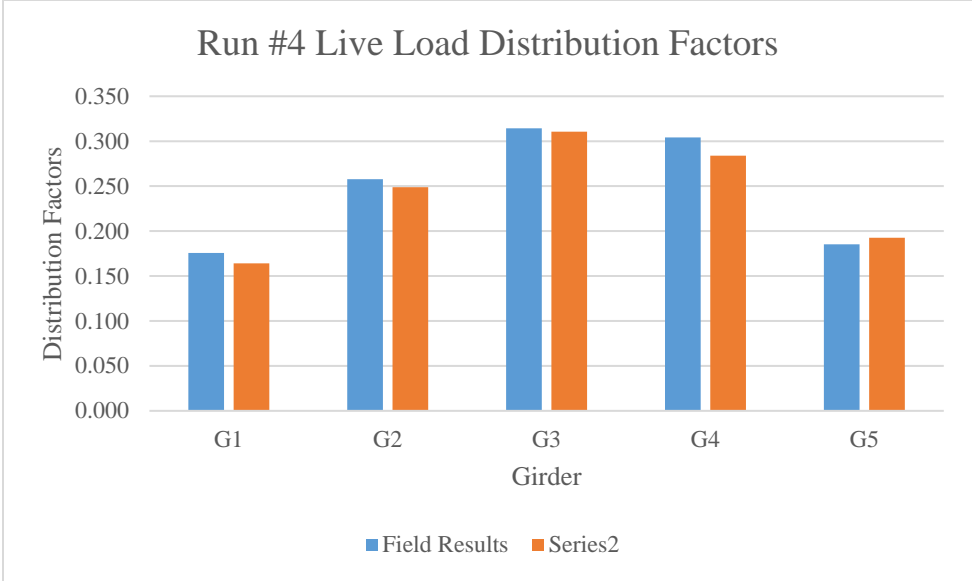
A.1.2 Finite Element Analysis Results

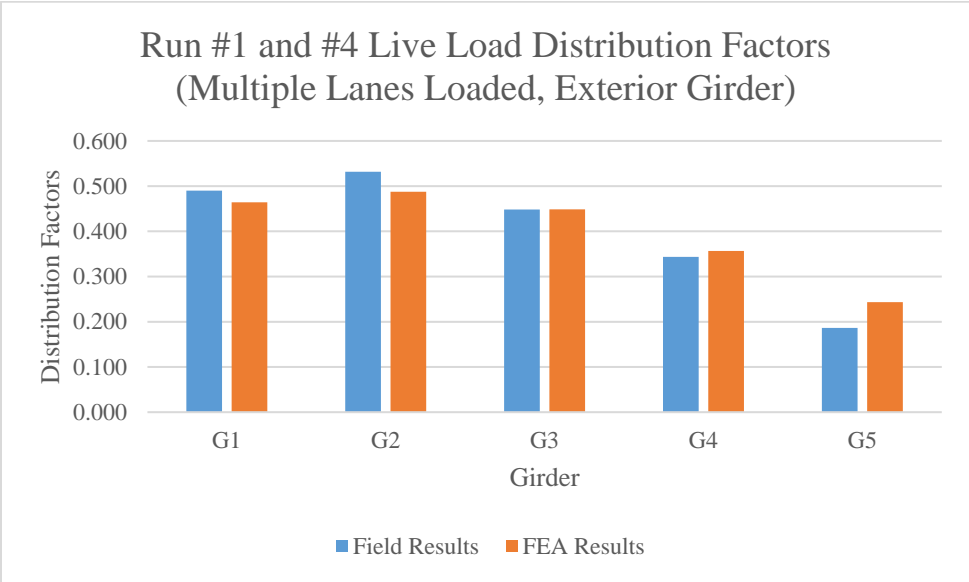
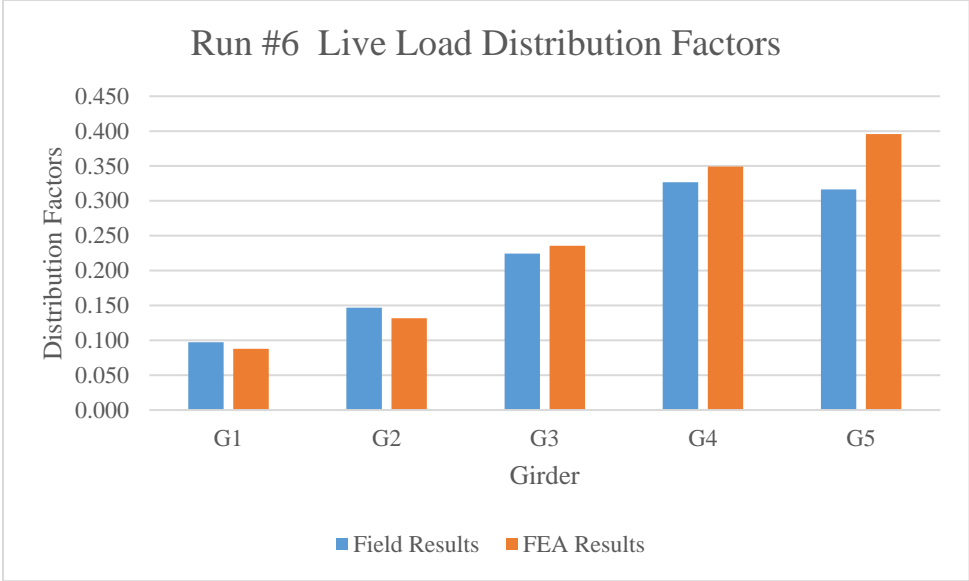
Summary of Live Load Distribution Factors (FEA)					
Truck Run	G1	G2	G3	G4	G5
Run 1	0.440	0.355	0.217	0.116	0.072
Run 2	0.411	0.354	0.231	0.127	0.077
Run 3	0.237	0.305	0.304	0.222	0.133
Run 4	0.164	0.249	0.311	0.284	0.193
Run 5	0.149	0.232	0.307	0.299	0.214
Run 6	0.088	0.132	0.236	0.349	0.396
Runs 1+4	0.502	0.503	0.440	0.334	0.221
Runs 2+5	0.464	0.487	0.449	0.356	0.243
Runs 3+6	0.269	0.362	0.449	0.477	0.443

A.1.3 Results Comparison: Live Load Field Test vs. Finite Element Analysis

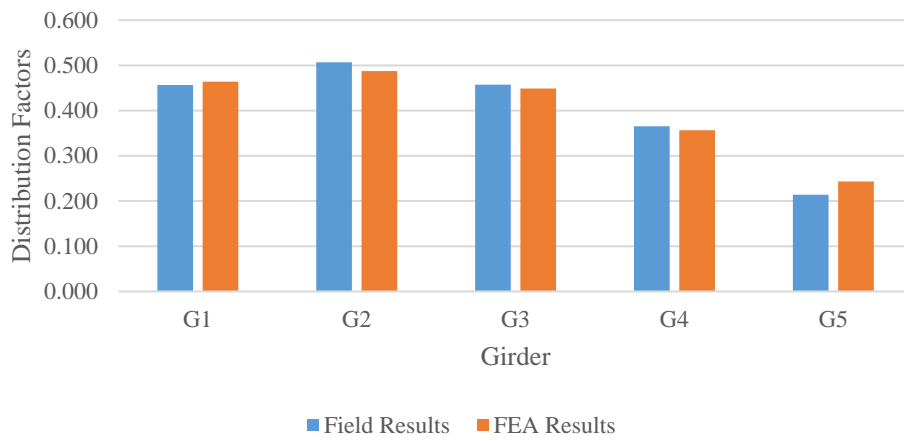




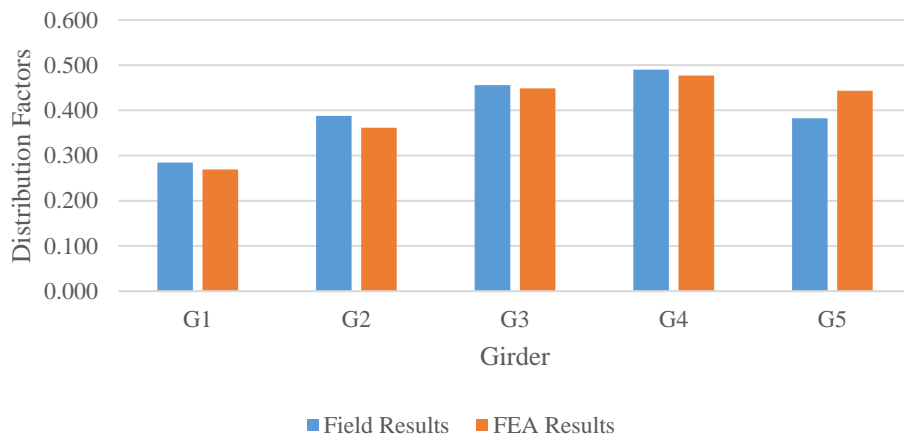




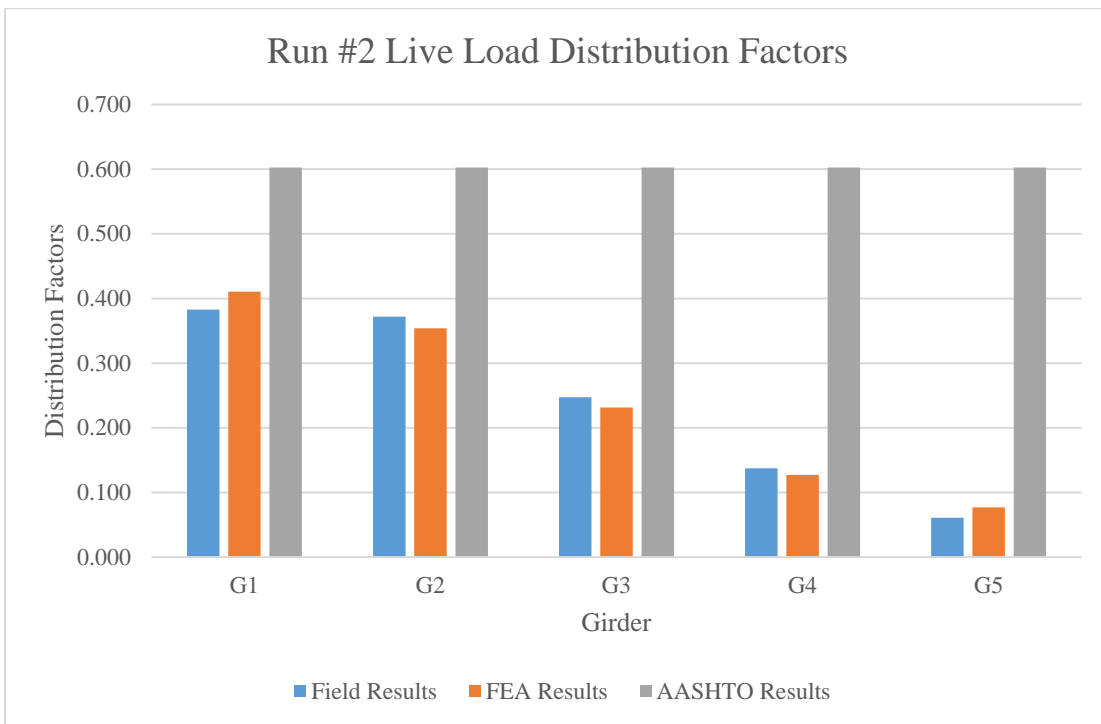
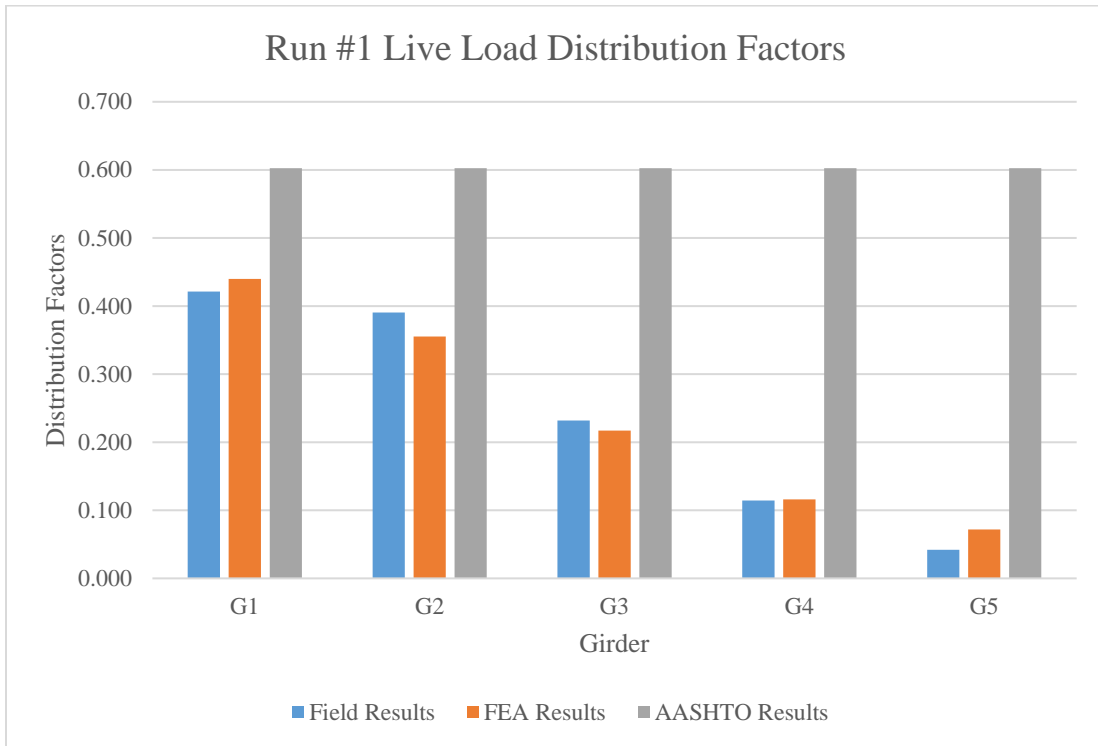
Run #2 and #5 Live Load Distribution Factors
(Multiple Lanes Loaded, Interior Girder)

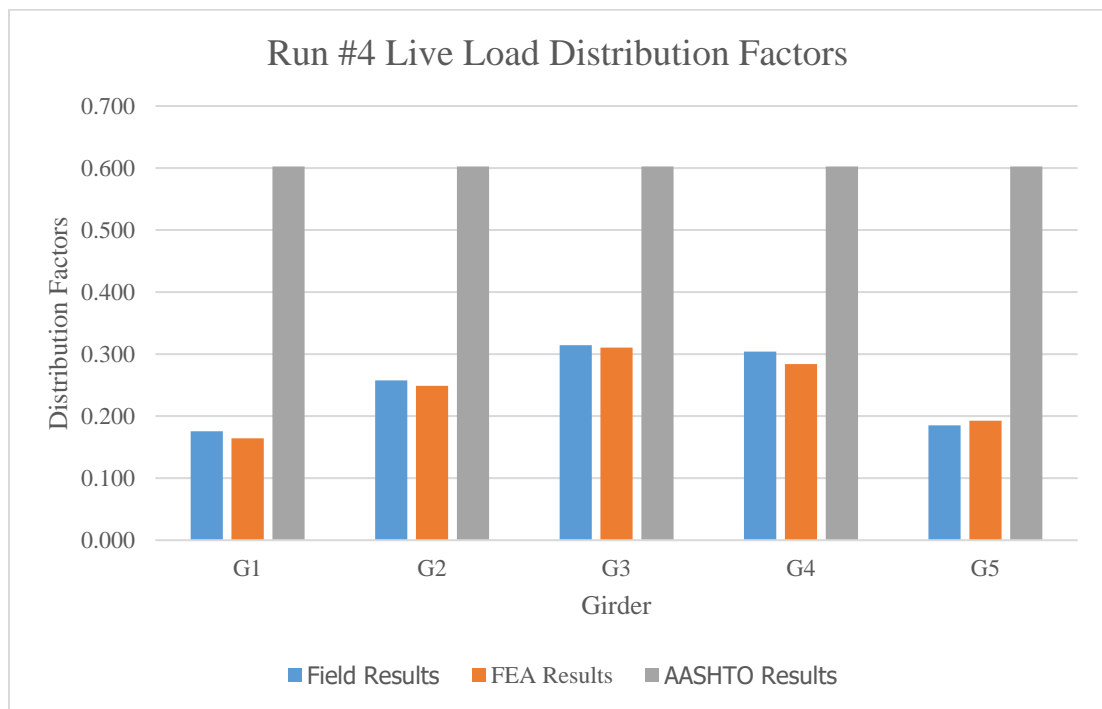


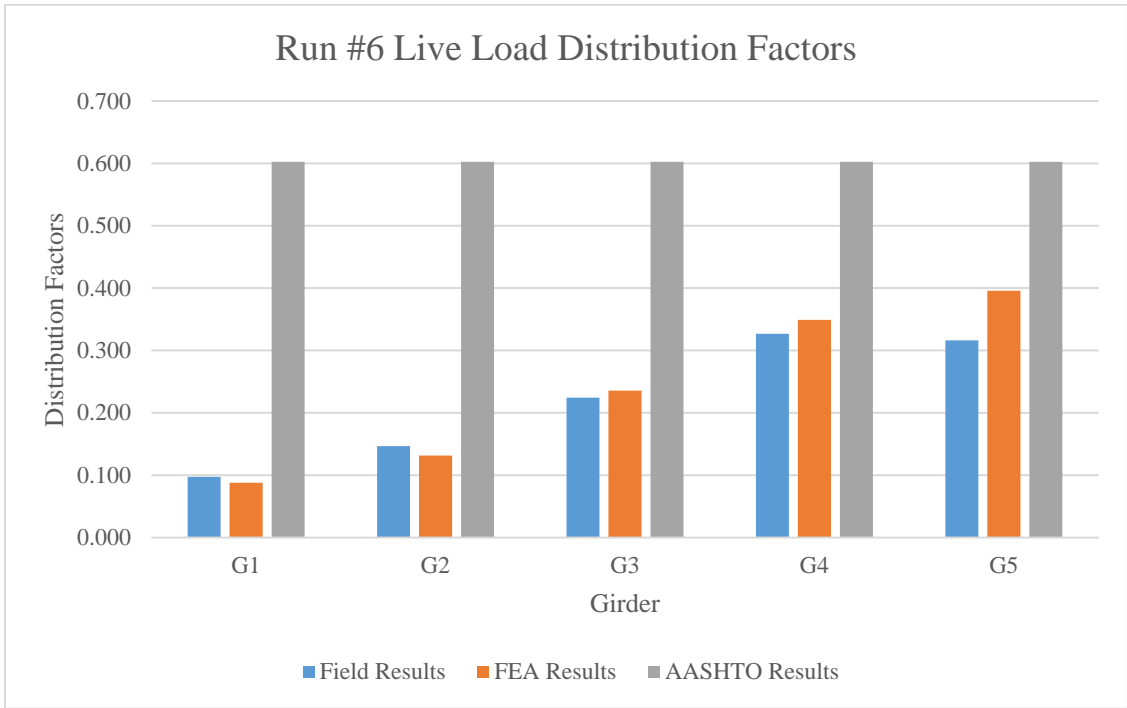
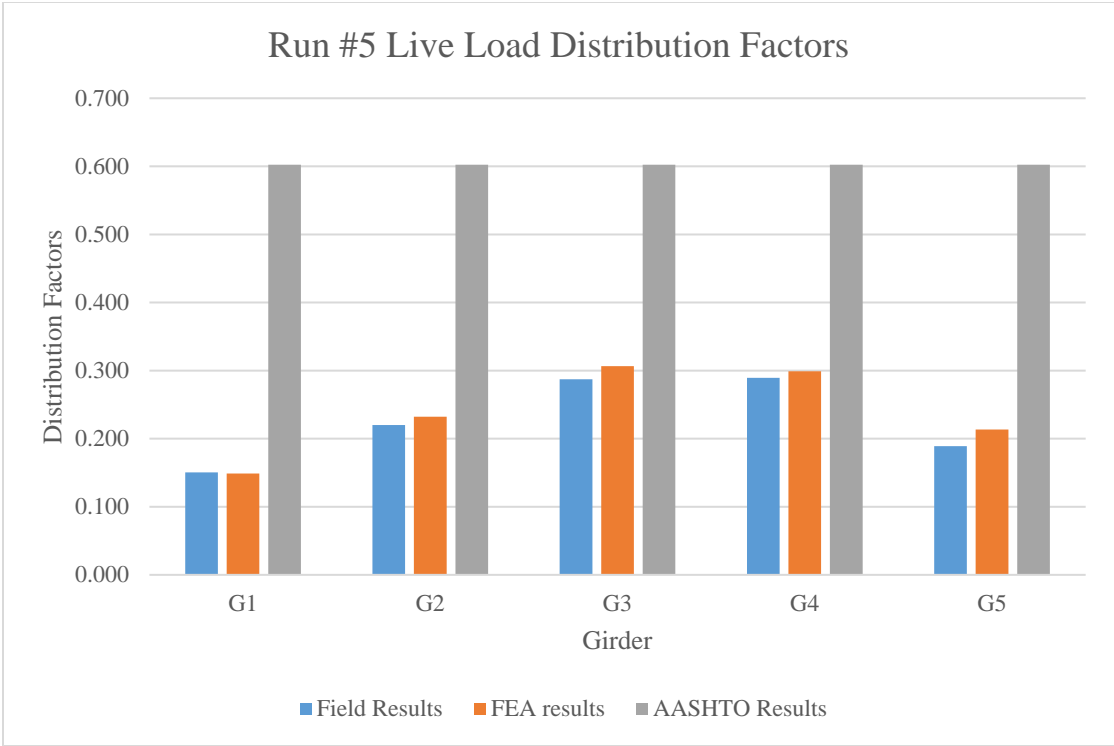
Run #3 and #6 Live Load Distribution Factors
(Multiple Lanes Loaded, Middle Interior Girder)

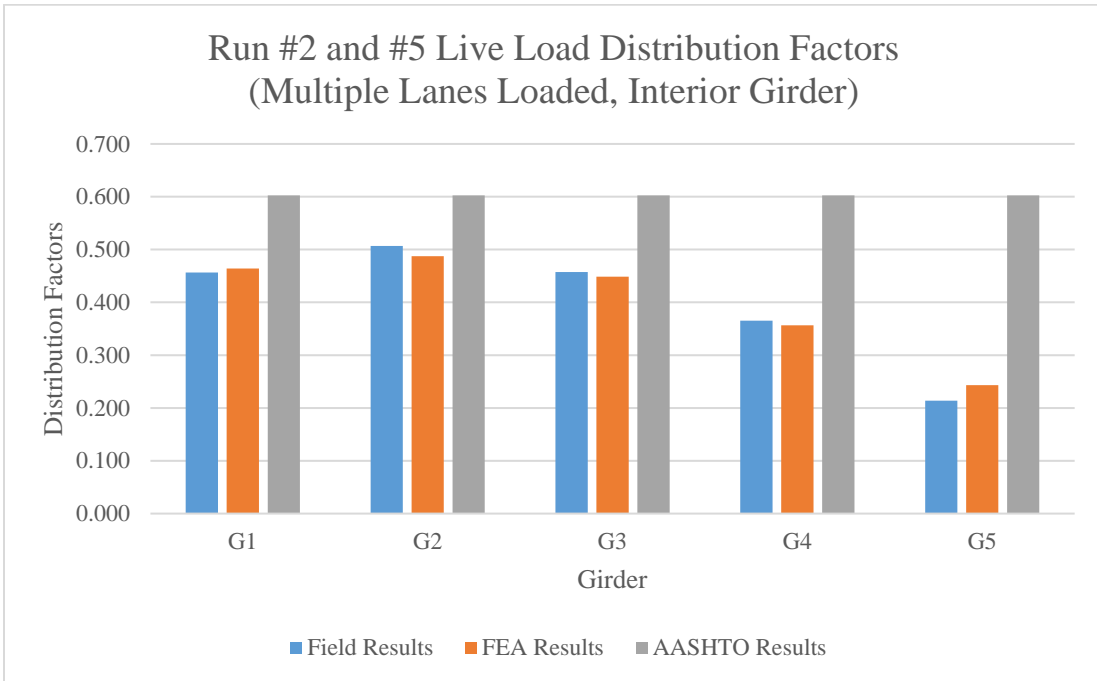
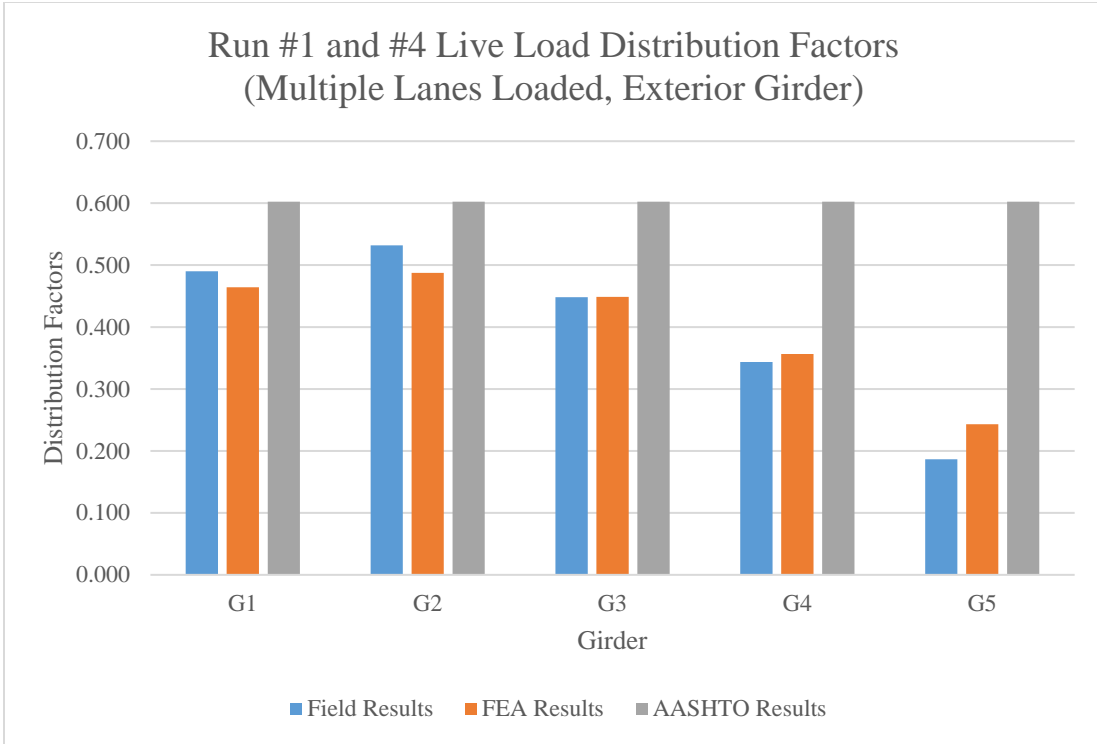


A.1.4 Results Comparison: Live Load Field Test, Finite Element Analysis, AASHTO Calculations

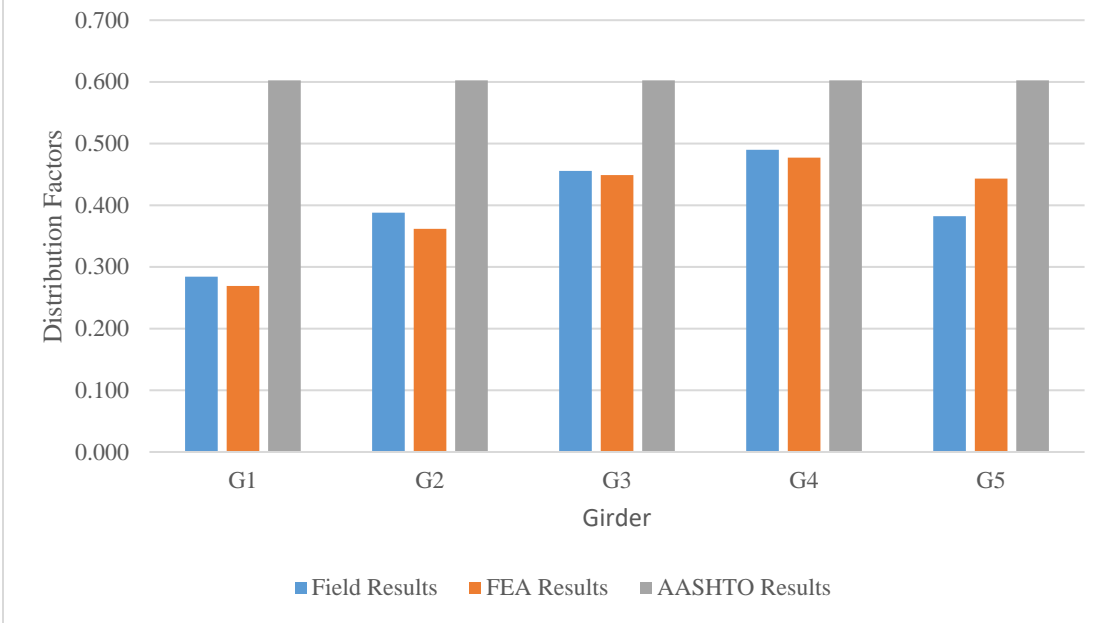








Run #3 and #6 Live Load Distribution Factors
(Multiple Lanes Loaded, Middle Interior Girder)



APPENDIX B: FINITE ELEMENT MODELING PROGRAM

This appendix documents the program written in MATLAB (The Mathworks, Inc., 2020) that were used in this research. The program “noncompv2.m” is used to preprocess .inp files that Abaqus will read to produce a finite element model. User inputs are used to generate the nodes and elements for the model under investigation. An outline of each section of the program is presented below:

- Part 0 reads the data necessary to generate the finite element mesh.
- Part 1 defines the longitudinal node layout of the girder.
- Part 2 defines the transverse node layout of the girder.
- Part 3 combines Part 3 and 4 to generate the three-dimensional mesh of the steel press-brake-formed tub girder.
- Part 4 defines the transverse node layout for the stiffener.
- Part 5 uses Part 4 to generate the three-dimensional mesh of the stiffener plates.
- Part 6 alters the geometry to consider geometric imperfection 1, flange tilt.
- Part 7 determines the centroid and shear center of the assembly.
- Part 8 alters the geometry to consider geometric imperfection 2, girder twist.
- Part 9 alters the girder geometry to consider geometric imperfection 3, web out of flatness.
- Part 10 alters the geometry of the stiffener plate to consider geometric imperfection 3, web out of flatness.
- Part 11 applies the loading and boundary conditions to specified nodes.
- Part 12 writes the .inp file with the information from Parts 0 through 11.

The MATLAB file is as follows (inputs for material properties and geometric imperfections are outlined in chapter 7):

```
fclose('all');

clc

clear

% =====

% PART 0: INPUT PARAMETERS

% =====

% 0.1 Girder Dimensions/Thicknesses

% -----

L=38;           % span length [ft]

w=84;           % standard mill plate width [in]

t=7/16;         % plate thickness [in]

t_BRG=3/4;      % bearing plate thickness [in]

d=23;           % total girder depth [in]

btf=6;          % top flange width [in]

Load_ap=33;     % applied load at midspan [kip]      From Lindsay Kelly Test 2
(Galvanized Girder)

% 0.2 Stiffener/Diaphragm Locations and Imperfection Anchors [ft]

% -----

% - There must be at least three locations: 0.0L, 0.5L and 1.0L.

Loc_St=[0;1/2;1]*L;
```

```

% 0.3 Locations of Lateral Support [ft]
% -----
% - There must be at least two locations: 0.0L and 1.0L.
Loc_Lat=[0;1]*L;

% 0.4 Transverse Node Layout Parameters
% -----
ne_bf=10;      % Number of elements along the bottom flange (MUST BE EVEN)
ne_w=12;      % Number of elements along the web
ne_b=03;      % Number of elements along the bend
ne_tf=05;      % Number of elements along the top flange (MUST BE EVEN)
le_L=3.0;     % Approximate length of element along the span [in]
Imp_Amp=1.0 ; % Imperfection Magnitude Amplification Factor

% 0.5 Imperfection I - Flange Tilt
% -----
% - There must be at least two locations: 0.0L and 1.0L.
Imp_St1=[0;1]*L; % Locations of imperfection [ft]
Imp_Mag1=Imp_Amp*btf*tan(1*pi/180); % Magnitude of maximum
imperfection [in]
Imp_Opt1=+1; % Option for imperfection orientation
% +1 for similar, -1 for opposite

% 0.6 Imperfection II - Girder Twist

```

```

% -----
% - There must be at least two locations: 0.0L and 1.0L.

Imp_St2=[0;1]*L;

% Imp_St2=[0;1/2;1]*L;           % Locations of imperfection [ft]

Imp_Mag2=Imp_Amp*1;              % Magnitude of maximum twist angle
[deg]

Imp_Opt2=1;                      % Option for origin of twist angle

% 0 for the centroid
% 1 for the shear center
% 0-1 for values between...

% 0.7 Imperfection III - Web Out of Flatness
% -----

% Note:

% - There must be at least two locations: 0.0L and 1.0L.

% - There must be a location that matches each stiffener.

Imp_St3=[0;1/4;1/2;3/4;1]*L;    % Locations of imperfection [ft]

Imp_Mag3=Imp_Amp*0;             % Magnitude of maximum imperfection
[in]

Imp_Opt3=-1;                    % Option for imperfection orientation

% +1 for similar, -1 for opposite

% =====

```

```

% PART 1: LONGITUDINAL NODE LAYOUT

% =====

% 1.1 Anchor Points for Stiffeners and Imperfections

% -----

Anchor_y=vertcat(Loc_St,Loc_Lat,Imp_St1,Imp_St2,Imp_St3)*12;

Anchor_y=unique(Anchor_y,'rows');

Anchor_y=sort(Anchor_y);

% 1.2 Number of Elements in Each Segment

% -----

id_e_y=zeros((length(Anchor_y)-1),1);

for i=1:length(id_e_y)

    y1=Anchor_y(i);

    y2=Anchor_y(i+1);

    id_e_y(i)=round((y2-y1)/le_L);

    clear y1 y2

end

clear ans i

% 1.3 Node Numbers at the Ends of Each Segment

% -----

id_n_y=zeros((length(id_e_y)+1),1);

id_n_y(1)=1;

for i=2:length(id_n_y)

```

```

        id_n_y(i)=id_n_y(i-1)+id_e_y(i-1);
end
clear ans i

% 1.4 Nodal Coordinates at the Ends of Each Segment
% -----
node_y=zeros(id_n_y(end),1);
for i=1:length(id_e_y)
    y1=Anchor_y(i);
    y2=Anchor_y(i+1);
    ne_y=round((y2-y1)/le_L);
    i1=id_n_y(i);
    i2=id_n_y(i+1);
    node_y(i1:i2)=y1:((y2-y1)/ne_y):y2;
    clear i1 i2 ne_y y1 y2
end
clear ans i

% 1.5 Adding 3" Past Bearing Stiffeners & Rounding of Nodal Coordinates
% -----
node_y=vertcat(-3,node_y,(L*12+3));
node_y=round(node_y*1e6)/1e6;
clear id_e_y id_n_y Anchor_y

% =====

```

```

% PART 2:  TRANSVERSE NODE LAYOUT (GIRDER)

% =====

% 2.1 General Paramters

% -----

slope=04;                                % slope ratio of web
r=11/2*t;                                % bend rad. at mid-thickness [in]
theta=pi/2-atan(1/slope);                % bend angle [rad]
L_R=theta*r;                              % arc length of bend [in]
Web_z=d-t+2*r*(1/(sqrt(slope^2+1))-1);    % Z-portion of straight web [in]
Web_x=Web_z/slope;                        % X-portion of straight web [in]
L_W=sqrt(Web_x^2+Web_z^2);                % length of straight web [in]
bbf=w-(4*L_R+2*L_W+2*btf);               % width of bottom flange [in]

% 2.2 Node Coordinates (Top Flange)

% -----

n_tf_x=((0):(btf/ne_tf):(btf))'+2*r*sin(theta)+Web_x+bbf/2;
n_tf_z=zeros(ne_tf+1,1)+d-t;
n_tf_x1=-n_tf_x;
n_tf_z1=n_tf_z;
n_tf_x2=n_tf_x;
n_tf_z2=n_tf_z;

clear n_tf_x n_tf_z

% 2.3 Node Coordinates (Top Flange Bends)

```

```

% -----
n_theta=(pi/2-theta):(theta/ne_b):(pi/2);
n_tb_x=-r*cos(n_theta)+2*r*sin(theta)+Web_x+bbf/2;
n_tb_z=r*sin(n_theta)-2*r*cos(theta)+Web_z+r;
n_tb_x1=-n_tb_x';
n_tb_z1=n_tb_z';
n_tb_x2=n_tb_x';
n_tb_z2=n_tb_z';
clear n_theta n_tb_x n_tb_z

% 2.4 Node Coordinates (Webs)
% -----
n_w_x=((0):(Web_x/ne_w):(Web_x))'+r*sin(theta)+bbf/2;
n_w_z=((0):(Web_z/ne_w):(Web_z))'+2*r*(sin(theta/2))^2;
n_w_x1=-n_w_x;
n_w_z1=n_w_z;
n_w_x2=n_w_x;
n_w_z2=n_w_z;
clear n_w_x n_w_z

% 2.5 Node Coordinates (Bottom Flange Bends)
% -----
n_theta=(3*pi/2):(theta/ne_b):(3*pi/2+theta);
n_bb_x=r*cos(n_theta)+bbf/2;
n_bb_z=r*sin(n_theta)+r;

```

```

n_bb_x1=-n_bb_x';
n_bb_z1=n_bb_z';
n_bb_x2=n_bb_x';
n_bb_z2=n_bb_z';
clear n_theta n_bb_x n_bb_z

% 2.6 Node Coordinates (Bottom Flange)
% -----

n_bf_x=(-bbf/2):(bbf/ne_bf):(bbf/2)';
n_bf_z=zeros(ne_bf+1,1);

% 2.7 Concatenation of Node Coordinates
% -----

nx1=vertcat(n_tf_x1,n_tb_x1,n_w_x1);
nx2=vertcat(n_bb_x1,n_bf_x,n_bb_x2);
nx3=vertcat(n_w_x2,n_tb_x2,n_tf_x2);
nx=vertcat(nx1,nx2,nx3);
nx=round(nx*1e6)/1e6;

nz1=vertcat(n_tf_z1,n_tb_z1,n_w_z1);
nz2=vertcat(n_bb_z1,n_bf_z,n_bb_z2);
nz3=vertcat(n_w_z2,n_tb_z2,n_tf_z2);
nz=vertcat(nz1,nz2,nz3);
nz=round(nz*1e6)/1e6;
node_cs=horzcat(nx,nz);
clear nx1 nx2 nx3

```

```

clear nz1 nz2 nz3

clear nx nz

node_cs=unique(node_cs,'rows');
node_x=node_cs(:,1);
node_z=node_cs(:,2);

% 2.8 Additional Clear Statements
% -----

clear L_R L_W Web_x Web_z theta

clear n_tf_x1 n_tb_x1 n_w_x1 n_tf_z1 n_tb_z1 n_w_z1
clear n_bb_x1 n_bf_x n_bb_x2 n_bb_z1 n_bf_z n_bb_z2
clear n_w_x2 n_tb_x2 n_tf_x2 n_w_z2 n_tb_z2 n_tf_z2

% =====

% PART 3:  NODE & ELEMENT LAYOUT (GIRDER)
% =====

% 3.1 Node Matrix
% -----

nn=((1):(1):(length(node_x)*length(node_y)))';
nx=repmat(node_x,length(node_y),1);
ny=repmat(node_y,1,length(node_x))';
ny=ny(:);
nz=repmat(node_z,length(node_y),1);

```

```

node_girder=horzcat(nn,nx,ny,nz);

clear nn nx ny nz

% 3.2 Element Matrix
% -----

ne_x_girder=length(node_x)-1; % number of girder elements [x-direction]
ne_y_girder=length(node_y)-1; % number of girder elements [y-direction]
nn_x_girder=ne_x_girder+1;
element_girder=zeros(ne_x_girder*ne_y_girder,5);
element_girder(:,1)=1:(ne_x_girder*ne_y_girder);
for i=1:ne_y_girder
    k1=ne_x_girder*i-ne_x_girder+1;
    k2=ne_x_girder*i;
    n1a=nn_x_girder*i-ne_x_girder;
    n1b=nn_x_girder*i-1;
    n2a=nn_x_girder*i-(ne_x_girder-1);
    n2b=nn_x_girder*i;
    n3a=nn_x_girder*i+2;
    n3b=nn_x_girder*i+nn_x_girder;
    n4a=nn_x_girder*i+1;
    n4b=nn_x_girder*i+ne_x_girder;
    element_girder(k1:k2,2)=node_girder(n1a:n1b,1);
    element_girder(k1:k2,3)=node_girder(n2a:n2b,1);
    element_girder(k1:k2,4)=node_girder(n3a:n3b,1);
    element_girder(k1:k2,5)=node_girder(n4a:n4b,1);
clear k1 k2 n1a n1b n2a n2b n3a n3b n4a n4b

```

```

end

clear ans i ne_x_girder ne_y_girder nn_x_girder

% 3.3 BC Identification
% -----

bc_g1=(1:(ne_bf+1))+ne_tf+2*ne_b+ne_w;
bc_g2=bc_g1+length(node_cs(:,1))*(length(node_y)-1);
bc_g1=bc_g1+length(node_cs(:,1));
bc_g2=bc_g2-length(node_cs(:,1));

% =====

% PART 4:  TRANSVERSE NODE LAYOUT (STIFFENER)
% =====

theta=pi/2-atan(1/slope);           % bend angle [rad]
L_R=theta*r;                        % arc length of bend [in]
Web_z=d-t+2*r*(1/(sqrt(slope^2+1))-1); % Z-portion of straight web [in]
Web_x=Web_z/slope;                  % X-portion of straight web [in]
L_W=sqrt(Web_x^2+Web_z^2);           % length of straight web [in]
bbf=w-(4*L_R+2*L_W+2*btf);          % width of bottom flange [in]
n_w_z=((0):(Web_z/ne_w):(Web_z))'+2*r*(sin(theta/2))^2;

% Node Layouts Along the Top/Bottom of the Diaphragm (X-direction)
% -----

```

```

st_px=Web_x+bbf/2;

n_top_x=(-st_px):(2*st_px/ne_bf):(st_px)';
n_bot_x=(-bbf/2):(bbf/ne_bf):(bbf/2)';

clear st_px

ns_x=length(n_top_x); % Number of unique stiffener nodes in the X-direction
ns_z=length(n_w_z)+1; % Number of unique stiffener nodes in the Z-direction
n_stiff=zeros(ns_x*ns_z,2);

% Node Layout for Generic Stiffener
% -----
for i=1:ns_x

    x1=round(n_top_x(i)*1e6)/1e6;

    z1=round((d-t)*1e6)/1e6;

    x2=round(n_bot_x(i)*1e6)/1e6;

    z2=0;

    if x1~=x2

        % z = m*x + b

        m=(z2-z1)/(x2-x1);

        b=z1-m*x1;

        for j=1:ns_z

            if j<ns_z

                z_index=n_w_z(j);

            else

                z_index=d-t/2;

```

```

        end

        x_index=(z_index-b)/m;

        n_stiff((i-1)*ns_z+j,1)=x_index;

        n_stiff((i-1)*ns_z+j,2)=z_index;

        clear x_index z_index

    end

    clear m

else

    % x = 0

    clear m b

    range=median(1:1:ns_x);

    for j=1:ns_z

        if j<ns_z

            z_index=n_w_z(j);

        else

            z_index=d-t/2;

        end

        n_stiff((range-1)*ns_z+j,1)=0;

        n_stiff((range-1)*ns_z+j,2)=z_index;

        clear z_index

    end

    clear j range

end

clear m b

end

clear ans i

```

```

clear x1 x2 z1 z2 z_index

n_stiff=round(n_stiff*1e6)/1e6;

% Additional Clear Statements

% -----

clear L_R L_W Web_x Web_z theta

clear bbf

% =====

% PART 5:  NODE & ELEMENT LAYOUT (STIFFENER)

% =====

nn_girder=length(node_girder(:,1));

ne_stiff=(ns_z)*(length(n_bot_x)-1)+2*(length(n_w_z)-1);

rect_stiff=zeros(ne_stiff*length(Loc_St),5);

rect_stiff(:,1)=(1:1:length(rect_stiff(:,1)))';

rect_stiff(:,1)=rect_stiff(:,1)+length(element_girder(:,1));

tri_stiff=zeros(4*length(Loc_St),4);

tri_stiff(:,1)=(1:1:length(tri_stiff(:,1)))';

tri_stiff(:,1)=tri_stiff(:,1)+length(element_girder(:,1));

tri_stiff(:,1)=tri_stiff(:,1)+length(rect_stiff(:,1));

% Node Matrix

```

```

% -----
node_stiff=zeros(length(n_stiff(:,1))*length(Loc_St),4);
for i=1:length(Loc_St)
    ind_stiff=((i-1)*length(n_stiff(:,1))+1):1:(i*length(n_stiff(:,1)));
    node_stiff(ind_stiff,2)=n_stiff(:,1);
    node_stiff(ind_stiff,3)=Loc_St(i)*12;
    node_stiff(ind_stiff,4)=n_stiff(:,2);
    clear ind_stiff
end
clear ans i
node_stiff(:,1)=(1:1:length(node_stiff(:,1)))+nn_girder;
node_stiff=round(node_stiff*1e6)/1e6;

% Element Matrix
% -----
for i=1:length(Loc_St)
    y_index=Loc_St(i)*12;          % Y-coordinate of individual stiff.
    cs_line=find(node_y==y_index); % Search for node loc. along girder

    ind_LW1=ne_tf+ne_b+1; % ind_LW1 = stiff. node on the LW (start)
    ind_LW2=ind_LW1+ne_w; % ind_LW2 = stiff. node on the LW (end)
    ind_BF1=ind_LW2+ne_b; % ind_BF1 = stiff. node on the BF (start)
    ind_BF2=ind_BF1+ne_bf; % ind_BF2 = stiff. node on the BF (end)
    ind_RW1=ind_BF2+ne_b; % ind_RW1 = stiff. node on the RW (start)
    ind_RW2=ind_RW1+ne_w; % ind_RW2 = stiff. node on the RW (end)
end

```

```

ind_LW1=ind_LW1+(cs_line-1)*length(node_cs); % Shift for ith stiff.
ind_LW2=ind_LW2+(cs_line-1)*length(node_cs); % Shift for ith stiff.
ind_BF1=ind_BF1+(cs_line-1)*length(node_cs); % Shift for ith stiff.
ind_BF2=ind_BF2+(cs_line-1)*length(node_cs); % Shift for ith stiff.
ind_RW1=ind_RW1+(cs_line-1)*length(node_cs); % Shift for ith stiff.
ind_RW2=ind_RW2+(cs_line-1)*length(node_cs); % Shift for ith stiff.

nn_LW=(ind_LW1:1:ind_LW2)'; % nn_LW = left web nodes
nn_BF=(ind_BF1:1:ind_BF2)'; % nn_BF = bottom flange nodes
nn_RW=(ind_RW1:1:ind_RW2)'; % nn_RW = right web nodes

clear ind_LW1 ind_LW2 ind_BF1 ind_BF2 ind_RW1 ind_RW2

% First Vertical Row of Elements
% -----
n1=nn_LW(2:1:end);
n1=n1(end:-1:1);
n2=(1:1:length(n_w_z(:,1))-1)';
n2=n2+nn_girder+(i-1)*ns_x*ns_z;
n3=(2:1:length(n_w_z(:,1)))';
n3=n3+nn_girder+(i-1)*ns_x*ns_z;
n4=nn_LW(1:1:(end-1));
n4=n4(end:-1:1);
es1=horzcat(n1,n2,n3,n4);

```

```

clear n1 n2 n3 n4

% Main Body of Elements
% -----

es2=zeros((ne_w+2)*(length(nn_BF)-1),4);

for j=1:(length(nn_BF)-1)

    v1=(((j-1)*(ns_z)+1):1:(j*ns_z))';
    v1=v1+nn_girder+(i-1)*ns_x*ns_z;
    vn1=vertcat(nn_BF(j,1),v1);

    clear v1

    v2=(((j*ns_z+1):1:((j+1)*(ns_z))))';
    v2=v2+nn_girder+(i-1)*ns_x*ns_z;
    vn2=vertcat(nn_BF(j+1,1),v2);

    clear v2

    n1=vn1(1:1:(end-1));
    n2=vn2(1:1:(end-1));
    n3=vn2(2:1:end);
    n4=vn1(2:1:end);

    es2((((j-1)*(ne_w+2)+1):1:(j*(ne_w+2))),:)=horzcat(n1,n2,n3,n4);

    clear vn1 vn2

end

clear ans j

% Last Vertical Row of Elements
% -----

```

```

n1=(ns_z*(ns_x-1)+1):1:(ns_x*ns_z-2)';
n1=n1+nn_girder+(i-1)*ns_x*ns_z;
n2=nn_RW(1:1:(end-1));
n3=nn_RW(2:1:end);
n4=(ns_z*(ns_x-1)+2):1:(ns_x*ns_z-1)';
n4=n4+nn_girder+(i-1)*ns_x*ns_z;
es3=horzcat(n1,n2,n3,n4);

clear n1 n2 n3 n4

% All Rectangular Elements
% -----
es=vertcat(es1,es2,es3);
rect_stiff(((i-1)*ne_stiff+1):1:(i*ne_stiff),(2:1:5))=es;
clear es es1 es2 es3

% All Triangular Elements
% -----
t11=nn_BF(1);
t12=length(node_girder(:,1))+(i-1)*ns_x*ns_z+1;
t13=nn_LW(end);
t21=nn_LW(1);
t22=length(node_girder(:,1))+(i-1)*ns_x*ns_z+ns_z-1;
t23=length(node_girder(:,1))+(i-1)*ns_x*ns_z+ns_z;
t31=nn_BF(end);
t32=nn_RW(1);

```

```

t33=length(node_girder(:,1))+(i-1)*ns_x*ns_z+(ns_x-1)*ns_z+1;

t41=length(node_girder(:,1))+(i-1)*ns_x*ns_z+(ns_x-1)*ns_z++ns_z-1;

t42=nn_RW(end);

t43=length(node_girder(:,1))+(i-1)*ns_x*ns_z+(ns_x-1)*ns_z++ns_z;

t1=[t11,t12,t13];

t2=[t21,t22,t23];

t3=[t31,t32,t33];

t4=[t41,t42,t43];

ele_t=[t1;t2;t3;t4];

i1=(i-1)*4+1;

i2=4*i;

tri_stiff(i1:i2,2:4)=ele_t;

clear t11 t12 t13 t21 t22 t23 t31 t32 t33 t41 t42 t43

clear t1 t2 t3 t4

clear i1 i2 ele_t

clear nn_LW nn_BF nn_RW

end

clear ans i y_index nn_stiff ne_stiff nn_girder

clear cs_line n_bot_x n_top_x n_stiff n_w_x n_w_z ns_x ns_z

```

```

% =====
% PART 6: IMPERFECTION I (FLANGE TILT)
% =====

% 6.1 Locating Nodes along Y-Axis
% -----

index_imp1=zeros(length(Imp_St1),1);

for i=1:length(index_imp1)

    i1=Imp_St1(i)*12;

    i1=round(i1*1e6)/1e6;

    for j=1:length(node_y)

        if i1==node_y(j)

            index_imp1(i)=j;

        end

    end

    clear ans i1 j

end

clear ans i

% 6.2 Base Imperfection Vector (Magnitude = 1.0)
% -----

base_imp1=zeros(length(node_y),1);

for i=1:(length(Imp_St1)-1)

    i1=index_imp1(i);

    i2=index_imp1(i+1);

```

```

y1=node_y(i1);
y2=node_y(i2);
x_imp=node_y(i1:i2)-y1;
y_imp=sin(pi*x_imp/(y2-y1));
if mod(i,2)==0
    y_imp=-y_imp;
else
    y_imp=+y_imp;
end
base_imp1(i1:i2)=y_imp;
clear i1 i2 y1 y2 x_imp y_imp
end
clear ans i

L_imp1=Imp_St1(2)-Imp_St1(1);
L_imp2=(Imp_St1(end)-Imp_St1(end-1));

base_imp1(1)=-sin(pi*3/(L_imp1*12));

if mod((length(Imp_St1)-1),2)==0
    base_imp1(end)=+sin(pi*3/(L_imp2*12));
else
    base_imp1(end)=-sin(pi*3/(L_imp2*12));
end
clear L_imp1 L_imp2

```

```

% 6.3 Locating Flange Nodes & Scaling Functions
% -----

impl_node_x1=(1:(ne_tf+1))';
impl_node_x2=((length(node_cs(:,1))-ne_tf):length(node_cs(:,1)))';
scale_imp1_x1=+(1:(-1/ne_tf):0);

if Imp_Opt1==+1
    scale_imp1_x2=+(0:(+1/ne_tf):1);
elseif Imp_Opt1==-1
    scale_imp1_x2=- (0:(+1/ne_tf):1);
end

impl_node=zeros(length(node_cs(:,1)),1);
impl_node(impl_node_x1)=scale_imp1_x1;
impl_node(impl_node_x2)=scale_imp1_x2;

clear impl_node_x1 impl_node_x2
clear scale_imp1_x1 scale_imp1_x2

% 6.4 Applying Imperfections to Girder Nodes
% -----

impl_girder_x=zeros(length(node_girder(:,1)),1);

for i=1:length(node_y)
    i1=(i-1)*length(node_cs(:,1))+1;
    i2=(i-0)*length(node_cs(:,1))+0;

```

```

    impl_girder_x(i1:i2)=base_impl(i);

    clear i1 i2
end

clear ans i

impl_girder_z= repmat(impl_node,length(node_y),1);
impl_girder=impl_girder_x.*impl_girder_z;
impl_girder=impl_girder*Imp_Mag1;
impl_girder=round(impl_girder*1e6)/1e6;

node_girder(:,4)=node_girder(:,4)+impl_girder;

clear impl_girder_x impl_girder_z impl_girder

% 6.5 Final Clear Statements
% -----

clear base_impl impl_node index_impl

% =====

% PART 7:  CENTROID & SHEAR CENTER
% =====

% 7.1 Element Breakdown for Section Properties
% -----

sne_tf=1;      % number of s.c. elements along the top flange
sne_b=100;    % number of s.c. elements along the bend

```

```

sne_w=1;      % number of s.c. elements along the web

sne_bf=1;     % number of s.c. elements along the bottom flange

% 7.2 Constant Values
% -----

% theta = bend angle (rad)

% L_bend = length of the bend region (in)

% Dx = length of the x-portion inclined web (in)

% Dy = length of the y-portion inclined web (in)

% bbf = bottom flange width (in)

theta=pi/2-atan(1/slope);

L_bend=r*atan(slope);

Dx=2*r/(slope*sqrt(slope^2+1))+(d-t-2*r)/slope;

Dy=d-t-2*r*(1-1/sqrt(slope^2+1));

D=(2*r+(d-t-2*r)*sqrt(slope^2+1))/slope;

bbf=w-(4*L_bend+2*D+2*btf);

% 7.3 Node Layout - Top Flange
% -----

n_tf_x=((0):(btf/sne_tf):(btf))+2*r*sin(theta)+Dx+bbf/2;

n_tf_y=zeros(sne_tf+1,1)+d-t;

n_tf_x1=-n_tf_x;    n_tf_y1=n_tf_y;

n_tf_x2=+n_tf_x;    n_tf_y2=n_tf_y;

clear n_tf_x n_tf_y

```

```

% 7.4 Node Layout - Top Bend Regions
% -----
n_theta=(pi/2-theta):(theta/sne_b):(pi/2);
n_tb_x=-r*cos(n_theta)+2*r*sin(theta)+Dx+bbf/2;
n_tb_y=r*sin(n_theta)-2*r*cos(theta)+Dy+r;

n_tb_x1=-n_tb_x';    n_tb_y1=n_tb_y';
n_tb_x2=+n_tb_x';    n_tb_y2=n_tb_y';
clear n_theta n_tb_x n_tb_y

% 7.5 Node Layout - Flat Web Regions
% -----
n_w_x=((0):(Dx/sne_w):(Dx))'+r*sin(theta)+bbf/2;
n_w_y=((0):(Dy/sne_w):(Dy))'+2*r*(sin(theta/2))^2;

n_w_x1=-n_w_x;      n_w_y1=n_w_y;
n_w_x2=+n_w_x;      n_w_y2=n_w_y;
clear n_w_x n_w_y

% 7.6 Node Layout - Bottom Bend Regions
% -----
n_theta=(3*pi/2):(theta/sne_b):(3*pi/2+theta);
n_bb_x=r*cos(n_theta)+bbf/2;
n_bb_y=r*sin(n_theta)+r;

```

```

n_bb_x1=-n_bb_x';    n_bb_x2=n_bb_x';
n_bb_y1=+n_bb_y';    n_bb_y2=n_bb_y';
clear n_theta n_bb_x n_bb_y

% 7.7 Node Layout - Bottom Flange
% -----
n_bf_x=(-bbf/2):(bbf/sne_bf):(bbf/2)';
n_bf_y=zeros(sne_bf+1,1);

% 7.8 Node Layout - Concatenation
% -----
nx1=vertcat(n_tf_x1,n_tb_x1,n_w_x1); ny1=vertcat(n_tf_y1,n_tb_y1,n_w_y1);
nx2=vertcat(n_bb_x1,n_bf_x,n_bb_x2); ny2=vertcat(n_bb_y1,n_bf_y,n_bb_y2);
nx3=vertcat(n_w_x2,n_tb_x2,n_tf_x2); ny3=vertcat(n_w_y2,n_tb_y2,n_tf_y2);

nx=vertcat(nx1,nx2,nx3);    ny=vertcat(ny1,ny2,ny3);
nx=round(nx*1e6)/1e6;    ny=round(ny*1e6)/1e6;
clear nx1 nx2 nx3 ny1 ny2 ny3

node=horzcat(nx,ny);
node=unique(node,'rows');
node(:,2)=node(:,2)+t/2;
node=round(node*1e6)/1e6;
clear nx ny

```

```

% 7.9 Node Layout - Clear Statements

% -----

clear n_tf_x1 n_tb_x1 n_w_x1    n_tf_y1 n_tb_y1 n_w_y1
clear n_bb_x1 n_bf_x n_bb_x2    n_bb_y1 n_bf_y n_bb_y2
clear n_w_x2 n_tb_x2 n_tf_x2    n_w_y2 n_tb_y2 n_tf_y2
clear theta L_bend Dx Dy D bbf
clear sne_tf sne_b sne_w sne_bf

% 7.10 Fundamental Terms

% -----

nnode=length(node(:,1)); % nnode = number of nodes
nele=nnode-1;           % nele = number of elements

% 7.11 Torsional Properties - Lengths & Area

% -----

Lij=zeros(nele,1); % Lij = length of each element (in)
Aij=zeros(nele,1); % Aij = area of each element (in^2)
for i=1:nele
    xi=node(i,1);
    xj=node(i+1,1);
    yi=node(i,2);
    yj=node(i+1,2);
    Lij(i)=sqrt((xj-xi)^2+(yj-yi)^2);
    Aij(i)=t*Lij(i);
    clear xi xj yi yj
end

```

```

end

clear ans i

A=sum(Aij);          % A = area of cross-section (in^2)

% 7.12 Torsional Properties - Center-of-Gravity
% -----
Qxij=zeros(nele,1); % Qxij = first moment of area about X-axis (in^3)
Qyij=zeros(nele,1); % Qyij = first moment of area about X-axis (in^3)
for i=1:nele
    xi=node(i,1);
    xj=node(i+1,1);
    yi=node(i,2);
    yj=node(i+1,2);
    Qxij(i)=(Aij(i)/2)*(xi+xj);
    Qyij(i)=(Aij(i)/2)*(yi+yj);
    clear xi xj yi yj
end

clear ans i

x_bar=sum(Qxij)/A; % x_bar = X-axis centroid (in)
y_bar=sum(Qyij)/A; % y_bar = Y-axis centroid (in)

% 7.13 Torsional Properties - Moments of Inertia
% -----
pij=zeros(nele,1); % pij = distances from elements to the C.G. (in)
Ixxij=zeros(nele,1); % Ixxij = X-axis element moment of inertia (in^4)

```

```

Iyyij=zeros(nele,1); % Iyyij = Y-axis element moment of inertia (in^4)

for i=1:nele

    xi=node(i,1)-x_bar;

    xj=node(i+1,1)-x_bar;

    yi=node(i,2)-y_bar;

    yj=node(i+1,2)-y_bar;

    pij(i)=(xi*yj-xj*yi)/Lij(i);

    Ixxij(i,1)=(Aij(i)/3)*(yi^2+yi*yj+yj^2);

    Iyyij(i,1)=(Aij(i)/3)*(xi^2+xi*xj+xj^2);

    clear xi xj yi yj

end

clear ans i

Iyy=sum(Iyyij); % Iyy = Y-axis moment of inertia (in^4)

% 7.14 Torsional Properties - Unit Warping (C.G.)

% -----

wij=zeros(nele,2); % wij = unit warp. with respect to the C.G. (in^2)

for i=1:nele

    if i==1

        wij(i,1)=0;

        wij(i,2)=pij(i)*Lij(i);

    else

        wij(i,1)=wij(i-1,2);

        wij(i,2)=wij(i,1)+pij(i)*Lij(i);

    end

end

end

```

```

clear ans i

% 7.15 Torsional Properties - Warping Products
% -----
Iwxij=zeros(nele,1); % Iwxij = X-axis element warp. prod. (in^5)
for i=1:nele
    xi=node(i,1)-x_bar;
    xj=node(i+1,1)-x_bar;
    wi=wij(i,1);
    wj=wij(i,2);
    Iwxij(i,1)=(Aij(i)/3)*(wi*xi+wj*xj)+(Aij(i)/6)*(wi*xj+wj*xi);
    clear xi xj yi yj wi wj
end
clear ans i
Iwx=sum(Iwxij); % Iwx = X-axis warping product of inertia (in^5)
Yo=-Iwx/Iyy; % Yo = Y-axis shear center (in)

% 7.16 Final Clear Statements
% -----
y_centroid=round(y_bar*1e6)/1e6;
y_shear=round(Yo*1e6)/1e6;

clear nnode nele node x_bar y_bar Yo
clear Lij Aij Qxij Qyij Ixxij Iyyij wij pij
clear A Iwxij Iwyij Iwx Iwy Ixx Iyy x_bar

```

```

% =====
% PART 8: IMPERFECTION II (GIRDER TWIST, APPLICATION TO GIRDER)
% =====

% 8.1 Locating Nodes along Y-Axis
% -----

index_imp2=zeros(length(Imp_St2),1);

for i=1:length(index_imp2)
    i1=Imp_St2(i)*12;
    i1=round(i1*1e6)/1e6;
    for j=1:length(node_y)
        if i1==node_y(j)
            index_imp2(i)=j;
        end
    end
    clear ans i1 j
end

clear ans i

% 8.2 Base Imperfection Vector
% -----

base_imp2=zeros(length(node_y),1);

for i=1:(length(Imp_St2)-1)

```

```

i1=index_imp2(i);
i2=index_imp2(i+1);
y1=node_y(i1);
y2=node_y(i2);
x_imp=node_y(i1:i2)-y1;
y_imp=sin(pi*x_imp/(y2-y1));
if mod(i,2)==0
    y_imp=-y_imp;
else
    y_imp+=y_imp;
end
base_imp2(i1:i2)=y_imp;
clear i1 i2 y1 y2 x_imp y_imp
end
clear ans i

L_imp1=Imp_St2(2)-Imp_St2(1);
L_imp2=(Imp_St2(end)-Imp_St2(end-1));

base_imp2(1)=-sin(pi*3/(L_imp1*12));

if mod((length(Imp_St2)-1),2)==0
    base_imp2(end)=+sin(pi*3/(L_imp2*12));
else
    base_imp2(end)=-sin(pi*3/(L_imp2*12));
end

```

```

end

clear L_imp1 L_imp2

% 8.3 Rotation of Cross-Section about Chosen Point
% -----

adj_cs=y_shear*(Imp_Opt2)+y_centroid*(1-Imp_Opt2);
node_adj_cs=node_cs;
node_adj_cs(:,2)=node_adj_cs(:,2)-adj_cs;
rotated_cs=zeros(length(node_adj_cs(:,2)),2);
for i=1:length(node_adj_cs(:,1))
    x_i=node_adj_cs(i,1);
    y_i=node_adj_cs(i,2);
    c_i=cos(-pi*Imp_Mag2/180);
    s_i=sin(-pi*Imp_Mag2/180);
    RM=[c_i,-s_i;s_i,c_i];
    r_i=RM*[x_i;y_i];
    rotated_cs(i,:)=r_i';
    clear x_i y_i c_i s_i RM r_i xr_i yr_i
end

clear ans i

% 8.4 Applying Imperfections to Girder Nodes
% -----

correct_cs=rotated_cs-node_cs;
correct_cs(:,2)=correct_cs(:,2)+adj_cs;

```

```

imp2_girder=zeros(length(node_girder(:,1)),3);

for i=1:length(node_y)

    i1=(i-1)*length(node_cs(:,1))+1;

    i2=(i-0)*length(node_cs(:,1))+0;

    imp2_girder(i1:i2,2)=correct_cs(:,1)*base_imp2(i);

    imp2_girder(i1:i2,4)=correct_cs(:,2)*base_imp2(i);

    clear i1 i2

end

clear ans i

imp2_girder=round(imp2_girder*1e6)/1e6;

node_girder(:,2)=node_girder(:,2)+imp2_girder(:,2);

node_girder(:,4)=node_girder(:,4)+imp2_girder(:,4);

clear correct_cs imp2_girder

% 8.5 Final Clear Statements
% -----

clear index_imp2 node_adj_cs

clear rotated_cs

% =====

% PART 9: IMPERFECTION II (GIRDER TWIST, APPLICATION TO STIFFENERS)

```

```

% =====

% 9.1 Base Imperfection Vector
% -----

ns_rot=length(node_stiff(:,1))/length(Loc_St);
node_rawstiff=node_stiff((1:ns_rot),[2,4]);
node_rawstiff(:,2)=node_rawstiff(:,2)-adj_cs;

adjusted_stiff=zeros(length(node_rawstiff(:,1)),2);
for i=1:length(adjusted_stiff(:,1))
    x_i=node_rawstiff(i,1);
    y_i=node_rawstiff(i,2);
    c_i=cos(-pi*Imp_Mag2/180);
    s_i=sin(-pi*Imp_Mag2/180);
    RM=[c_i,-s_i;s_i,c_i];
    r_i=RM*[x_i;y_i];
    adjusted_stiff(i,:)=r_i';
    clear x_i y_i c_i s_i RM r_i xr_i yr_i
end

clear ans i

% 9.2 Rotation Magnitudes at the Stiffeners
% -----

mag_rotation=zeros(length(Loc_St),1);
for i=1:length(mag_rotation)

```

```

ind_mag=Loc_St(i)*12;

ind_mag=round(ind_mag*1e6)/1e6;

for j=1:length(node_y)

    if ind_mag==node_y(j)

        mag_rotation(i)=base_imp2(j);

    end

end

clear ans j

end

clear ans i

% 9.3 Imperfections at all Stiffeners
% -----
correct_stiff=adjusted_stiff-node_rawstiff;
correct_stiff(:,2)=correct_stiff(:,2);
imp2_stiff=zeros(length(node_stiff(:,1)),2);
for i=1:length(mag_rotation)

    i1=(i-1)*length(correct_stiff(:,1))+1;

    i2=(i-0)*length(correct_stiff(:,1))+0;

    imp2_stiff(i1:i2,1)=correct_stiff(:,1)*mag_rotation(i);

    imp2_stiff(i1:i2,2)=correct_stiff(:,2)*mag_rotation(i);

    clear i1 i2

end

clear ans i

imp2_stiff=round(imp2_stiff*1e6)/1e6;

node_stiff(:,2)=node_stiff(:,2)+imp2_stiff(:,1);

```

```

node_stiff(:,4)=node_stiff(:,4)+imp2_stiff(:,2);

% 9.4 Final Clear Statements
% -----

clear base_imp2 node_rawstiff adjusted_stiff correct_stiff
clear ind_mag mag_rotation
clear y_shear y_centroid adj_cs ns_rot

% =====

% PART 10: IMPERFECTION III (WEB OUT-OF-FLATNESS)
% =====

% 10.1 Locating Nodes along Y-Axis
% -----

index_imp3=zeros(length(imp_st3),1);
for i=1:length(index_imp3)
    i1=imp_st3(i)*12;
    i1=round(i1*1e6)/1e6;
    for j=1:length(node_y)
        if i1==node_y(j)
            index_imp3(i)=j;
        end
    end
end
end

```

```

clear ans i1 j
end
clear ans i

% 10.2 Base Imperfection Vector (Longitudinal)
% -----
base_imp3=zeros(length(node_y),1);
for i=1:(length(Imp_St3)-1)
    i1=index_imp3(i);
    i2=index_imp3(i+1);
    y1=node_y(i1);
    y2=node_y(i2);
    x_imp=node_y(i1:i2)-y1;
    y_imp=sin(pi*x_imp/(y2-y1));
    if mod(i,2)==0
        y_imp=-y_imp;
    else
        y_imp=+y_imp;
    end
    base_imp3(i1:i2)=y_imp;
    clear i1 i2 y1 y2 x_imp y_imp
end
clear ans i

L_imp1=Imp_St3(2)-Imp_St3(1);

```

```

L_imp2=(Imp_St3(end)-Imp_St3(end-1));

base_imp3(1)=-sin(pi*3/(L_imp1*12));

if mod((length(Imp_St3)-1),2)==0
    base_imp3(end)=+sin(pi*3/(L_imp2*12));
else
    base_imp3(end)=-sin(pi*3/(L_imp2*12));
end
clear L_imp1 L_imp2

% 10.3 Base Imperfection Vector (Transverse)
% -----
slope=04; % slope ratio of web
r=11/2*t; % bend rad. at mid-thickness [in]
Web_z=d-t+2*r*(1/(sqrt(slope^2+1))-1); % Z-portion of straight web [in]
Web_x=Web_z/slope; % X-portion of straight web [in]
L_W=sqrt(Web_x^2+Web_z^2); % length of straight web [in]
clear Web_x Web_z

ni_wx=((0):(L_W/ne_w):(L_W))';
ni_wy=sin(pi*ni_wx/L_W);

new_1=1+ne_tf+ne_b;
new_2=new_1+ne_w;

```

```

new_3=new_2+2*ne_b+ne_bf;
new_4=new_3+ne_w;
base_twist=zeros(length(node_cs(:,1)),1);
base_twist(new_1:new_2)=ni_wy;
if Imp_Opt3==+1
    base_twist(new_3:new_4)=+ni_wy;
elseif Imp_Opt3==-1
    base_twist(new_3:new_4)=-ni_wy;
end
clear new_1 new_2 new_3 new_4 ni_wx ni_wy

% 10.4 Base Imperfection Vector (Girder)
% -----
base_girder=zeros(length(node_girder(:,1)),1);
for i=1:length(node_y)
    i1=(i-1)*length(base_twist(:,1))+1;
    i2=(i-0)*length(base_twist(:,1))+0;
    base_girder(i1:i2)=base_twist*base_imp3(i);
    clear i1 i2
end
clear ans i

base_trig=zeros(length(node_girder(:,1)),2);
t_comp_x=cos(atan(1/slope));
t_comp_z=sin(atan(1/slope));

```

```

base_trig(:,1)=base_girder*t_comp_x;
base_trig(:,2)=base_girder*t_comp_z;
base_trig=base_trig*Imp_Mag3;
base_trig=round(base_trig*1e6)/1e6;
clear t_comp_x t_comp_z

% 10.5 Imperfection Application and Clear Statements
% -----

node_girder(:,2)=node_girder(:,2)+base_trig(:,1);
node_girder(:,4)=node_girder(:,4)+base_trig(:,2);
clear base_imp3 base_girder base_twist base_trig index_imp3 L_W

% =====
% PART 11:  LOADING, BOUNDARY CONDITIONS & DATA COLLECTION
% =====

% 11.1 Loading Applied at Midspan
% -----

nn_1_stiff=length(node_stiff(:,1))/length(Loc_St);
for i=1:length(Loc_St)
    si=round(Loc_St(i)*12*1e6)/1e6;
    Ls=round(L*12/2*1e6)/1e6;
    if si==Ls

```

```

        stiff_index=i;

    end

    clear si Ls

end

clear ans i

k1=(stiff_index-1)*nn_1_stiff+1;
k2=(stiff_index-0)*nn_1_stiff+0;
single_stiff=node_stiff((k1:k2),:);
single_stiff=round(single_stiff*1e6)/1e6;
imp_loadstiff=imp2_stiff((k1:k2),:);
imp_loadstiff=round(imp_loadstiff*1e6)/1e6;
clear k1 k2

single_stiff(:,2)=single_stiff(:,2)-imp_loadstiff(:,1);
single_stiff(:,4)=single_stiff(:,4)-imp_loadstiff(:,2);
single_stiff=round(single_stiff*1e6)/1e6;

z_max=max(single_stiff(:,4));

search_stiff=zeros(nn_1_stiff,4);
for i=1:nn_1_stiff
    if single_stiff(i,4)==z_max
        search_stiff(i,:)=single_stiff(i,:);
    end
end

```

```

end

clear ans i

load_stiff=search_stiff(any(search_stiff,2),:); % removes zero rows
load_stiff=load_stiff(:,1);

load_mag=zeros(length(load_stiff),1);
load_mag=load_mag+1;
load_mag(1)=1/2;
load_mag(end)=1/2;
load_mag=load_mag/sum(load_mag);
load_mag=-load_mag*Load_ap;
load_mag=round(load_mag*1e6)/1e6;

load=zeros(length(load_stiff),3);
load(:,1)=load_stiff;
load(:,2)=3;
load(:,3)=load_mag;

clear mn_l_stiff stiff_index single_stiff search_stiff z_max
clear load_stiff load_mag imp2_stiff

% 11.2 Boundary Conditions
% -----
bc_i1=1+ne_tf+ne_b;

```

```

bc_i2=bc_i1+ne_w;
bc_i3=bc_i2+2*ne_b+ne_bf;
bc_i4=bc_i3+ne_w;
bc_g3=vertcat((bc_i1:bc_i2)',(bc_i3:bc_i4)');
clear bc_i1 bc_i2 bc_i3 bc_i4

ind_bcx=zeros(length(Loc_Lat(:,1)),1);
for i=1:length(Loc_Lat)
    index_lat=Loc_Lat(i)*12;
    index_lat=round(index_lat*1e6)/1e6;
    for j=1:length(node_y)
        if index_lat==node_y(j)
            ind_bcx(i)=j;
        end
    end
    clear ans j
    clear index_lat
end
clear ans i

node_bcx=zeros(length(Loc_Lat(:,1))*length(bc_g3),1);
for i=1:length(ind_bcx)
    i1=(i-1)*length(bc_g3(:,1))+1;
    i2=(i-0)*length(bc_g3(:,1))+0;
    mult_bc=(ind_bcx(i)-1)*length(node_cs(:,1));

```

```

    node_bcx(i1:i2)=bc_g3+mult_bc;

    clear i1 i2 mult_bc
end

clear ans i

node_bcy=bc_g1';
node_bcz=vertcat(bc_g1',bc_g2');

clear ind_bcx

clear bc_g1 bc_g2 bc_g3

% =====
% PART 12:  ABAQUS INPUT FILE
% =====

% 12.1 Input File Creation & Heading
% -----

inputfile=strcat('noncompositeimpv2intbrace','.inp');

fid=fopen(inputfile,'wt');

fprintf(fid,'** Gregory K. Michaelson, Ph.D., P.E.\n');
fprintf(fid,'** Karl E. Barth, Ph.D.\n');
fprintf(fid,'** %s\n',datestr(now,0));
fprintf(fid,'**\n');

clear date

```

```

fprintf(fid, '** BRIDGE/GIRDER PARAMETERS\n');
fprintf(fid, '** -----\n');
fprintf(fid, '** Span Length [ft] = ');
fprintf(fid, '%10.6f\n', L);
fprintf(fid, '** Std. Mill Plate Width [in] = ');
fprintf(fid, '%10.2f\n', w);
fprintf(fid, '** Std. Mill Plate Thickness [in] = ');
fprintf(fid, '%10.6f\n', t);
fprintf(fid, '** Bearing Plate Thickness [in] = ');
fprintf(fid, '%10.6f\n', t_BRG);
fprintf(fid, '** Total Steel Girder Depth [in] = ');
fprintf(fid, '%10.2f\n', d);
fprintf(fid, '** Top Flange Width [in] = ');
fprintf(fid, '%10.2f\n', btf);
fprintf(fid, '**\n');
fprintf(fid, '** FINITE ELEMENT MODELING PARAMETERS\n');
fprintf(fid, '** -----\n');
fprintf(fid, '** No. of Elements along the Bottom Flange = ');
fprintf(fid, '%10.0f\n', ne_bf);
fprintf(fid, '** No. of Elements along the Web = ');
fprintf(fid, '%10.0f\n', ne_w);
fprintf(fid, '** No. of Elements along Bend Regions = ');
fprintf(fid, '%10.0f\n', ne_b);
fprintf(fid, '** No. of Elements along the Top Flange = ');
fprintf(fid, '%10.0f\n', ne_tf);
fprintf(fid, '** Longitudinal Element Length [in] = ');

```

```

fprintf(fid, '%10.2f\n', le_L);

fprintf(fid, '**\n');

% 12.2 Nodes

% -----

fprintf(fid, '*NODE\n');

for i=1:length(node_girder(:,1))

    fprintf(fid, '%10.0f, %15.6f, %15.6f, %15.6f\n', node_girder(i, :));

end

clear ans i node_girder

for i=1:length(node_stiff(:,1))

    fprintf(fid, '%10.0f, %15.6f, %15.6f, %15.6f\n', node_stiff(i, :));

end

clear ans i node_stiff

% 12.3 Elements

% -----

fprintf(fid, '*ELEMENT, TYPE=S4R, ELSET=GIRDER\n');

for i=1:length(element_girder(:,1))

    fprintf(fid, '%10.0f, %10.0f, %10.0f, %10.0f, %10.0f\n', element_girder(i, :));

end

clear ans i element_girder

fprintf(fid, '*ELEMENT, TYPE=S4R, ELSET=STIFFENER\n');

for i=1:length(rect_stiff(:,1))

    fprintf(fid, '%10.0f, %10.0f, %10.0f, %10.0f, %10.0f\n', rect_stiff(i, :));

end

```

```

end

clear ans i rect_stiff

fprintf(fid, '*ELEMENT, TYPE=S3R, ELSET=STIFFENER\n');

for i=1:length(tri_stiff(:,1))
    fprintf(fid, '%10.0f, %10.0f, %10.0f, %10.0f\n', tri_stiff(i, :));
end

clear ans i tri_stiff

% 12.4 Sets for Boundary Conditions & Data Collection
% -----

fprintf(fid, '*NSET, NSET=BCX\n');

for i=1:length(node_bcx(:,1))
    fprintf(fid, '%10.0f, \n', node_bcx(i, :));
end

clear ans i node_bcx

fprintf(fid, '*NSET, NSET=BCY\n');

for i=1:length(node_bcy(:,1))
    fprintf(fid, '%10.0f, \n', node_bcy(i, :));
end

clear ans i node_bcy

fprintf(fid, '*NSET, NSET=BCZ\n');

for i=1:length(node_bcz(:,1))
    fprintf(fid, '%10.0f, \n', node_bcz(i, :));
end

clear ans i node_bcz

```

```

% 12.5 MPCs & Boundary Conditions
% -----
fprintf(fid, '*BOUNDARY\n');
fprintf(fid, '      BCX,      1\n');
fprintf(fid, '      BCY,      2\n');
fprintf(fid, '      BCZ,      3\n');

% 12.6 Materials & Section Sets
% -----
%Steel Material Model  Added 04/15/2020

E=29559.160900899;      % modulus of elasticity (ksi)
ssy=60.9620413788773;  % static yield strength (ksi)
s02=63.05;             % offset yield strength (ksi)
est=0.0178825333333333; % strain at the onset of strain hardening
Est=1033.46262739326;  % strain hardening modulus (ksi)
su=84.3821008182302;   % tensile strength (ksi)
eu=0.131645626079353;  % strain at the tensile strength

e1=ssy/E;   e2=est;   e3=(eu-est)/10+est;
s1=ssy;     s2=ssy;   s3=Est*(eu-est)/10+ssy;

e6=eu-(eu-est)/10;      e7=eu;
s6=(ssy/s02)*su-(100*(eu-est))/Est;  s7=(ssy/s02)*su;

```

```

e4=2*(e6-e3)/7+e3;      e5=2*(e6-e3)/7+e4;
s4=4*(s6-s3)/7+s3;      s5=2*(s6-s3)/7+s4;

e_eng=[e1;e2;e3;e4;e5;e6;e7];
s_eng=[s1;s2;s3;s4;s5;s6;s7];

e_true=log(1+e_eng);
e_true=e_true-e_true(1);
s_true=s_eng.*(1+e_eng);

steel=horzcat(s_true,e_true);

%End of addition 04/15/2020

fprintf(fid,'*MATERIAL, NAME=STEEL\n');
fprintf(fid,'*DENSITY\n');
fprintf(fid,'%10.6e\n',(0.49/(12^3))/386.08858267716533);
fprintf(fid,'*ELASTIC\n');
fprintf(fid,'%10.0f,%10.2f\n',[29000,0.3]);
fprintf(fid,'*PLASTIC \n');
for i=1:length(steel(:,1))
    fprintf(fid,'%12.3f, %12.7f',steel(i,:));
    fprintf(fid,'\n');
end

```

```

%end of addition 04/15/2020

fprintf(fid, '*SHELL SECTION, ELSET=GIRDER, MATERIAL=STEEL\n');

fprintf(fid, '%10.6f\n', t);

fprintf(fid, '*SHELL SECTION, ELSET=STIFFENER, MATERIAL=STEEL\n');

fprintf(fid, '%10.6f\n', t_BRG);

% 12.7 Static Step & Load Application

% -----

% fprintf(fid, '*STEP, NAME=LOAD, NLGEOM=NO, INC=1\n');

% fprintf(fid, '*STATIC\n');

% fprintf(fid, '%10.0f, %10.0f, %10.6f, %10.0f\n', [1, 1, 1e-5, 1]);

% fprintf(fid, '*CLOAD\n');

% for i=1:length(load(:,1))

%     fprintf(fid, '%10.0f, %10.0f, %10.6f\n', load(i, :));

% end

% clear ans i load

% fprintf(fid, '*OUTPUT, HISTORY, VARIABLE=PRESELECT\n');

% fprintf(fid, '*OUTPUT, FIELD, VARIABLE=PRESELECT\n');

% % fprintf(fid, '*EL PRINT, ELSET=DF, FREQUENCY=1, POSITION=CENTROIDAL\n');

% % fprintf(fid, '          S22\n');

% fprintf(fid, '*END STEP');

% 12.7 Static Riks Step and Load Application (04/16/2020)

% -----

fprintf(fid, '*STEP, NLGEOM=YES, INC=2000 \n');

```

```

fprintf(fid, '*STATIC, RIKS \n');

fprintf(fid, '%10.4f, %10.2f, %10.7f, %10.1f, %10.1f', [0.005, 1, 1e-7, 2, 1]);

fprintf(fid, '\n');

%fprintf(fid, '*NODE PRINT, FREQUENCY=1, NSET=DEFL-CL \n');

%fprintf(fid, 'U3, \n');

fprintf(fid, '*CLOAD, OP=NEW \n');

for i=1:length(load(:,1))

    %fprintf(fid, '%15.0f, %15.0f, %15.6f, ', cload(i, :));

    %fprintf(fid, '\n');

    fprintf(fid, '%10.0f, %10.0f, %10.6f\n', load(i, :));    %From static general

end

clear ans i load

fprintf(fid, '*OUTPUT, HISTORY, VARIABLE=PRESELECT\n');    %From old code

fprintf(fid, '*OUTPUT, FIELD, VARIABLE=PRESELECT\n');    %From Old code

fprintf(fid, '*END STEP');

%End Added Code (04/16/2020)

% 12.8 Close Input File

% -----

fclose('all');

clear ans fid inputfile

```

APPENDIX C: FOURTEEN MILE BRIDGE DESIGN PLANS

The following appendix includes the detail plans from J.B. Turman Engineering, PLLC for the Fourteen Mile Bridge. These plans are not the final construction plans on file with the West Virginia Division of Highways. Note that these plans have been converted from their original 11"x17" format to 8 ½" x 11" for presentation in this report.

PROJECT NO.	SECTION	DATE	BY
18022-37-128 00	SP-000100RD	2/19	UMK
WV 2			

QUANTITY	UNIT	REMARKS
1	LN	SECTION
2	LN	SECTION



EDGE OF SHOULDER



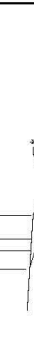
SHOULDER P.I. W/O GUARDRAIL



SHOULDER P.I. WITH GUARDRAIL



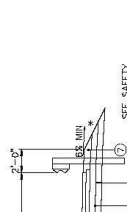
GUARDRAIL AS SHOWN ON PLANS



GUARDRAIL DETAIL

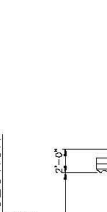


TYPICAL HEEL-IN DETAIL



WV 37 - DETOUR CROWN SECTION

STA. 204+01.25 TO STA. 204+13.69
STA. 204+14.33 TO STA. 204+63.36
STA. 204+68.36 TO STA. 204+100.00



WV 37 - DETOUR SUPERELEVATED SECTION CURVE LEFT

STA. 201+56.81 TO STA. 203+01.25



WV 37 - DETOUR SUPERELEVATED SECTION CURVE RIGHT

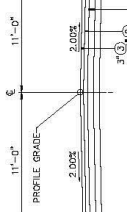
STA. 204+14.43 TO STA. 204+68.36



DRIVEWAY - DETOUR CROWN SECTION

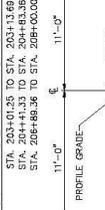
STA. 300+97.62 TO STA. 301+15.99

* SLOPES VARY - SEE CROSS SECTIONS



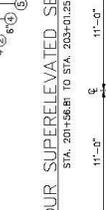
WV 37 - SUPERELEVATED SECTION CURVE RIGHT

STA. 100+60.00 TO STA. 102+00.00
STA. 105+40.00 TO STA. 107+52.11



WV 37 - SUPERELEVATED SECTION CURVE RIGHT

STA. 102+00.00 TO STA. 102+38.12



WV 37 - SUPERELEVATED SECTION CURVE RIGHT

STA. 103+11.81 TO STA. 104+68.60



WV 37 - SUPERELEVATED SECTION CURVE RIGHT

STA. 104+68.60 TO STA. 104+68.60

ITEM	DESCRIPTION	UNITS
------	-------------	-------

- 1 MARSHALL ASPHALT WEARING COURSE, STONE OR GRAVEL (OR SLAG), TYPE 1
- 2 MARSHALL ASPHALT BASE COURSE, STONE OR GRAVEL (OR SLAG), TYPE 1
- 3 MARSHALL ASPHALT BASE COURSE, STONE OR GRAVEL (OR SLAG), TYPE 2
- 4 AGGREGATE BASE COURSE, CLASS 1
- 5 FABRIC FOR SEPARATION
- 6 SUBGRADE
- 7 AGGREGATE BASE COURSE, CLASS 10
- 8 AGGREGATE BASE COURSE, CLASS 3
- 9 STANDARD MILLING
- 10 ASPHALT MATERIAL
- 11 TYPE 1 GUARDRAIL, CLASS 1
- 12 ASPHALT
- 13 ASPHALT
- 14 ASPHALT
- 15 ASPHALT
- 16 ASPHALT
- 17 ASPHALT
- 18 ASPHALT
- 19 ASPHALT
- 20 ASPHALT

THE WEST VIRGINIA DEPARTMENT OF TRANSPORTATION

FOURTEEN MILE BRIDGE
WV 37 OVER
FOURTEENMILE CREEK

P.O. Box 483
Beech Grove, WV 25504
www.jbengineering.com
304-733-1336

J.B. TURMAN ENGINEERING, PLLC

REVISION

DATE

BY

TITLE

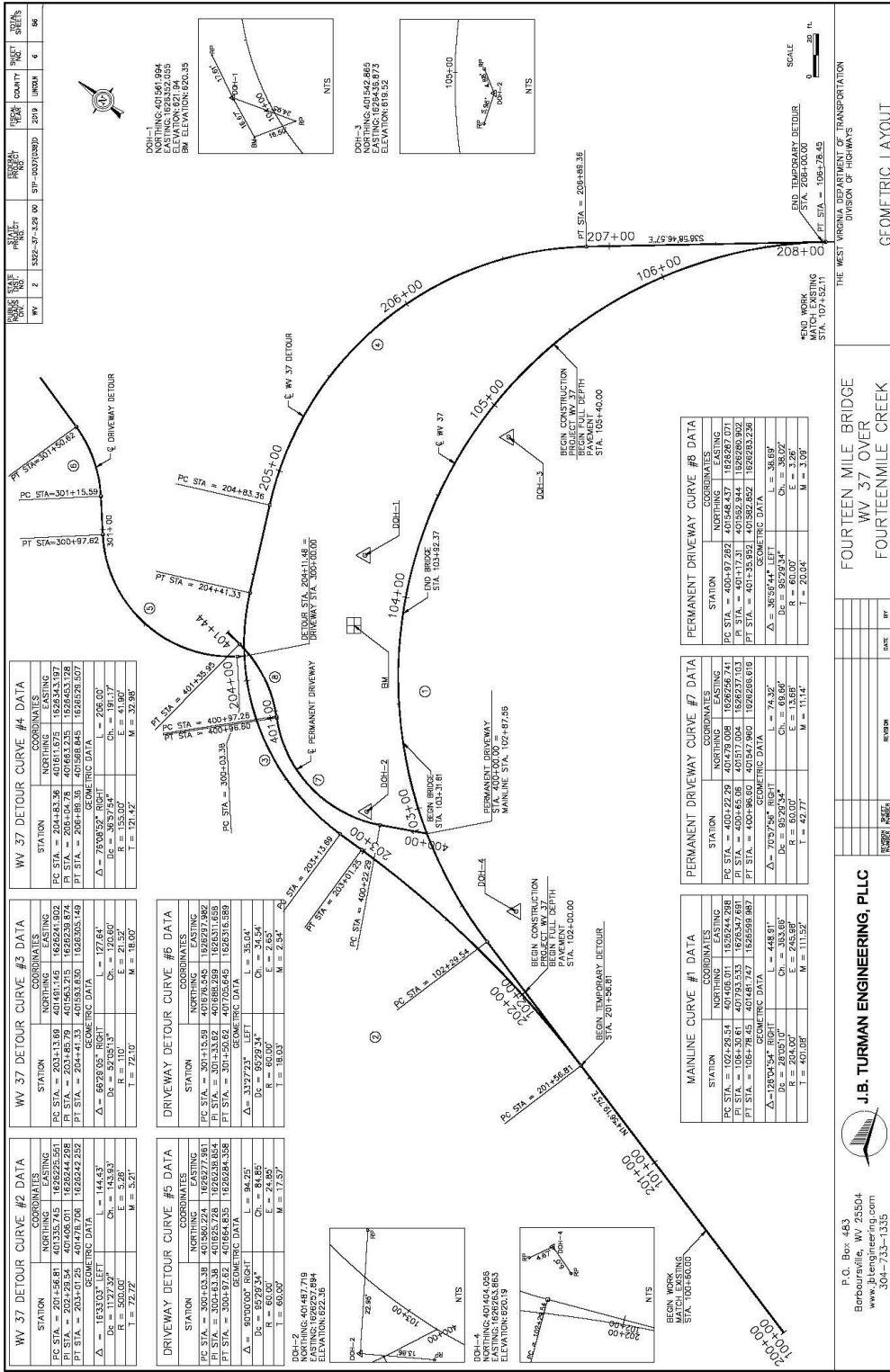
SCALE

SUMMARY OF ESTIMATED QUANTITIES

ITEM	ALT	DESCRIPTION	UNIT	QUANTITY
527096-001		200 LB CHANNEL POST	LF	32
661001-001		0.080 IN FLAT SHEET SIGN	SF	12
663001-026		EDGE LINE, TYPE II - 6 IN	LF	662
665002-040		CENTERLINE, TYPE II - 6 IN	LF	662
401001-020	AA1	MARSHALL ASPHALT BASE COURSE, SS, TYPE 1	TN	365
401001-021	AA2	MARSHALL ASPHALT BASE COURSE, S, TYPE 1	TN	376
401001-023	BB1	MARSHALL ASPHALT BASE COURSE, SS, TYPE 2	TN	249
401001-024	BB2	MARSHALL ASPHALT BASE COURSE, S, TYPE 2	TN	237
401001-020	CC1	MARSHALL ASPHALT WEARING COURSE, SS, TYPE 1	TN	101
401002-021	CC2	MARSHALL ASPHALT WEARING COURSE, S, TYPE 1	TN	98
203001-000		DISMANTLING STRUCTURE	LS	1
212001-000		STRUCTURE EXCAVATION	CY	508
216001-000		UTILITY PROTECTION	CY	216
601001-001		CLASS II CONCRETE	CY	10
601003-001		CLASS K CONCRETE	CY	10
601000-001		ULTRA HIGH PERFORMANCE CONCRETE	CY	5
602002-001		REINFORCING STEEL BAR	LB	15,369
610001-001		EPOXY COATED REINFORCING STEEL BAR	LB	2,615
610002-001		NON-COATED BEARING ELASTOMER	EA	10
619001-001		PRECAST CONCRETE	LS	1
619002-001		CONSTRUCTION LAYOUT STAKE	LS	1
619003-001		PRE-FABRICATED BRIDGE ELEMENT SUPERSTRUCTURE	EA	5

SUMMARY OF ESTIMATED QUANTITIES

ITEM	ALT	DESCRIPTION	UNIT	QUANTITY
201001-000		CLEARING AND GRUBBING	LS	1
204001-000		MOBILIZATION	LS	1
207001-001		UNCLASSIFIED EXCAVATION	CY	4334
207002-000		SHORING	SY	246
207004-000		FABRIC FOR SEPARATION	SY	3343
211001-000		UNCLASSIFIED BORROW EXCAVATION	CY	3668
307001-000		AGGREGATE BASE COURSE, CLASS 1	CY	1462
307001-000		AGGREGATE BASE COURSE, CLASS 3	CY	98
307001-000		AGGREGATE BASE COURSE, CLASS 10	CY	120
456002-001		ASPHALT MATERIAL	GAU	131
459002-001		STANDARD MILLING	SY	1065
502001-012		12 IN PORTLAND CEMENT CONCRETE APPROACH SLAB	SY	129
607001-001		TYPE I GUARDRAIL, CLASS 1	LF	79
607003-001		THREE BEAM GUARDRAIL BRIDGE TRANSITION	EA	4
607004-001		FLARED END TERMINAL	EA	3
636005-001		TEMPORARY STRUCTURE FOR MAINTAINING TRAFFIC	LS	1
636007-001		ERADICATION OF PAVEMENT MARKINGS	LF	300
636008-002		TEMPORARY PAVEMENT MARKINGS - PAINT 6 IN	EA	892
636012-001		INDIVIDUAL TRAFFIC CONTROL DEVICE CLEANING	IN	6770
636013-001		INDIVIDUAL TRAFFIC CONTROL DEVICE CLEANING	EA	98
636014-001		FLAGGER	HR	360
636019-001		TEMPORARY GUARDRAIL BARRIER	LF	791
636022-001		CHANGEABLE MESSAGE SIGN	DAY	28
636025-001		WARNING LIGHTS, TYPE B	DAY	2320
636032-001		RIGHT OF WAY MARKER	EA	6
636031-001		CONSTRUCTION LAYOUT STAKE	LS	1
640002-001		LARGE FIELD OFFICE AND STORAGE BUILDING	MG	12
640003-001		BUILDING EQUIPMENT	LS	1
642004-003		SEED MIXTURE D	LB	49
642005-001		LIQUID NITROGEN OR LIQUID	TN	1.46
642006-001		FERTILIZER	TN	0.37
642010-001		AGRICULTURAL LIMESTONE	TN	1.09
642012-001		SILT FENCE	LF	2373
642013-001		DITCH CHECK	EA	11
642040-001		INLET PROTECTION	EA	1
645001-001		PRIMARY REINFORCEMENT, 2400 LB/FT	SY	2072
652001-001		AGRICULTURAL LIMESTONE	TN	1.09
652002-001		FERTILIZER	TN	0.17
652003-002		FERTILIZER, UREA FORMALDEHYDE	TN	0.17
652003-001		SEED MIXTURE C-2	LB	49
652004-001		STRAW OR HAY MULCH	TN	1.46



ROUTE	PROJECT NO.	DATE	SCALE	SHEET NO.	TOTAL SHEETS
WV 2	SS02-37-120 00	SP-0001000D	2019	WORK	6

STATION	NORTHING	EASTING
PC STA = 204+13.36	407611.675	1626241.902
PI STA = 204+104.78	407663.235	1626453.178
PT STA = 204+185.38	407688.845	1626529.507
GEOMETRIC DATA		
Δ = 78°05'32" RIGHT	L = 206.00'	
Dc = 38.9754'	Ch = 191.17'	
R = 155.00'	E = 41.90'	
T = 12.14'	M = 31.96'	

STATION	NORTHING	EASTING
PC STA = 204+13.36	407611.675	1626241.902
PI STA = 204+104.78	407663.235	1626453.178
PT STA = 204+185.38	407688.845	1626529.507
GEOMETRIC DATA		
Δ = 69°28'05" RIGHT	L = 127.64'	
Dc = 52.95'13"	Ch = 128.60'	
R = 110'	E = 21.59'	
T = 72.0'	M = 18.65'	

STATION	NORTHING	EASTING
PC STA = 203+13.89	407481.146	1626241.902
PI STA = 203+145.79	407563.215	1626248.874
PT STA = 203+185.38	407688.845	1626529.507
GEOMETRIC DATA		
Δ = 78°05'32" RIGHT	L = 206.00'	
Dc = 38.9754'	Ch = 191.17'	
R = 155.00'	E = 41.90'	
T = 12.14'	M = 31.96'	

STATION	NORTHING	EASTING
PC STA = 203+13.89	407481.146	1626241.902
PI STA = 203+145.79	407563.215	1626248.874
PT STA = 203+185.38	407688.845	1626529.507
GEOMETRIC DATA		
Δ = 33°27'31"	L = 35.64'	
Dc = 65.79'34"	Ch = 34.54'	
R = 60.00'	E = 2.85'	
T = 18.03'	M = 2.54'	

STATION	NORTHING	EASTING
PC STA = 202+13.89	407481.146	1626241.902
PI STA = 202+145.79	407563.215	1626248.874
PT STA = 202+185.38	407688.845	1626529.507
GEOMETRIC DATA		
Δ = 69°28'05" RIGHT	L = 127.64'	
Dc = 52.95'13"	Ch = 128.60'	
R = 110'	E = 21.59'	
T = 72.0'	M = 18.65'	

STATION	NORTHING	EASTING
PC STA = 201+26.81	407408.011	1626244.298
PI STA = 201+78.45	407481.747	1626268.184
PT STA = 201+104.78	407563.215	1626248.874
GEOMETRIC DATA		
Δ = 128°39'58" RIGHT	L = 448.91'	
Dc = 166.69'	Ch = 448.91'	
R = 204.00'	E = 245.89'	
T = 401.09'	M = 111.59'	

STATION	NORTHING	EASTING
PC STA = 201+26.81	407408.011	1626244.298
PI STA = 201+78.45	407481.747	1626268.184
PT STA = 201+104.78	407563.215	1626248.874
GEOMETRIC DATA		
Δ = 79°37'55" RIGHT	L = 74.32'	
Dc = 60.00'	Ch = 74.32'	
R = 60.00'	E = 13.88'	
T = 42.77'	M = 11.14'	

STATION	NORTHING	EASTING
PC STA = 200+17.292	407548.437	1626287.071
PI STA = 200+113.82	407562.842	1626323.224
PT STA = 200+104.78	407563.215	1626248.874
GEOMETRIC DATA		
Δ = 38°55'44" LEFT	L = 38.69'	
Dc = 60.00'	Ch = 38.69'	
R = 60.00'	E = 3.26'	
T = 20.04'	M = 3.09'	

STATION	NORTHING	EASTING
PC STA = 400+17.292	401548.437	1626287.071
PI STA = 400+113.82	401562.842	1626323.224
PT STA = 400+104.78	401563.215	1626248.874
GEOMETRIC DATA		
Δ = 38°55'44" LEFT	L = 38.69'	
Dc = 60.00'	Ch = 38.69'	
R = 60.00'	E = 3.26'	
T = 20.04'	M = 3.09'	

STATION	NORTHING	EASTING
PC STA = 400+17.292	401548.437	1626287.071
PI STA = 400+113.82	401562.842	1626323.224
PT STA = 400+104.78	401563.215	1626248.874
GEOMETRIC DATA		
Δ = 79°37'55" RIGHT	L = 74.32'	
Dc = 60.00'	Ch = 74.32'	
R = 60.00'	E = 13.88'	
T = 42.77'	M = 11.14'	

STATION	NORTHING	EASTING
PC STA = 102+26.34	407408.011	1626244.298
PI STA = 102+78.45	407481.747	1626268.184
PT STA = 102+104.78	407563.215	1626248.874
GEOMETRIC DATA		
Δ = 128°39'58" RIGHT	L = 448.91'	
Dc = 166.69'	Ch = 448.91'	
R = 204.00'	E = 245.89'	
T = 401.09'	M = 111.59'	

STATION	NORTHING	EASTING
PC STA = 102+26.34	407408.011	1626244.298
PI STA = 102+78.45	407481.747	1626268.184
PT STA = 102+104.78	407563.215	1626248.874
GEOMETRIC DATA		
Δ = 79°37'55" RIGHT	L = 74.32'	
Dc = 60.00'	Ch = 74.32'	
R = 60.00'	E = 13.88'	
T = 42.77'	M = 11.14'	

P.O. Box 483
Bencouville, WV 25504
www.jbturmanengineering.com
304-733-1338

J.B. TURMAN ENGINEERING, PLLC

FOURTEEN MILE BRIDGE
WV 37 OVER
FOURTEENMILE CREEK

THE WEST VIRGINIA DEPARTMENT OF TRANSPORTATION
DIVISION OF HIGHWAYS

GEOMETRIC LAYOUT

PROJECT NAME	DATE	BY	CHKD	DATE	BY	CHKD
13322-3P-138 00	10/24/13	MM	MM	10/24/13	MM	MM

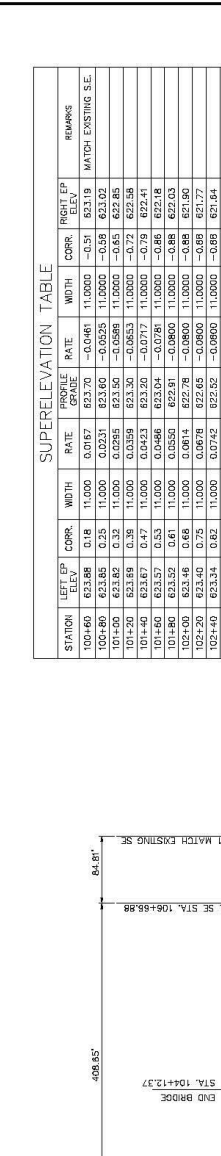
DATE	BY	CHKD	DATE	BY	CHKD
10/24/13	MM	MM	10/24/13	MM	MM

DATE	BY	CHKD	DATE	BY	CHKD
10/24/13	MM	MM	10/24/13	MM	MM

DATE	BY	CHKD	DATE	BY	CHKD
10/24/13	MM	MM	10/24/13	MM	MM

DATE	BY	CHKD	DATE	BY	CHKD
10/24/13	MM	MM	10/24/13	MM	MM

STATION	LEFT E.P.	CORR.	WIDTH	RATE	PROFILE	RATE	WIDTH	CORR.	RIGHT E.P.	REMARKS
102+40	623.86	0.18	11.000	0.0167	623.70	-0.0461	11.0000	-0.51	631.19	
102+60	623.65	0.25	11.000	0.0231	623.60	-0.0525	11.0000	-0.58	631.02	
102+80	623.62	0.32	11.000	0.0285	623.56	-0.0588	11.0000	-0.65	622.85	
101+20	623.69	0.38	11.000	0.0359	623.30	-0.0653	11.0000	-0.71	622.58	
101+40	623.67	0.47	11.000	0.0423	623.20	-0.0717	11.0000	-0.79	622.41	
101+60	623.57	0.53	11.000	0.0486	623.04	-0.0781	11.0000	-0.86	622.18	
101+80	623.52	0.61	11.000	0.0550	622.91	-0.0845	11.0000	-0.88	622.03	
102+00	623.49	0.68	11.000	0.0614	622.78	-0.0909	11.0000	-0.88	621.99	
102+20	623.46	0.75	11.000	0.0678	622.68	-0.0973	11.0000	-0.88	621.99	
102+40	623.34	0.82	11.000	0.0742	622.54	-0.0990	11.0000	-0.89	621.84	
102+58.12	623.28	0.85	11.000	0.0800	622.40	-0.0990	11.0000	-0.88	621.52	BEGIN FULL S.E.
102+60	623.27	0.85	11.000	0.0800	622.38	-0.0990	11.0000	-0.88	621.51	
102+80	623.15	0.85	11.000	0.0800	622.27	-0.0990	11.0000	-0.88	621.39	
103+00	623.03	0.85	11.000	0.0800	622.16	-0.0990	11.0000	-0.88	621.28	
103+20	622.93	0.85	11.000	0.0800	622.05	-0.0990	11.0000	-0.88	621.17	
103+40	622.81	0.85	11.000	0.0800	621.94	-0.0990	11.0000	-0.88	621.06	
103+60	622.70	0.85	11.000	0.0800	621.82	-0.0990	11.0000	-0.88	620.94	
103+80	622.58	0.85	11.000	0.0800	621.70	-0.0990	11.0000	-0.89	620.82	
104+00	622.47	0.85	11.000	0.0800	621.59	-0.0990	11.0000	-0.88	620.71	
104+20	622.35	0.85	11.000	0.0800	621.47	-0.0990	11.0000	-0.89	620.59	
104+40	622.24	0.85	11.000	0.0800	621.35	-0.0990	11.0000	-0.88	620.48	
104+60	622.13	0.85	11.000	0.0800	621.25	-0.0990	11.0000	-0.88	620.37	
104+80	622.01	0.85	11.000	0.0800	621.14	-0.0990	11.0000	-0.88	620.25	
105+00	621.90	0.85	11.000	0.0800	621.03	-0.0990	11.0000	-0.88	620.14	
105+20	621.78	0.85	11.000	0.0800	620.94	-0.0990	11.0000	-0.88	620.06	
105+40	621.66	0.85	11.000	0.0800	620.86	-0.0990	11.0000	-0.89	619.90	
105+60	621.54	0.85	11.000	0.0800	620.78	-0.0990	11.0000	-0.89	619.85	
105+80	621.42	0.85	11.000	0.0800	620.70	-0.0990	11.0000	-0.89	619.80	
106+00	621.30	0.85	11.000	0.0800	620.63	-0.0990	11.0000	-0.89	619.45	
106+20	621.18	0.85	11.000	0.0800	620.57	-0.0990	11.0000	-0.89	619.49	
106+40	621.06	0.85	11.000	0.0800	620.50	-0.0990	11.0000	-0.89	619.32	
106+60	620.94	0.85	11.000	0.0800	620.43	-0.0990	11.0000	-0.88	619.22	
106+80	620.82	0.85	11.000	0.0800	620.36	-0.0990	11.0000	-0.88	619.14	
106+96.88	620.60	0.85	11.000	0.0800	619.72	-0.0990	11.0000	-0.88	618.92	END FULL S.E.
106+80	620.42	0.82	11.000	0.0744	619.60	-0.0990	11.0000	-0.88	618.72	
107+00	620.12	0.72	11.000	0.0658	619.40	-0.0990	11.0000	-0.88	618.52	
107+20	619.93	0.63	11.000	0.0573	619.30	-0.0990	11.0000	-0.88	618.42	
107+40	619.74	0.54	11.000	0.0488	619.20	-0.0990	11.0000	-0.88	618.32	
107+52.11	619.63	0.48	11.000	0.0409	619.18	-0.0990	11.0000	-0.88	618.30	MATCH EXISTING S.E.



SUPERELEVATION TABLE

STATION	LEFT E.P.	CORR.	WIDTH	RATE	PROFILE	RATE	WIDTH	CORR.	RIGHT E.P.	REMARKS
102+40	623.86	0.18	11.000	0.0167	623.70	-0.0461	11.0000	-0.51	631.19	
102+60	623.65	0.25	11.000	0.0231	623.60	-0.0525	11.0000	-0.58	631.02	
102+80	623.62	0.32	11.000	0.0285	623.56	-0.0588	11.0000	-0.65	622.85	
101+20	623.69	0.38	11.000	0.0359	623.30	-0.0653	11.0000	-0.71	622.58	
101+40	623.67	0.47	11.000	0.0423	623.20	-0.0717	11.0000	-0.79	622.41	
101+60	623.57	0.53	11.000	0.0486	623.04	-0.0781	11.0000	-0.86	622.18	
101+80	623.52	0.61	11.000	0.0550	622.91	-0.0845	11.0000	-0.88	622.03	
102+00	623.49	0.68	11.000	0.0614	622.78	-0.0909	11.0000	-0.88	621.99	
102+20	623.46	0.75	11.000	0.0678	622.68	-0.0973	11.0000	-0.88	621.99	
102+40	623.34	0.82	11.000	0.0742	622.54	-0.0990	11.0000	-0.89	621.84	
102+58.12	623.28	0.85	11.000	0.0800	622.40	-0.0990	11.0000	-0.88	621.52	BEGIN FULL S.E.
102+60	623.27	0.85	11.000	0.0800	622.38	-0.0990	11.0000	-0.88	621.51	
102+80	623.15	0.85	11.000	0.0800	622.27	-0.0990	11.0000	-0.88	621.39	
103+00	623.03	0.85	11.000	0.0800	622.16	-0.0990	11.0000	-0.88	621.28	
103+20	622.93	0.85	11.000	0.0800	622.05	-0.0990	11.0000	-0.88	621.17	
103+40	622.81	0.85	11.000	0.0800	621.94	-0.0990	11.0000	-0.88	621.06	
103+60	622.70	0.85	11.000	0.0800	621.82	-0.0990	11.0000	-0.88	620.94	
103+80	622.58	0.85	11.000	0.0800	621.70	-0.0990	11.0000	-0.89	620.82	
104+00	622.47	0.85	11.000	0.0800	621.59	-0.0990	11.0000	-0.88	620.71	
104+20	622.35	0.85	11.000	0.0800	621.47	-0.0990	11.0000	-0.89	620.59	
104+40	622.24	0.85	11.000	0.0800	621.35	-0.0990	11.0000	-0.88	620.48	
104+60	622.13	0.85	11.000	0.0800	621.25	-0.0990	11.0000	-0.88	620.37	
104+80	622.01	0.85	11.000	0.0800	621.14	-0.0990	11.0000	-0.88	620.25	
105+00	621.90	0.85	11.000	0.0800	621.03	-0.0990	11.0000	-0.88	620.14	
105+20	621.78	0.85	11.000	0.0800	620.94	-0.0990	11.0000	-0.88	620.06	
105+40	621.66	0.85	11.000	0.0800	620.86	-0.0990	11.0000	-0.89	619.90	
105+60	621.54	0.85	11.000	0.0800	620.78	-0.0990	11.0000	-0.89	619.85	
105+80	621.42	0.85	11.000	0.0800	620.70	-0.0990	11.0000	-0.89	619.80	
106+00	621.30	0.85	11.000	0.0800	620.63	-0.0990	11.0000	-0.89	619.45	
106+20	621.18	0.85	11.000	0.0800	620.57	-0.0990	11.0000	-0.89	619.49	
106+40	621.06	0.85	11.000	0.0800	620.50	-0.0990	11.0000	-0.89	619.32	
106+60	620.94	0.85	11.000	0.0800	620.43	-0.0990	11.0000	-0.88	619.22	
106+80	620.82	0.85	11.000	0.0800	620.36	-0.0990	11.0000	-0.88	619.14	
106+96.88	620.60	0.85	11.000	0.0800	619.72	-0.0990	11.0000	-0.88	618.92	END FULL S.E.
106+80	620.42	0.82	11.000	0.0744	619.60	-0.0990	11.0000	-0.88	618.72	
107+00	620.12	0.72	11.000	0.0658	619.40	-0.0990	11.0000	-0.88	618.52	
107+20	619.93	0.63	11.000	0.0573	619.30	-0.0990	11.0000	-0.88	618.42	
107+40	619.74	0.54	11.000	0.0488	619.20	-0.0990	11.0000	-0.88	618.32	
107+52.11	619.63	0.48	11.000	0.0409	619.18	-0.0990	11.0000	-0.88	618.30	MATCH EXISTING S.E.

SUPERELEVATION TABLE

FOURTEEN MILE BRIDGE
WV 37 OVER
FOURTEENMILE CREEK

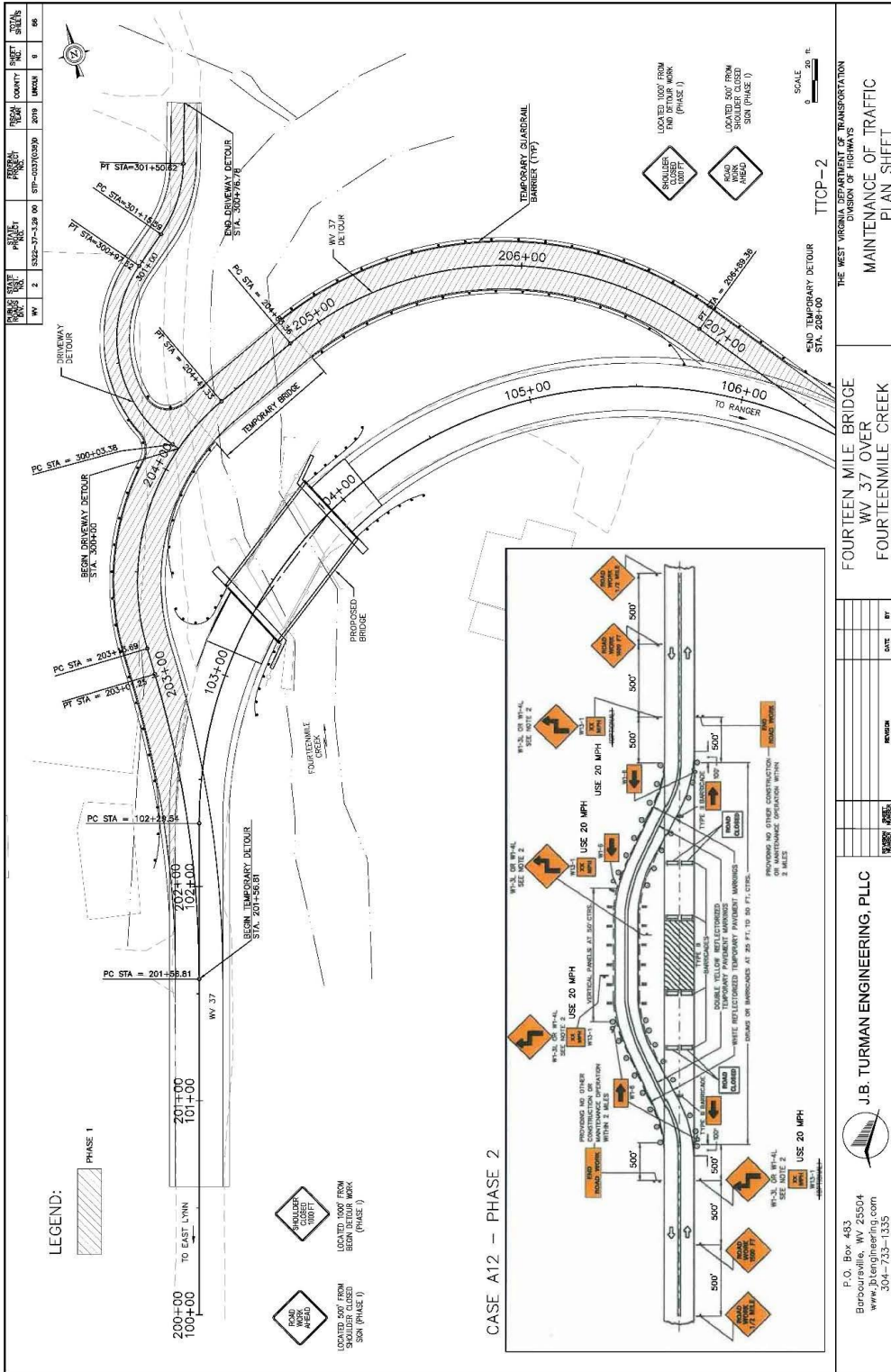
THE WEST VIRGINIA DEPARTMENT OF TRANSPORTATION
DIVISION OF HIGHWAYS

SUPERELEVATION DIAGRAM

SCALE
0 50 100
FEET

P.O. Box 483
Bellefonte, WV 25504
www.jbenengineering.com
304-233-1335

J.B. TURMAN ENGINEERING, PLLC



PROJECT NO.	13222-77-128 00	DATE	08/11/10
SCALE	1" = 40'	PROJECT	TRAFFIC CONTROL
DATE	08/11/10	CONTRACT	13222-77-128 00
NO.	2	NO.	6

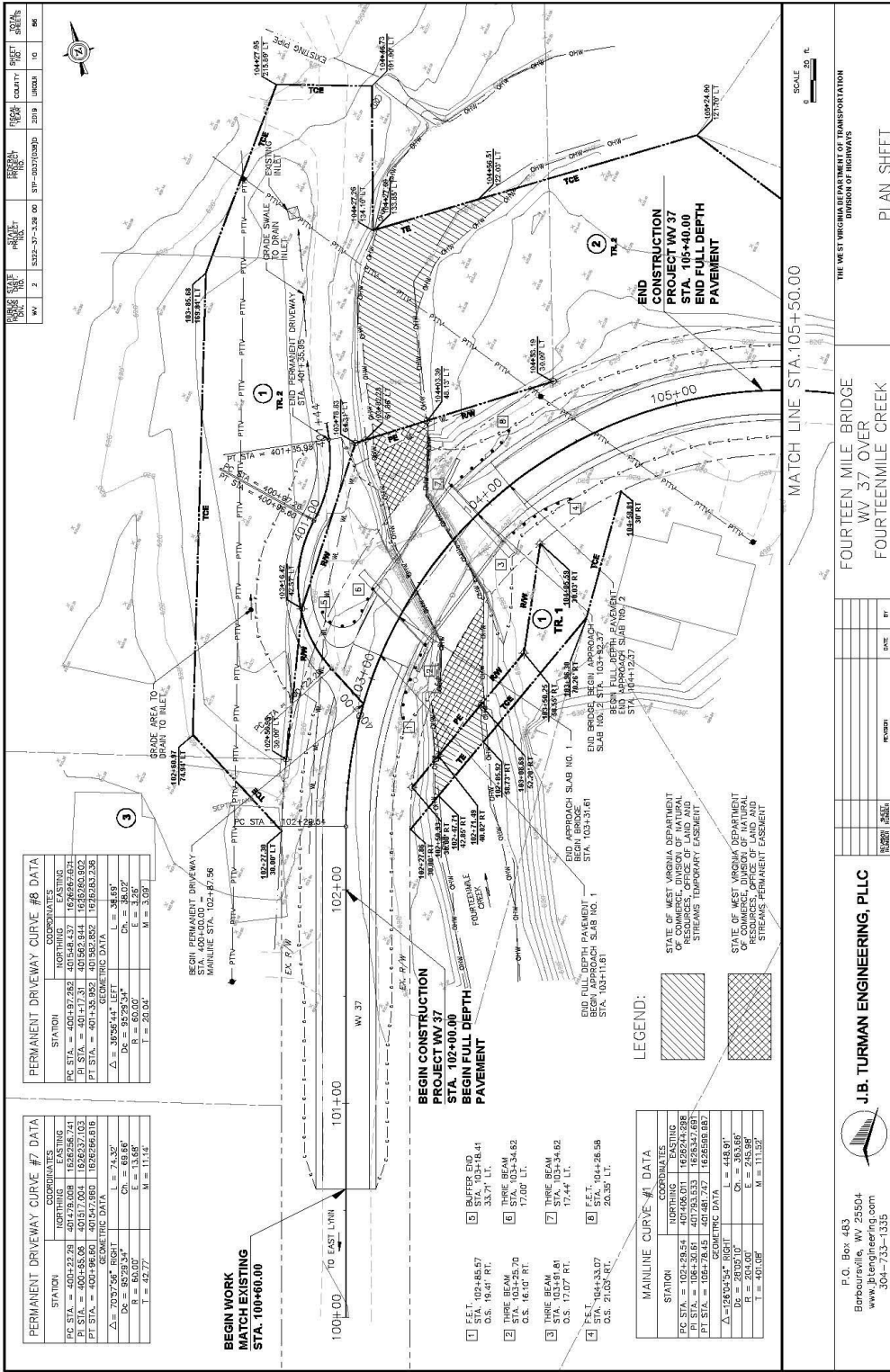
DATE	08/11/10	NO.	6
NO.	6	NO.	6

THE WEST VIRGINIA DEPARTMENT OF TRANSPORTATION
DIVISION OF HIGHWAYS
MAINTENANCE OF TRAFFIC
PLAN SHEET

FOURTEEN MILE BRIDGE
WV 37 OVER
FOURTEENMILE CREEK

J.B. TURMAN ENGINEERING, PLLC
P.O. Box 483
Barbourville, WV 25504
www.tbengineering.com
304-733-1335

TTCP-2
SCALE 1" = 40' F.
FOURTEEN MILE BRIDGE
WV 37 OVER
FOURTEENMILE CREEK



PERMANENT DRIVEWAY CURVE #7 DATA

STATION	COORDINATES
PC STA. = 400+222.29	401548.437 1626256.741
PI STA. = 400+556.06	401617.31 1626257.103
PT STA. = 400+969.60	401852.832 1626256.816
GEOMETRIC DATA	
$\Delta = 70.9756^\circ$ RIGHT	$L = 74.32'$
$D_c = 85.79'$	$C_h = 69.66'$
$R = 60.07'$	$E = 13.68'$
$T = 49.77'$	$M = 11.14'$

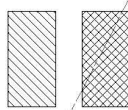
PERMANENT DRIVEWAY CURVE #8 DATA

STATION	COORDINATES
PC STA. = 400+197.262	401548.437 1626256.741
PI STA. = 401+17.31	401862.944 1626260.802
PT STA. = 401+55.952	401852.832 1626256.816
GEOMETRIC DATA	
$\Delta = 95.5844^\circ$ LEFT	$L = 38.68'$
$D_c = 95.79'$	$C_h = 38.07'$
$R = 60.07'$	$E = 3.26'$
$T = 28.93'$	$M = 3.05'$

BEGIN WORK MATCH EXISTING STA. 100+60.00

BEGIN CONSTRUCTION PROJECT WV 37 BEGIN FULL DEPTH PAVEMENT

LEGEND:



STATE OF WEST VIRGINIA DEPARTMENT OF COMMERCE, DIVISION OF NATURAL RESOURCES
 STATE OF WEST VIRGINIA DEPARTMENT OF COMMERCE, DIVISION OF NATURAL RESOURCES
 STREAMS PERMANENT CASSETT
 STREAMS TEMPORARY EXPOSURE

MAINLINE CURVE #1 DATA

STATION	COORDINATES
PC STA. = 102+29.54	401406.011 1626244.898
PI STA. = 103+25.70	401481.707 1626256.887
PT STA. = 104+26.58	401481.707 1626256.887
GEOMETRIC DATA	
$\Delta = 189.933^\circ$ RIGHT	$L = 448.91'$
$D_c = 203.00'$	$C_h = 448.91'$
$R = 203.00'$	$E = 2.63.98'$
$T = 401.08'$	$M = 111.52'$

- 1 F.E.T. 102+46.67
O.S. 18.41' RT.
- 2 THREE BEAM
STA. 103+25.70
O.S. 16.10' RT.
- 3 THREE BEAM
STA. 103+34.82
O.S. 17.07' RT.
- 4 F.E.T. 104+26.58
O.S. 21.03' RT.
- 5 BUFFER END
O.S. 18.41' RT.
- 6 THREE BEAM
STA. 103+34.82
O.S. 16.10' RT.
- 7 THREE BEAM
STA. 103+34.82
O.S. 17.07' RT.
- 8 F.E.T. 104+26.58
O.S. 21.03' RT.

J.B. TURMAN ENGINEERING, PLLC

P.O. Box 483
 Berea, WV 25504
 www.tbengineering.com
 304-733-1335

FOURTEEN MILE BRIDGE
 WV 37 OVER
 FOURTEENMILE CREEK

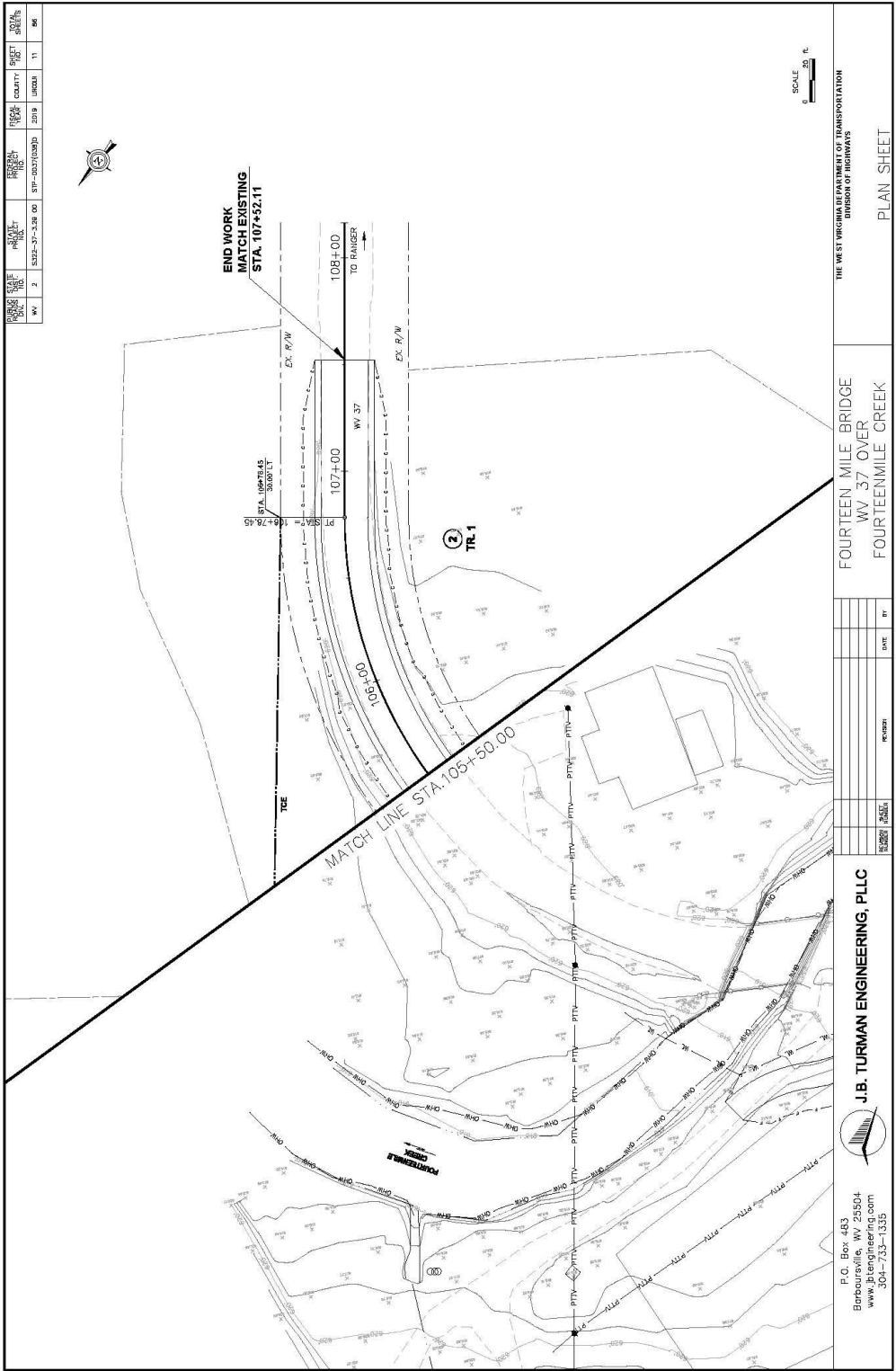
THE WEST VIRGINIA DEPARTMENT OF TRANSPORTATION
 DIVISION OF HIGHWAYS

PLAN SHEET

MATCH LINE STA. 105+50.00

SCALE 0 20 40 FT.

PROJECT NO.	1000000000
DATE	10/1/2010
DESIGNER	J.B. TURMAN ENGINEERING, PLLC
CHECKER	J.B. TURMAN ENGINEERING, PLLC
DATE	10/1/2010
PROJECT	FOURTEEN MILE BRIDGE
SHEET	10
DATE	10/1/2010



PROJECT NO.	DATE	BY	CHECKED	SCALE
107-37-128-00	10/11/11	WV	2	AS SHOWN
SPR-0021049D	2011	UNITS	11	SHEET
				56

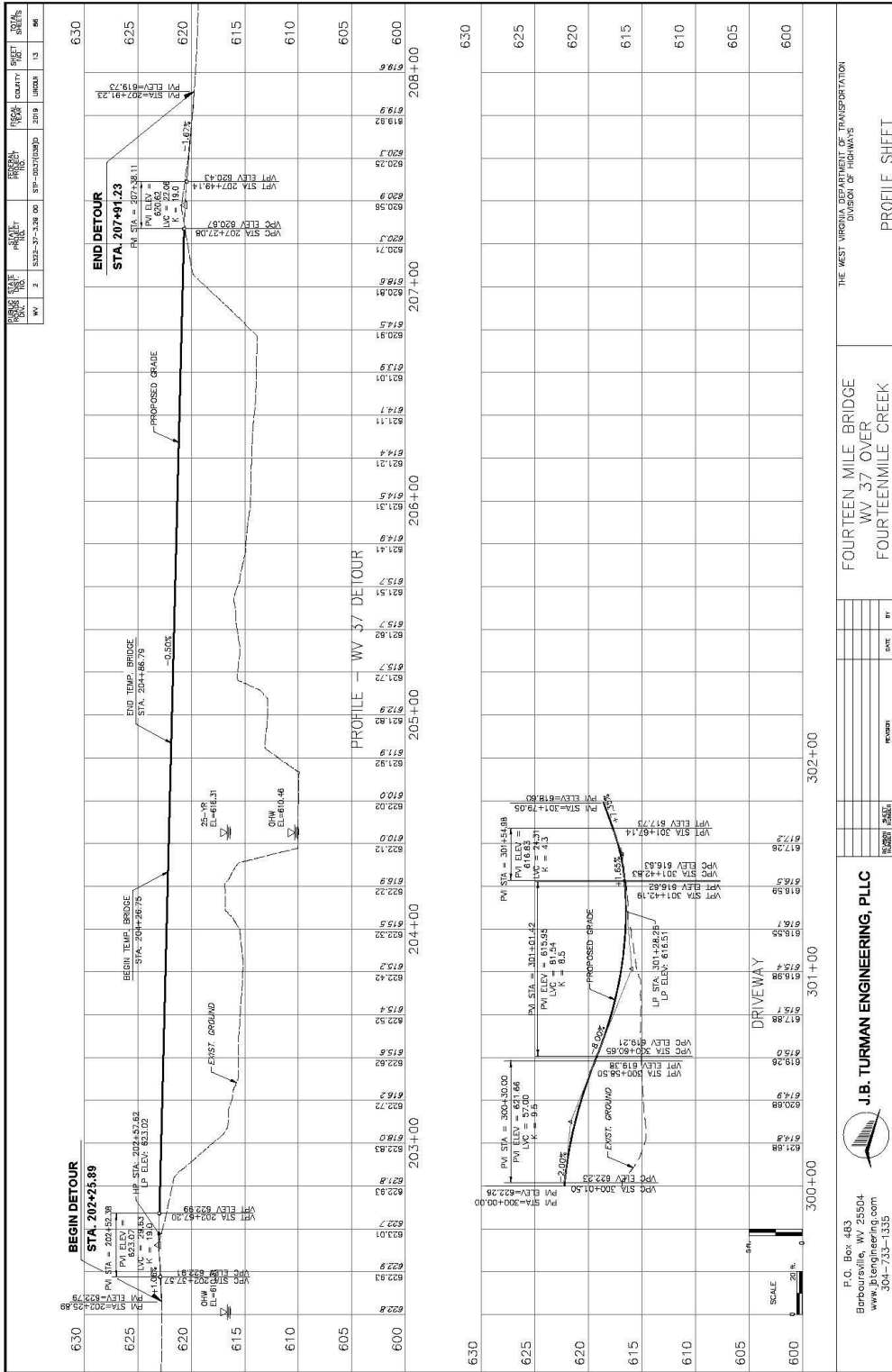
THE WEST VIRGINIA DEPARTMENT OF TRANSPORTATION
DIVISION OF HIGHWAYS

PLAN SHEET

FOURTEEN MILE BRIDGE
WV 37 OVER
FOURTEENMILE CREEK

NO.	DATE	BY	REVISION


J.B. TURMAN ENGINEERING, PLLC
 P.O. Box 483
 Bercoeurville, WV 25504
 www.jbtengineering.com
 304-733-1335



THE WEST VIRGINIA DEPARTMENT OF TRANSPORTATION
DIVISION OF HIGHWAYS

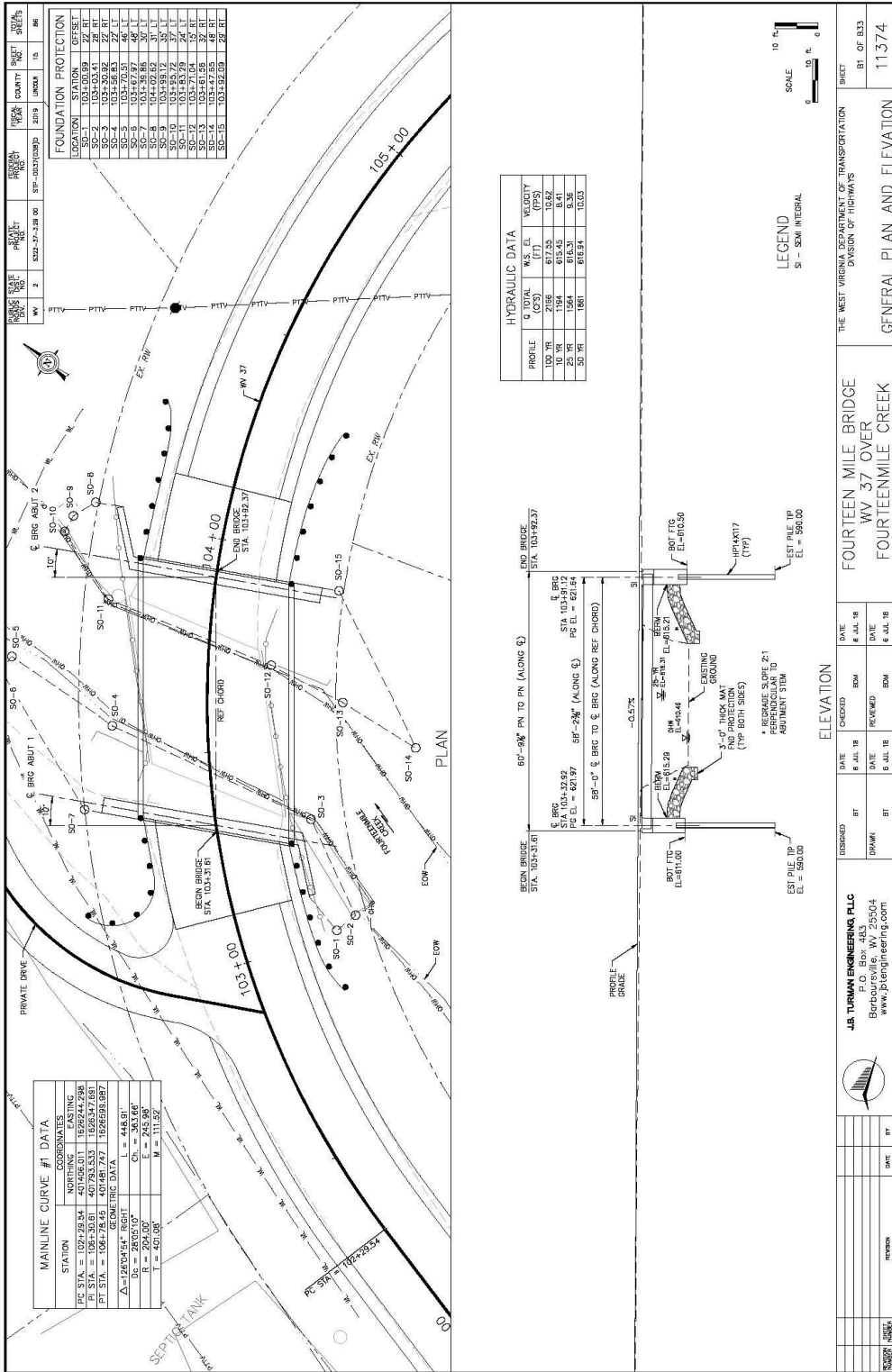
FOURTEEN MILE BRIDGE
WV 37 OVER
FOURTEENMILE CREEK

NO.	DATE	BY

J.B. TURMAN ENGINEERING, PLLC

P.O. Box 483
Berkeley, WV 25504
www.jbturman.com
304-733-1335

PROFILE SHEET



MAINLINE CURVE #1 DATA

STATION	NORTHING	EASTING
PC STA = 102+29.54	401496.011	1529244.298
PT STA = 106+29.54	401496.011	1529244.298
PI STA = 104+29.54	401496.011	1529244.298

GEOMETRIC DATA

$\Delta = 128.94^\circ$	RIGHT
$L = 445.81'$	
$R = 224.20'$	
$T = 401.00'$	
$M = 111.92'$	

FOUNDATION PROTECTION

LOCATION	STATION	DEPTH	DIAMETER
SO-1	103+00.00	24' RI	24" RI
SO-2	103+03.41	28' RI	24" RI
SO-3	103+06.82	24' RI	24" RI
SO-4	103+10.23	24' RI	24" RI
SO-5	103+13.64	24' RI	24" RI
SO-6	103+17.05	24' RI	24" RI
SO-7	103+20.46	24' RI	24" RI
SO-8	103+23.87	24' RI	24" RI
SO-9	103+27.28	24' RI	24" RI
SO-10	103+30.69	24' RI	24" RI
SO-11	103+34.10	24' RI	24" RI
SO-12	103+37.51	24' RI	24" RI
SO-13	103+40.92	24' RI	24" RI
SO-14	103+44.33	24' RI	24" RI
SO-15	103+47.74	24' RI	24" RI

HYDRAULIC DATA

PROFILE	Q TOTAL (CFS)	WS. EL. (FT)	VELOCITY (FPS)
100 YR	2188	877.55	10.62
10 YR	1194	815.45	8.41
25 YR	1564	816.31	8.36
50 YR	1881	816.14	10.03



J.B. TURMAN ENGINEERING, PLLC
P.O. Box 483
Burlington, WV 25504
www.jbturmanengineering.com

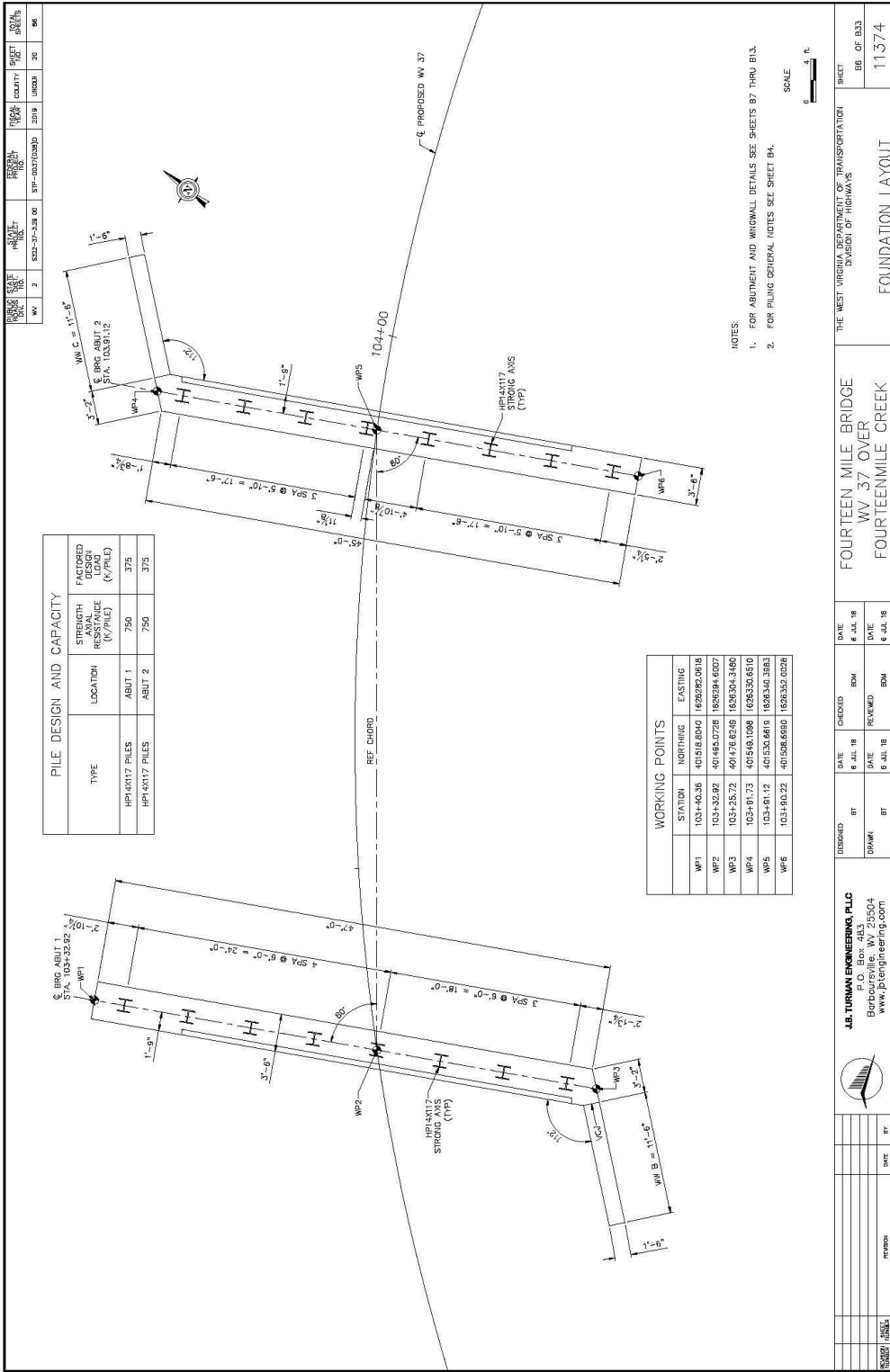
DESIGNED [] **CHECKED** [] **DATE** []
BY [] **BY** [] **DATE** []

THE WEST VIRGINIA DEPARTMENT OF TRANSPORTATION
DIVISION OF HIGHWAYS

FOURTEEN MILE BRIDGE
WV 37 OVER
FOURTEENMILE CREEK

GENERAL PLAN AND ELEVATION

SHEET 11374
BT OF 833



TYPE	LOCATION	STRENGTH RESISTANCE (K/PILE)	FACTORED DESIGN LOAD (K/PILE)
HP14X17 PILES	ABUT 1	750	375
HP14X17 PILES	ABUT 2	750	375

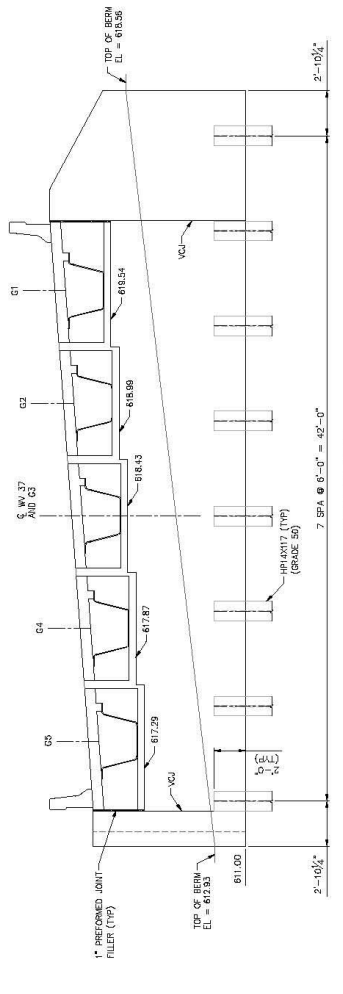
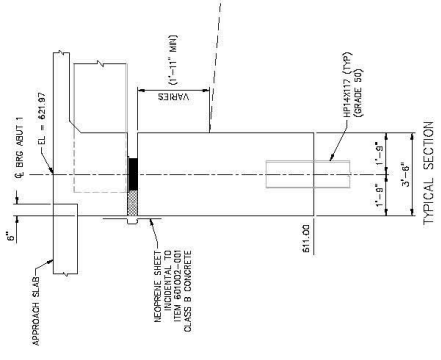
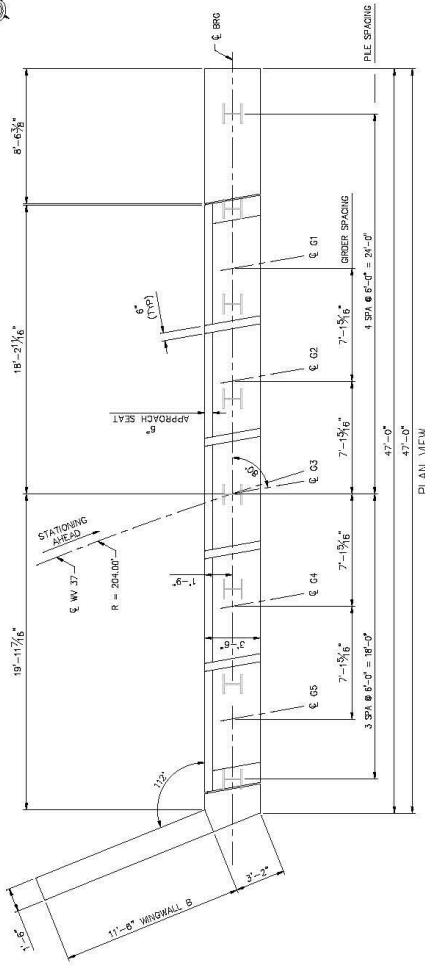
STATION	NORTHING	EASTING
WP1	1031+60.36	401618.040
WP2	1031+32.82	401462.0728
WP3	1031+25.72	401782.8248
WP4	1031+91.73	401849.1088
WP5	1031+91.12	401532.8419
WP6	1031+93.22	401598.6990

- NOTES:
- FOR ABUTMENT AND WINGWALL DETAILS SEE SHEETS B7 THRU B10.
 - FOR PILING GENERAL NOTES SEE SHEET B4.

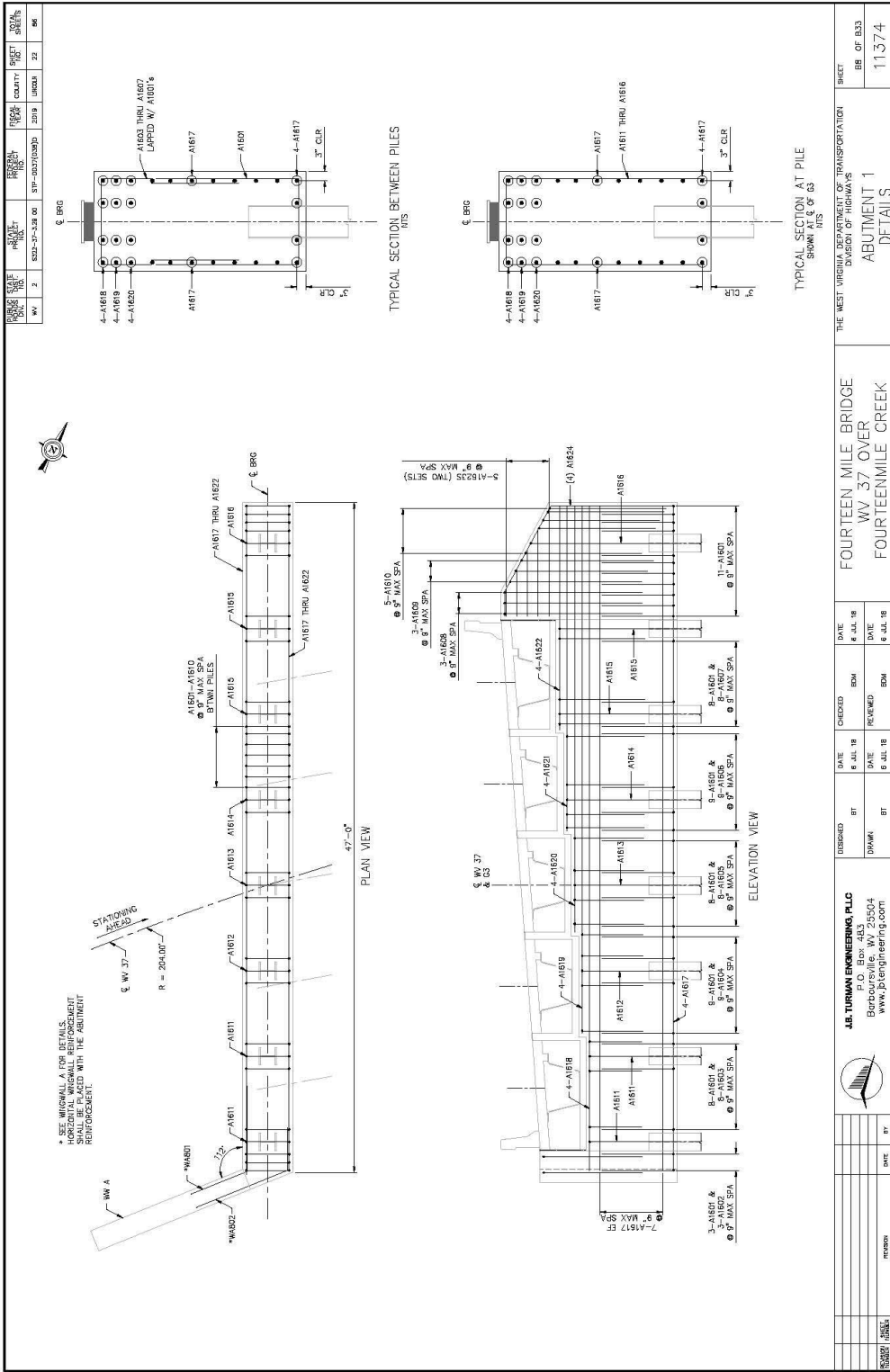
SCALE
0 4 ft.

J.R. TURMAN ENGINEERING, PLLC P.O. Box 483 Barboursville, WV 25504 www.jrturmanengineering.com		THE WEST VIRGINIA DEPARTMENT OF TRANSPORTATION DIVISION OF HIGHWAYS	
DESIGNED BY	BT	CHECKED BY	BTM
DATE	6 JUL 18	DATE	6 JUL 18
PROJECT NO.	11374	SHEET NO.	BB OF B33
FOURTEEN MILE BRIDGE		FOUNDATION LAYOUT	
WV 37 OVER		FOURTEENMILE CREEK	

PROJECT NO.	DATE	BY	CHECKED	DATE	BY
14-0001	10/18/18	BT	BT	10/18/18	BT
REV	DATE	BY	REASON		
1	10/18/18	BT	ISSUED FOR PERMITS		
2	10/18/18	BT	ISSUED FOR CONSTRUCTION		



J.R. TURMAN ENGINEERING, PLLC P.O. Box 483 Barboursville, WV 25504 www.jrturmanengineering.com				THE WEST VIRGINIA DEPARTMENT OF TRANSPORTATION DIVISION OF HIGHWAYS			
DESIGNED	BT	CHECKED	BT	DATE	8 JUL 18	PROJECT NO.	14-0001
DRAWN	BT	REVIEWED	BT	DATE	8 JUL 18	SHEET	87 OF 833
DATE	BT			DATE	8 JUL 18	ABUTMENT 1 PLAN AND ELEVATION	
						11374	



PROJECT NO.	4322-37-2A.00	DESIGN NO.	110	DATE	2018	UNITS	MM/KN	SHEET NO.	22	TOTAL SHEETS	26
WV	2	SP	00010000	2018	UNITS	MM/KN	SHEET NO.	22	TOTAL SHEETS	26	

DESIGNED BY	BT	DATE	6 JUL 18
CHECKED BY	BT	DATE	6 JUL 18
DESIGNED BY	BT	DATE	6 JUL 18
CHECKED BY	BT	DATE	6 JUL 18

THE WEST VIRGINIA DEPARTMENT OF TRANSPORTATION
 DIVISION OF HIGHWAYS
 FOURTEEN MILE BRIDGE
 W/ 37 OVER
 FOURTEENMILE CREEK

PROJECT NO.	4322-37-2A.00	DESIGN NO.	110	DATE	2018	UNITS	MM/KN	SHEET NO.	22	TOTAL SHEETS	26
-------------	---------------	------------	-----	------	------	-------	-------	-----------	----	--------------	----

PROJECT NO.	4322-37-2A.00	DESIGN NO.	110	DATE	2018	UNITS	MM/KN	SHEET NO.	22	TOTAL SHEETS	26
-------------	---------------	------------	-----	------	------	-------	-------	-----------	----	--------------	----

J.R. TURMAN ENGINEERING, PLLC
 P.O. Box 483
 Barboursville, WV 25504
 www.jrturmanengineering.com

PROJECT NO.	DATE	BY	CHKD.	DATE	BY	CHKD.
WV 2	8/22/18	WV	WV	8/22/18	WV	WV

PROJECT NAME	PROJECT NO.	PROJECT DATE	PROJECT LOCATION
WINGWALL A	WV 2	8/22/18	FOURTEEN MILE BRIDGE

DESIGNER	CHECKER	DATE	BY	CHKD.
JR TURMAN	WV	8/22/18	WV	WV

PROJECT NO.	DATE	BY	CHKD.	DATE	BY	CHKD.
WV 2	8/22/18	WV	WV	8/22/18	WV	WV

PROJECT NAME	PROJECT NO.	PROJECT DATE	PROJECT LOCATION
WINGWALL A	WV 2	8/22/18	FOURTEEN MILE BRIDGE

DESIGNER	CHECKER	DATE	BY	CHKD.
JR TURMAN	WV	8/22/18	WV	WV

PROJECT NO.	DATE	BY	CHKD.	DATE	BY	CHKD.
WV 2	8/22/18	WV	WV	8/22/18	WV	WV

PROJECT NAME	PROJECT NO.	PROJECT DATE	PROJECT LOCATION
WINGWALL A	WV 2	8/22/18	FOURTEEN MILE BRIDGE

DESIGNER	CHECKER	DATE	BY	CHKD.
JR TURMAN	WV	8/22/18	WV	WV

PROJECT NO.	DATE	BY	CHKD.	DATE	BY	CHKD.
WV 2	8/22/18	WV	WV	8/22/18	WV	WV

PROJECT NAME	PROJECT NO.	PROJECT DATE	PROJECT LOCATION
WINGWALL A	WV 2	8/22/18	FOURTEEN MILE BRIDGE

DESIGNER	CHECKER	DATE	BY	CHKD.
JR TURMAN	WV	8/22/18	WV	WV

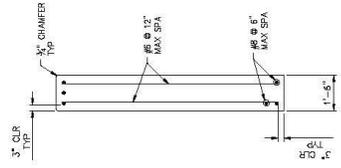
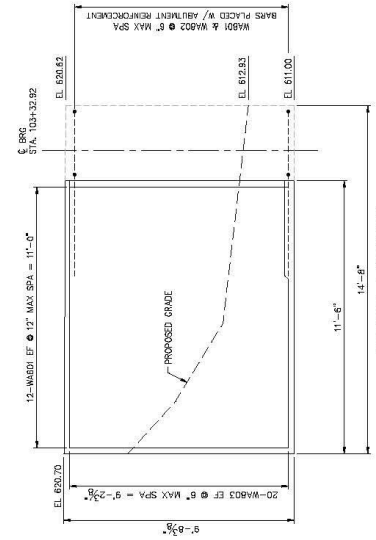
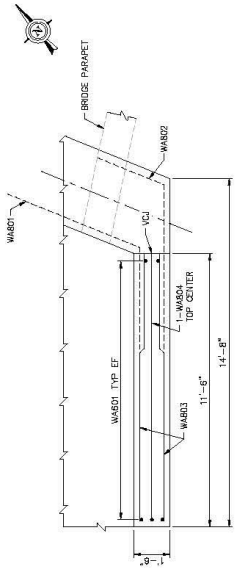
PROJECT NO.	DATE	BY	CHKD.	DATE	BY	CHKD.
WV 2	8/22/18	WV	WV	8/22/18	WV	WV

PROJECT NAME	PROJECT NO.	PROJECT DATE	PROJECT LOCATION
WINGWALL A	WV 2	8/22/18	FOURTEEN MILE BRIDGE

DESIGNER	CHECKER	DATE	BY	CHKD.
JR TURMAN	WV	8/22/18	WV	WV

PROJECT NO.	DATE	BY	CHKD.	DATE	BY	CHKD.
WV 2	8/22/18	WV	WV	8/22/18	WV	WV

PROJECT NAME	PROJECT NO.	PROJECT DATE	PROJECT LOCATION
WINGWALL A	WV 2	8/22/18	FOURTEEN MILE BRIDGE



PROJECT NO.	DATE	BY	CHKD.	DATE	BY	CHKD.
WV 2	8/22/18	WV	WV	8/22/18	WV	WV

PROJECT NAME	PROJECT NO.	PROJECT DATE	PROJECT LOCATION
WINGWALL A	WV 2	8/22/18	FOURTEEN MILE BRIDGE

DESIGNER	CHECKER	DATE	BY	CHKD.
JR TURMAN	WV	8/22/18	WV	WV

PROJECT NO.	DATE	BY	CHKD.	DATE	BY	CHKD.
WV 2	8/22/18	WV	WV	8/22/18	WV	WV

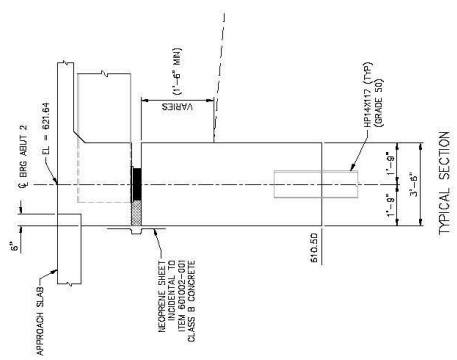
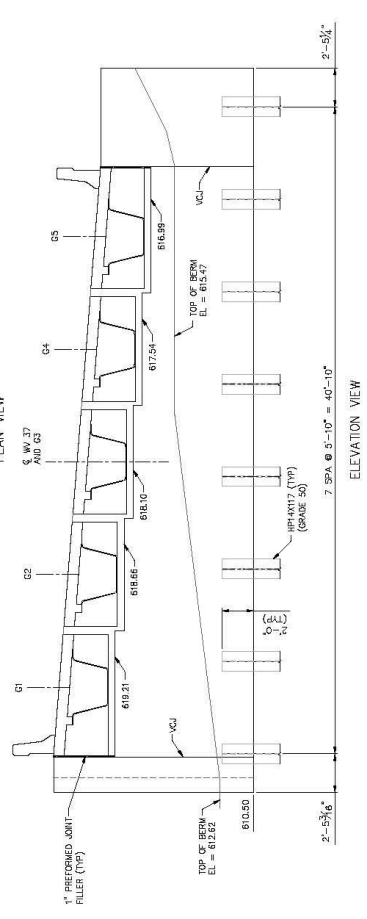
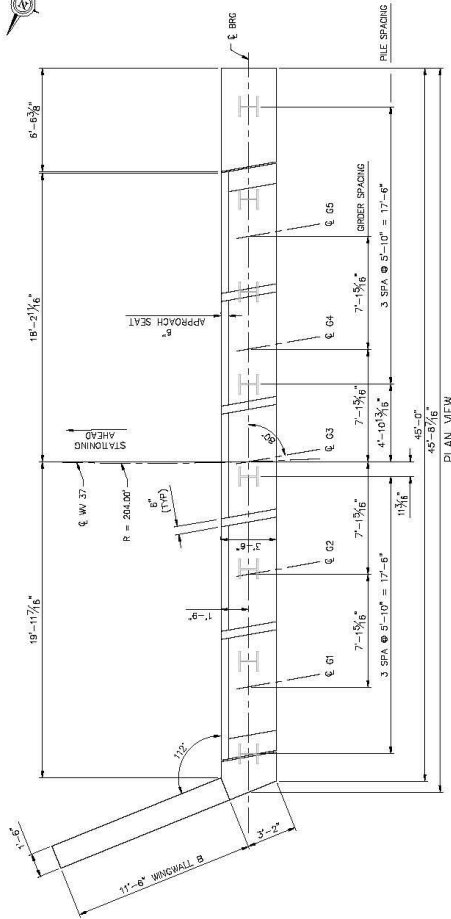
PROJECT NAME	PROJECT NO.	PROJECT DATE	PROJECT LOCATION
WINGWALL A	WV 2	8/22/18	FOURTEEN MILE BRIDGE

DESIGNER	CHECKER	DATE	BY	CHKD.
JR TURMAN	WV	8/22/18	WV	WV

PROJECT NO.	DATE	BY	CHKD.	DATE	BY	CHKD.
WV 2	8/22/18	WV	WV	8/22/18	WV	WV

PROJECT NAME	PROJECT NO.	PROJECT DATE	PROJECT LOCATION
WINGWALL A	WV 2	8/22/18	FOURTEEN MILE BRIDGE

PROJECT NO.	DATE	BY	REVISION
WV 2	03/22/17	SP	001/001/001
PROJECT NAME	PROJECT NO.	PROJECT YEAR	PROJECT SHEET NO.
BRIDGE	14	2018	24
LOCATION	SECTION	DATE	BY

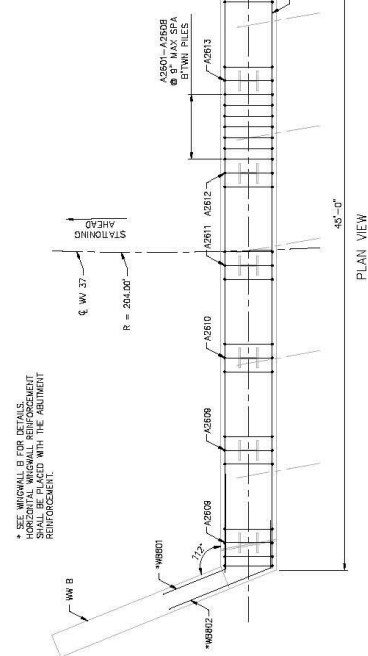


DESIGNED BY	DATE	DESIGNED BY	DATE	DESIGNED BY	DATE	DESIGNED BY	DATE
J.B. TURMAN ENGINEERING, PLLC P.O. Box 483 Barboursville, WV 25504 www.tbengineering.com				THE WEST VIRGINIA DEPARTMENT OF TRANSPORTATION DIVISION OF HIGHWAYS ABUTMENT 2 PLAN AND ELEVATION			
CHECKED BY DATE				REVIEWED BY DATE			
DRAWN BY DATE				SHOWN BY DATE			
PROJECT NO. DATE				SHEET NO. DATE			
PROJECT NAME DATE				SHEET NO. DATE			
LOCATION DATE				SHEET NO. DATE			
SECTION DATE				SHEET NO. DATE			
REVISION DATE				SHEET NO. DATE			

PROJECT NO.	DATE	BY	CHKD.	DATE	BY	CHKD.
14-00000000	03/20/18	JL	JL	03/20/18	JL	JL
REV.	DATE	BY	CHKD.	DATE	BY	CHKD.
1	03/20/18	JL	JL	03/20/18	JL	JL
2	03/20/18	JL	JL	03/20/18	JL	JL

PROJECT NO.	DATE	BY	CHKD.	DATE	BY	CHKD.
14-00000000	03/20/18	JL	JL	03/20/18	JL	JL
REV.	DATE	BY	CHKD.	DATE	BY	CHKD.
1	03/20/18	JL	JL	03/20/18	JL	JL
2	03/20/18	JL	JL	03/20/18	JL	JL

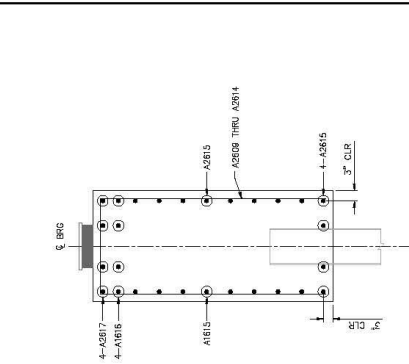
SEE DRAWING FOR DETAILS.
HORIZONTAL WALL REINFORCEMENT
SHALL BE PLACED WITH THE ABUTMENT
REINFORCEMENT.



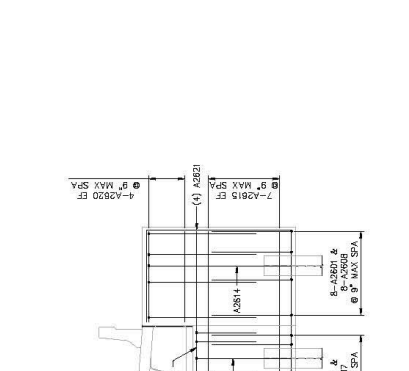
PLAN VIEW



TYPICAL SECTION BETWEEN PILES



TYPICAL SECTION AT PILE

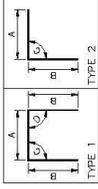


ELEVATION VIEW

		J.R. TURMAN ENGINEERING, PLLC P.O. Box 483 Barboursville, WV 25504 www.jrturmanengineering.com		DESIGNED BY DATE	CHECKED BY DATE	DATE 8 JUL 18	DATE 8 JUL 18	THE WEST VIRGINIA DEPARTMENT OF TRANSPORTATION DIVISION OF HIGHWAYS ABUTMENT 2 DETAILS	SHEET 11374
PROJECT NO. 14-00000000		PROJECT NAME FOURTEEN MILE BRIDGE WV 37 OVER FOURTEENMILE CREEK		DESIGNED BY JLM	CHECKED BY JLM	DATE 8 JUL 18	DATE 8 JUL 18	PROJECT NO. 14-00000000	SHEET 11374

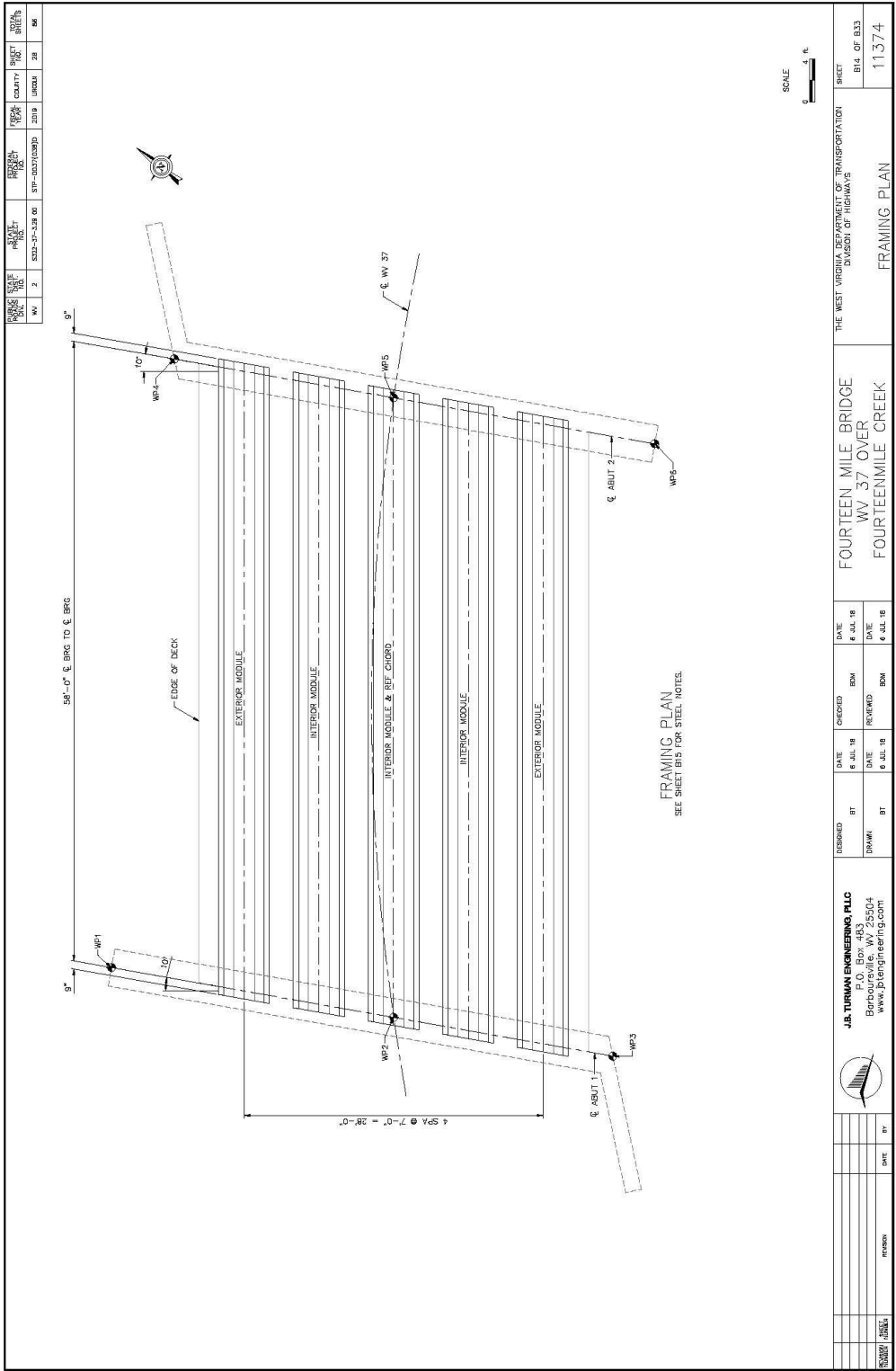
PROJECT NO.	WV 2	DATE	5/22/2018	SCALE	AS SHOWN	PROJECT	BRIDGE	NO.	110	DATE	5/22/2018	SCALE	AS SHOWN	PROJECT	BRIDGE	NO.	110
-------------	------	------	-----------	-------	----------	---------	--------	-----	-----	------	-----------	-------	----------	---------	--------	-----	-----

ABUTMENT AND WINGWALL REINFORCEMENT									
MARK	TYPE	NUMBER REQUIRED	LENGTH (FT)	602001-001	602002-001	A	B	C	D
WINGWALL A									
WAB01	STR	24	9' - 2"	331					
WAB02	STR	20	10' - 3"	548		4' - 3"	5' - 0"	112'	
WAB03	STR	40	11' - 3"	1202		6' - 11"	3' - 0"	112'	
WAB04	STR	1	17' - 3"	47		11' - 3"	3' - 0"	80'	90'
TOTAL				2658					
WINGWALL B									
WBB01	STR	24	12' - 3"	438					
WBB02	STR	2	10' - 0"	685		4' - 3"	5' - 0"	112'	
WBB03	STR	50	11' - 3"	1502		6' - 11"	3' - 0"	112'	
WBB04	STR	1	17' - 3"	47		11' - 3"	3' - 0"	80'	90'
TOTAL				3335					



ABUTMENT AND WINGWALL REINFORCEMENT									
MARK	TYPE	NUMBER REQUIRED	LENGTH (FT)	602001-001	602002-001	A	B	C	D
ABUTMENT NO. 1									
A1E01	STR	56	13' - 0"	1094		3' - 0"	5' - 0"	90'	90'
A1E02	STR	3	16' - 10"	76		3' - 0"	6' - 11"	90'	90'
A1E03	STR	8	11' - 8"	152		3' - 0"	4' - 3"	80'	80'
A1E04	STR	1	11' - 8"	152		3' - 0"	4' - 3"	80'	80'
A1E05	STR	8	12' - 8"	153		3' - 0"	4' - 10"	90'	90'
A1E06	STR	1	13' - 10"	167		3' - 0"	5' - 5"	80'	90'
A1E07	STR	8	13' - 10"	167		3' - 0"	5' - 5"	80'	90'
A1E08	STR	3	22' - 4"	101		3' - 0"	9' - 6"	80'	90'
A1E09	STR	3	22' - 4"	101		3' - 0"	9' - 6"	80'	90'
A1E10	STR	3	22' - 4"	101		3' - 0"	9' - 6"	80'	90'
A1E11	STR	2	14' - 8"	45		3' - 0"	5' - 10"	80'	80'
A1E12	STR	1	15' - 10"	24		3' - 0"	5' - 10"	80'	90'
A1E13	STR	1	16' - 10"	26		3' - 0"	6' - 11"	80'	90'
A1E14	STR	1	16' - 10"	26		3' - 0"	6' - 11"	80'	90'
A1E15	STR	2	19' - 0"	58		3' - 0"	7' - 6"	90'	90'
A1E16	STR	1	19' - 0"	58		3' - 0"	7' - 6"	90'	90'
A1E17	STR	18	24' - 10"	2458		3' - 0"	10' - 0"	90'	90'
A1E18	STR	4	46' - 8"	280		3' - 0"	10' - 0"	90'	90'
A1E19	STR	4	37' - 0"	223		3' - 0"	10' - 0"	90'	90'
A1E20	STR	4	29' - 10"	180		3' - 0"	6' - 11"	80'	90'
A1E21	STR	4	22' - 9"	137		3' - 0"	6' - 11"	80'	90'
A1E22	STR	4	15' - 8"	95		3' - 0"	10' - 0"	90'	90'
A1E23	STR	2 EACH MARK	1' - 10" TO 1' - 10" TO	71					
A1E24	STR	4	17' - 1"	103				152'	116'
TOTAL				4878					
ABUTMENT NO. 2									
A2E01	STR	54	13' - 0"	1065		3' - 0"	5' - 0"	90'	90'
A2E02	STR	2	22' - 10"	89		3' - 0"	9' - 11"	90'	90'
A2E03	STR	8	13' - 0"	303		3' - 0"	5' - 0"	80'	80'
A2E04	STR	1	13' - 0"	303		3' - 0"	5' - 0"	80'	80'
A2E05	STR	8	12' - 10"	174		3' - 0"	4' - 11"	80'	80'
A2E06	STR	1	11' - 8"	141		3' - 0"	4' - 4"	90'	90'
A2E07	STR	1	10' - 6"	142		3' - 0"	3' - 9"	80'	90'
A2E08	STR	1	16' - 5"	199		3' - 0"	6' - 9"	80'	90'
A2E09	STR	2	19' - 6"	58		3' - 0"	6' - 9"	80'	90'
A2E10	STR	1	17' - 2"	26		3' - 0"	7' - 1"	80'	90'
A2E11	STR	1	17' - 2"	26		3' - 0"	7' - 1"	80'	90'
A2E12	STR	1	16' - 0"	25		3' - 0"	6' - 6"	80'	80'
A2E13	STR	2	15' - 0"	46		3' - 0"	6' - 0"	80'	90'
A2E14	STR	1	21' - 0"	32		3' - 0"	5' - 0"	80'	90'
A2E15	STR	22	44' - 6"	1471					
A2E16	STR	4	30' - 5"	143					
A2E17	STR	4	30' - 5"	143					
A2E18	STR	4	16' - 3"	98					
A2E19	STR	4	9' - 1"	55					
A2E20	STR	8	5' - 8"	70		5' - 9"	5' - 2"	80'	
A2E21	STR	2	14' - 11"	90					
TOTAL				4497					

	J.B. TURMAN ENGINEERING, PLC P.O. Box 483 Barboursville, WV 25504 www.jbturmanengineering.com		CHECKED DATE: 6 JUL 18 BY:	DESIGNED DATE: 6 JUL 18 BY:	DATE: 6 JUL 18 BY:	THE WEST VIRGINIA DEPARTMENT OF TRANSPORTATION DIVISION OF HIGHWAYS FOURTEEN MILE BRIDGE WV 37 OVER FOURTEENMILE CREEK ABUTMENT AND WINGWALL REINFORCING	SHEET BL3 OF B33 11374
	DATE: 6 JUL 18 BY:	DATE: 6 JUL 18 BY:	DATE: 6 JUL 18 BY:	DATE: 6 JUL 18 BY:	DATE: 6 JUL 18 BY:	DATE: 6 JUL 18 BY:	DATE: 6 JUL 18 BY:



PROJECT NO.	DATE	BY	CHKD
WV 2	5/22/18	JTB	JTB

REGION	COUNTY	PROJECT	SHEET
SP-00010000	WV	11374	28

DESIGNED	DATE	BY
JTB	6 JUL 18	JTB

CHECKED	DATE	BY
JTB	6 JUL 18	JTB

DESIGNED	DATE	BY
JTB	6 JUL 18	JTB

REVIEWED	DATE	BY
JTB	6 JUL 18	JTB

DESIGNED	DATE	BY
JTB	6 JUL 18	JTB

REVIEWED	DATE	BY
JTB	6 JUL 18	JTB

DESIGNED	DATE	BY
JTB	6 JUL 18	JTB

REVIEWED	DATE	BY
JTB	6 JUL 18	JTB

DESIGNED	DATE	BY
JTB	6 JUL 18	JTB

REVIEWED	DATE	BY
JTB	6 JUL 18	JTB

DESIGNED	DATE	BY
JTB	6 JUL 18	JTB

J.B. TURMAN ENGINEERING, PLLC
P.O. Box 483
Barboursville, WV 25504
www.jbturmanengineering.com

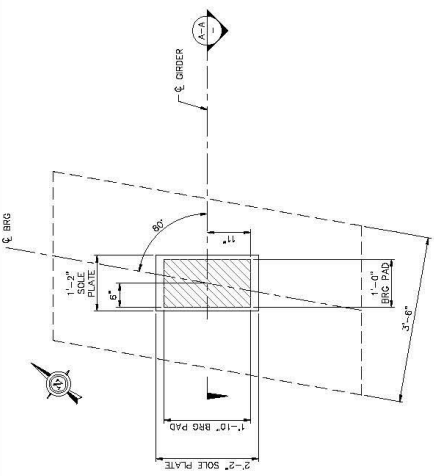
THE WEST VIRGINIA DEPARTMENT OF TRANSPORTATION
DIVISION OF HIGHWAYS

FOURTEEN MILE BRIDGE
WV 37 OVER
FOURTEENMILE CREEK

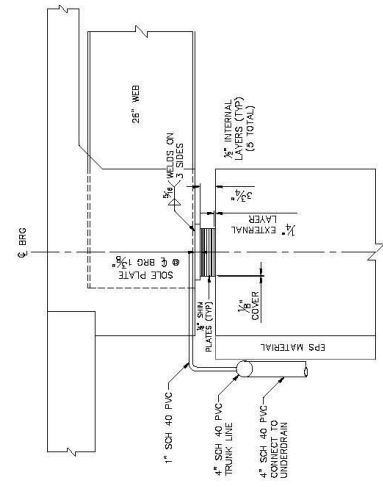
FRAMING PLAN
SHEET B14 OF B33
11374

PROJECT NO.	1000	SECTION NO.	1000	DATE	10/11/18
DATE	10/11/18	BY	1000	DATE	10/11/18
BY	1000	DATE	10/11/18	BY	1000

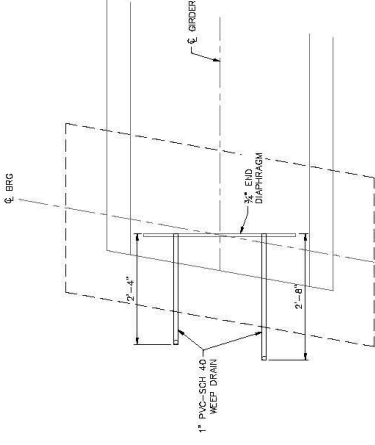
- NOTES:
1. PROVIDE ELASTOMER WITH A SHEAR MODULUS G=130 PSI +/- 15% AT 73° F.
 2. BEARINGS SHALL BE SUBJECT TO TESTING REQUIREMENTS IN ACCORDANCE WITH AASHTO LFD0 CONSTRUCTION SPECIFICATION SECTION 18, CORRESPONDING TO DESIGN METHOD B.
 3. MATERIALS SHALL CONFORM TO AASHTO M281 (STANDARD SPECIFICATIONS FOR PLAN AND ELEVATION ELASTOMERIC BEARINGS), STEEL SHIMS SHALL BE ASTM A307, GRADE 50 (MIN).
 4. (NOTED) SURFACES SHALL BE FINISHED TO THE BOTTOM SURFACES OF THE SOLE PLATE AND TO THE TOP SURFACE OF THE CONCRETE THAT IS IN CONTACT WITH THE ELASTOMERIC PAD, PLUS AN ADDITIONAL 1/2" IN ALL DIRECTIONS. SEE SPECIAL PROVISIONS FOR ADDITIONAL DETAILS.
 5. CAUTION SHALL BE EXERCISED WHERE A FIELD WELD WILL BE MADE WHILE ELASTOMERIC BEARING PAD IS IN CONTACT WITH METAL. IN NO CASE SHALL THE ELASTOMER BE EXPOSED TO WELDING SPATTER. WELDING SHALL BE LIMITED TO THE ELASTOMERIC BEARING DUE TO WELDING WILL BE CAUSE FOR REJECTION. TEMPERATURES SHALL BE DETERMINED BY TEMPERATURE INDICATING DEVICES OR OTHER SUITABLE MEANS.
 6. SIDES OF SOLE PLATE THAT ARE NOT WELDED SHALL BE CAULKED WITH A MATERIAL MATCHING THE COLOR OF THE STEEL.
 7. THE SOLE PLATE SHALL MEET THE REQUIREMENTS OF AASHTO M270, GRADE 50.
 8. THE ELASTOMERIC PAD SHALL BE PAID FOR UNDER ITEM 61929-001, NON-GUIDED BEARINGS, ELASTOMERIC.
 9. BEARINGS SHALL BE VERTICAL AT TEMPERATURE BETWEEN 40° AND 80° F.



PLAN VIEW BEARING
ABUTMENT 1 SHOWN, ABUTMENT 2 OPPOSITE HEAD



ELEVATION



PLAN VIEW WEEP DRAINS

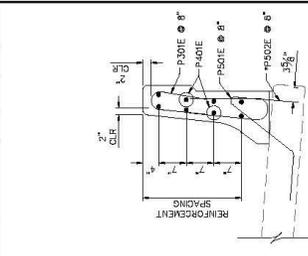
PROJECT NO.	1000	SECTION NO.	1000	DATE	10/11/18
DATE	10/11/18	BY	1000	DATE	10/11/18
BY	1000	DATE	10/11/18	BY	1000

DESIGNED	BT	CHECKED	BT	DATE	8 JUL 18
DRAWN	BT	REVIEWED	BT	DATE	8 JUL 18

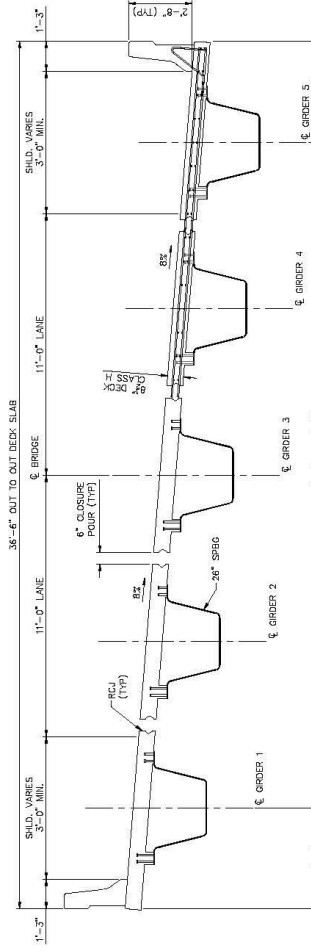
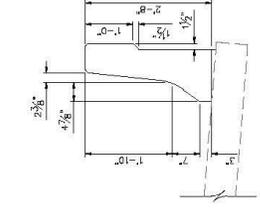
J.R. TURMAN ENGINEERING, PLLC P.O. Box 483 Barboursville, WV 25504 www.jrturmanengineering.com	THE WEST VIRGINIA DEPARTMENT OF TRANSPORTATION DIVISION OF HIGHWAYS
--	--

SHEET BT7 OF B33 11374	BEARING DETAILS
------------------------------	-----------------

PROJECT NO.	SP-2010-0010	SECTION	BRIDGE	DATE	11/11/10
NO.	2	NO.	2	NO.	2
DATE	11/11/10	DATE	11/11/10	DATE	11/11/10

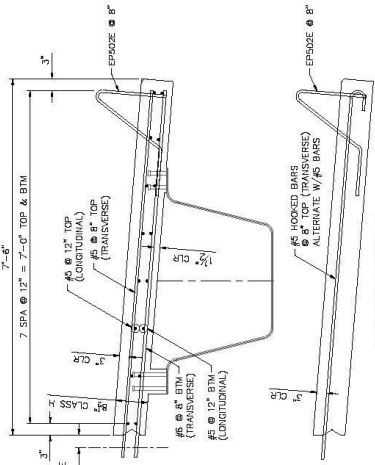


PARAPET REINFORCING ON BRIDGE
 *P-ROD TO BE LAPPED WITH EXTERIOR MODULE PRECASTING

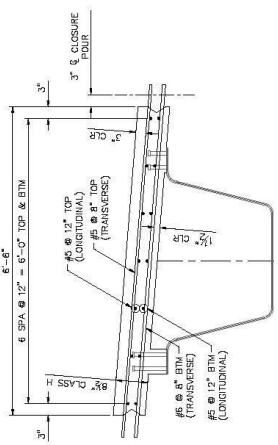


TYPICAL SECTION
 LOOKING EAST ON WEIR

- NOTES:**
1. PRECASTING TO INCLUDE THE DECK AND CONCRETE OVERLAY AT THE ABUTMENT.
 2. PRECAST DECK THICKNESS TO BE 8", ALLOWING 1/2" FOR DIAMOND GRINDING. SEE SHEET BA FOR DIAMOND GRINDING NOTE.
 3. THAT OVERHANGS THE GIRDERS. SHALL CONSIST OF REMOVABLE FORMS FOR ANY SECTION.
 4. STAKEOUT AND THE BEARING SHALL BE USED OVER THE GIRDERS TO ALLOW FOR IN SERVICE SETTLEMENTS. THE BEARING SHALL BE APPROVED BY THE PROJECT ENGINEER FOR APPROVAL. IF ANY PIECES OF THE FORM MAY BE SUBMITTED TO THE PROJECT ENGINEER FOR APPROVAL. ALL FALSE WORK MUST BE STAMPED BY A LICENSED WEST VIRGINIA ENGINEER.
 5. WEST VIRGINIA ENGINEER. SHALL BE COMPLETED USING ULTRA HIGH PERFORMANCE CONCRETE.
 6. PARAPET WALLS TO BE CONSTRUCTED IN THE FIELD.



EXTERIOR MODULE



INTERIOR MODULE

THE WEST VIRGINIA DEPARTMENT OF TRANSPORTATION DIVISION OF HIGHWAYS				SHEET B18 OF B33	
FOURTEEN MILE BRIDGE WV 37 OVER FOURTEENMILE CREEK				DECK TYPICAL SECTION 11374	
DESIGNED BY	DATE	CHECKED BY	DATE	DESIGNED BY	DATE
DRM/	8 JUL 10	BM	8 JUL 10	DRM/	8 JUL 10
BY	8 JUL 10	BY	8 JUL 10	BY	8 JUL 10
REVISION	DATE	BY			
J.B. TURMAN ENGINEERING, PLLC P.O. Box 483 Barboursville, WV 25504 www.jbturmanengineering.com					

PROJECT NO.	DATE	BY	CHKD.	APP'D.
100-000000	10/1/00	WV	2	100-000000

STATE	COUNTY	SHEET
WV	17	33

DATE	BY	CHKD.	APP'D.
8 JUL 18	BT	BT	BT
8 JUL 18	BT	BT	BT

PROJECT NO.	DATE	BY	CHKD.	APP'D.
100-000000	10/1/00	WV	2	100-000000

STATE	COUNTY	SHEET
WV	17	33

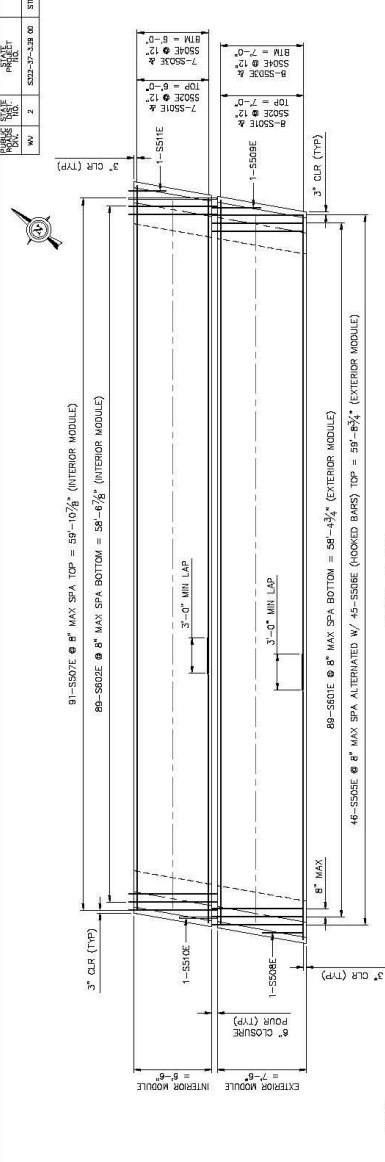
DATE	BY	CHKD.	APP'D.
8 JUL 18	BT	BT	BT
8 JUL 18	BT	BT	BT

PROJECT NO.	DATE	BY	CHKD.	APP'D.
100-000000	10/1/00	WV	2	100-000000

STATE	COUNTY	SHEET
WV	17	33

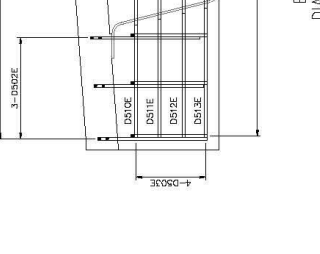
DATE	BY	CHKD.	APP'D.
8 JUL 18	BT	BT	BT
8 JUL 18	BT	BT	BT

PROJECT NO.	DATE	BY	CHKD.	APP'D.
100-000000	10/1/00	WV	2	100-000000

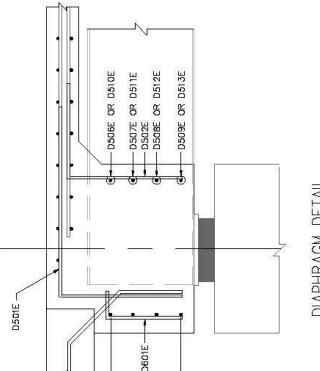


DECK PLAN

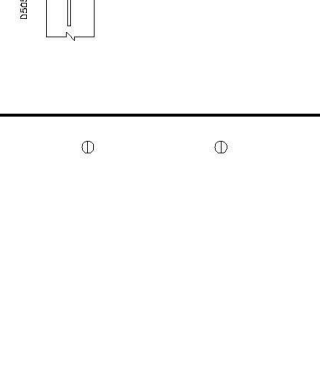
- NOTES:
1. CONTRACTOR SHALL USE CAUTION WHEN SETTING PRECAST MODULES AS TO NOT CAUSE DAMAGE TO THEM.
 2. TO NOT CAUSE DAMAGE TO THEM, PRECAST CONCRETE SHALL BE UTILIZED IN THE CLOSURE POLES.
 3. LOCATION AND TYPE OF LIFTING LOOPS ON THE PRECAST MODULES CONTRACTOR SHALL BE A MINIMUM OF FOUR PICK POINTS FOR EACH MODULE. THE LIFTING LOOPS SHALL BE LOCATED AT THE FACE, MINIMUM FACTOR OF SAFETY OF THE LIFTING LOOPS AND THEIR LOCATION SHALL BE SUBMITTED WITH THE SHOP DRAWINGS.



DIAPHRAGM DETAIL



EXTERIOR MODULE DIAPHRAGM ELEVATION



INTERIOR MODULE DIAPHRAGM ELEVATION

PROJECT NO.	DATE	BY	CHKD.	APP'D.
100-000000	10/1/00	WV	2	100-000000

STATE	COUNTY	SHEET
WV	17	33

DATE	BY	CHKD.	APP'D.
8 JUL 18	BT	BT	BT
8 JUL 18	BT	BT	BT

PROJECT NO.	DATE	BY	CHKD.	APP'D.
100-000000	10/1/00	WV	2	100-000000

STATE	COUNTY	SHEET
WV	17	33

DATE	BY	CHKD.	APP'D.
8 JUL 18	BT	BT	BT
8 JUL 18	BT	BT	BT

PROJECT NO.	DATE	BY	CHKD.	APP'D.
100-000000	10/1/00	WV	2	100-000000

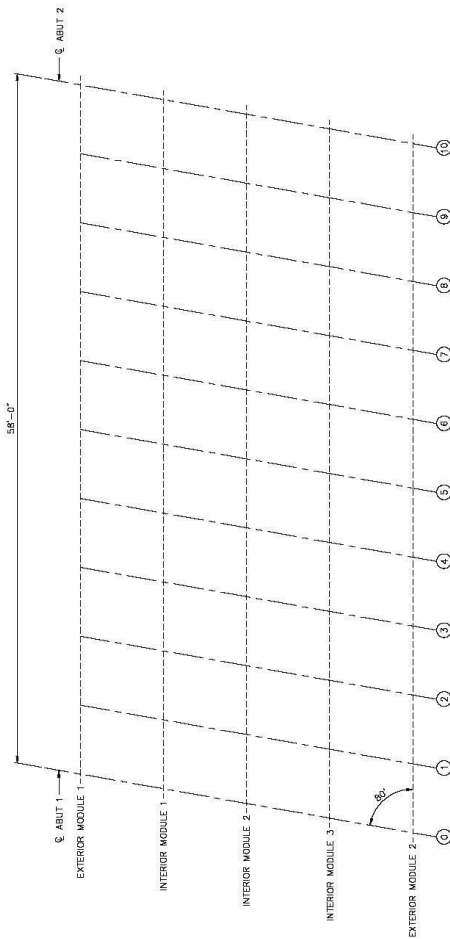
STATE	COUNTY	SHEET
WV	17	33

STATE	PROJECT	REGION	YEAR	SHEET
WV	5322-37-426.00	2019	10004	54

DECK ELEVATIONS

LOCATION	EXTERIOR PROFILE ELEVATION	INTERIOR PROFILE ELEVATION	EXTERIOR GRADE ELEVATION	INTERIOR GRADE ELEVATION	EXTERIOR ELEVATION	INTERIOR ELEVATION
ABUT 1 - 0	623.08	622.53	621.97	621.41	620.86	620.86
1	623.05	622.50	621.84	621.36	620.83	620.83
2	623.01	622.46	621.90	621.34	620.79	620.79
3	622.98	622.43	621.87	621.31	620.76	620.76
4	622.95	622.40	621.84	621.28	620.73	620.73
5	622.92	622.37	621.81	621.25	620.70	620.70
6	622.88	622.33	621.77	621.21	620.66	620.66
7	622.85	622.30	621.74	621.18	620.63	620.63
8	622.82	622.27	621.71	621.15	620.60	620.60
9	622.78	622.23	621.67	621.11	620.56	620.56
ABUT 2 - 10	622.75	622.20	621.64	621.08	620.53	620.53

DECK NOTE:
 DECK ELEVATIONS REFLECT THE
 FINISHED GRADE. THE
 DIAMOND GRINDING HAS BEEN
 PERFORMED. SEE NOTES
 FOR ADDITIONAL DETAILS ON
 DIAMOND GRINDING.



DESIGNED BY	DATE	CHECKED BY	DATE	DESIGNED BY	DATE	PROJECT	SHEET
JLB TURMAN ENGINEERING, PLLC P.O. Box 483 Bartonsville, WV 25504 www.jtengineering.com	6 JUL 18	JLB	6 JUL 18	JLB	6 JUL 18	FOURTEEN MILE BRIDGE WV 37 OVER FOURTEENMILE CREEK	B2D OF B33 11374
DESIGNED BY	DATE	CHECKED BY	DATE	DESIGNED BY	DATE	PROJECT	SHEET
JLB TURMAN ENGINEERING, PLLC P.O. Box 483 Bartonsville, WV 25504 www.jtengineering.com	6 JUL 18	JLB	6 JUL 18	JLB	6 JUL 18	FOURTEEN MILE BRIDGE WV 37 OVER FOURTEENMILE CREEK	B2D OF B33 11374

PROJECT NO.	DATE	BY	CHECKED	DATE	BY
14-0001	11/18/14	WV	WV	11/18/14	WV
PROJECT NAME	PROJECT NO.	PROJECT DATE	PROJECT BY	PROJECT CHECKED	PROJECT DATE
SP-1001(100)	14-0001	11/18/14	WV	WV	11/18/14

MARK	TYPE	NUMBER REQUIRED	LENGTH (FT)	602001-001	602002-001	A	B	C	D	E
------	------	-----------------	-------------	------------	------------	---	---	---	---	---

PRECAST DIAPHRAGM AND PARAPET REINFORCEMENT										
DIMENSION										

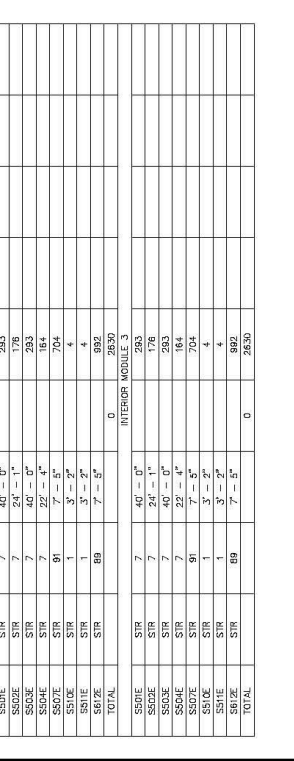
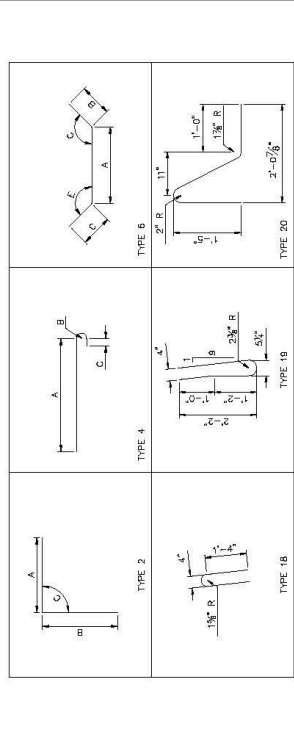
PRECAST SLAB REINFORCEMENT										
DIMENSION										

PRECAST DIAPHRAGM AND PARAPET REINFORCEMENT										
DIMENSION										

PRECAST SLAB REINFORCEMENT										
DIMENSION										

PRECAST DIAPHRAGM AND PARAPET REINFORCEMENT										
DIMENSION										

PRECAST SLAB REINFORCEMENT										
DIMENSION										



MARK	TYPE	NUMBER REQUIRED	LENGTH (FT)	602001-001	602002-001	A	B	C	D	E
TOTAL										

MARK	TYPE	NUMBER REQUIRED	LENGTH (FT)	602001-001	602002-001	A	B	C	D	E
TOTAL										

DATE	BY	CHECKED	DATE	BY	REVIEWED	DATE	BY
11/18/14	WV	WV	11/18/14	WV	WV	11/18/14	WV

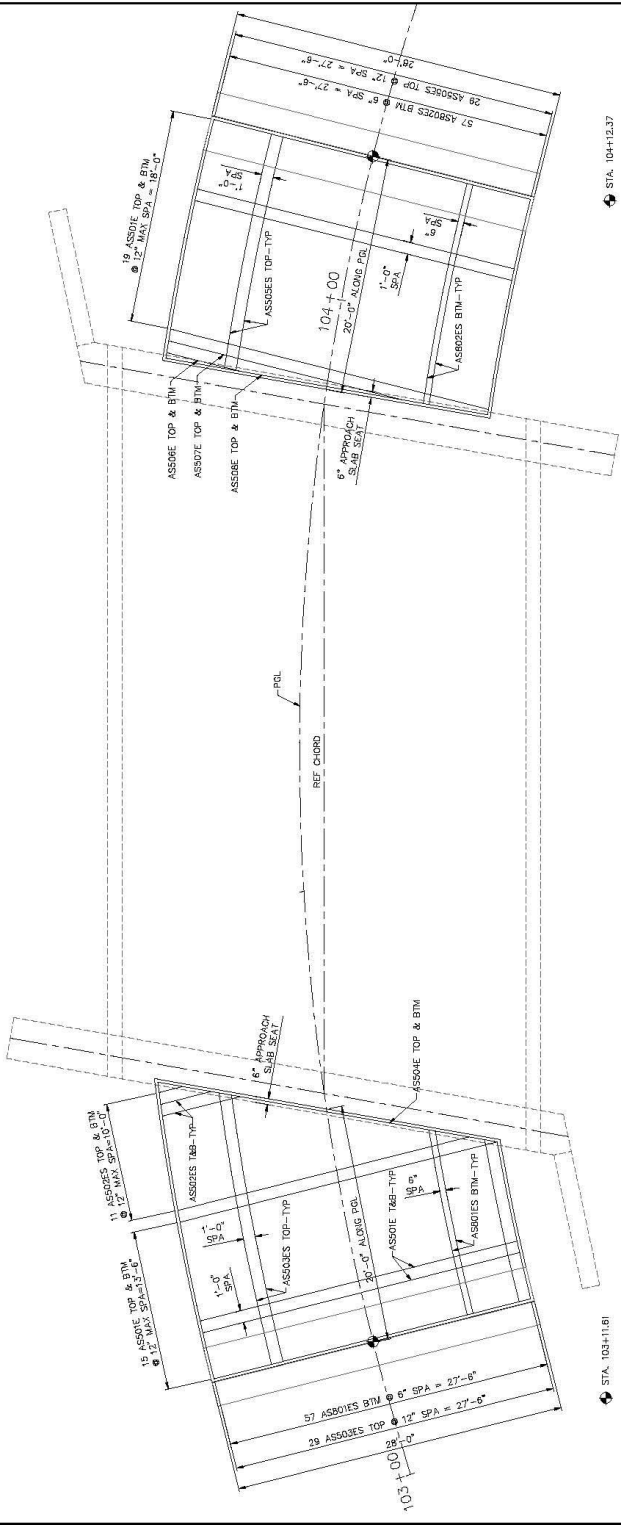
J.B. TURMAN ENGINEERING, PLLC
P.O. Box 483
Burlington, WV 25804
www.tbengineering.com

FOURTEEN MILE BRIDGE
WV 37 OVER
FOURTEENMILE CREEK

THE WEST VIRGINIA DEPARTMENT OF TRANSPORTATION
DIVISION OF HIGHWAYS
SUPERSTRUCTURE
REINFORCING

SHOULDER
BPI OF B33
11374

PROJECT NO.	DATE	BY	CHKD	DATE	BY	CHKD
WV 2	5/22/17	JTB	JTB	5/22/17	JTB	JTB

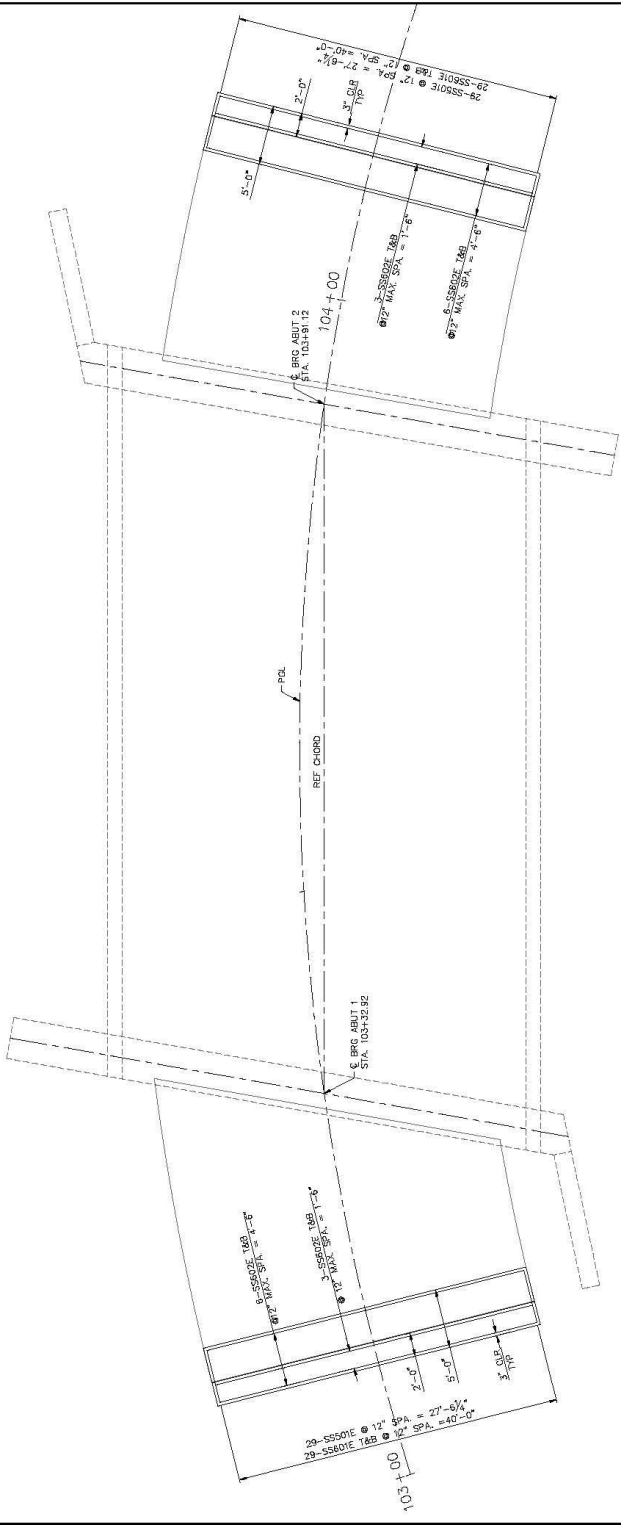


ABUTMENT 1 APPROACH SLAB

ABUTMENT 2 APPROACH SLAB

DESIGNED	DATE	BY	CHKD	DATE	BY	CHKD
	8 JUL 18	JTB	JTB	8 JUL 18	JTB	JTB
DRAWN	DATE	BY	CHKD	DATE	BY	CHKD
	8 JUL 18	JTB	JTB	8 JUL 18	JTB	JTB
<p style="text-align: center;">J.B. TURMAN ENGINEERING, PLLC P.O. Box 483 Barboursville, WV 25504 www.jbturmanengineering.com</p>						
<p style="text-align: center;">THE WEST VIRGINIA DEPARTMENT OF TRANSPORTATION DIVISION OF HIGHWAYS</p>				<p style="text-align: center;">FOURTEEN MILE BRIDGE WV 37 OVER FOURTEENMILE CREEK</p>		
<p style="text-align: center;">APPROACH SLAB PLAN</p>				<p style="text-align: center;">SHEET B23 OF B33 11374</p>		

PROJECT NO.	DATE	BY	CHKD.	DATE	BY	CHKD.
WV 2	5/22/17	JTB	JTB	5/22/17	JTB	JTB



ABUTMENT 1 SLEEPER SLAB

ABUTMENT 2 SLEEPER SLAB

DESIGNED BY	DATE	CHECKED BY	DATE	DESIGNED BY	DATE	CHECKED BY	DATE	PROJECT NO.	SHEET NO.	SHEET TOTAL
<p>J.B. TURMAN ENGINEERING, PLLC P.O. Box 483 Berbersville, WV 25804 www.jbturmanengineering.com</p>								<p>THE WEST VIRGINIA DEPARTMENT OF TRANSPORTATION DIVISION OF HIGHWAYS</p>		
<p>FOURTEEN MILE BRIDGE WV 37 OVER FOURTEENMILE CREEK</p>								<p>SLEEPER SLAB PLAN</p>		
								<p>BP4 OF B33</p>		
								<p>11374</p>		

PROJECT NO.	DATE	BY	CHKD
1302-37-126.00	5/22/18	JTB	JTB
WV 2			

PROJECT NAME	PROJECT NO.	PROJECT DATE
1302-37-126.00	1302-37-126.00	5/22/18

PROJECT LOCATION	PROJECT NO.	PROJECT DATE
1302-37-126.00	1302-37-126.00	5/22/18

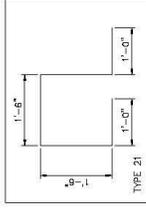
PROJECT NO.	DATE	BY	CHKD
1302-37-126.00	5/22/18	JTB	JTB

PROJECT NAME	PROJECT NO.	PROJECT DATE
1302-37-126.00	1302-37-126.00	5/22/18

PROJECT LOCATION	PROJECT NO.	PROJECT DATE
1302-37-126.00	1302-37-126.00	5/22/18

APPROACH SLAB AND SLEEPER SLAB REINFORCEMENT

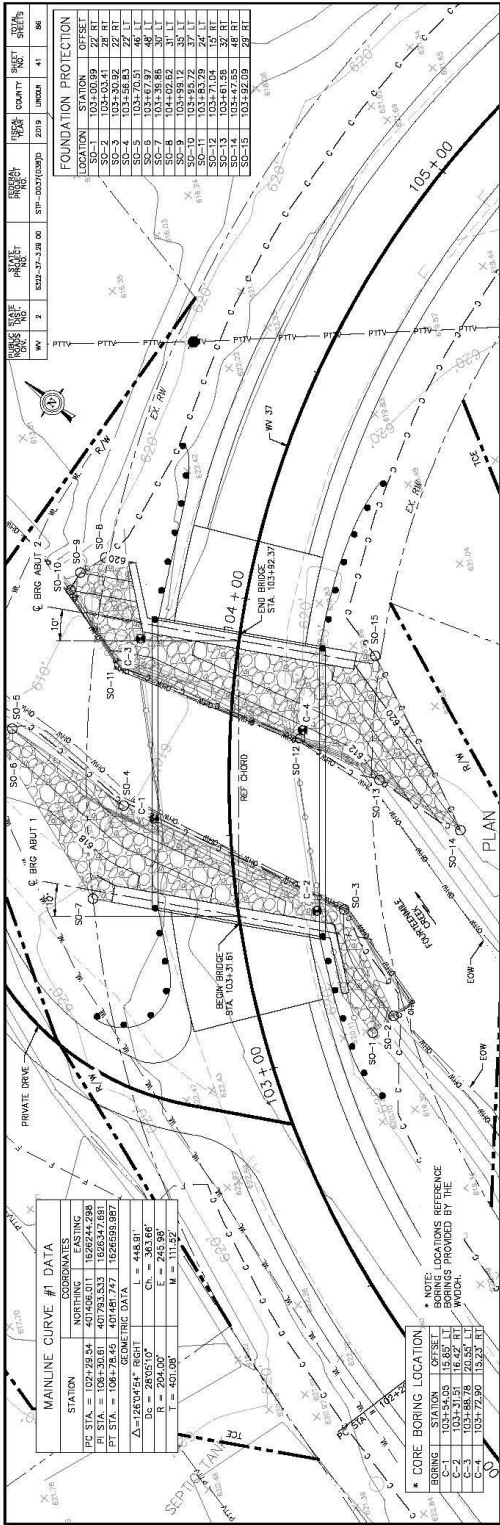
MARK	TYPE	NUMBER REQUIRED	LENGTH (FT)	ADJUSTMENT	DIMENSIONS			
					A	B	C	D
ADJUSTMENT NO. 1, APPROACH SLAB								
ASB01E	STR	30	27'-6"	0				
ASB02E	STR	2 EACH MARK	VARIES FROM 1'-0" TO 25'	VARIES FROM 1'-0" TO 25'				
ASB03E	STR	2 EACH MARK	VARIES FROM 13'-6" TO 25'	VARIES FROM 13'-6" TO 25'				
ASB04E	STR	1	28'-11"	0				
ASB05E	STR	1 EACH MARK	VARIES FROM 13'-6" TO 25'	VARIES FROM 13'-6" TO 25'				
TOTAL					0			
ADJUSTMENT NO. 2, APPROACH SLAB								
ASB06E	STR	19	27'-6"	0				
ASB07E	STR	1 EACH MARK	VARIES FROM 18'-0" TO 20'-6"	VARIES FROM 18'-0" TO 20'-6"				
ASB08E	STR	1	6'-6"	0				
ASB09E	STR	1	20'-6"	0				
ASB10E	STR	1 EACH MARK	VARIES FROM 18'-0" TO 20'-6"	VARIES FROM 18'-0" TO 20'-6"				
TOTAL					0			
SLEEPER SLAB								
SSB01E	STR	28	5'-0"	0				
SSB02E	STR	18	4'-6"	0				
SSB03E	STR	18	27'-7"	0				
TOTAL					0			
SLEEPER SLAB 2								
SSB04E	STR	28	5'-0"	0				
SSB05E	STR	18	4'-6"	0				
SSB06E	STR	18	27'-7"	0				
TOTAL					0			



DESIGNED BY	DATE	DESIGNED BY	DATE	DESIGNED BY	DATE	DESIGNED BY	DATE
JTB	5/22/18	JTB	5/22/18	JTB	5/22/18	JTB	5/22/18
CHECKED BY	DATE	CHECKED BY	DATE	CHECKED BY	DATE	CHECKED BY	DATE
JTB	5/22/18	JTB	5/22/18	JTB	5/22/18	JTB	5/22/18
PROJECT NO.	PROJECT NAME	PROJECT NO.	PROJECT NAME	PROJECT NO.	PROJECT NAME	PROJECT NO.	PROJECT NAME
1302-37-126.00	1302-37-126.00	1302-37-126.00	1302-37-126.00	1302-37-126.00	1302-37-126.00	1302-37-126.00	1302-37-126.00
PROJECT LOCATION	PROJECT NO.	PROJECT DATE	PROJECT LOCATION	PROJECT NO.	PROJECT DATE	PROJECT LOCATION	PROJECT NO.
1302-37-126.00	1302-37-126.00	5/22/18	1302-37-126.00	1302-37-126.00	5/22/18	1302-37-126.00	1302-37-126.00
PROJECT NAME	PROJECT NO.	PROJECT DATE	PROJECT NAME	PROJECT NO.	PROJECT DATE	PROJECT NAME	PROJECT NO.
1302-37-126.00	1302-37-126.00	5/22/18	1302-37-126.00	1302-37-126.00	5/22/18	1302-37-126.00	1302-37-126.00
PROJECT LOCATION	PROJECT NO.	PROJECT DATE	PROJECT LOCATION	PROJECT NO.	PROJECT DATE	PROJECT LOCATION	PROJECT NO.
1302-37-126.00	1302-37-126.00	5/22/18	1302-37-126.00	1302-37-126.00	5/22/18	1302-37-126.00	1302-37-126.00


J.B. TURMAN ENGINEERING, PLLC
 P.O. Box 483
 Barboursville, WV 25504
 www.jbturmanengineering.com

THE WEST VIRGINIA DEPARTMENT OF TRANSPORTATION
 DIVISION OF HIGHWAYS
**FOURTEEN MILE BRIDGE
 WV 37 OVER
 FOURTEENMILE CREEK**
 SLAB REINFORCING
 SHEET
 B26 OF B33
 11374



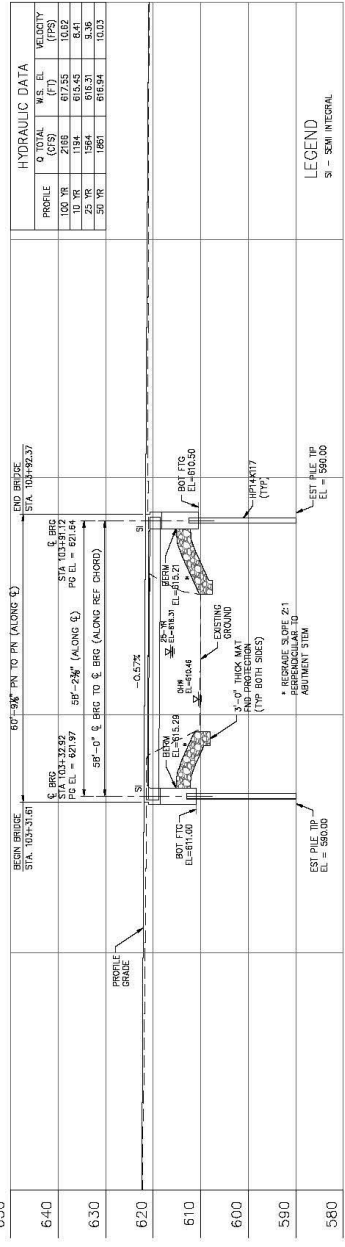
MAINLINE CURVE #1 DATA

STATION	NORTHING	EASTING
PC STA. = 102+29.24	401496.011	1629244.298
PT STA. = 104+28.46	401483.747	1629250.897
Δ = 128°45'48"	L = 448.91'	
R = 254.00'	CE = 245.95'	
T = 401.09'	M = 111.92'	

CORE BORING LOCATION

BORING	STATION	OFFSET
C-1	103+54.00	15.82' L
C-2	103+31.51	16.42' L
C-3	103+27.90	15.23' L
C-4	103+27.90	15.23' L

NOTE: COORDINATE REFERENCE BORINGS PROVIDED BY THE WAGOH.



HYDRAULIC DATA

PROFILE	Q TOTAL (CFS)	W.S. EL. (FT)	VELOCITY (FPS)
100 YR	1184	615.45	8.41
25 YR	1584	615.31	9.36
50 YR	1881	615.54	10.53



LEGEND
S - SEMI INTEGRAL

DESIGNED BY	DATE	CHECKED BY	DATE	DESIGNED BY	DATE	CHECKED BY	DATE
BT	6 JUL 18	BT	6 JUL 18	BT	6 JUL 18	BT	6 JUL 18

J.B. TURMAN ENGINEERING, P.L.C.
P.O. Box 483
Burlington, WV 25504
www.jbturmanengineering.com

EST PILE TIP EL. = 580.00
EST PILE TIP EL. = 580.00
EST PILE TIP EL. = 580.00

102+50 103+00 103+50 ELEVATION 104+00 104+50 105+00

FOURTEEN MILE BRIDGE
WV 37 OVER
FOURTEENMILE CREEK

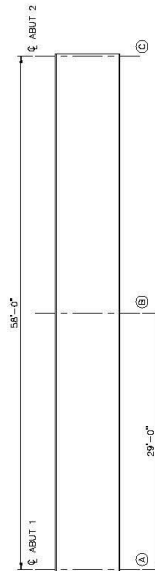
THE WEST VIRGINIA DEPARTMENT OF TRANSPORTATION
DIVISION OF HIGHWAYS

SHEET 11374
B27 OF B33

MEMBER	SPAN	SECTION LOCATION	TOP FLANGE			BOTTOM FLANGE			WEB			NON-COMPOSITE (CONCRETE WITH 3% AGGREGATE FIBERS)			1% COMPOSITE FOR GIRDER AND CONCRETE WITH 3% AGGREGATE FIBERS			DESIGN SERVICE MOMENT AND SHEAR										
			WIDTH (IN)	THICKNESS (IN)	FIELD STRENGTH (KSI)	WIDTH (IN)	THICKNESS (IN)	FIELD STRENGTH (KSI)	DEPTH (IN)	THICKNESS (IN)	FIELD STRENGTH (KSI)	S-TOP F.L.O.	S-TOP F.L.O.	S-TOP F.L.O.	S-TOP F.L.O.	S-TOP F.L.O.	S-TOP F.L.O.	S-TOP F.L.O.	S-TOP F.L.O.	DC1 MOMENT (K-FT)	DC1 SHEAR (K)	DC2 MOMENT (K-FT)	DC2 SHEAR (K)	DC3 MOMENT (K-FT)	DC3 SHEAR (K)	DM MOMENT (K-FT)	DM SHEAR (K)	FACTORED CAPACITY (K-FT)
EXTERIOR	1	A	6	0.5	50	29.79	0.5	50	26	0.5	50	26	0.5	50	306	443	1705	653	7406	734	0.00	216.80	0.00	3.59	0.00	4.98	3296	389
EXTERIOR	1	B	6	0.5	50	29.79	0.5	50	26	0.5	50	26	0.5	50	306	443	1705	653	7406	734	0.00	216.80	0.00	3.59	0.00	4.98	3296	389
EXTERIOR	1	C	6	0.5	50	29.79	0.5	50	26	0.5	50	26	0.5	50	306	443	1705	653	7406	734	0.00	216.80	0.00	3.59	0.00	4.98	3296	389
INTERIOR	1	A	6	0.5	50	29.79	0.5	50	26	0.5	50	26	0.5	50	306	443	1705	653	7406	734	0.00	216.80	0.00	3.59	0.00	4.98	3296	389
INTERIOR	1	B	6	0.5	50	29.79	0.5	50	26	0.5	50	26	0.5	50	306	443	1705	653	7406	734	0.00	216.80	0.00	3.59	0.00	4.98	3296	389
INTERIOR	1	C	6	0.5	50	29.79	0.5	50	26	0.5	50	26	0.5	50	306	443	1705	653	7406	734	0.00	216.80	0.00	3.59	0.00	4.98	3296	389

LIVE LOAD MOMENTS AND SHEARS (REFINED ANALYSIS)

MEMBER	SPAN	SECTION LOCATION	HL-93			S14			S16			S17			WV-552		
			LI+ MOMENT (K-FT)	LI+ SHEAR (K)	LI- MOMENT (K-FT)	LI+ MOMENT (K-FT)	LI+ SHEAR (K)	LI- MOMENT (K-FT)	LI+ MOMENT (K-FT)	LI+ SHEAR (K)	LI- MOMENT (K-FT)	LI+ MOMENT (K-FT)	LI+ SHEAR (K)	LI- MOMENT (K-FT)	LI+ MOMENT (K-FT)	LI+ SHEAR (K)	LI- MOMENT (K-FT)
EXTERIOR	1	A	-18	53	-12	31	-14	34	-15	38	-15	39	-15	40	-14	36	
EXTERIOR	1	B	689	32	407	21	471	-23	514	-24	571	23	622	21	443	23	
EXTERIOR	1	C	-60	2	-56	2	-44	2	-46	2	-46	2	-42	2	-42		
INTERIOR	1	A	-18	41	-12	25	-13	27	-14	28	-13	30	-13	32	-13	28	
INTERIOR	1	B	584	-30	348	20	385	23	431	24	477	21	517	19	374	-22	
INTERIOR	1	C	-46	-4	-28	4	-30	4	-33	4	-35	5	-36	5	-33		



LEGAL LOAD RATING

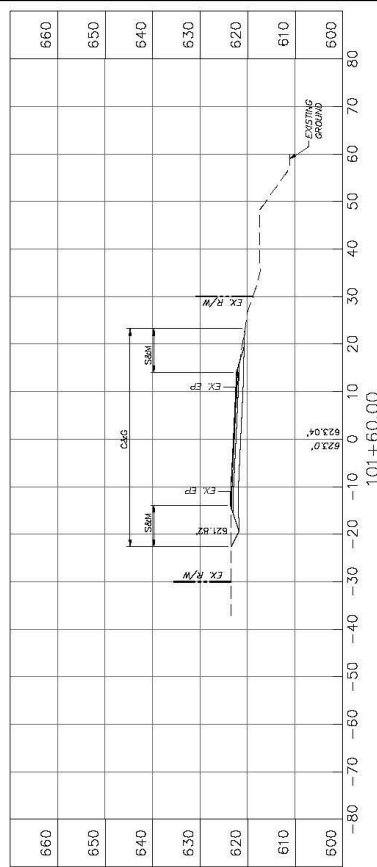
MEMBER	LIMIT STATE	DESIGN LOAD RATING (PL-93)	OPERATING (RF)	INVENTORY (RF)	FL	S14	S16	S18	S19	S20	WV-552
EXTERIOR	STRENGTH	2.18	2.83	4.62	3.99	3.65	3.29	3.02	4.25		
EXTERIOR	SHEAR	3.70	4.80	7.82	7.22	6.46	6.29	6.14	6.46		
INTERIOR	STRENGTH	2.81	3.39	5.47	4.83	4.43	4.00	3.69	5.10		
INTERIOR	SHEAR	4.63	6.28	8.90	8.16	8.53	8.29	7.73	8.53		

PROJECT NO.	SECTION	DATE	BY
101-460	101-460	10/1/13	JTB

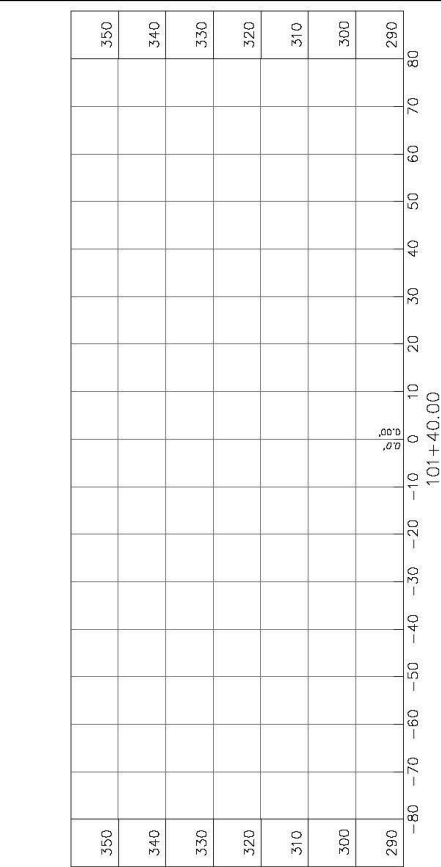
STATE	COUNTY	SHEET NO.	TOTAL SHEETS
WV	2	1328	1328

PROJECT	SECTION	DATE	BY
101-460	101-460	10/1/13	JTB

PROJECT	SECTION	DATE	BY
101-460	101-460	10/1/13	JTB



STATION	SEEDING & MULCHING		CLEARING & GRUBBING		EXCAVATION		EMBANKMENT	
	LENGTH FT	AREA SF	WIDTH FT	AREA SF	UNCLASSIFIED CY	UNSUITABLE SF	UNCLASSIFIED SF	SELECT EMBANKMENT SF
101+460	20	180	0	461	0	21.85	0	0
101+480	0	0	0	0	0	0	0	0



STATION	SEEDING & MULCHING		CLEARING & GRUBBING		EXCAVATION		EMBANKMENT	
	LENGTH FT	AREA SF	WIDTH FT	AREA SF	UNCLASSIFIED CY	UNSUITABLE SF	UNCLASSIFIED SF	SELECT EMBANKMENT SF
101+460	20	180	0	461	0	21.85	0	0
101+480	0	0	0	0	0	0	0	0

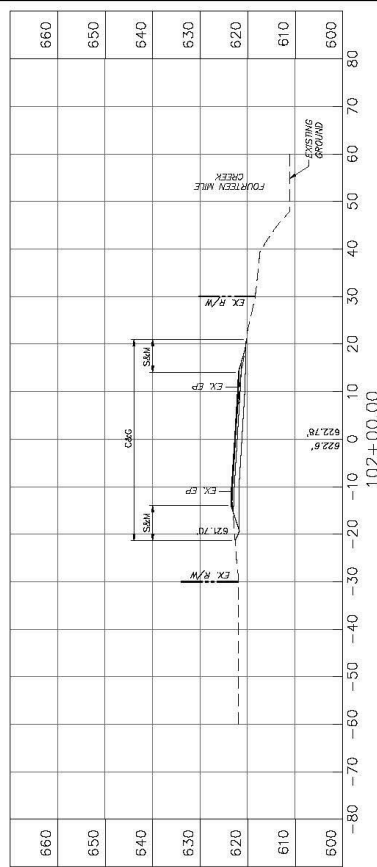


J.B. TURMAN ENGINEERING, PLLC
 P.O. Box 483
 Berneville, WV 25504
 www.jbtengineering.com
 304-733-1335

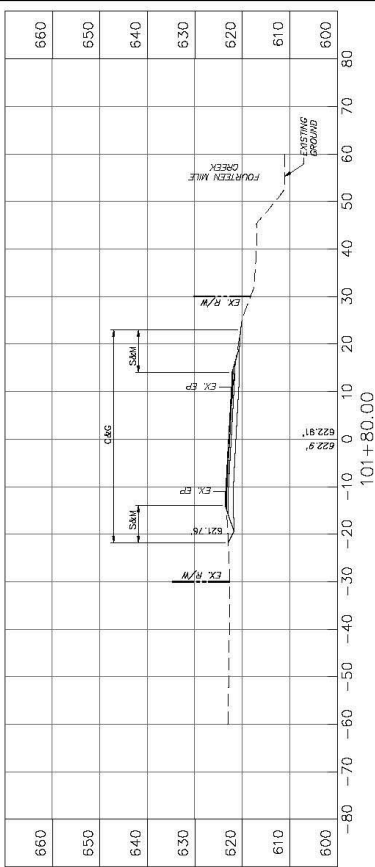
THE WEST VIRGINIA DEPARTMENT OF TRANSPORTATION
 DIVISION OF HIGHWAYS
**FOURTEEN MILE BRIDGE
 WV 37 OVER
 FOURTEENMILE CREEK**

CROSS SECTIONS

PROJECT NO.	1322	SECTION	1322-37-138.00	DATE	10/11/11	SCALE	AS SHOWN
STATE	WV	ROUTE	37	POST MILE	138.00	PROJECT	1322
COUNTY	JEFFERSON	SECTION	1322-37-138.00	DATE	10/11/11	SCALE	AS SHOWN
COUNTY	JEFFERSON	SECTION	1322-37-138.00	DATE	10/11/11	SCALE	AS SHOWN



LOCATION	SEEDING & MULCHING		CLEARING & GRUBBING		EXCAVATION		EMBANKMENT	
	LENGTH FT	AREA SF	WIDTH FT	AREA SF	UNCLASSIFIED SF	UNSATURABLE SF	UNCLASSIFIED SF	SELECT EMBANKMENT SF
102+00	20	310	42	870	58	43.33	0	0
101+60	17	45	45	870	59	---	0	---



LOCATION	SEEDING & MULCHING		CLEARING & GRUBBING		EXCAVATION		EMBANKMENT	
	LENGTH FT	AREA SF	WIDTH FT	AREA SF	UNCLASSIFIED SF	UNSATURABLE SF	UNCLASSIFIED SF	SELECT EMBANKMENT SF
101+80	20	350	45	910	59	43.70	0	---
101+60	18	45	45	870	59	---	0	---

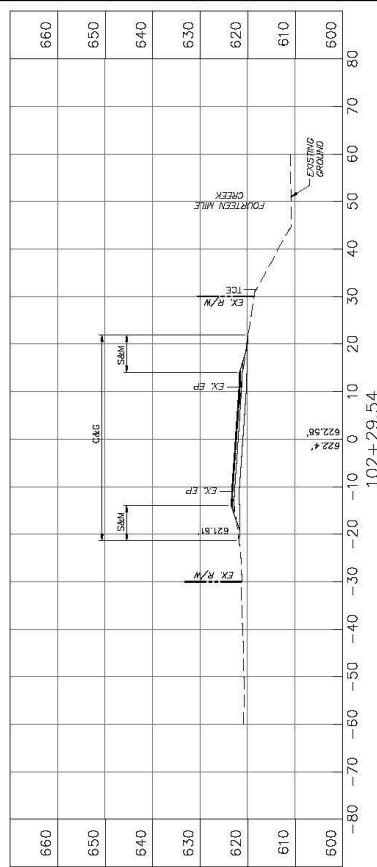


J.B. TURMAN ENGINEERING, PLLC
 P.O. Box 483
 Berneville, WV 25504
 www.jbtengineering.com
 304-733-1335

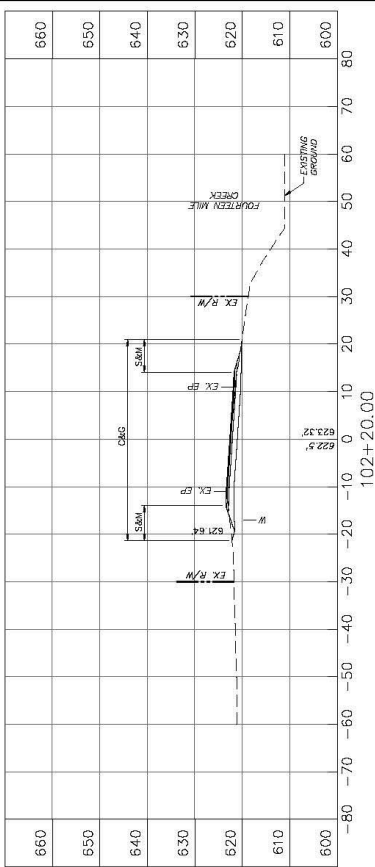
THE WEST VIRGINIA DEPARTMENT OF TRANSPORTATION
 DIVISION OF HIGHWAYS
FOURTEEN MILE BRIDGE
WV 37 OVER
FOURTEENMILE CREEK

CROSS SECTIONS

PROJECT NO.	13322-37-1.20 00	SECTION NO.	102+29.54	DATE	12/28/14
STATE	WV	COUNTY	JEFFERSON	PROJECT	STATE ROUTE 37
DATE	12/28/14	SCALE	AS SHOWN	PROJECT	STATE ROUTE 37
DATE	12/28/14	SCALE	AS SHOWN	PROJECT	STATE ROUTE 37



LOCATION	SEEDING & MULCHING		CLEARING & GRUBBING		EXCAVATION		EMBANKMENT	
	LENGTH FT	WIDTH FT	AREA SF	AREA SF	UNCLASSIFIED SF	UNUSABLE SF	UNCLASSIFIED SF	SELECT EMBANKMENT SF
102+29.54	15	43	143.10	405.45	57	19.43	0	0
102+40	14	42	143.10	405.45	57	19.43	0	0



LOCATION	SEEDING & MULCHING		CLEARING & GRUBBING		EXCAVATION		EMBANKMENT	
	LENGTH FT	WIDTH FT	AREA SF	AREA SF	UNCLASSIFIED SF	UNUSABLE SF	UNCLASSIFIED SF	SELECT EMBANKMENT SF
102+20	15	43	143.10	405.45	57	19.43	0	0
102+40	14	42	143.10	405.45	57	19.43	0	0



FOURTEEN MILE BRIDGE
WV 37 OVER
FOURTEENMILE CREEK

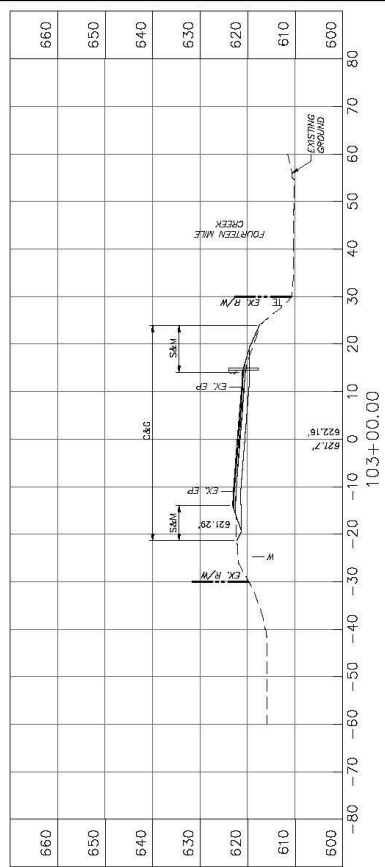
THE WEST VIRGINIA DEPARTMENT OF TRANSPORTATION
 DIVISION OF HIGHWAYS

J.B. TURMAN ENGINEERING, PLLC
 P.O. Box 483
 Berneville, WV 25504
 www.jbtengineering.com
 304-733-1335

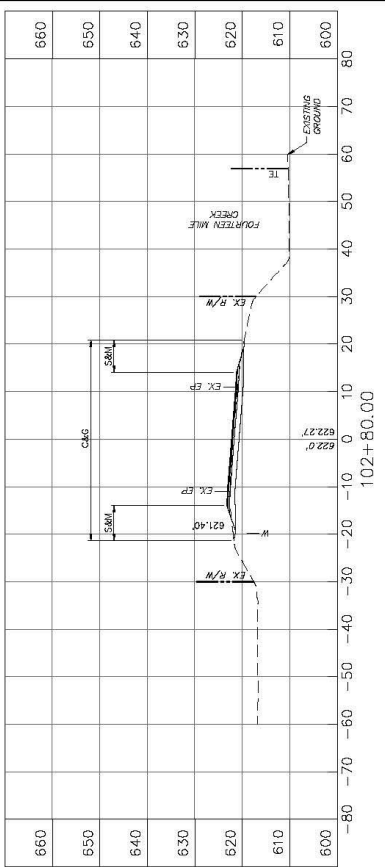
REVISION: _____ DATE: _____ BY: _____

CROSS SECTIONS

STATE	COUNTY	PROJECT	SHEET
WV	2	1322-37-1-28 00	08
DATE	BY	APP'D	CHK'D



LOCATION	SEEDING & MULCHING		CLEARING & GRUBBING		EXCAVATION		EMBANKMENT	
	LENGTH FT	WIDTH SP	AREA SF	AREA SF	UNCLASSIFIED CY	UNUSABLE SF	UNCLASSIFIED CY	SELECT EMBANKMENT SF
103+00	20	17	310	45	870	41.11	0	0.74
102+60	20	14	310	42	870	53	0	---



LOCATION	SEEDING & MULCHING		CLEARING & GRUBBING		EXCAVATION		EMBANKMENT	
	LENGTH FT	WIDTH SP	AREA SF	AREA SF	UNCLASSIFIED CY	UNUSABLE SF	UNCLASSIFIED CY	SELECT EMBANKMENT SF
102+80	20	14	310	42	870	39.28	0	---
102+60	20	17	310	45	870	53	0	---



THE WEST VIRGINIA DEPARTMENT OF TRANSPORTATION
DIVISION OF HIGHWAYS

**FOURTEEN MILE BRIDGE
WV 37 OVER
FOURTEENMILE CREEK**

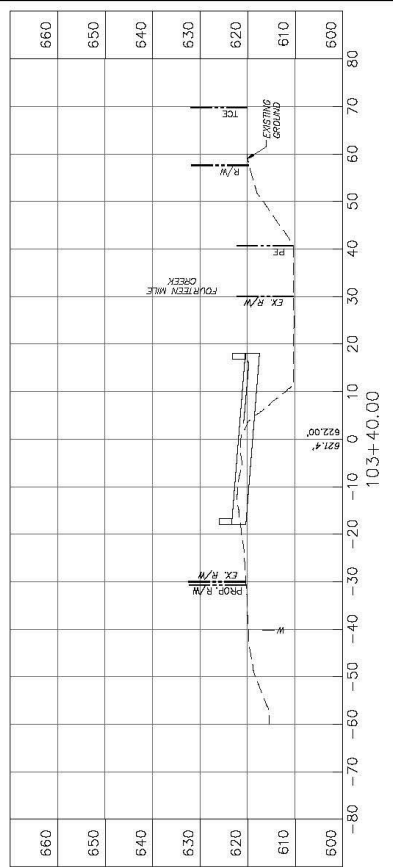
CROSS SECTIONS

P.O. Box 483
Berkeley Springs, WV 25504
www.jbturmanengineering.com
304-733-1335

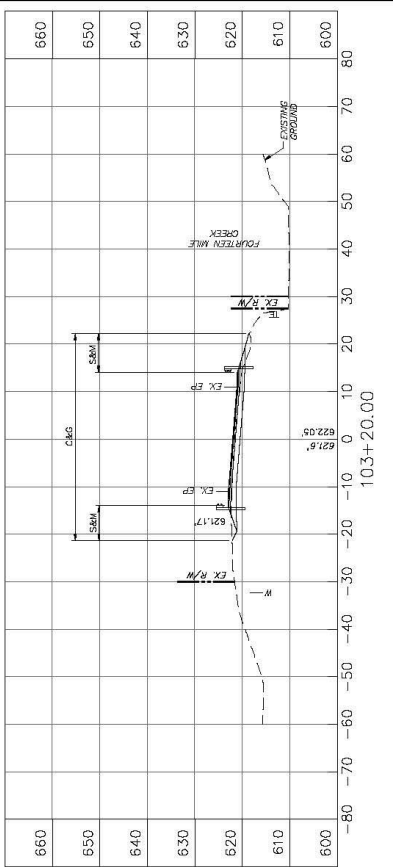
J.B. TURMAN ENGINEERING, PLLC

DATE: _____ BY: _____

PROJECT NO.	13322-37-130 00	SECTION	1300	DATE	12/28/14
DATE	12/28/14	BY	WV	2	
PROJECT NAME	FOURTEEN MILE BRIDGE				
STATE	WV	COUNTY	JEFFERSON	SHEET NO.	51
ROUTE	103	SECTION	40.00	DATE	12/28/14



LOCATION	SEEDING & MULCHING		CLEARING & GRUBBING		EXCAVATION		EMBANKMENT	
	LENGTH (L)	WIDTH (W)	AREA (SF)	AREA (CY)	UNCLASSIFIED (SF)	UNCLASSIFIED (CY)	UNCLASSIFIED (SF)	UNCLASSIFIED (CY)
103+40	20	16	320	44	35	12.95	5	1.85



LOCATION	SEEDING & MULCHING		CLEARING & GRUBBING		EXCAVATION		EMBANKMENT	
	LENGTH (L)	WIDTH (W)	AREA (SF)	AREA (CY)	UNCLASSIFIED (SF)	UNCLASSIFIED (CY)	UNCLASSIFIED (SF)	UNCLASSIFIED (CY)
103+20	20	17	340	45	35	34.44	2	2.59



THE WEST VIRGINIA DEPARTMENT OF TRANSPORTATION
DIVISION OF HIGHWAYS

**FOURTEEN MILE BRIDGE
WV 37 OVER
FOURTEEN MILE CREEK**

CROSS SECTIONS

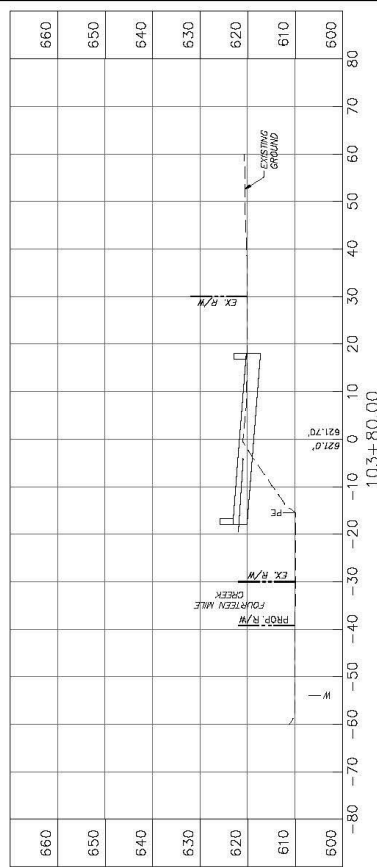
P.O. Box 483
Berkeley, WV 25504
www.jbturmanengineering.com
304-733-1335

J.B. TURMAN ENGINEERING, PLLC

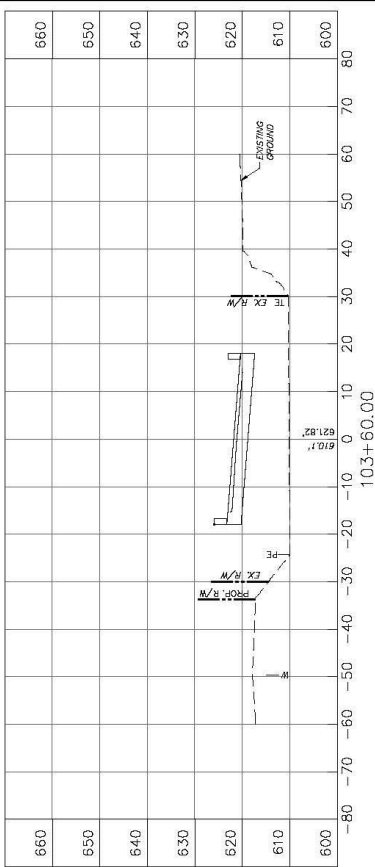
DATE: _____ BY: _____

REVISION: _____

PROJECT NO.	13222-37-1.20 00	REGION	SP-00000000	DATE	10/11/11	PROJECT	STATE	COUNTY	SHEET	TOTAL SHEETS
WV	2								54	54



LOCATION	SEEDING & MULCHING		CLEARING & GRUBBING		EXCAVATION		EMBANKMENT	
	LENGTH FT.	AREA SF.	WIDTH FT.	AREA SF.	UNCLASSIFIED SF.	UNCLASSIFIED SF.	UNCLASSIFIED SF.	SELECT EMBANKMENT SF.
103+80	20	0	0	0	0	0	0	0



LOCATION	SEEDING & MULCHING		CLEARING & GRUBBING		EXCAVATION		EMBANKMENT	
	LENGTH FT.	AREA SF.	WIDTH FT.	AREA SF.	UNCLASSIFIED SF.	UNCLASSIFIED SF.	UNCLASSIFIED SF.	SELECT EMBANKMENT SF.
103+60	20	0	0	0	0	0	0	0

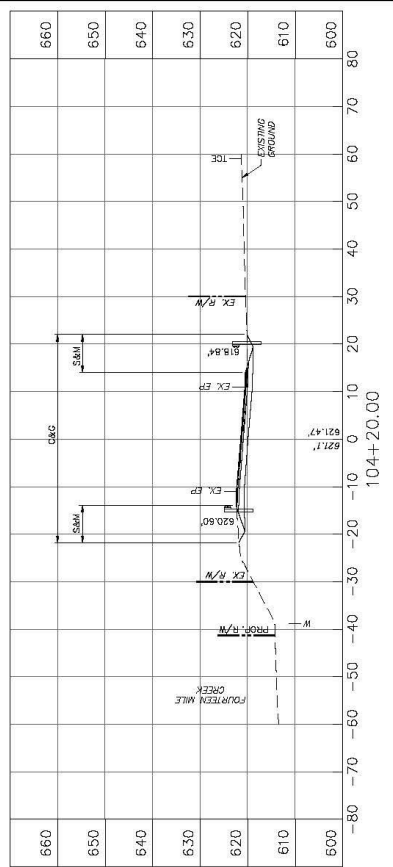


J.B. TURMAN ENGINEERING, PLLC
 P.O. Box 483
 Bercoeurville, WV 25504
 www.jbengineering.com
 304-733-1335

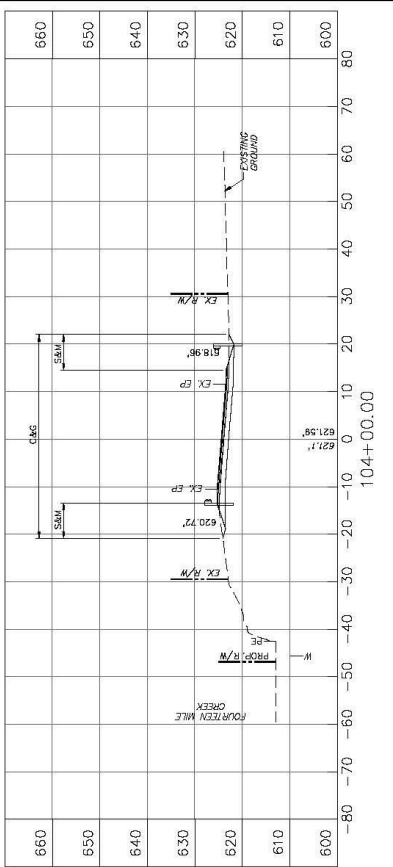
THE WEST VIRGINIA DEPARTMENT OF TRANSPORTATION
 DIVISION OF HIGHWAYS
FOURTEEN MILE BRIDGE
WV 37 OVER
FOURTEENMILE CREEK

CROSS SECTIONS

PROJECT NO.	13322-37-1.28.00	SECTION	104+00 TO 104+20
DATE	08/14/13	SCALE	1" = 20'
BY	WJ	CHECKED	WJ
APP'D		DATE	



LOCATION	SEEDING & MULCHING		CLEARING & GRUBBING		EXCAVATION		EMBANKMENT	
	WIDTH	AREA	WIDTH	AREA	UNCLASSIFIED	UNUSABLE	UNCLASSIFIED	SELECT EMBANKMENT
STATION	FT.	SF	FT.	SF	CV	SF	CV	CV
104+00	15	310	44	870	53	39.26	0	0
104+20	15	310	44	870	53	39.26	0	0



LOCATION	SEEDING & MULCHING		CLEARING & GRUBBING		EXCAVATION		EMBANKMENT	
	WIDTH	AREA	WIDTH	AREA	UNCLASSIFIED	UNUSABLE	UNCLASSIFIED	SELECT EMBANKMENT
STATION	FT.	SF	FT.	SF	CV	SF	CV	CV
104+00	15	310	44	870	53	19.63	0	0
104+20	15	310	44	870	53	19.63	0	0



P.O. Box 483
Berkeleyville, WV 25504
www.jbturmanengineering.com
304-733-1335

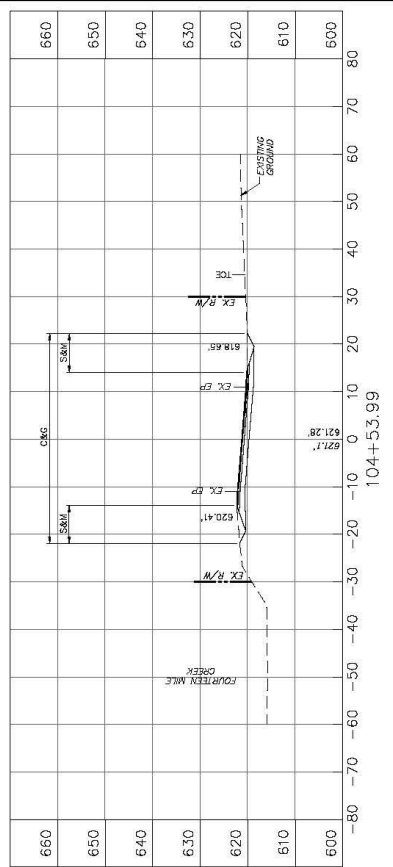
THE WEST VIRGINIA DEPARTMENT OF TRANSPORTATION
DIVISION OF HIGHWAYS

**FOURTEEN MILE BRIDGE
WV 37 OVER
FOURTEEN MILE CREEK**

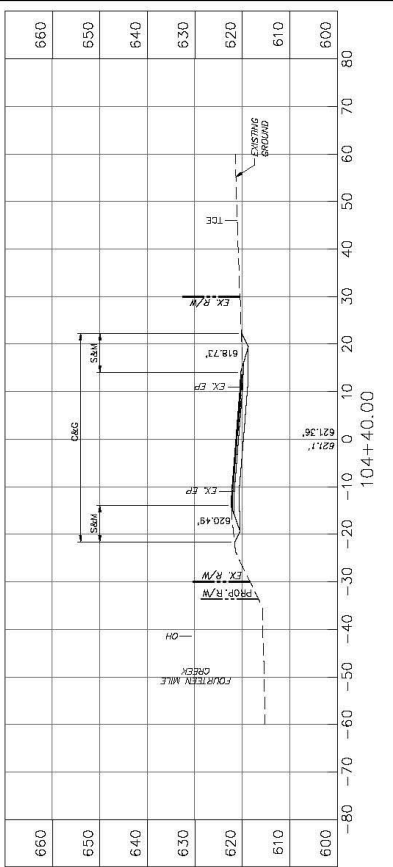
CROSS SECTIONS

NO.	DATE	BY

PROJECT NO.	13322-37-1.28.00	SECTION NO.	2011
DATE	12/28/11	SCALE	AS SHOWN
BY	WV	CHKD	WV



LOCATION	SEEDING & MULCHING		CLEARING & GRUBBING		EXCAVATION		EMBANKMENT	
	WIDTH	AREA	WIDTH	AREA	UNCLASSIFIED	UNUSABLE	UNCLASSIFIED	SELECT EMBANKMENT
104+53.99	16	223.84	44	615.56	53	27.46	0	0
104+40	16	223.84	44	615.56	53	27.46	0	0



LOCATION	SEEDING & MULCHING		CLEARING & GRUBBING		EXCAVATION		EMBANKMENT	
	WIDTH	AREA	WIDTH	AREA	UNCLASSIFIED	UNUSABLE	UNCLASSIFIED	SELECT EMBANKMENT
104+40	16	223.84	44	615.56	53	27.46	0	0
104+20	16	223.84	44	615.56	53	27.46	0	0



THE WEST VIRGINIA DEPARTMENT OF TRANSPORTATION
DIVISION OF HIGHWAYS

**FOURTEEN MILE BRIDGE
WV 37 OVER
FOURTEENMILE CREEK**

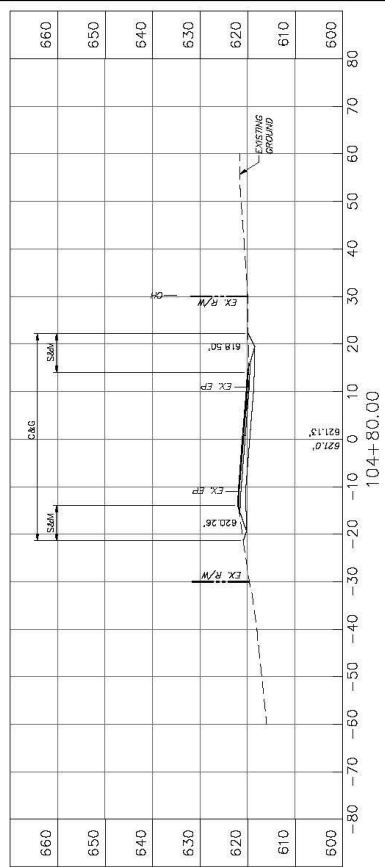
CROSS SECTIONS

P.O. Box 483
Berkeley, WV 25504
www.jbenengineering.com
304-733-1335

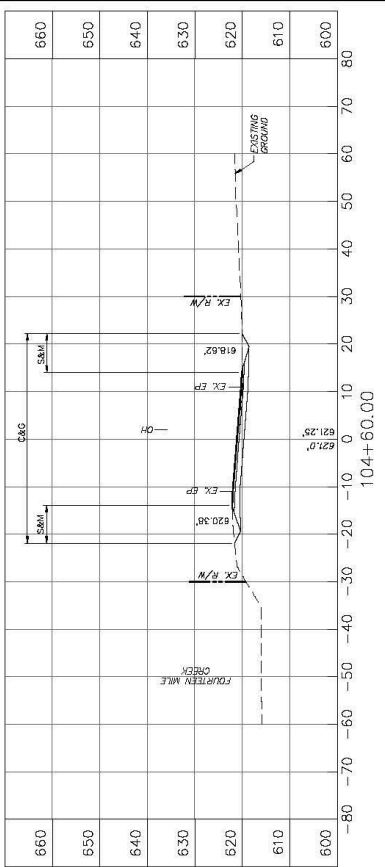
J.B. TURMAN ENGINEERING, PLLC

DATE: _____ BY: _____

PROJECT NO.	13322-37-1.28.00	SECTION NO.	001
DATE	12/28/14	SCALE	AS SHOWN
BY	WV	CHKD	WV



LOCATION	SEEDING & MULCHING		CLEARING & GRUBBING		EXCAVATION		EMBANKMENT	
	LENGTH	AREA	WIDTH	AREA	UNCLASSIFIED	UNUSABLE	UNCLASSIFIED	SELECT EMBANKMENT
104+80	20	320	44	880	53	39.28	0	0
	16		44		53		0	



LOCATION	SEEDING & MULCHING		CLEARING & GRUBBING		EXCAVATION		EMBANKMENT	
	LENGTH	AREA	WIDTH	AREA	UNCLASSIFIED	UNUSABLE	UNCLASSIFIED	SELECT EMBANKMENT
104+60	6.01	86.16	44	264.44	11.80		0	
104+53.58	16		44		53		0	



FOURTEEN MILE BRIDGE
WV 37 OVER
FOURTEENMILE CREEK

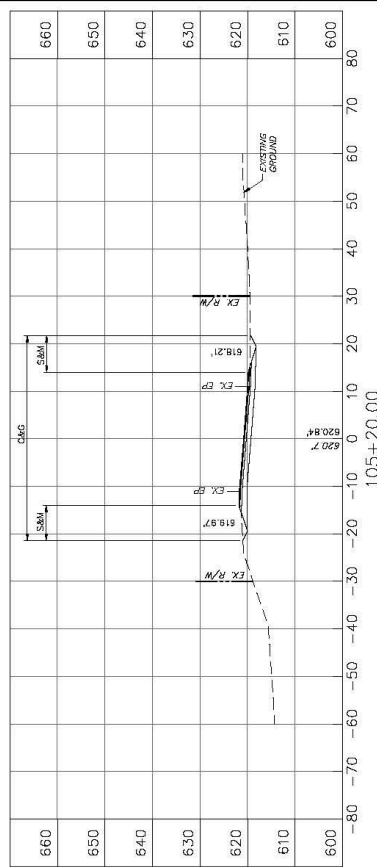
THE WEST VIRGINIA DEPARTMENT OF TRANSPORTATION
 DIVISION OF HIGHWAYS

J.B. TURMAN ENGINEERING, PLLC
 P.O. Box 483
 Berneville, WV 25504
 www.jbtengineering.com
 304-733-1335

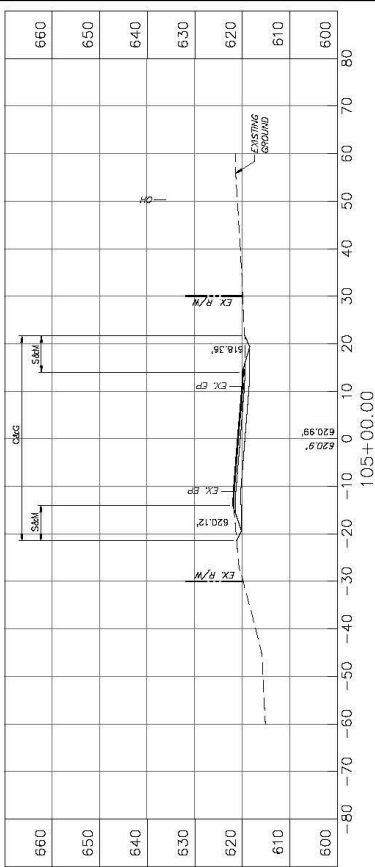
REVISION: _____ DATE: _____ BY: _____

CROSS SECTIONS

PROJECT NO.	13322-37-1.28.00	SECTION	1011	DATE	08
DATE	08/14/13	BY	WV	2	13322-37-1.28.00
SCALE	AS SHOWN	PROJECT	STATE	COUNTY	SHEET



LOCATION	LENGTH FT.	SEEDING & CLEARING & MULCHING		EXCAVATION		EMBANKMENT	
		AREA SF	WIDTH FT	UNCLASSIFIED SF	SUITABLE CY	UNCLASSIFIED SF	SELECT EMBANKMENT CY
105+20	15	300	43	53	0	0	0
105+100	15	300	43	53	0	0	0



LOCATION	LENGTH FT.	SEEDING & CLEARING & MULCHING		EXCAVATION		EMBANKMENT	
		AREA SF	WIDTH FT	UNCLASSIFIED SF	SUITABLE CY	UNCLASSIFIED SF	SELECT EMBANKMENT CY
105+00	15	310	44	53	0	0	0
104+80	20	310	44	53	0	0	0



P.O. Box 483
Berkeleyville, WV 25504
www.jbengineering.com
304-733-1335

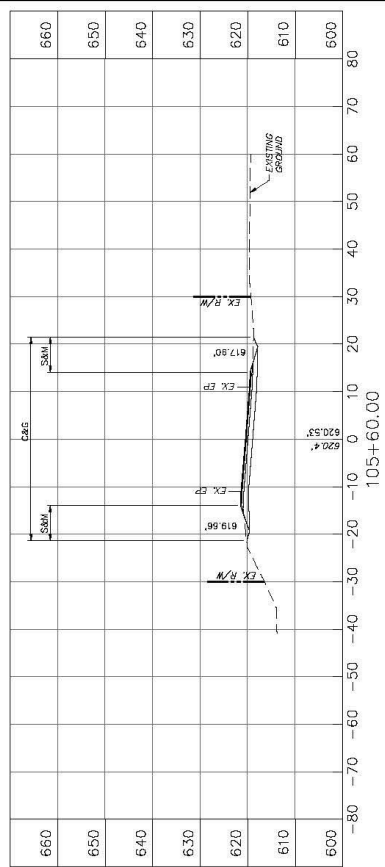
THE WEST VIRGINIA DEPARTMENT OF TRANSPORTATION
DIVISION OF HIGHWAYS

**FOURTEEN MILE BRIDGE
WV 37 OVER
FOURTEENMILE CREEK**

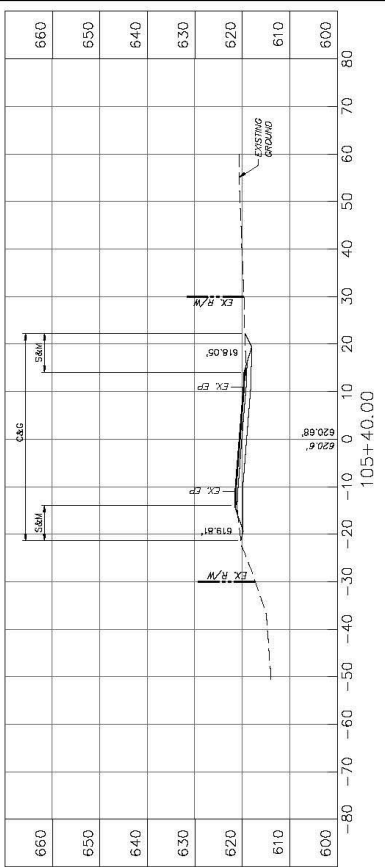
CROSS SECTIONS

NO.	DATE	BY

PROJECT NO.	13322-37-1.28.00	SECTION	1011	DATE	08/11/11
DATE	08/11/11	BY	WJ	CHKD	WJ



LOCATION	SEEDING & MULCHING			CLEARING & GRUBBING			EXCAVATION			EMBANKMENT		
	LENGTH FT	WIDTH FT	AREA SF	LENGTH FT	WIDTH FT	AREA SF	UNCLASSIFIED CY	UNUSABLE SF	UNCLASSIFIED CY	UNCLASSIFIED SF	UNUSABLE CY	SELECT EMBANKMENT CY
105+60	20	16	310	43	310	13230	53	---	53	0	---	---
105+40	20	16	310	44	310	13620	53	---	53	0	---	---



LOCATION	SEEDING & MULCHING			CLEARING & GRUBBING			EXCAVATION			EMBANKMENT		
	LENGTH FT	WIDTH FT	AREA SF	LENGTH FT	WIDTH FT	AREA SF	UNCLASSIFIED CY	UNUSABLE SF	UNCLASSIFIED CY	UNCLASSIFIED SF	UNUSABLE CY	SELECT EMBANKMENT CY
105+40	20	16	310	44	310	13620	53	---	53	0	---	---
105+20	20	16	310	44	310	13620	53	---	53	0	---	---



J.B. TURMAN ENGINEERING, PLLC
 P.O. Box 483
 Bercooreville, WV 25504
 www.jbtengineering.com
 304-733-1335

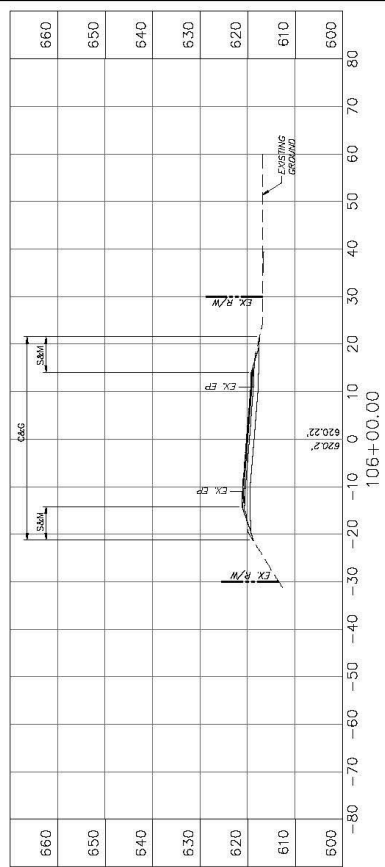
THE WEST VIRGINIA DEPARTMENT OF TRANSPORTATION
 DIVISION OF HIGHWAYS

**FOURTEEN MILE BRIDGE
 WV 37 OVER
 FOURTEENMILE CREEK**

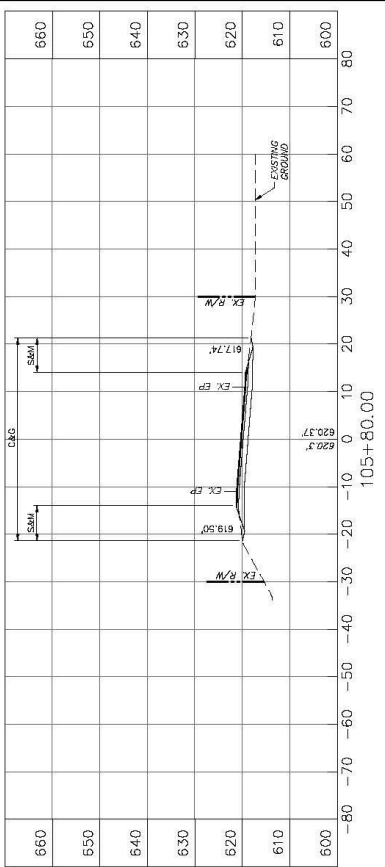
CROSS SECTIONS

NO.	DATE	BY

PROJECT NO.	13322-37-1.2B.00	SECTION NO.	001
DATE	12/28/11	PROJECT NAME	13322-37-1.2B.00
SCALE	AS SHOWN	PROJECT NO.	13322-37-1.2B.00
DATE	12/28/11	SECTION NO.	001



LOCATION	SEEDING & MULCHING		CLEARING & GRUBBING		EXCAVATION		EMBANKMENT	
	LENGTH FT.	AREA SF	WIDTH FT.	AREA SF	UNCLASSIFIED CY	UNUSABLE SF	UNCLASSIFIED CY	SELECT EMBANKMENT SF
106+00	20	300	43	860	53	39.28	0	0
106+80	15	300	43	860	53	39.28	0	0



LOCATION	SEEDING & MULCHING		CLEARING & GRUBBING		EXCAVATION		EMBANKMENT	
	LENGTH FT.	AREA SF	WIDTH FT.	AREA SF	UNCLASSIFIED CY	UNUSABLE SF	UNCLASSIFIED CY	SELECT EMBANKMENT SF
105+80	20	300	43	860	53	39.28	0	0
105+60	15	300	43	860	53	39.28	0	0



J.B. TURMAN ENGINEERING, PLLC
 P.O. Box 483
 Bercooreville, WV 25504
 www.jbtengineering.com
 304-733-1335

THE WEST VIRGINIA DEPARTMENT OF TRANSPORTATION
 DIVISION OF HIGHWAYS
**FOURTEEN MILE BRIDGE
 WV 37 OVER
 FOURTEENMILE CREEK**

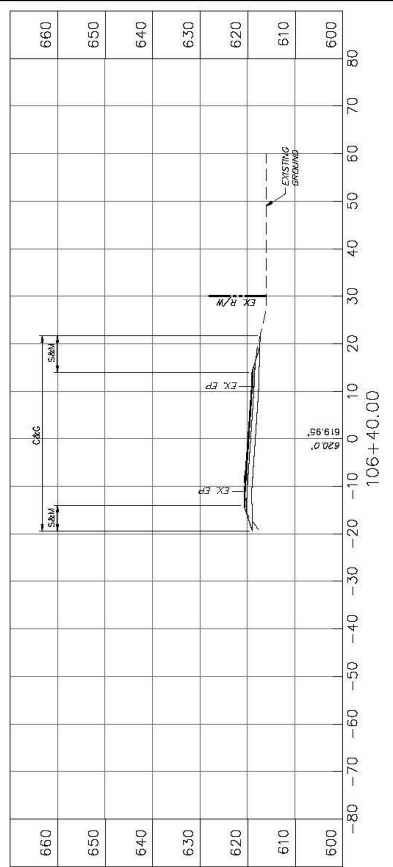
CROSS SECTIONS

PROJECT NO.	DATE	BY	CHKD BY	DATE	BY
106+40.00	10/1/14	WV	2	10/1/14	WV

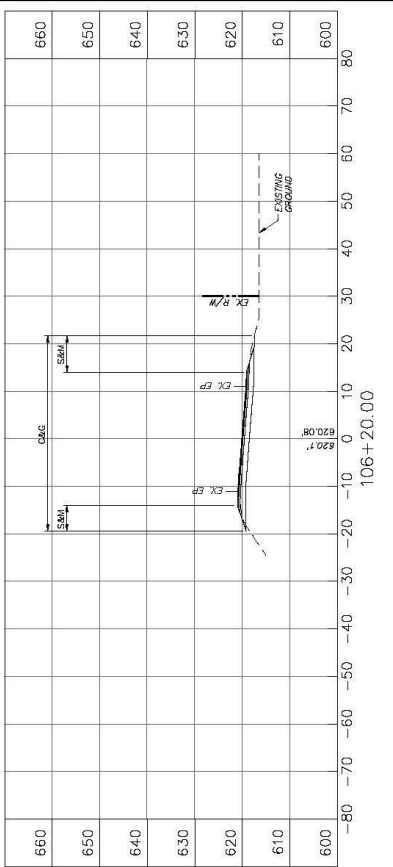
SECTION	DATE	BY	CHKD BY	DATE	BY
106+40.00	10/1/14	WV	2	10/1/14	WV

PROJECT NO.	DATE	BY	CHKD BY	DATE	BY
106+40.00	10/1/14	WV	2	10/1/14	WV

PROJECT NO.	DATE	BY	CHKD BY	DATE	BY
106+40.00	10/1/14	WV	2	10/1/14	WV



LOCATION	SEEDING & MULCHING		CLEARING & GRUBBING		EXCAVATION		EMBANKMENT	
	LENGTH FT	WIDTH FT	AREA SQ	AREA CY	UNCLASSIFIED SQ	UNCLASSIFIED CY	UNCLASSIFIED SQ	UNCLASSIFIED CY
106+40	13	41	53	31.26	0	0	0	0
106+20	13	41	53	31.26	0	0	0	0



LOCATION	SEEDING & MULCHING		CLEARING & GRUBBING		EXCAVATION		EMBANKMENT	
	LENGTH FT	WIDTH FT	AREA SQ	AREA CY	UNCLASSIFIED SQ	UNCLASSIFIED CY	UNCLASSIFIED SQ	UNCLASSIFIED CY
106+20	13	41	53	31.26	0	0	0	0
106+00	13	41	53	31.26	0	0	0	0



J.B. TURMAN ENGINEERING, PLLC
 P.O. Box 483
 Bercooreville, WV 25504
 www.jbtengineering.com
 304-733-1535

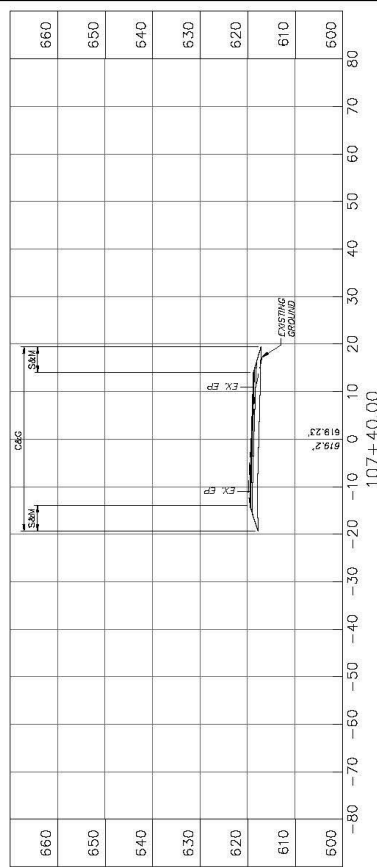
THE WEST VIRGINIA DEPARTMENT OF TRANSPORTATION
 DIVISION OF HIGHWAYS

**FOURTEEN MILE BRIDGE
 WV 37 OVER
 FOURTEENMILE CREEK**

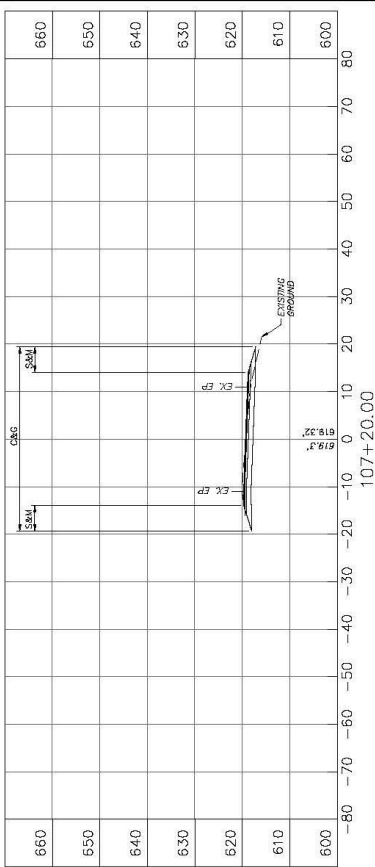
CROSS SECTIONS

PROJECT NO.	DATE	BY
106+40.00	10/1/14	WV

PROJECT NO.	13322-37-1.28.00	SECTION	107+40.00
DATE	12/28/2011	BY	AS



LOCATION	SEEDING & MULCHING		CLEARING & GRUBBING		EXCAVATION		EMBANKMENT	
	LENGTH	WIDTH	AREA	WIDTH	AREA	UNCLASSIFIED	UNCLASSIFIED	SELECT EMBANKMENT
1074.40	11	38	418	38	780	53	0	0
1074.20	11	38	418	38	780	53	0	0



LOCATION	SEEDING & MULCHING		CLEARING & GRUBBING		EXCAVATION		EMBANKMENT	
	LENGTH	WIDTH	AREA	WIDTH	AREA	UNCLASSIFIED	UNCLASSIFIED	SELECT EMBANKMENT
1074.20	11	38	418	38	780	53	0	0
1074.00	11	38	418	38	780	53	0	0

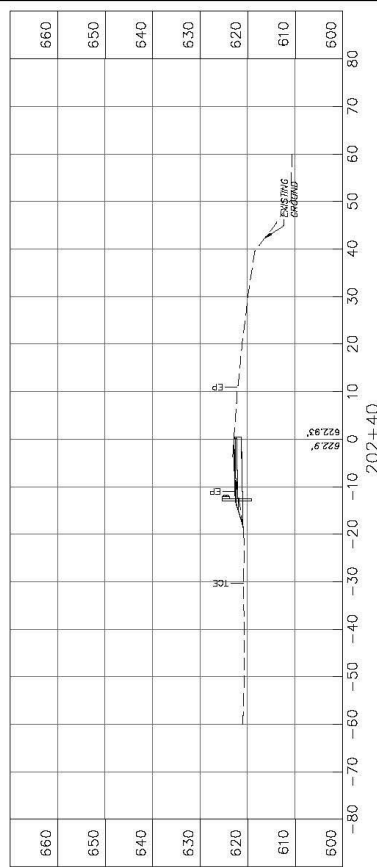


J.B. TURMAN ENGINEERING, PLLC
 P.O. Box 483
 Bercoeurville, WV 25504
 www.jbtengineering.com
 304-733-1335

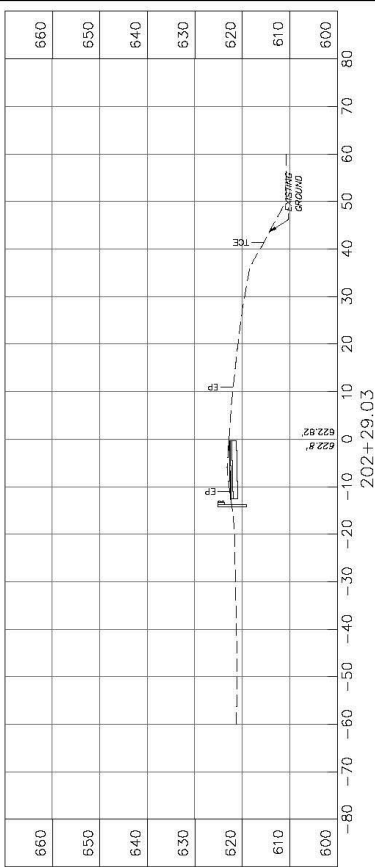
THE WEST VIRGINIA DEPARTMENT OF TRANSPORTATION
 DIVISION OF HIGHWAYS
FOURTEEN MILE BRIDGE
WV 37 OVER
FOURTEENMILE CREEK

CROSS SECTIONS

PROJECT NO.	DATE	PROJECT NAME	SCALE	SHEET NO.	TOTAL SHEETS
WV 2	12/22/2011	1322-37-128.00	1"=20'	10	10
DATE	BY	CHECKED	DATE	BY	DATE



LOCATION	SEEDING & MULCHING		CLEARING & GRUBBING		EXCAVATION		EMBANKMENT	
	LENGTH (FT)	AREA (SF)	WIDTH (FT)	AREA (SF)	UNCLASSIFIED (CY)	UNSUITABLE (SF)	UNCLASSIFIED (CY)	SELECT EMBANKMENT (SF)
202+40	10.67	0	0	0	20.86	0	0	0
202+29.03	0	0	0	0	22.48	8.81	0	0



LOCATION	SEEDING & MULCHING		CLEARING & GRUBBING		EXCAVATION		EMBANKMENT	
	LENGTH (FT)	AREA (SF)	WIDTH (FT)	AREA (SF)	UNCLASSIFIED (CY)	UNSUITABLE (SF)	UNCLASSIFIED (CY)	SELECT EMBANKMENT (SF)
202+29.03	9.03	0	0	0	22.48	4.37	0	0
202+20	0	0	0	0	0	0	0	0



P.O. Box 483
Bourbonville, WV 25504
www.jbengineering.com
304-733-1335

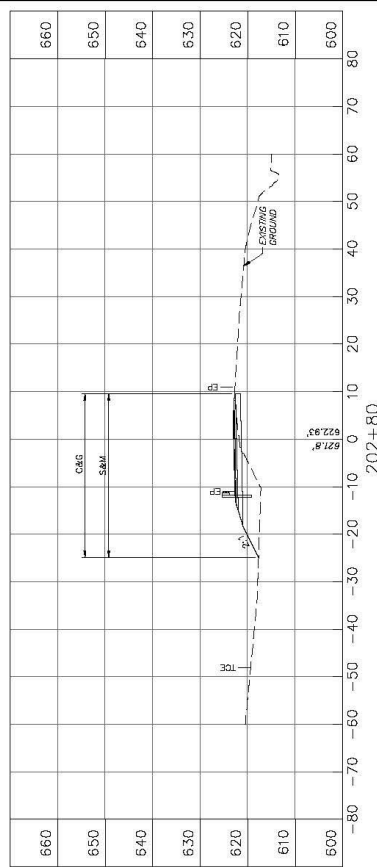
THE WEST VIRGINIA DEPARTMENT OF TRANSPORTATION
DIVISION OF HIGHWAYS

**FOURTEEN MILE BRIDGE
WV 37 OVER
FOURTEENMILE CREEK**

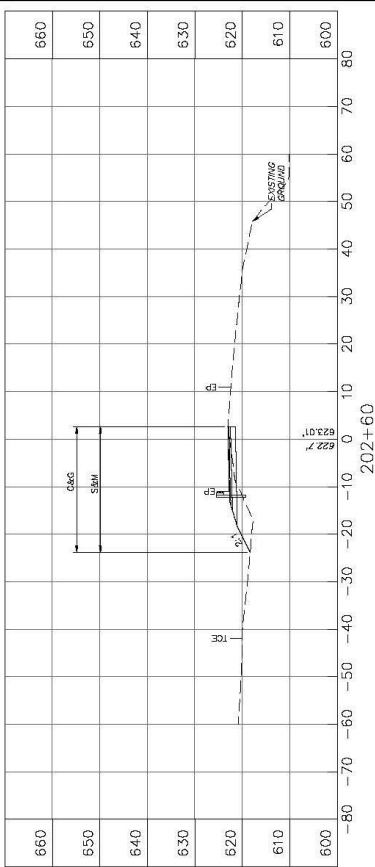
DETOUR
CROSS SECTIONS

DATE	BY

STATE	PROJECT NO.	SECTION	DATE	SCALE	SHEET NO.	TOTAL SHEETS
WV	2	1322-37-138 00	08/11/2011	1"=40'	108	110



LOCATION	SEEDING & MULCHING		CLEARING & GRUBBING		EXCAVATION		EMBANKMENT	
	LENGTH FT.	AREA SF	WIDTH FT.	AREA SF	UNCLASSIFIED CY	UNSUITABLE SF	UNCLASSIFIED SF	SELECT EMBANKMENT CY
202+80	20	608.40	34.42	608.40	6.86	571.5	30.30	---
202+80	20	26.42	26.42	10.35	7.11	---	26.19	---



LOCATION	SEEDING & MULCHING		CLEARING & GRUBBING		EXCAVATION		EMBANKMENT	
	LENGTH FT.	AREA SF	WIDTH FT.	AREA SF	UNCLASSIFIED CY	UNSUITABLE SF	UNCLASSIFIED SF	SELECT EMBANKMENT CY
202+60	20	264.20	26.42	264.20	10.35	11.56	0	9.70
202+60	20	26.42	26.42	20.68	---	---	---	---



P.O. Box 483
Berkeley, WV 25504
www.jbturmanengineering.com
304-733-1335

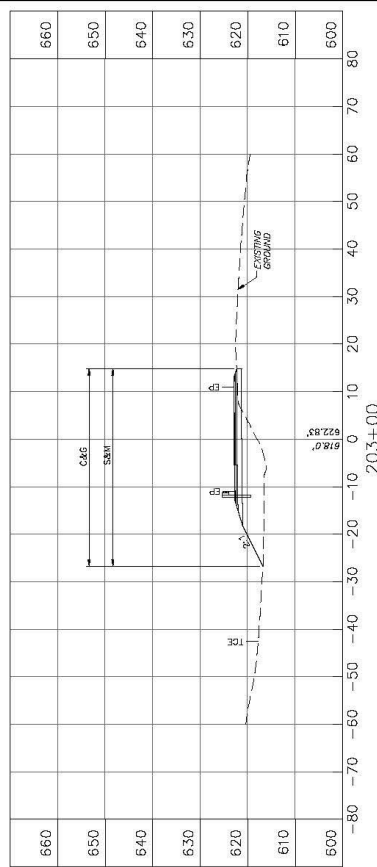
THE WEST VIRGINIA DEPARTMENT OF TRANSPORTATION
DIVISION OF HIGHWAYS

FOURTEEN MILE BRIDGE
WV 37 OVER
FOURTEENMILE CREEK

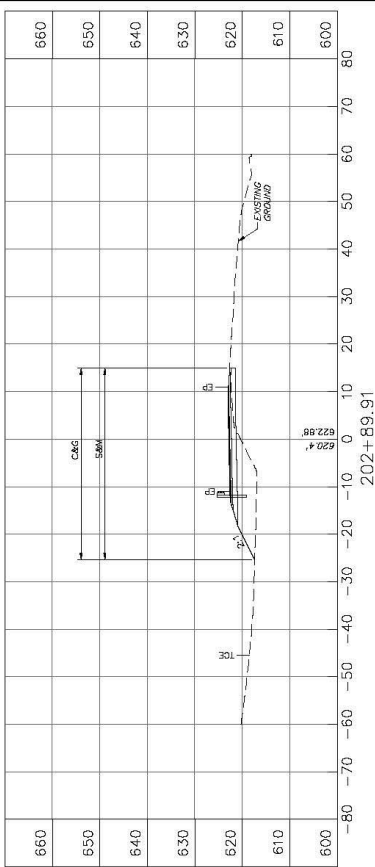
DETOUR
CROSS SECTIONS

NO.	DATE	BY

PROJECT NO.	DATE	BY	CHKD	DATE	BY	CHKD
1322-37-138 02	10/11/11	WV	2	10/11/11	WV	2



LOCATION	SEEDING & MULCHING		CLEARING & GRUBBING		EXCAVATION		EMBANKMENT	
	WIDTH FT	AREA SF	WIDTH FT	AREA SF	UNCLASSIFIED SF	UNSATURABLE SF	UNCLASSIFIED SF	SELECT EMBANKMENT SF
203+00	41.59	413.24	41.59	413.24	6.37	2.84	112.77	35.59
202+85 SF	40.32	403.24	40.32	413.24	9.35	---	77.71	---



LOCATION	SEEDING & MULCHING		CLEARING & GRUBBING		EXCAVATION		EMBANKMENT	
	WIDTH FT	AREA SF	WIDTH FT	AREA SF	UNCLASSIFIED SF	UNSATURABLE SF	UNCLASSIFIED SF	SELECT EMBANKMENT SF
202+89.91	40.32	370.34	40.32	370.34	6.35	3.34	77.71	24.77
202+80	34.42	344.2	34.42	344.2	6.86	---	57.25	---

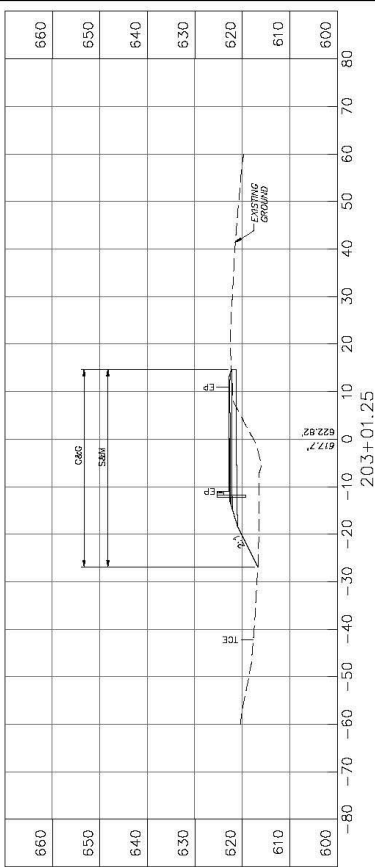
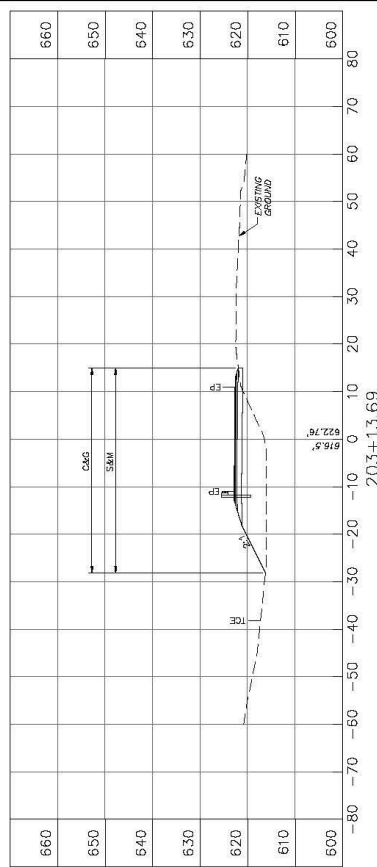


J.B. TURMAN ENGINEERING, PLLC
 P.O. Box 483
 Bercooreville, WV 25504
 www.jbtengineering.com
 304-733-1335

THE WEST VIRGINIA DEPARTMENT OF TRANSPORTATION
 DIVISION OF HIGHWAYS
**FOURTEEN MILE BRIDGE
 WV 37 OVER
 FOURTEENMILE CREEK**
 DETOUR
 CROSS SECTIONS

PROJECT NO.	DATE	BY
1322-37-138 02		

STATE	PROJECT	SECTION	SHEET
WV	2	203+00 TO 203+100	10
DATE	BY	SCALE	PROJECT
			1:1



LOCATION	SEEDING & MULCHING		CLEARING & GRUBBING		EXCAVATION		EMBANKMENT	
	LENGTH	AREA	WIDTH	AREA	UNCLASSIFIED	UNUSABLE	UNCLASSIFIED	SELECT EMBANKMENT
STATION	FT	SF	FT	SF	CU	SF	CU	SF
203+13.69	11	43.19	43.19	577.58	2.81	---	146.54	---
203+01.25	12.44	41.63	41.63	577.58	5.96	---	116.95	---

LOCATION	SEEDING & MULCHING		CLEARING & GRUBBING		EXCAVATION		EMBANKMENT	
	LENGTH	AREA	WIDTH	AREA	UNCLASSIFIED	UNUSABLE	UNCLASSIFIED	SELECT EMBANKMENT
STATION	FT	SF	FT	SF	CU	SF	CU	SF
203+01.25	1.20	41.59	41.59	52.01	6.37	---	112.77	5.32
203+00	---	---	---	---	---	---	---	---



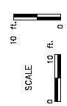
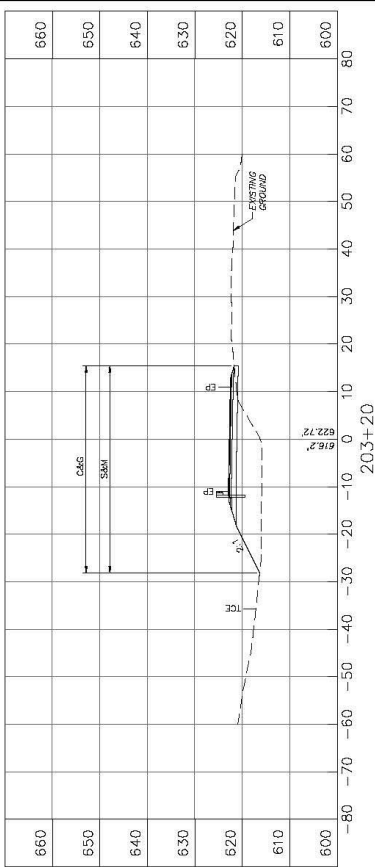
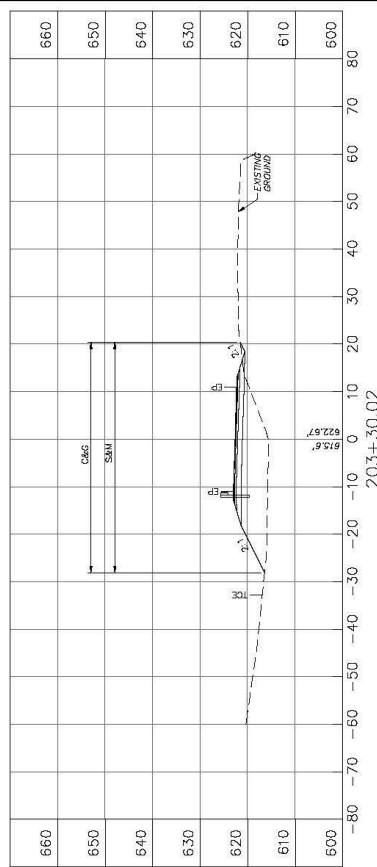
P.O. Box 483
Berkeleyville, WV 25504
www.jbenengineering.com
304-733-1335

THE WEST VIRGINIA DEPARTMENT OF TRANSPORTATION
DIVISION OF HIGHWAYS

FOURTEEN MILE BRIDGE
WV 37 OVER
FOURTEENMILE CREEK

DETOUR
CROSS SECTIONS

PROJECT NO.	DATE	BY	CHKD	DATE	BY	CHKD	DATE	BY
1322-37-1.00.02	10/02	WV	2	10/02	WV	2	10/02	WV

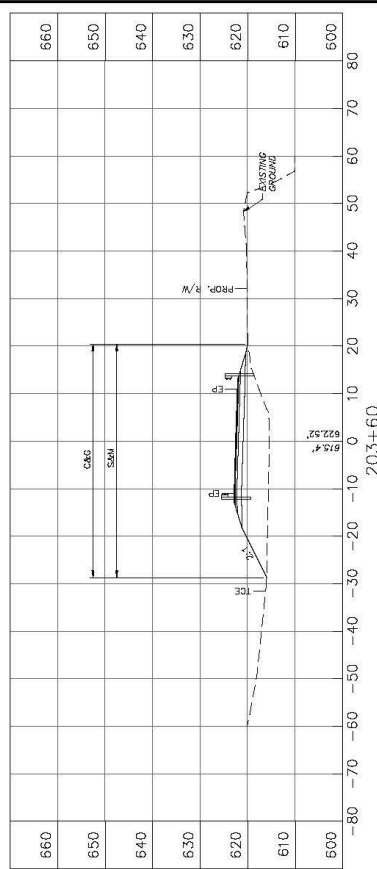


J.B. TURMAN ENGINEERING, PLLC
 P.O. Box 483
 Bercoeurville, WV 25504
 www.jbtengineering.com
 304-733-1335

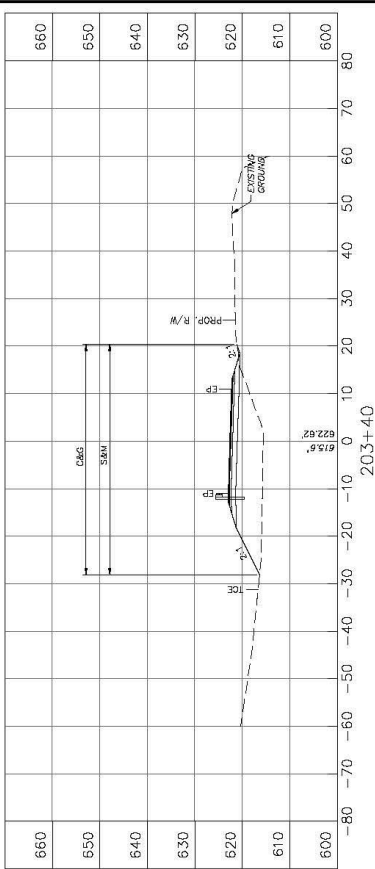
THE WEST VIRGINIA DEPARTMENT OF TRANSPORTATION
 DIVISION OF HIGHWAYS
FOURTEEN MILE BRIDGE
WV 37 OVER
FOURTEENMILE CREEK
 DETOUR
 CROSS SECTIONS

NO.	DATE	BY

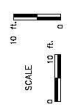
PROJECT NO.	13322-37-1.28.00	PROJECT NAME	SR-600/600B	DATE	2011	DESIGNER	UNION	NO.	70	DATE	2011	BY	MS
STATE	WV	SECTION	2										



LOCATION	SEEDING & MULCHING		CLEARING & GRUBBING		EXCAVATION		EMBANKMENT	
	WIDTH	AREA	WIDTH	AREA	UNCLASSIFIED	UNUSABLE	UNCLASSIFIED	SELECT EMBANKMENT
STATION	FT.	SF	FT.	SF	CV	SF	SF	CV
203+60	49.11	4856	49.11	4856	0	1847.5	177.06	137.71
203+60	20	4856	48.53	4848	0.82	177.06	177.06	137.71



LOCATION	SEEDING & MULCHING		CLEARING & GRUBBING		EXCAVATION		EMBANKMENT	
	WIDTH	AREA	WIDTH	AREA	UNCLASSIFIED	UNUSABLE	UNCLASSIFIED	SELECT EMBANKMENT
STATION	FT.	SF	FT.	SF	CV	SF	SF	CV
203+40	48.53	4848	48.53	4848	0.82	177.06	177.06	137.71
203+50.02	48.53	4848	48.53	4848	2.79	167.00	167.00	137.71

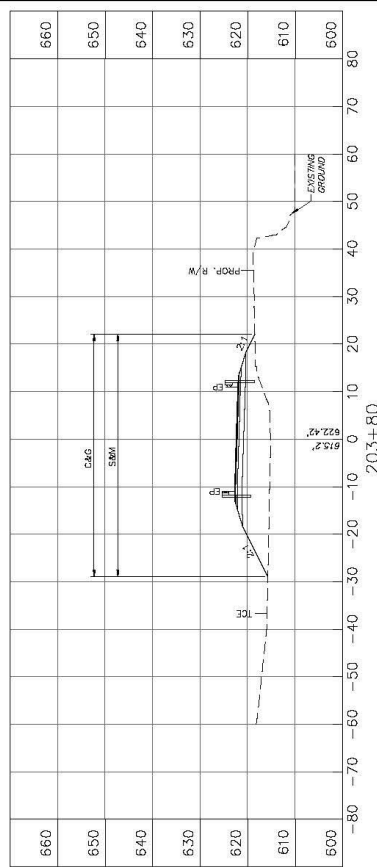


J.B. TURMAN ENGINEERING, PLLC
 P.O. Box 483
 Bercooreville, WV 25504
 www.jbtengineering.com
 304-733-1335

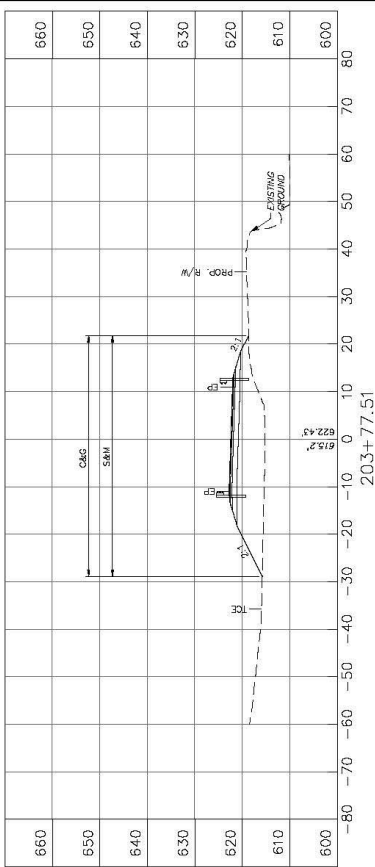
THE WEST VIRGINIA DEPARTMENT OF TRANSPORTATION
 DIVISION OF HIGHWAYS
FOURTEEN MILE BRIDGE
WV 37 OVER
FOURTEENMILE CREEK
 DETOUR
 CROSS SECTIONS

DATE	BY

PROJECT NO.	13322-37-1.28.00	SECTION	2011	DATE	11/11/11
WV	2	SECTION	2011	DATE	11/11/11



LOCATION	SEEDING & MULCHING		CLEARING & GRUBBING		EXCAVATION		EMBANKMENT	
	WIDTH	AREA	WIDTH	AREA	UNCLASSIFIED	UNUSABLE	UNCLASSIFIED	SELECT EMBANKMENT
STATION	LENGTH	FT	FT	SF	CV	SF	CV	SF
203+80	2.49	51.06	51.06	176.75	0	0	0	194.4
203+77.5		50.75	50.75	176.75	0	0	209.58	---



LOCATION	SEEDING & MULCHING		CLEARING & GRUBBING		EXCAVATION		EMBANKMENT	
	WIDTH	AREA	WIDTH	AREA	UNCLASSIFIED	UNUSABLE	UNCLASSIFIED	SELECT EMBANKMENT
STATION	LENGTH	FT	FT	SF	CV	SF	CV	SF
203+77.5	17.5	56.75	56.75	874.27	0	0	209.58	131.1
203+80		49.11	49.11	874.27	0	0	194.75	---

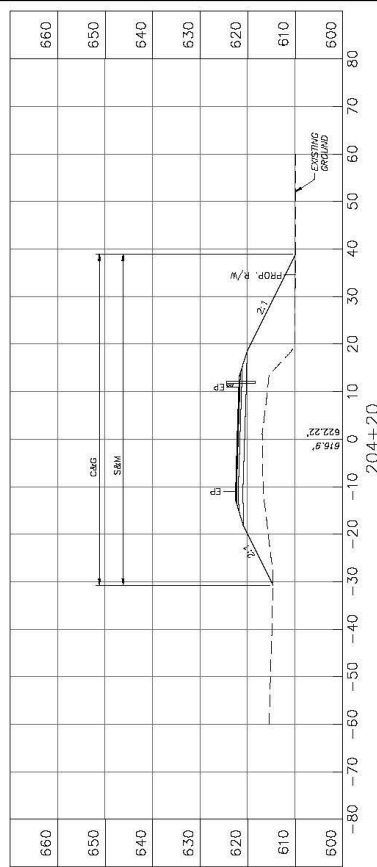


J.B. TURMAN ENGINEERING, PLLC
 P.O. Box 483
 Berneville, WV 25504
 www.jbtengineering.com
 304-733-1335

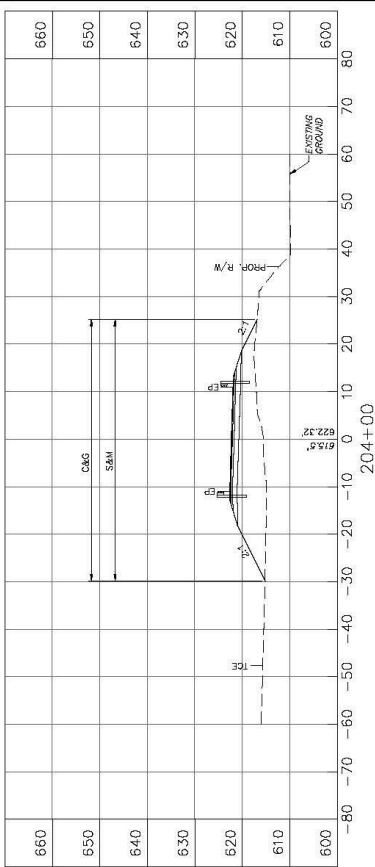
THE WEST VIRGINIA DEPARTMENT OF TRANSPORTATION
 DIVISION OF HIGHWAYS
FOURTEEN MILE BRIDGE
WV 37 OVER
FOURTEENMILE CREEK
 DETOUR
 CROSS SECTIONS

DATE	BY

PROJECT NO.	DATE	DESIGN NO.	SCALE	SHEET NO.	TOTAL SHEETS
WV 2	12/22/11	1322-37-130-00	1"=40'	17	17



LOCATION	SEEDING & MULCHING		CLEARING & GRUBBING		EXCAVATION		EMBANKMENT	
	WIDTH	AREA	WIDTH	AREA	UNCLASSIFIED	UNUSABLE	UNCLASSIFIED	SELECT EMBANKMENT
STATION	FT.	SF	FT.	SF	CV	SF	CV	CV
204+20	48.72	1247.60	69.72	1247.60	0	0	304.42	193.00
204+00	56.04	1247.60	56.04	1247.60	0	0	216.88	---



LOCATION	SEEDING & MULCHING		CLEARING & GRUBBING		EXCAVATION		EMBANKMENT	
	WIDTH	AREA	WIDTH	AREA	UNCLASSIFIED	UNUSABLE	UNCLASSIFIED	SELECT EMBANKMENT
STATION	FT.	SF	FT.	SF	CV	SF	CV	CV
204+00	56.04	1247.60	56.04	1247.60	0	0	216.88	158.33
204+80	51.06	1091	51.06	1091	0	0	211.30	---



P.O. Box 483
Berkeley, WV 25504
www.jbturmanengineering.com
304-733-1335

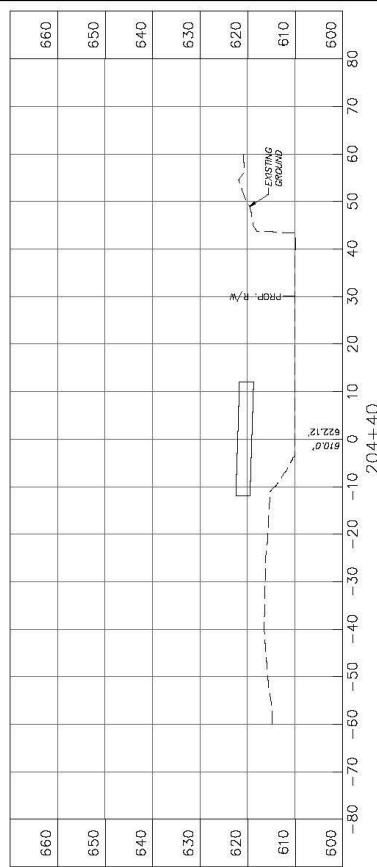
THE WEST VIRGINIA DEPARTMENT OF TRANSPORTATION
DIVISION OF HIGHWAYS

**FOURTEEN MILE BRIDGE
WV 37 OVER
FOURTEENMILE CREEK**

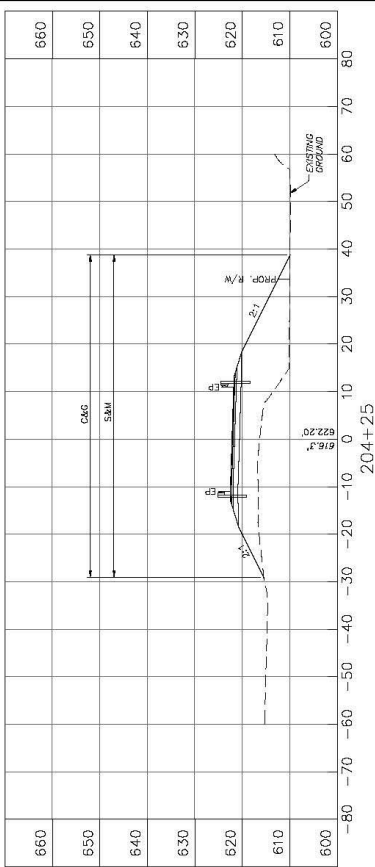
DETOUR
CROSS SECTIONS

NO.	DATE	BY

PROJECT NO.	13322-37-1.20 00	SECTION NO.	2
DATE	12/20/11	SCALE	AS SHOWN
DESIGNED BY	J.B. TURMAN	CHECKED BY	J.B. TURMAN
DATE	12/20/11	SCALE	AS SHOWN
PROJECT NO.	13322-37-1.20 00	SECTION NO.	2
DATE	12/20/11	SCALE	AS SHOWN
DESIGNED BY	J.B. TURMAN	CHECKED BY	J.B. TURMAN
DATE	12/20/11	SCALE	AS SHOWN



LOCATION	SEEDING & MULCHING		CLEARING & GRUBBING		EXCAVATION		EMBANKMENT	
	WIDTH	AREA	WIDTH	AREA	UNCLASSIFIED	UNUSABLE	UNCLASSIFIED	SELECT EMBANKMENT
STATION	FT.	SF	FT.	SF	CV	SF	CV	SF
204+40	0	0	0	0	0	0	0	0
204+25	67.85	508.88	67.85	508.88	0	0	398.26	563.3



LOCATION	SEEDING & MULCHING		CLEARING & GRUBBING		EXCAVATION		EMBANKMENT	
	WIDTH	AREA	WIDTH	AREA	UNCLASSIFIED	UNUSABLE	UNCLASSIFIED	SELECT EMBANKMENT
STATION	FT.	SF	FT.	SF	CV	SF	CV	SF
204+25	67.85	508.88	67.85	508.88	0	0	398.26	563.3
204+20	69.72	483.93	69.72	483.93	0	0	304.42	444.0

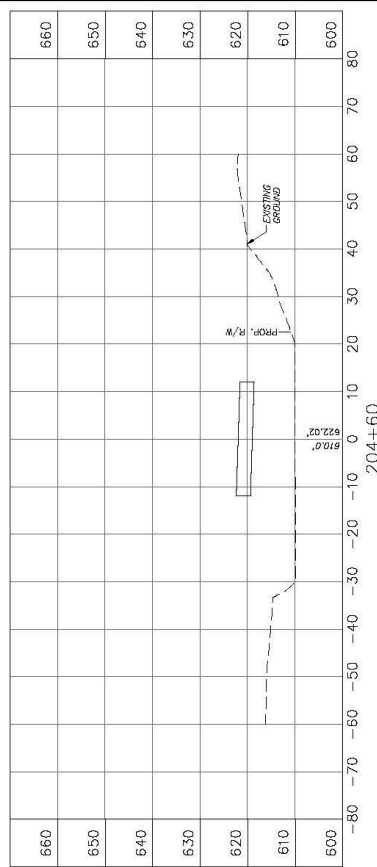


J.B. TURMAN ENGINEERING, PLLC
 P.O. Box 483
 Bercooreville, WV 25504
 www.jbtengineering.com
 304-733-1335

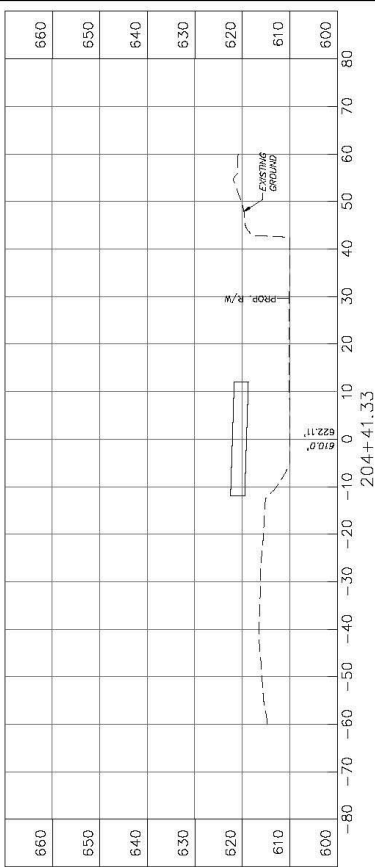
THE WEST VIRGINIA DEPARTMENT OF TRANSPORTATION
 DIVISION OF HIGHWAYS
FOURTEEN MILE BRIDGE
WV 37 OVER
FOURTEENMILE CREEK
 DETOUR
 CROSS SECTIONS

DATE	BY

PROJECT NO.	1332-37-128 00	PROJECT NAME	SR-60010000	DATE	10/11
WV 2		SECTION	SECTION	SECTION	SECTION



LOCATION	SEEDING & MULCHING		CLEARING & GRUBBING		EXCAVATION		EMBANKMENT	
	LENGTH FT	AREA SF	WIDTH FT	AREA SF	UNCLASSIFIED SF	UNCLASSIFIED SF	UNCLASSIFIED SF	SELECT EMBANKMENT SF
204+60	0	0	0	0	0	0	0	0
204+41.33	0	0	0	0	0	0	0	0



LOCATION	SEEDING & MULCHING		CLEARING & GRUBBING		EXCAVATION		EMBANKMENT	
	LENGTH FT	AREA SF	WIDTH FT	AREA SF	UNCLASSIFIED SF	UNCLASSIFIED SF	UNCLASSIFIED SF	SELECT EMBANKMENT SF
204+41.33	1.33	0	0	0	0	0	0	0
204+40	0	0	0	0	0	0	0	0



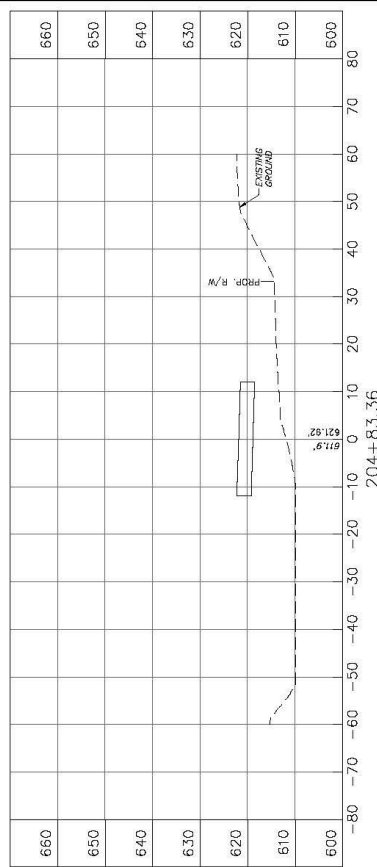
P.O. Box 483
Berkeleyville, WV 25504
www.jbturmanengineering.com
304-733-1335

THE WEST VIRGINIA DEPARTMENT OF TRANSPORTATION
DIVISION OF HIGHWAYS

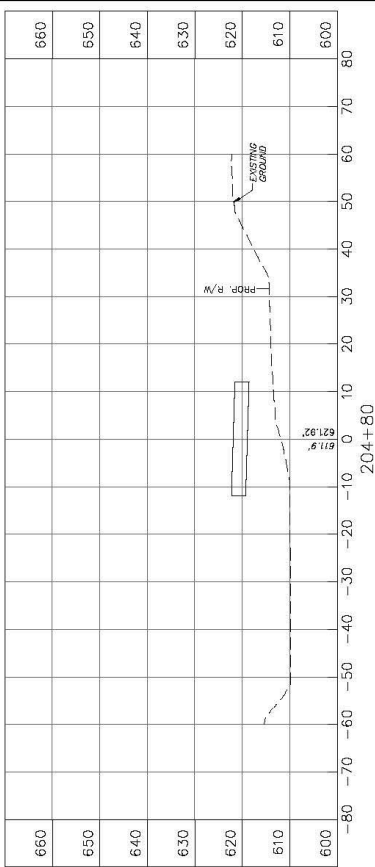
**FOURTEEN MILE BRIDGE
WV 37 OVER
FOURTEENMILE CREEK**

DETOUR
CROSS SECTIONS

STATE	PROJECT	SECTION	DATE
WV	1332-37-128 00	811-0001000	2011
NO.	REV.	BY	DATE
2			



LOCATION	SEEDING & MULCHING		CLEARING & GRUBBING		EXCAVATION		EMBANKMENT	
	LENGTH FT	AREA SF	WIDTH FT	AREA SF	UNCLASSIFIED CY	UNUSABLE SF	UNCLASSIFIED CY	SELECT EMBANKMENT SF
204+83.36	0	0	0	0	0	0	0	0
204+80	3.36	0	0	0	0	0	0	0



LOCATION	SEEDING & MULCHING		CLEARING & GRUBBING		EXCAVATION		EMBANKMENT	
	LENGTH FT	AREA SF	WIDTH FT	AREA SF	UNCLASSIFIED CY	UNUSABLE SF	UNCLASSIFIED CY	SELECT EMBANKMENT SF
204+80	0	0	0	0	0	0	0	0
204+80	0	0	0	0	0	0	0	0



P.O. Box 483
Berkeley, WV 25504
www.jbturmanengineering.com
304-733-1335

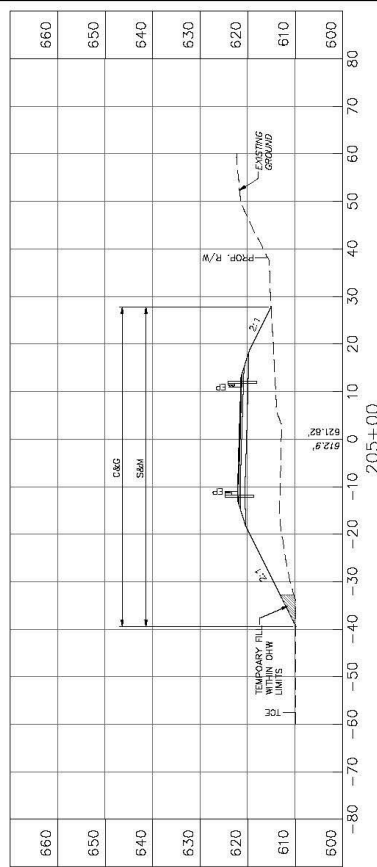
THE WEST VIRGINIA DEPARTMENT OF TRANSPORTATION
DIVISION OF HIGHWAYS

FOURTEEN MILE BRIDGE
WV 37 OVER
FOURTEENMILE CREEK

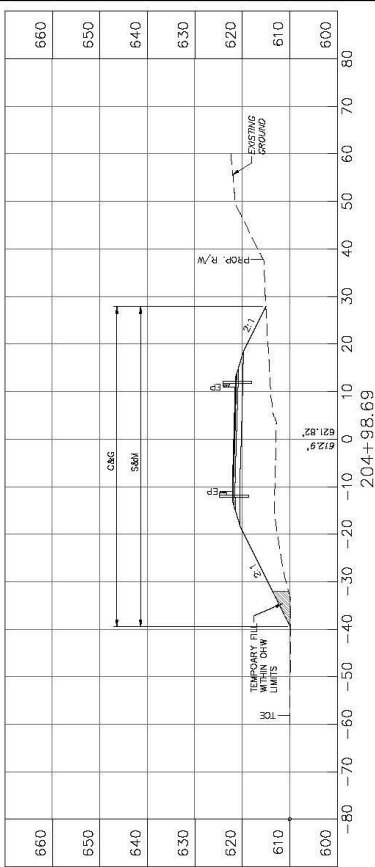
DETOUR
CROSS SECTIONS

DATE	BY

PROJECT NO.	DATE	PROJECT NAME	PROJECT LOCATION	PROJECT SHEET NO.	TOTAL SHEETS
WV 2	12/22/2011	1322-37-128.00	SPR-00010000	2011	UNKN
DATE	BY	PROJECT NAME	PROJECT LOCATION	PROJECT SHEET NO.	TOTAL SHEETS
12/22/2011	JTB	1322-37-128.00	SPR-00010000	2011	UNKN



LOCATION	SEEDING & MULCHING		CLEARING & GRUBBING		EXCAVATION		EMBANKMENT	
	WIDTH	AREA	WIDTH	AREA	UNCLASSIFIED	UNUSABLE	UNCLASSIFIED	SELECT EMBANKMENT
205+00	67.31	44.09	67.31	44.09	0	0	354.36	0
204+98.68	67.36	44.09	67.36	44.09	0	0	362.44	0



LOCATION	SEEDING & MULCHING		CLEARING & GRUBBING		EXCAVATION		EMBANKMENT	
	WIDTH	AREA	WIDTH	AREA	UNCLASSIFIED	UNUSABLE	UNCLASSIFIED	SELECT EMBANKMENT
204+98.69	67.36	44.09	67.36	44.09	0	0	362.44	0
204+83.16	67.36	44.09	67.36	44.09	0	0	362.44	0



THE WEST VIRGINIA DEPARTMENT OF TRANSPORTATION
DIVISION OF HIGHWAYS

**FOURTEEN MILE BRIDGE
WV 37 OVER
FOURTEENMILE CREEK**

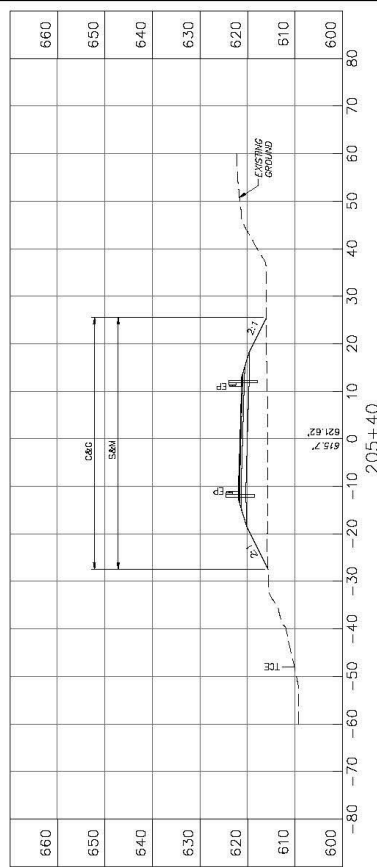
DETOUR
CROSS SECTIONS

P.O. Box 483
Berkeley, WV 25504
www.jbturmanengineering.com
304-733-1335

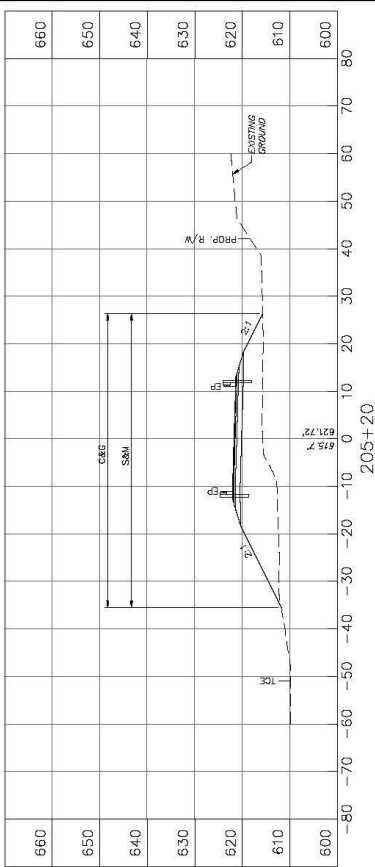
J.B. TURMAN ENGINEERING, PLLC

DATE: _____ BY: _____

STATE	PROJECT NO.	SECTION NO.	DATE	BY
WV	5322-37-128 00	1328	12/28/11	AS



LOCATION	SEEDING & MULCHING		CLEARING & GRUBBING		EXCAVATION		EMBANKMENT	
	LENGTH FT.	WIDTH FT.	AREA SF.	WIDTH FT.	AREA SF.	UNCLASSIFIED SP.	UNCLASSIFIED SP.	UNCLASSIFIED SP.
205+40	20	61.88	1282	53.01	1148	0	0	188.01
205+50	20	61.88	1282	61.88	1148	0	0	253.93



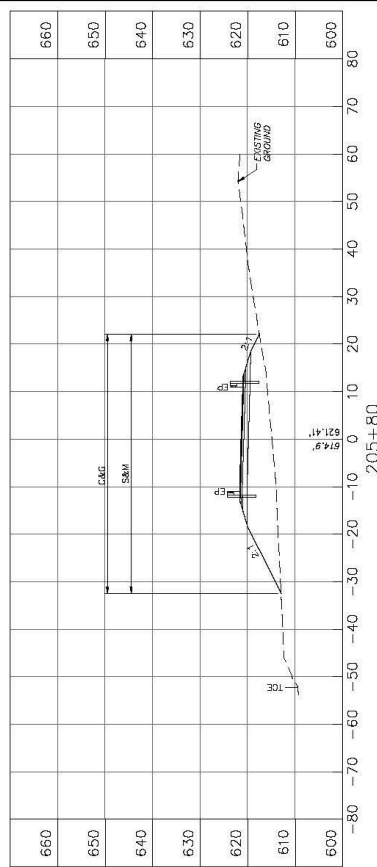
LOCATION	SEEDING & MULCHING		CLEARING & GRUBBING		EXCAVATION		EMBANKMENT	
	LENGTH FT.	WIDTH FT.	AREA SF.	WIDTH FT.	AREA SF.	UNCLASSIFIED SP.	UNCLASSIFIED SP.	UNCLASSIFIED SP.
205+20	20	61.88	1282	61.88	1282	0	0	253.93
205+50	20	61.88	1282	61.88	1282	0	0	394.35



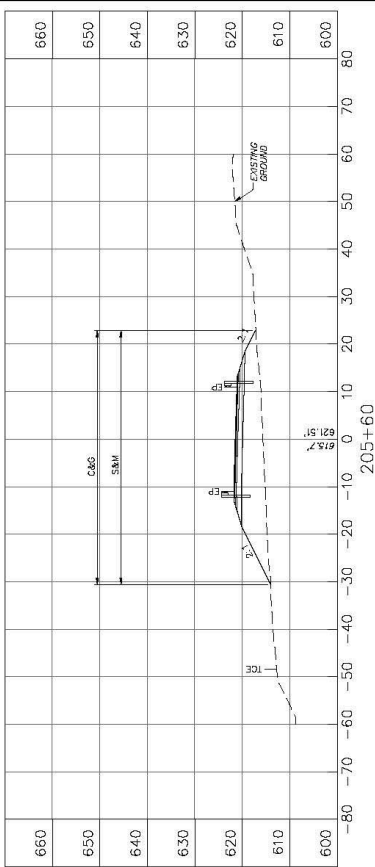
J.B. TURMAN ENGINEERING, PLLC
 P.O. Box 483
 Bercooreville, WV 25504
 www.jbtengineering.com
 304-733-1335

THE WEST VIRGINIA DEPARTMENT OF TRANSPORTATION
 DIVISION OF HIGHWAYS
**FOURTEEN MILE BRIDGE
 WV 37 OVER
 FOURTEENMILE CREEK**
 DETOUR
CROSS SECTIONS

STATE	PROJECT NO.	SECTION	DATE	BY
WV	1332-37-128 00	1332-37-128 00	2011	WJ



LOCATION	SEEDING & MULCHING		CLEARING & GRUBBING		EXCAVATION		EMBANKMENT		
	LENGTH FT	WIDTH SP	AREA SF	WIDTH SP	AREA SF	UNCLASSIFIED CY	UNUSABLE CY	UNCLASSIFIED CY	SELECT EMBANKMENT CY
205+80	20	53.96	1080.90	54.53	1080.90	0	0	226.78	154.87
205+80	20	53.96	1080.90	53.96	1080.90	0	0	181.36	---



LOCATION	SEEDING & MULCHING		CLEARING & GRUBBING		EXCAVATION		EMBANKMENT		
	LENGTH FT	WIDTH SP	AREA SF	WIDTH SP	AREA SF	UNCLASSIFIED CY	UNUSABLE CY	UNCLASSIFIED CY	SELECT EMBANKMENT CY
205+60	20	53.96	1085.70	53.96	1085.70	0	0	181.36	140.93
205+60	20	53.96	1085.70	53.01	1085.70	0	0	188.01	---



P.O. Box 483
Berkeley, WV 25504
www.jbengineering.com
304-733-1335

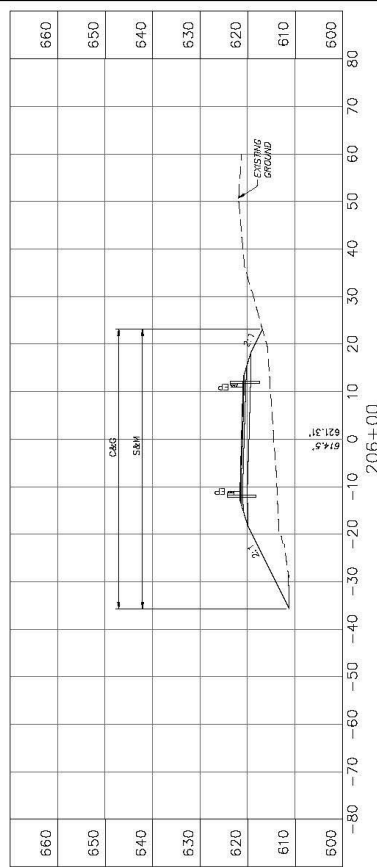
THE WEST VIRGINIA DEPARTMENT OF TRANSPORTATION
DIVISION OF HIGHWAYS

**FOURTEEN MILE BRIDGE
WV 37 OVER
FOURTEENMILE CREEK**

DETOUR
CROSS SECTIONS

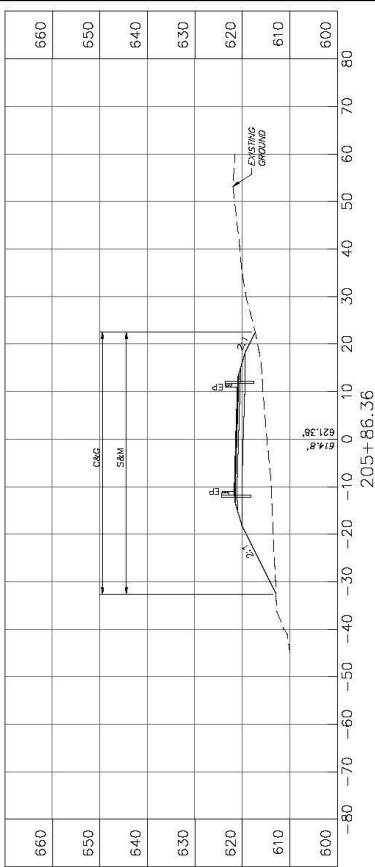
NO.	DATE	BY

STATE	PROJECT NO.	SECTION NO.	DATE	BY
WV	15322-37-1-28 00	15322-37-1-28 00		



LOCATION	SEEDING & MULCHING		CLEARING & GRUBBING		EXCAVATION		EMBANKMENT	
	WIDTH	AREA	WIDTH	AREA	UNCLASSIFIED	UNUSABLE	UNCLASSIFIED	SELECT EMBANKMENT
STATION	FT	SF	FT	SF	CY	CY	CY	CY
205+00	58.84	3428.46	58.84	3428.46	0	0	263.47	0
205+86.36	55.05	3030.46	776.73	61256.73	0	0	234.06	126.67

206+00



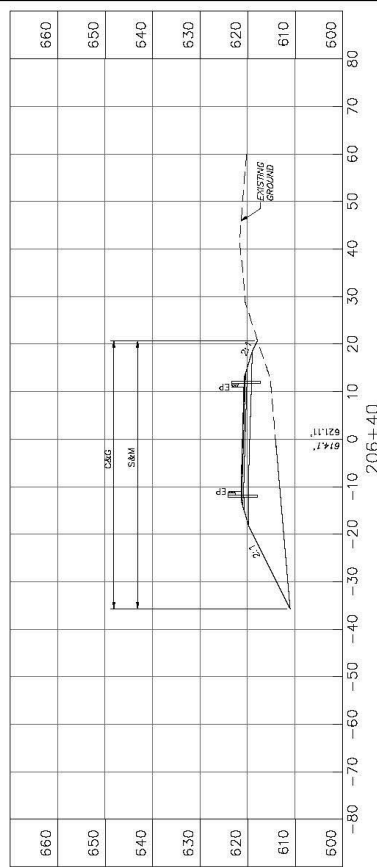
LOCATION	SEEDING & MULCHING		CLEARING & GRUBBING		EXCAVATION		EMBANKMENT	
	WIDTH	AREA	WIDTH	AREA	UNCLASSIFIED	UNUSABLE	UNCLASSIFIED	SELECT EMBANKMENT
STATION	FT	SF	FT	SF	CY	CY	CY	CY
205+86.36	55.05	3030.46	55.05	3030.46	0	0	234.06	0
205+86.36	54.53	2967.46	54.53	2967.46	0	0	236.78	0

205+86.36

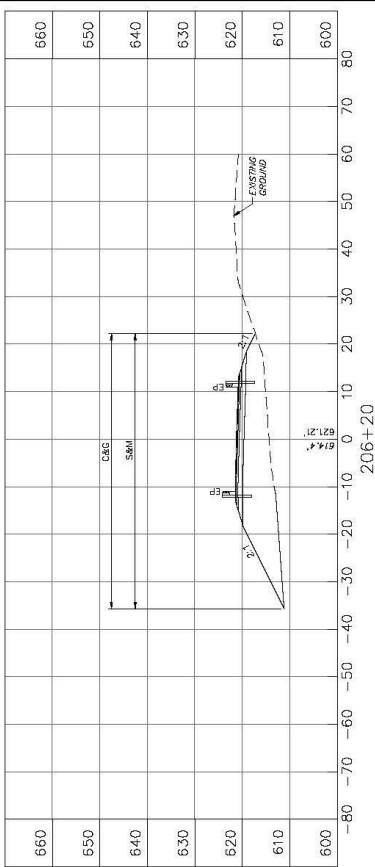


J.B. TURMAN ENGINEERING, PLLC P.O. Box 483 Berneville, WV 25504 www.jbtengineering.com 304-733-1335		THE WEST VIRGINIA DEPARTMENT OF TRANSPORTATION DIVISION OF HIGHWAYS FOURTEEN MILE BRIDGE WV 37 OVER FOURTEENMILE CREEK DETOUR CROSS SECTIONS	
REVISION	DATE	BY	APP

STATE	PROJECT NO.	PROJECT NAME	SECTION	DATE	BY
WV	2	15322-37-1-28 00	15322-37-1-28 00		



LOCATION	SEEDING & MULCHING		CLEARING & GRUBBING		EXCAVATION		EMBANKMENT	
	WIDTH	AREA	WIDTH	AREA	UNCLASSIFIED	UNSUITABLE	UNCLASSIFIED	SELECT EMBANKMENT
STATION	FT	SF	FT	SF	CV	CV	CV	CV
206+40	56.36	1142.20	56.36	1142.20	0	0	257.61	194.38
206+20	57.86	1142.20	57.86	1142.20	0	0	267.21	---



LOCATION	SEEDING & MULCHING		CLEARING & GRUBBING		EXCAVATION		EMBANKMENT	
	WIDTH	AREA	WIDTH	AREA	UNCLASSIFIED	UNSUITABLE	UNCLASSIFIED	SELECT EMBANKMENT
STATION	FT	SF	FT	SF	CV	CV	CV	CV
206+20	57.86	1187	57.86	1187	0	0	262.61	196.50
206+00	56.84	1187	56.84	1187	0	0	263.47	---



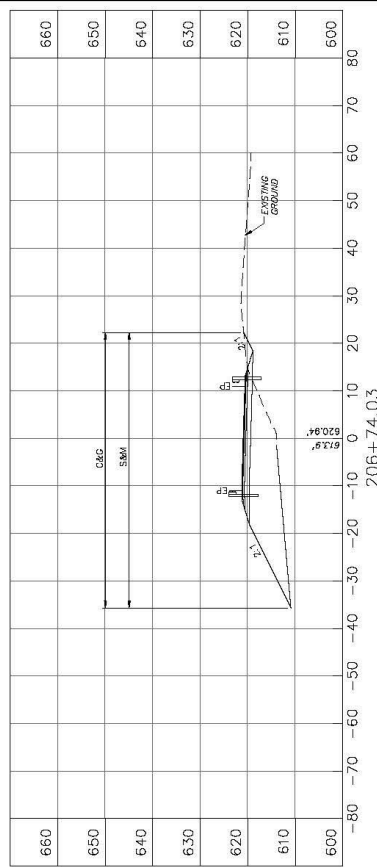
P.O. Box 483
Berkeley, WV 25504
www.jbturmanengineering.com
304-733-1335

THE WEST VIRGINIA DEPARTMENT OF TRANSPORTATION
DIVISION OF HIGHWAYS

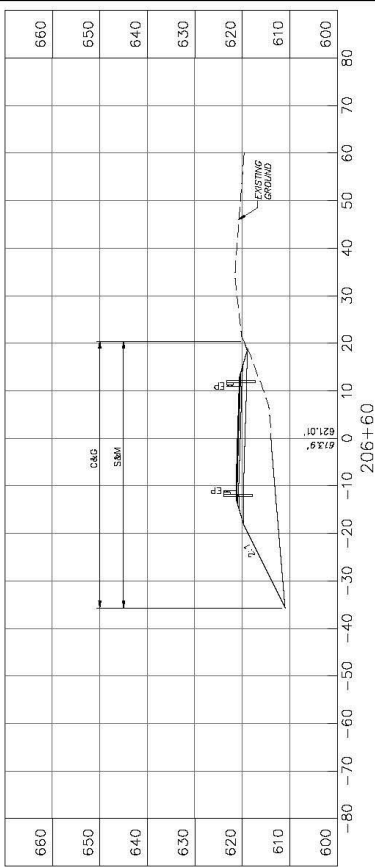
**FOURTEEN MILE BRIDGE
WV 37 OVER
FOURTEENMILE CREEK**

DETOUR
CROSS SECTIONS

STATE	PROJECT	SECTION	DATE	BY
WV	15322-37-128.00	15322-37-128.00	2011	UNSM



LOCATION	SEEDING & MULCHING		CLEARING & GRUBBING		EXCAVATION		EMBANKMENT		
	LENGTH	WIDTH	AREA	WIDTH	AREA	UNCLASSIFIED	UNCLASSIFIED	UNCLASSIFIED	SELECT
STATION	FT	FT	SF	FT	SF	CY	SF	CY	EMBANKMENT
206+74.03	11	57.83	799.64	57.83	799.64	9.16	212.77	0	118.96
206+80	14.03	56.06	799.64	56.06	799.64	0	245.11	0	118.96



LOCATION	SEEDING & MULCHING		CLEARING & GRUBBING		EXCAVATION		EMBANKMENT		
	LENGTH	WIDTH	AREA	WIDTH	AREA	UNCLASSIFIED	UNCLASSIFIED	UNCLASSIFIED	SELECT
STATION	FT	FT	SF	FT	SF	CY	SF	CY	EMBANKMENT
206+60	20	56.06	1124.20	56.06	1124.20	0	245.11	188.19	---
206+40	20	56.36	1124.20	56.36	1124.20	0	257.61	---	---



THE WEST VIRGINIA DEPARTMENT OF TRANSPORTATION
 DIVISION OF HIGHWAYS

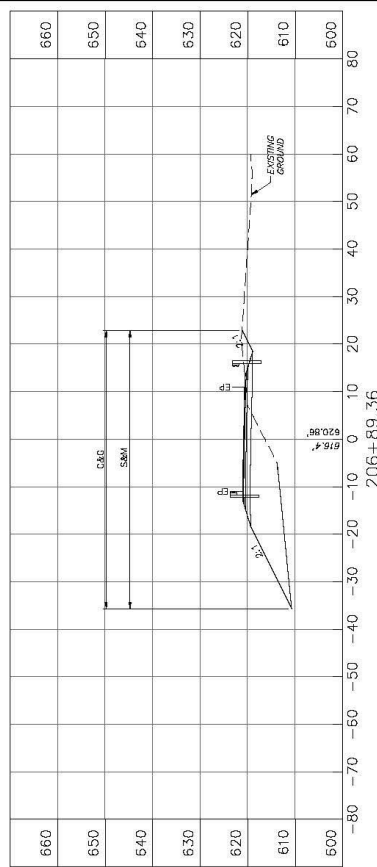
FOURTEEN MILE BRIDGE
WV 37 OVER
FOURTEENMILE CREEK

J.B. TURMAN ENGINEERING, PLLC
 P.O. Box 483
 Berneville, WV 25504
 www.jbtengineering.com
 304-733-1335

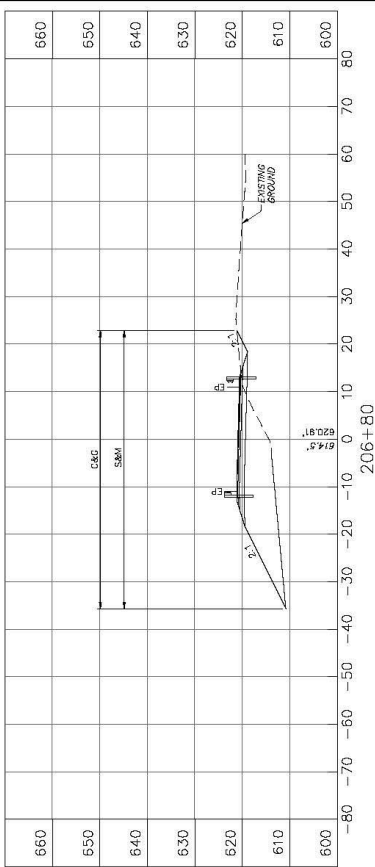
DETOUR
 CROSS SECTIONS

DATE	BY

PROJECT NO.	DATE	BY	CHKD.	DATE	BY	CHKD.
13322-37-128.00	10/11/11	WV	2	10/11/11	WV	2



LOCATION	SEEDING & MULCHING		CLEARING & GRUBBING		EXCAVATION		EMBANKMENT		
	LENGTH FT	WIDTH SF	AREA SF	WIDTH SF	AREA SF	UNCLASSIFIED CY	UNCLASSIFIED SF	UNCLASSIFIED SF	SELECT EMBANKMENT SF
206+89.36	9.36	58.56	548.12	58.56	548.12	15.07	22.83	173.41	571.9
206+80		58.56	548.12	58.56	548.12	15.07	22.83	173.41	571.9



LOCATION	SEEDING & MULCHING		CLEARING & GRUBBING		EXCAVATION		EMBANKMENT		
	LENGTH FT	WIDTH SF	AREA SF	WIDTH SF	AREA SF	UNCLASSIFIED CY	UNCLASSIFIED SF	UNCLASSIFIED SF	SELECT EMBANKMENT SF
206+80	8.97	58.56	524.72	57.93	524.72	2.88	15.07	158.80	452.29
206+74.03		57.83	524.72	57.93	524.72	2.88	15.07	158.80	452.29



P.O. Box 483
Berkeley, WV 25504
www.jbenengineering.com
304-733-1335

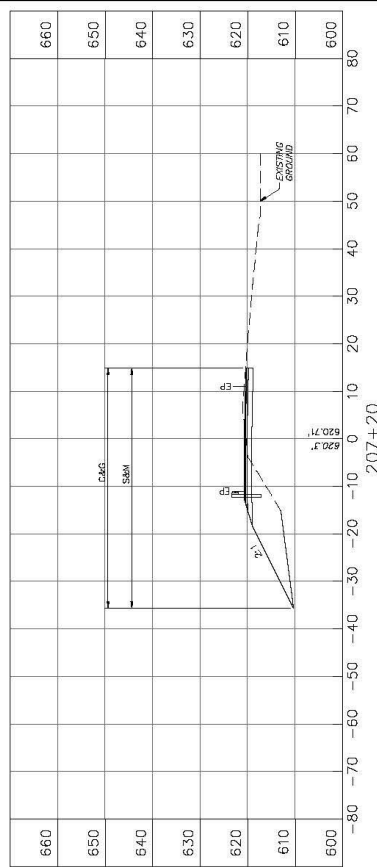
THE WEST VIRGINIA DEPARTMENT OF TRANSPORTATION
DIVISION OF HIGHWAYS

**FOURTEEN MILE BRIDGE
WV 37 OVER
FOURTEENMILE CREEK**

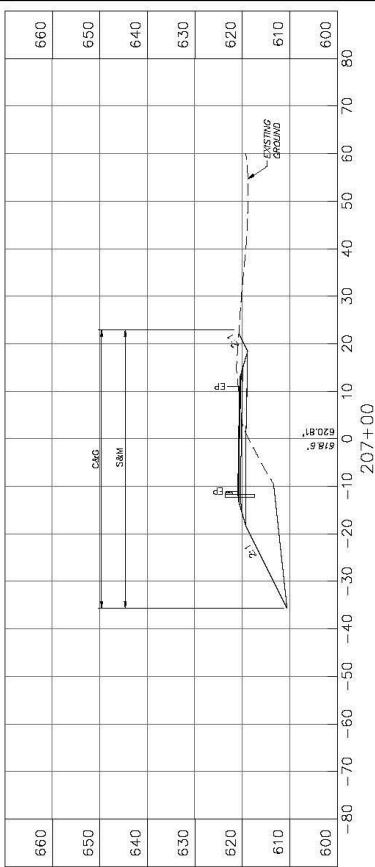
DETOUR
CROSS SECTIONS

NO.	DATE	BY

PROJECT NO.	DATE	BY	CHKD	DATE	BY	CHKD
1322-37-128 00	10/11/11	WV	2	10/11/11	WV	2



LOCATION	SEEDING & MULCHING		CLEARING & GRUBBING		EXCAVATION		EMBANKMENT	
	WIDTH	AREA	WIDTH	AREA	UNCLASSIFIED	UNUSABLE	UNCLASSIFIED	SELECT EMBANKMENT
207+20	58.56	1091	58.56	1091	31.06	37.06	106.19	93.30
207+40	58.56	1091	58.56	1091	31.16	37.06	145.72	---



LOCATION	SEEDING & MULCHING		CLEARING & GRUBBING		EXCAVATION		EMBANKMENT	
	WIDTH	AREA	WIDTH	AREA	UNCLASSIFIED	UNUSABLE	UNCLASSIFIED	SELECT EMBANKMENT
207+00	58.56	1091	58.56	1091	31.16	37.06	145.72	93.30
207+40	58.56	1091	58.56	1091	31.16	37.06	173.41	---



THE WEST VIRGINIA DEPARTMENT OF TRANSPORTATION
DIVISION OF HIGHWAYS

**FOURTEEN MILE BRIDGE
WV 37 OVER
FOURTEENMILE CREEK**

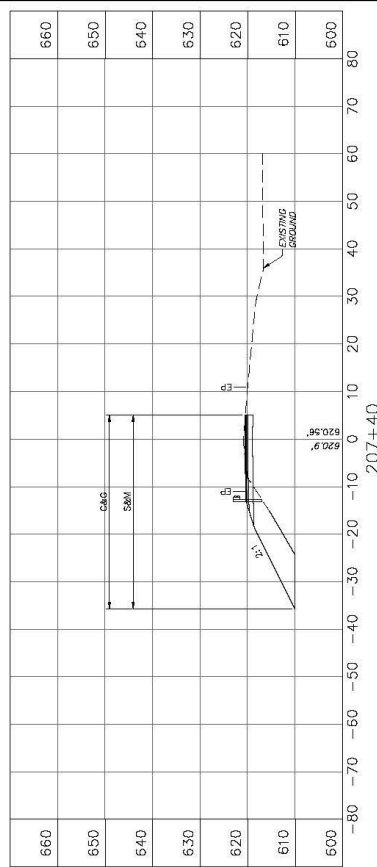
DETOUR
CROSS SECTIONS

J.B. TURMAN ENGINEERING, PLLC

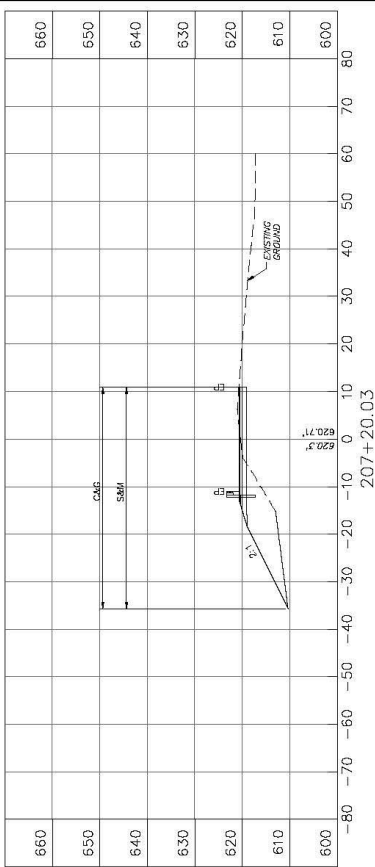
P.O. Box 483
Berkeley, WV 25504
www.jbtengineering.com
304-733-1335

DATE: _____ BY: _____

PROJECT NO.	DATE	BY	SCALE	PROJECT	DATE	BY	SCALE
1322-37-128.00	10/11/11	WV	1"=20'	1322-37-128.00	10/11/11	WV	1"=20'



LOCATION	SEEDING & MULCHING		CLEARING & GRUBBING		EXCAVATION		EMBANKMENT		
	LENGTH FT	WIDTH FT	AREA SF	WIDTH FT	AREA SF	UNCLASSIFIED SF	UNCLASSIFIED SF	UNCLASSIFIED SF	SELECT EMBANKMENT SF
207+40	19.97	46.55	919.28	40.71	800.51	22.53	87.06	71.44	---
207+20.03	0.03	50.54	1,48	46.55	2,148	22.38	106.12	---	---



LOCATION	SEEDING & MULCHING		CLEARING & GRUBBING		EXCAVATION		EMBANKMENT	
	LENGTH FT	WIDTH FT	AREA SF	WIDTH FT	AREA SF	UNCLASSIFIED SF	UNCLASSIFIED SF	SELECT EMBANKMENT SF
207+20.03	0.03	50.54	1,48	46.55	2,148	22.38	106.12	0.06
207+20	0.03	50.54	1,48	46.55	2,148	22.38	106.12	---



P.O. Box 483
Berkeley, WV 25504
www.jbenengineering.com
304-733-1335

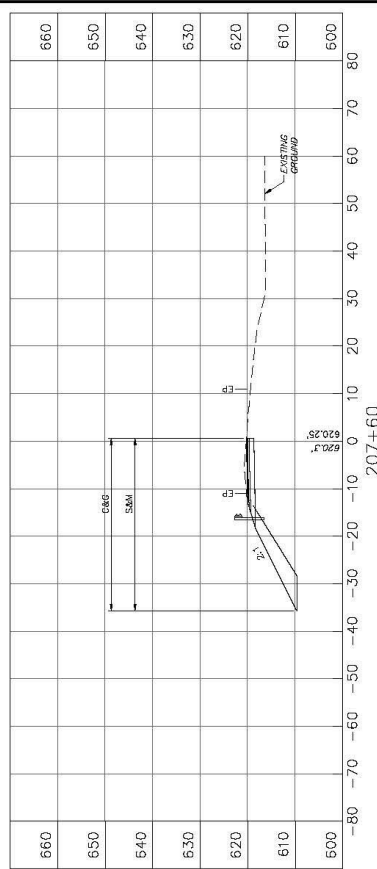
THE WEST VIRGINIA DEPARTMENT OF TRANSPORTATION
DIVISION OF HIGHWAYS

FOURTEEN MILE BRIDGE
WV 37 OVER
FOURTEENMILE CREEK

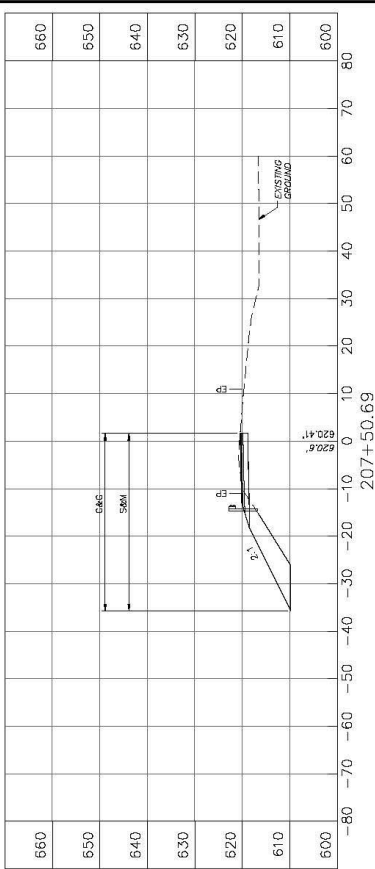
DETOUR
CROSS SECTIONS

NO.	DATE	BY

STATE	PROJECT NO.	SECTION	DATE	BY
WV	15322-37-1-28.00	15322-37-1-28.00	2011	MS



LOCATION	SEEDING & MULCHING		CLEARING & GRUBBING		EXCAVATION		EMBANKMENT	
	WIDTH	AREA	WIDTH	AREA	UNCLASSIFIED	UNUSABLE	UNCLASSIFIED	SELECT EMBANKMENT
STATION	FT	SF	FT	SF	CY	SF	SF	CY
207+60	36.21	342.10	36.21	25.06	8.29	---	49.15	---
207+50.69	37.28	342.10	37.28	27.41	---	---	67.30	---



LOCATION	SEEDING & MULCHING		CLEARING & GRUBBING		EXCAVATION		EMBANKMENT	
	WIDTH	AREA	WIDTH	AREA	UNCLASSIFIED	UNUSABLE	UNCLASSIFIED	SELECT EMBANKMENT
STATION	FT	SF	FT	SF	CY	SF	SF	CY
207+50.69	37.28	418.86	37.28	418.86	8.90	---	67.30	30.96
207+40	40.71	407.1	40.71	22.53	---	---	67.06	---

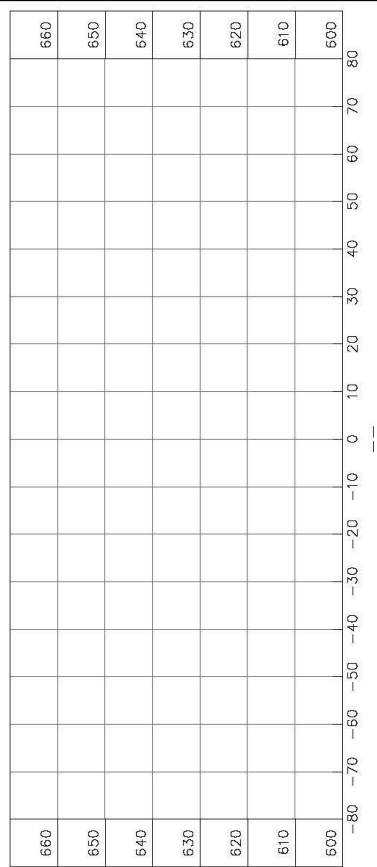


J.B. TURMAN ENGINEERING, PLLC
 P.O. Box 483
 Berneville, WV 25504
 www.jbtengineering.com
 304-733-1335

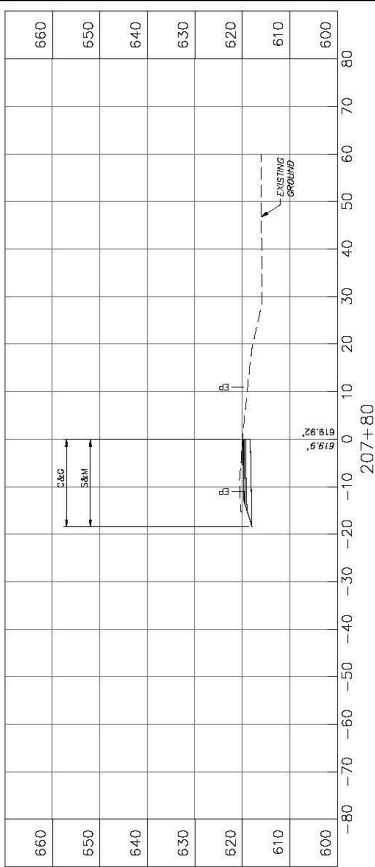
THE WEST VIRGINIA DEPARTMENT OF TRANSPORTATION
 DIVISION OF HIGHWAYS
FOURTEEN MILE BRIDGE
WV 37 OVER
FOURTEENMILE CREEK
 DETOUR
 CROSS SECTIONS

PROJECT NO.	DATE	BY

PROJECT NO.	DATE	DESIGNER	PROJECT NAME	DATE	PROJECT NO.	DATE
WV 2	12/22/2011	J.B. TURMAN ENGINEERING, PLLC	FOURTEEN MILE BRIDGE	12/22/2011	WV 2	12/22/2011



STATION	SEEDING & MULCHING		CLEARING & GRUBBING		EXCAVATION		EMBANKMENT	
	LENGTH (FT)	AREA (SF)	WIDTH (FT)	AREA (SF)	UNCLASSIFIED (CY)	UNSUITABLE (SF)	UNCLASSIFIED (CY)	SELECT EMBANKMENT (SF)
207+80	20	543.20	18.31	343.20	18.32	24.34	0	18.20
207+60	20	36.21	36.21	25.66	49.15	0	0	0



STATION	SEEDING & MULCHING		CLEARING & GRUBBING		EXCAVATION		EMBANKMENT	
	LENGTH (FT)	AREA (SF)	WIDTH (FT)	AREA (SF)	UNCLASSIFIED (CY)	UNSUITABLE (SF)	UNCLASSIFIED (CY)	SELECT EMBANKMENT (SF)
207+80	20	543.20	18.31	343.20	18.32	24.34	0	18.20
207+60	20	36.21	36.21	25.66	49.15	0	0	0



J.B. TURMAN ENGINEERING, PLLC
 P.O. Box 483
 Bercooreville, WV 25504
 www.jbtengineering.com
 304-733-1335

THE WEST VIRGINIA DEPARTMENT OF TRANSPORTATION
 DIVISION OF HIGHWAYS
FOURTEEN MILE BRIDGE
WV 37 OVER
FOURTEENMILE CREEK
 DETOUR
 CROSS SECTIONS

PROJECT NO.	DATE	BY